NATURAL PRODUCTS FROM MARINE DERIVED MICRO-ORGANISMS

A thesis
submitted in partial fulfilment
of the requirements for the degree
of
Doctor of Philosophy in Chemistry
in the
University of Canterbury
by
Richard K. Phipps

University of Canterbury
2002

ABSTRACT

A large number of micro-organisms were cultured from marine substrates collected from multiple sites along the coast of the South Island of New Zealand. Depending on growth rate and colony morphology the micro-organisms were classified as terrestrial, facultative marine or obligate marine. Micro-organisms were selected for large scale culture and extraction based on either apparent unusual morphology or observed cytotoxicity in small scale extracts.

Two very pale yellow compounds were isolated from cytotoxic extracts prepared from culture broths of a *Fusarium* sp. The first compound (**A**) was identified as a novel trichothecene called 4-deacetoxy-8-isobutyrylneosolaniol. The second compound (**B**) was identified as the 4-hydroxy derivative of **A**, previously only known through semi-synthetic preparation.

The known compound cephalochromin (**C**) was purified from the culture broths of two unidentified *Cephalosporium*-like Hyphomycetes. The identity with cephalochromin was confirmed by comparison of published NMR and circular dichroism spectroscopy.

An intense yellow compound was isolated from an extract prepared from culture broths of an *Alternaria* sp. This compound was identified by NMR spectroscopy as a novel altersolanol called altersolanol J (**D**).

The known compound 1-hydroxyaclacinomycin T (**E**) was isolated from the culture broths of a *Streptomyces* sp. A further five related compounds (**F** - **J**) were also isolated the culture broths. Compounds **F** and **G**, were shown by NMR spectroscopy to be stereoisomers of pyrromycin called 9-*epi*-pyrromycin and (7*R**9*R**10*R**)-pyrromycin respectively. The low isolated mass of compound **H** prevented a complete identification but was tentatively assigned by NMR spectroscopy as an *N*-demethyl derivative of pyrromycin. Compounds **I** and **J** were both shown by NMR spectroscopy to be novel pyrromycin derivatives called 1-hydroxyauramycin T and 1-hydroxysulfurmycin T respectively.

The known compounds actinomycin V (**K**), actinomycin X_0 (**L**) and actinomycin D (**M**) were purified from extracts of the culture broths of three *Streptomyces* sp.

The identities of all these compounds were established by 1D and 2D NMR spectroscopy and comparison to previously reported data.

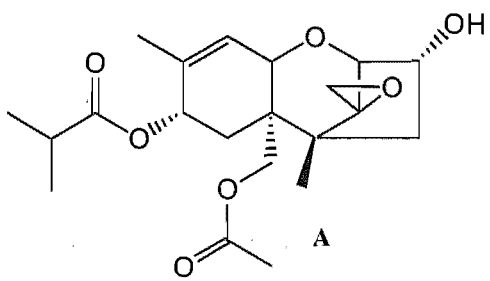

A

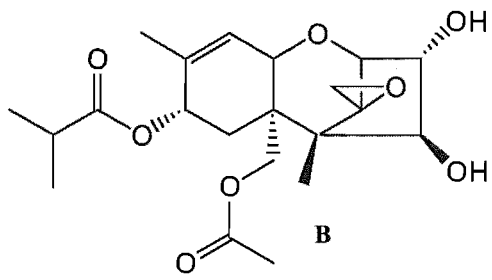

B

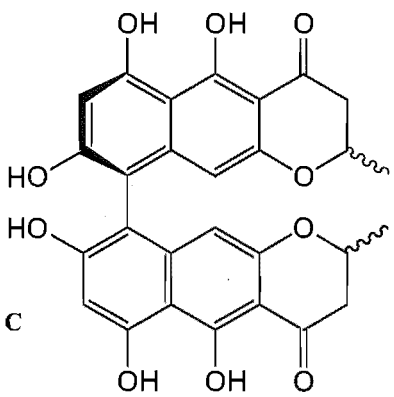

C

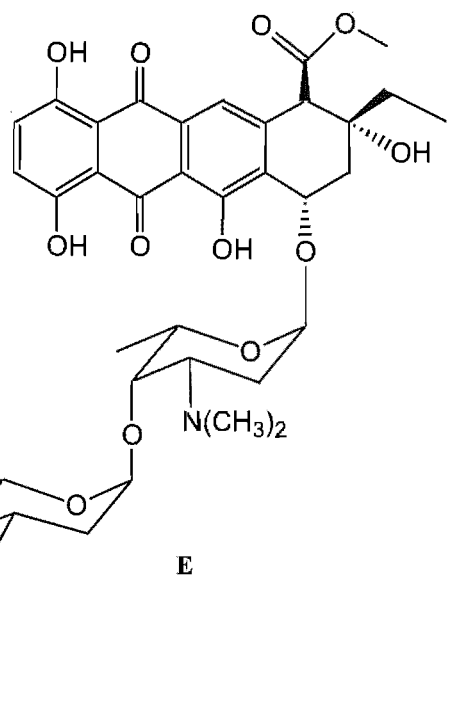

E

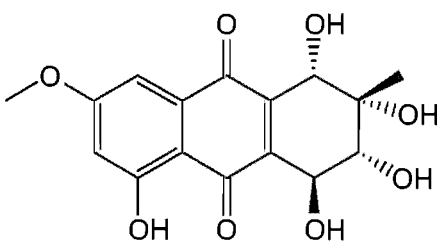

D

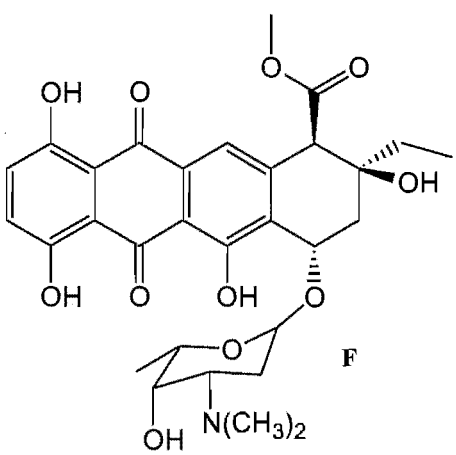

F

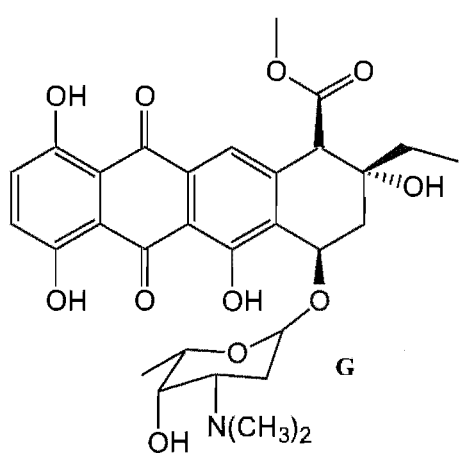

G

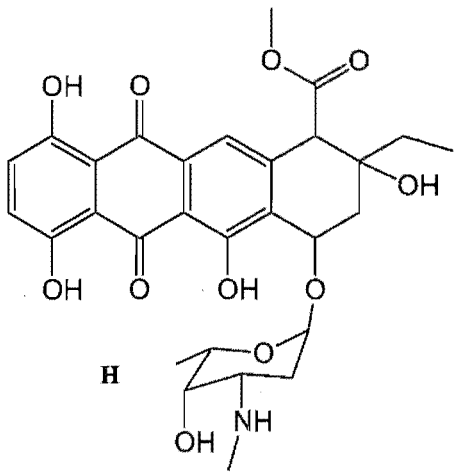
OH
O
O
O
OH
OH
O
OH
O
O
O
OH
NH

H

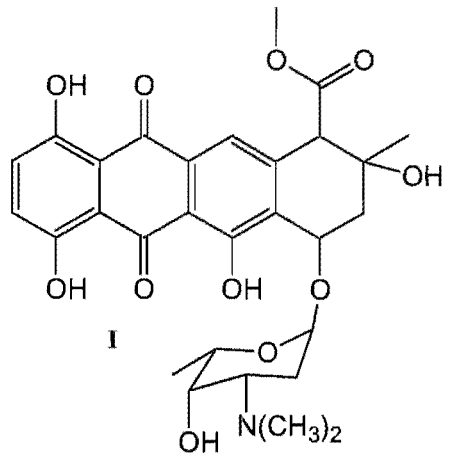
O
O
OH
O
OH
OH
O
OH
O
O
OH
N(CH3)2

I

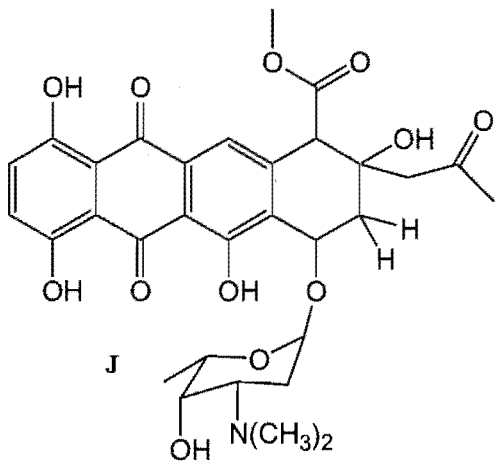
O
O
OH
O
OH
O
H
H
OH
O
OH
O
O
OH
N(CH3)2

J

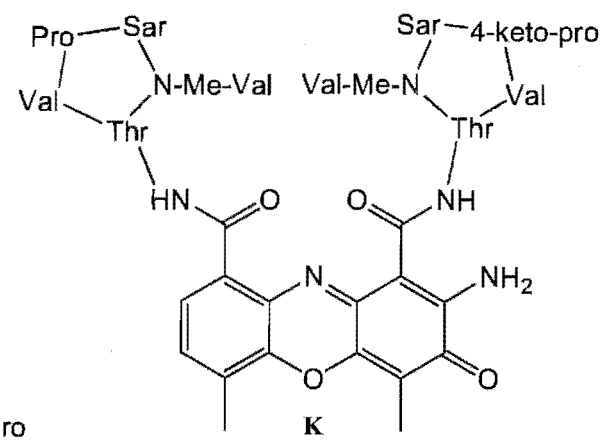
Pro
Sar
Val
N-Me-Val
Thr
HN
O
Sar
4-keto-pro
Val-Me-N
Val
Thr
O
NH
N
NH2
O
O

K

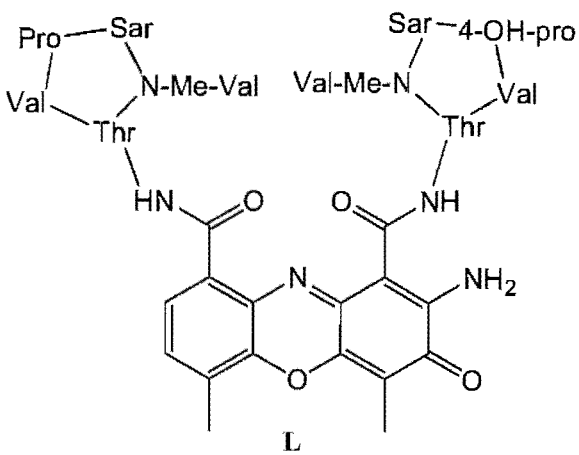
Pro
Sar
Val
N-Me-Val
Thr
HN
O
Sar
4-OH-pro
Val-Me-N
Val
Thr
O
NH
N
NH2
O
O

L

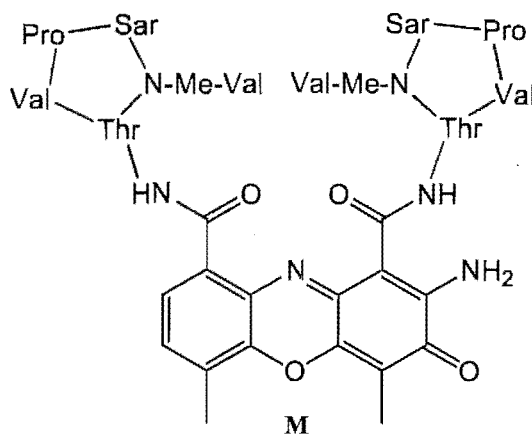
Pro
Sar
Val
N-Me-Val
Thr
HN
O
Sar
Pro
Val-Me-N
Val
Thr
O
NH
N
NH2
O
O

M

ACKNOWLEDGEMENTS

First, I would like to thank my Supervisors, Professor Murray Munro and Professor John Blunt of the Chemistry Department and Associate Professor Anthony Cole of the Department of Plant and Microbial Sciences for all their help, guidance and advice during the course of this thesis. I would also like to thank BioMar SA for the financial assistance and two powdered extracts provided during the course of this work.

The technical staff in both the Chemistry Department and the Department of Plant and Microbial Sciences have provided a great deal of technical expertise during the course of this study. I would especially like to thank Gill Ellis for the opportunity to understand the biological assays at first hand and Bruce Clark for running the myriad mass spectra required during the course of this study. Many thanks also go to those members of the Department of Plant and Microbial Sciences who have helped in some way, but especially Matt Walters and Dougal Holmes. Matt for the invaluable assistance with collecting samples from the field and Dougal for the almost endless photos required to help keep track of the fungi being isolated. I would also like to thank Craig Galilee and Nic Cummings for the microbiological help.

There have been many students from both departments who have provided advice and made my time at the University of Canterbury much more enjoyable. These people include, but are not limited to, Wenxu Jiao, Dr Yunjiang Feng, Sonia van der Sar, Warren Maclean, Scott Bringans, Marie Squire, Sean Devenish and Dr Sylvia Urban.

An extra special thanks goes to my partner, Angela Cone, who provided a great deal of help with the field work and general support, without whom things would not have progressed so well. Finally, a very special thanks goes to my family for all the support and meals provided during the course of this study and during my entire time at University.

ABBREVIATIONS

ACN	Acetonitrile
APcI	Atmospheric Pressure chemical Ionisation
APT	Attached Proton Test
ATA	Alimentary Toxic Aleukia
BNPD	Berdy Natural Products Database
CBA	Carboxylic Acid
CD	Circular Dichroism
CD_3OD	Deuterated Methanol
$CDCl_3$	Deuterated Chloroform
d	doublet (in connection with NMR data)
DCM	Dichloromethane
DEA	Diethylamine
DMSO-d_6	Deuterated Dimethylsulphoxide
EtOAc	Ethyl acetate
HPLC	High Pressure Liquid Chromatography
HS	Host Specific
Hz	Hertz
IC_{50}	50 % Inhibitory Concentration
m	multiplet (in connection with NMR data)
MeOH	Methanol
MHz	Megahertz
min	minutes
nm	10^{-9} meter
NMR	Nuclear Magnetic Resonance
PDA	Potato Dextrose Agar
PDB	Potato Dextrose Broth
Pet. Ether	Petroleum Ether
q	quartet (in connection with NMR data)
s	singlet (in connection with NMR data)
SA	Seawater Agar
sp.	species
t	triplet (in connection with NMR data)
TFA	Trifluoroacetic Acid
UV	Ultra-Violet
VLC	Vacuum Liquid Chromatography

TABLE OF CONTENTS

CHAPTER ONE

INTRODUCTION

1.1 Natural products

Until the late 19th Century the major source of drugs was from terrestrial plants. After the discovery of penicillin (**1**) in the early 1900's however, interest was directed towards bioactive secondary metabolites from terrestrial micro-organisms. Extensive studies were carried out and these yielded a dazzling array of bioactive metabolites. Since the early 1940's over 5,000 antibiotic agents have been identified, primarily from actinomycetes. Antibiotic production by fungi is second only to the actinomycetes with approximately 1,600 compounds characterised.[1] Of the top ten commercially used antibiotics or antibiotic classes isolated from fungi, the penicillins such as penicillin G (**1**), the cephalosporins such as cephalosporin C (**2**), griseofulvin (**3**) and fusidic acid (**4**) have been the most important.

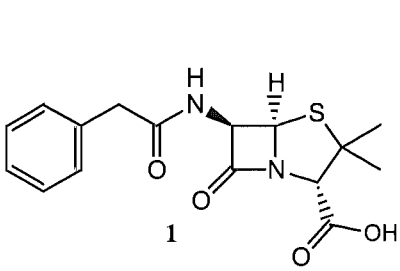

1

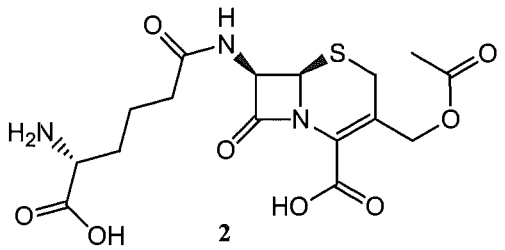

2

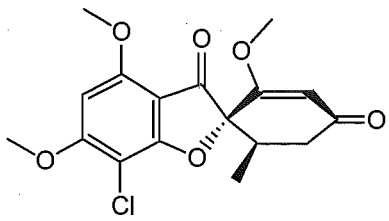

3

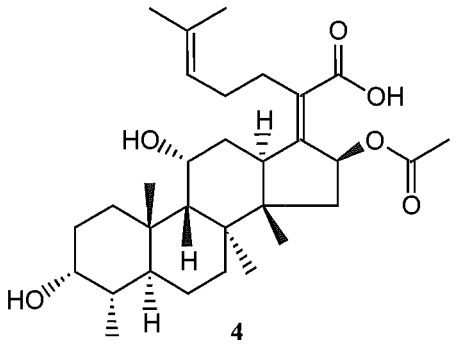

4

1.2 A brief history of bioactive compounds

Fewer than 10% of the total terrestrial organisms have been examined for biologically active compounds.[2] Fungi comprise a large number of those terrestrial organisms that have been examined.[2] Including undescribed species the number of fungi are estimated to be in excess of 1.5 million,[3] but only a fraction of these, approximately 5 %,[1] have been described, let alone examined in the full range of possible assays for biological activity.

Most bioactive compounds produced in nature are typically secondary metabolites which are not essential for the growth of an organism, but have been shown to confer selective advantages to the organism, such as antifeeding.[4, 5] Perhaps the most famous class of these secondary metabolites would be the penicillins which inhibited the growth of other micro-organisms, but had no effect on the fungus producing it.

Other well known fungal compounds used in medicine are cyclosporin A and the cholesterol biosynthesis inhibitors, the statins. Cyclosporin A (**5**) was initially discovered as an antifungal agent from *Tolypocladium inflatum*.[6] Further work however, found it to possess excellent immunosuppressant activity.[7] The cholesterol-lowering agent mevastatin (**6**) was originally isolated from *Penicillium citrinum* in 1976.[8] The statins are perhaps one of the most important classes of compounds to

enter the pharmaceutical market within the last 20 years with over US$ 7.52 billion dollars per year generated from sales in 1997. Indeed one of this group, simvastatin was the second highest selling drug world-wide that year.[9]

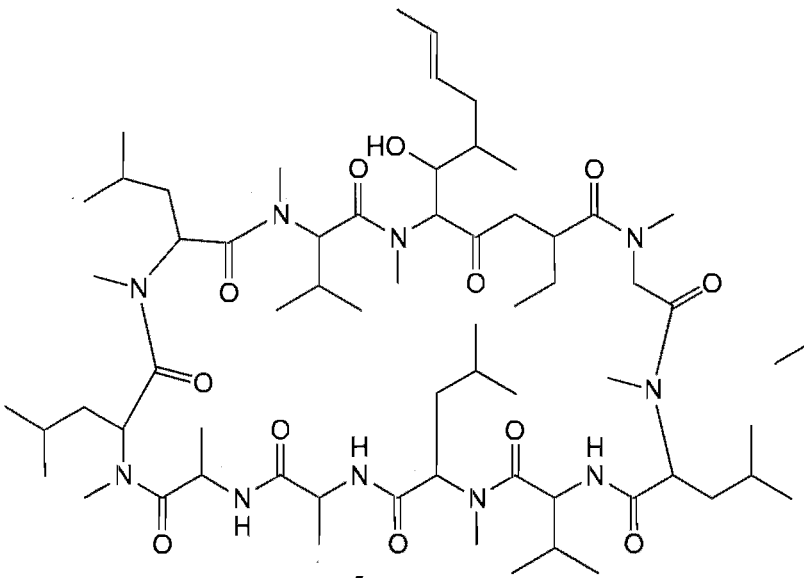

5

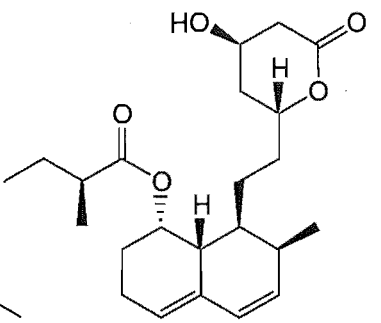

6

Even some fungal metabolites that have been known for a long time are finding new uses in medicine today. Mycophenolic acid (7), a highly toxic metabolite from various species of *Penicillium*, originally discovered in 1896 with the structure reported in 1952,[10] was recently found to have immunosuppressant activity.[11] The mycophenolic acid (7) prodrug, Mofetil (8), is broken down in the body to release mycophenolic acid, which subsequently inhibits proliferation of cells involved in the immune response.[7] This compound has also recently been isolated from several species of fungi in the Marine Chemistry Group at the University of Canterbury.

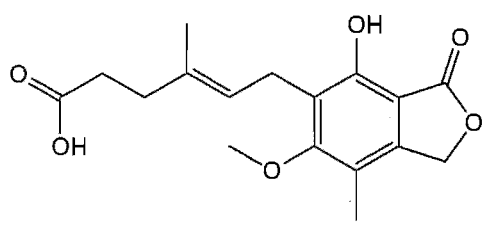

7

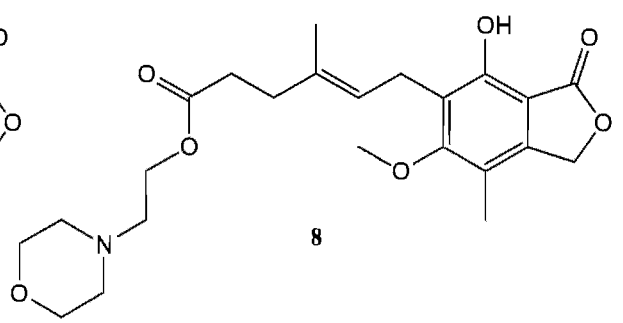

8

Of all the compounds with biological activity isolated to date, terrestrial organisms have been the most common source. Unfortunately, the yield of potentially useful new

compounds from terrestrial organisms has been in decline for some time, due mostly to the rediscovery of known compounds. However, the need for new bioactive compounds is not declining, but rather is still increasing. This is not only because new diseases are still being discovered, but also because existing disease-causing agents can easily mutate into strains resistant to the array of pharmaceuticals in use today.

Within the last 30 years the focus has turned towards the marine environment. This is because it covers over 70 % of the Earth's surface and is over 95 % of the earth's biosphere[12] with diverse habitats ranging from hot tropical environments to cold polar ones. Some of these habitats, such as tropical coral reefs, display extreme biodiversity (high abundance of different animal and plant species).

Nearly all forms of marine life have been examined with sponges topping the list of those investigated. Compounds isolated from the marine environment are extremely diverse in their chemistry, with a higher percentage of halogenated compounds being found,[13] such as agelongine (**9**) from the marine sponge *Agelas longissima*,[14] due in part to the higher natural abundance of halogens in seawater.

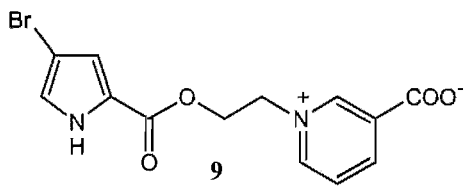

9

Most of these natural products have been implicated either in chemical defence or competition.

1.3 Biodiversity in the marine environment

The number of marine animal and micro-organism species is estimated to be in excess of 2 million and constitutes a greater diversity at higher taxonomic levels than seen in terrestrial ecosystems.[12] Since the early 1970's a vast succession of novel metabolites has been isolated from marine animals, yet less than 0.5 % have actually been screened for antineoplastic activity and even fewer have been examined for activity against infectious diseases.[12]

Table 1.1 shows some novel metabolites reported from the marine environment between 1970 and 2000. As can be seen, there are a larger number of sponge metabolites being found, however this is most likely because the Porifera has been one of the more intensely investigated phyla.

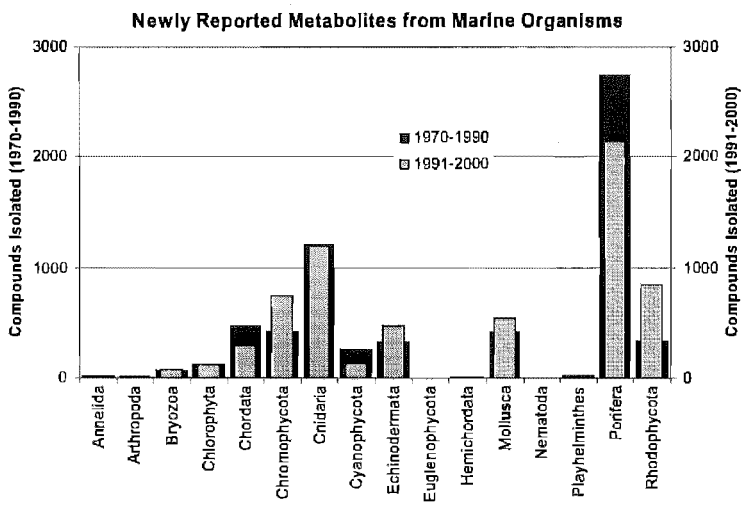

Table 1.1: Newly reported metabolites from various marine phyla.
Adapted from Urban *et al.*[15]

Table 1.2 shows the number of compounds isolated from marine phyla over the last 30 years. From 1970 to 1991 the number of natural products being isolated from marine organisms steadily increased from just 17 in 1970 to over 600 in 1991. Since 1991 an average of over 650 new metabolites have been discovered each year.

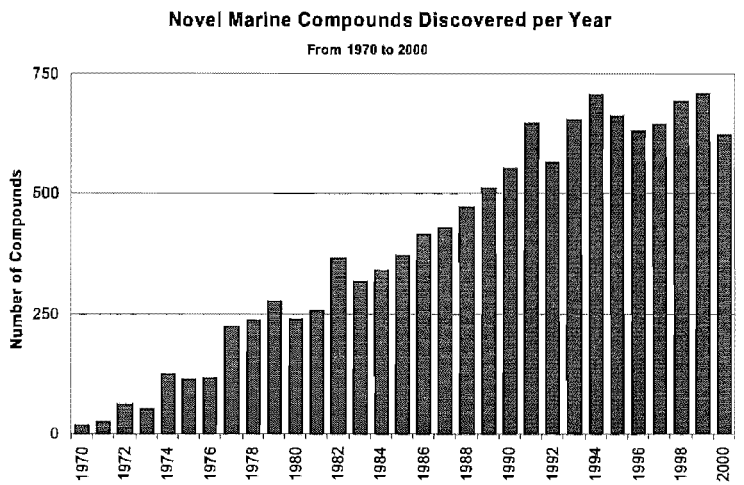

Table 1.2: The number of novel compounds from marine phyla reported each year.
Adapted from Blunt *et al.*[16]

1.3.1 Natural products from the marine environment

Compounds isolated from marine animals have displayed a wide range of biological activities, such as antimicrobial and anticancer activity. By 2001 over 12,000 marine natural products had been isolated from a wide variety of organisms, several of these exhibiting potent biological activity.[16]

The production of bioactive secondary metabolites from marine macroorganisms is well documented with new compounds constantly being discovered.[17, 18] Table 1.3 shows some novel compounds isolated from marine macro organisms.

Source Organism	*Metabolites Identified*	*Activity*
Ecteinascidia turbinata	Ecteinascidin 743 (**10**)[19]	Cytotoxic
Conus magus	ω-conotoxin MVIIA (**11**)[20]	Analgesic
Aplidium lobatum (Australian tunicate)	Lobatamide A (**12**)[21] Lobatamide B (**13**) Lobatamide C (**14**) Lobatamide D (**15**) Lobatamide E (**16**) Lobatamide F (**17**)	Cytotoxic
Pseudopterogorgia elisabethae (West-Indian sea whip)	Elisabethin A (**18**)[22]	
	Elisabethin B (**19**)	Antitumour
	Elisabethin C (**20**)	Anti tuberculosis
	Elisabanolide (**21**)	Anti tuberculosis
Sigmosceptrella sp (Marine sponge)	Sigmosceptrin A (**22**)[23] Sigmosceptrin B (**23**) Sigmosceptrin C (**24**)	Not tested
Cytoseira tamariscifolia (Brown alga)	Methoxybifurcarenone (**25**)[24]	Antimicrobial

Table 1.3: Some bioactive metabolites isolated from marine macro organisms

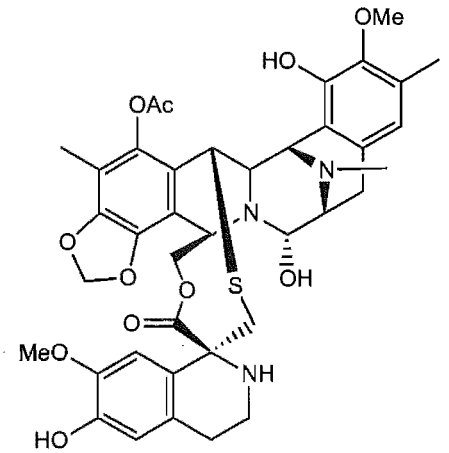

10

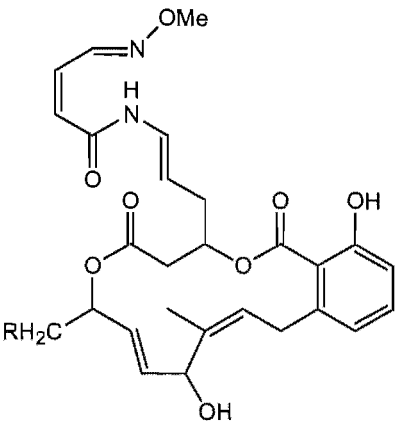

12 R=H
15 R=OH

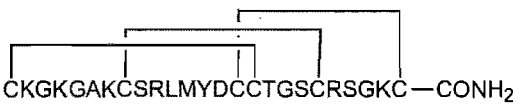

11

The letters in structure **11** refer to the single letter abbreviations commonly used to illustrate the 20 amino acids most frequently found in nature.[25]

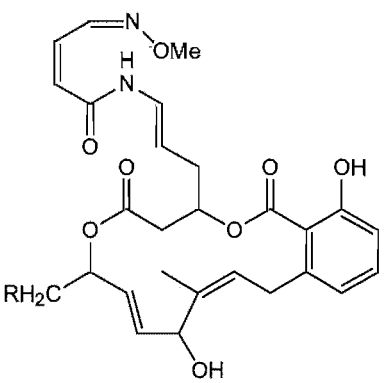

13: R=H
16: R=OH

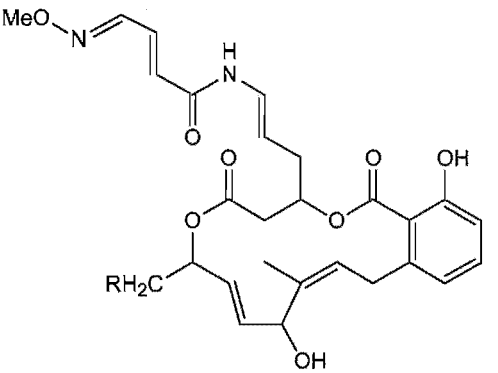

14: R=H
17: R=OH

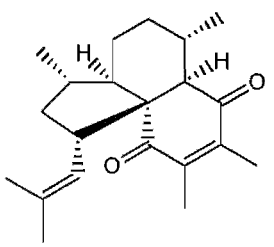

18

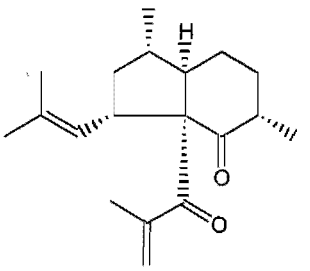

19

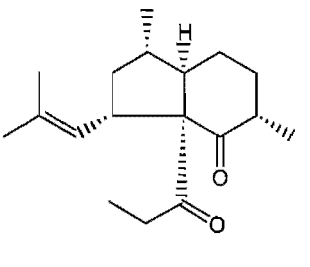

20

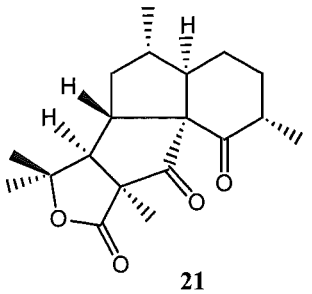

21

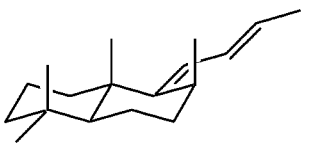

22

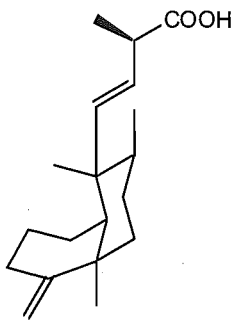

23

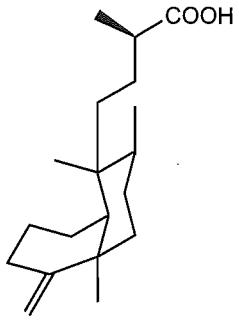

24

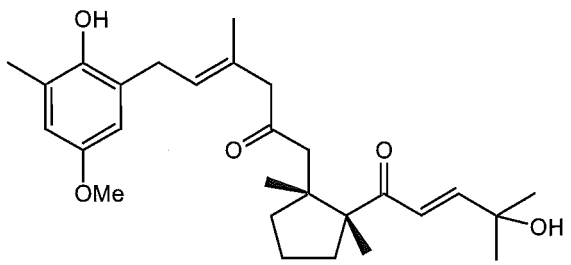

25

Although all these compounds show potent biological activity of some kind, to date only ecteinascidin 743 and ω-conotoxin MVIIA have progressed to clinical trials, with ecteinascidin 743 expected to enter phase III trials in 2002.[26]

Ziconotide (**11**) (ω-conotoxin MVIIA), a peptide toxin isolated from various species of cone snail, is very good at alleviating intractable pain and, unlike regular painkillers such as morphine, is not addictive, and is expected to be approved for use as a painkiller in early 2002.[27]

Even though marine organisms are known to produce some of the most toxic compounds so far discovered,[28] the supply of the metabolite of interest from these organisms is often limited. This led to the hypothesis that some of the biologically active components of marine organisms could actually have been derived from symbiotic micro-organisms. As a result of this, attention has been directed towards both free living and symbiotic marine micro-organisms, both of which have previously shown good potential as a source of novel metabolites.

1.4 Marine micro-organisms – An overview

It has been estimated that over 99 % of symbiotic marine micro-organisms are 'unculturable' with current techniques.[29] Techniques developed to help find the 'unculturable' micro-organisms include 16s rRNA work on microbial polyketide synthases.[30] One major problem associated with isolating microbial symbionts from their hosts, is that there may be metabolite flow between the host and symbiont, and disrupting this flow may cause the production of unusual secondary metabolites to cease unless nutritive media similar to those found in the host organism's cells is used.

One of the first reported cases of production of a natural product by a symbiont was of tetrodotoxin (**26**). This compound, originally isolated from many different organisms, was later found to be produced by a marine bacterium. The paralytic shellfish toxin, saxitoxin (**27**), was found to be produced by dinoflagellates from the genus *Gonyaulax*, and okadaic acid (**28**) originally isolated from the sponge *Halichondria okadai*, has since been found in the dinoflagellate *Prorocentrum lima*.[31]

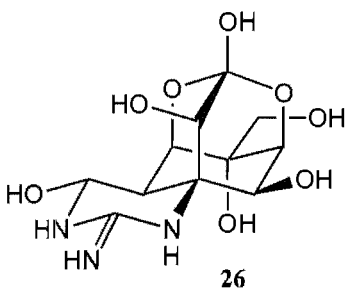

26

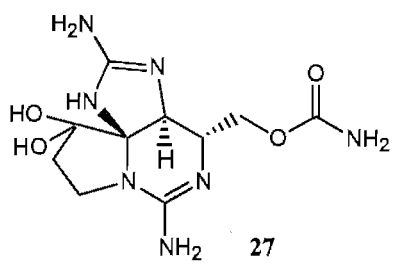

27

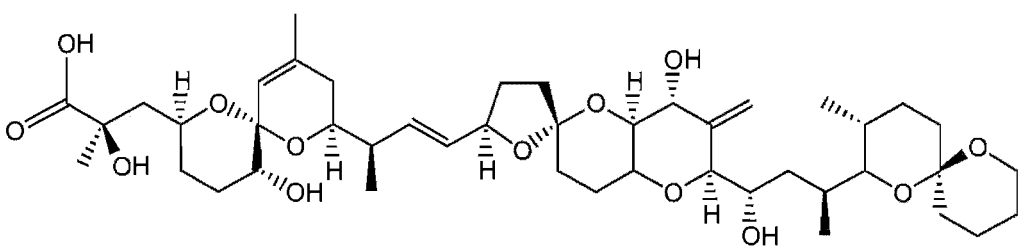

28

Similarities between compounds isolated from terrestrial micro-organisms and some sponge metabolites have also been observed. The sponge *Discodermia dissoluta* produces discodermide (**29**), of which the photodegradation product (**30**) is very similar in structure to alteramide (**31**), produced by a marine *Alteromonas* bacterium, and ikarngamycin (**32**), a metabolite from a species of terrestrial *Streptomycete*.[31]

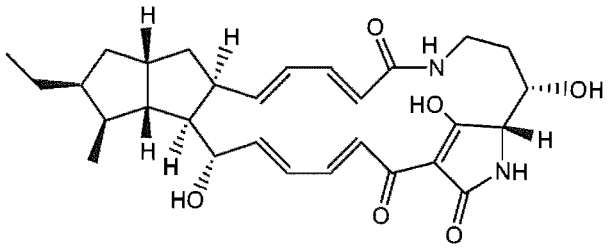

29

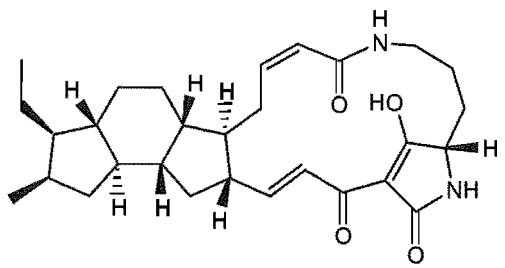

31

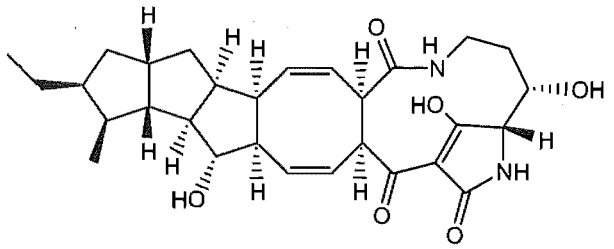

30

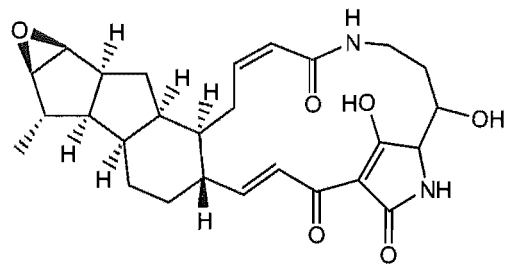

32

1.5 Marine fungi - A brief history

Early investigations into the marine environment found only a few species of marine fungi. Up until the late 18th Century numerous authors had noted the presence of threads or filaments present in marine invertebrates, but none of these structures were considered to be fungal hyphae.[32] This was because seawater was generally considered to be a fungistatic medium. In fact, investigations of fresh seawater found an unknown mycostatic agent present which prevented terrestrial spores from germinating, but not marine spores, and was destroyed during heat sterilisation.[33]

Since the early investigations into the marine environment many marine fungi have been isolated, such as the ascomycete *Sphaeria posidoniae (Halotthia posidoniae).*[34] Up until the mid 1940's only a few marine fungi had been discovered every decade, such as those found by Fischer and Sparrow.[35, 36] In 1944, a paper on marine fungi by Linder and Barghoorn[37] stimulated a great deal of interest in marine fungi resulting in increased numbers of marine fungi being isolated. However, even when fungi were isolated from the marine environment it was observed that most were common species of terrestrial fungi, most being various species of *Penicillium* and *Aspergillus.*[38] Later

reports show that marine fungi are generally distributed across all major mycological genera.[39] This leads to the question "what is a marine fungus?"

1.5.1 What is a marine fungus?

Many different theories have been put forward to explain or classify exactly what is a marine fungus. The definition of marine fungi has been examined from many different perspectives, such as physiological and ecological. Answers to this question range from the suggestion that fungi could not occur in seawater due to a lack of dissolved oxygen,[40] to those that said a true marine fungus grows and sporulates exclusively in the marine environment.[41]

Initial attempts to define marine fungi introduced the term 'thalassiomycetes', meaning 'fungi of the sea'.[42] Thalassiomycetes were defined as fungi of any class isolated from the marine environment, however this did not take into account those fungi that could have been washed into the ocean, via rivers, rainfall or land run-off and simply be existing as hardy, resistant spores until conditions become favourable for growth again. Nor does it account for those fungi originally from a terrestrial environment that have managed to adapt, if only slightly, to the high saline marine environment, and as a result the term thalassiomycete has fallen into disfavour.

In 1960 Ritchie[43] proposed that "...a fungus is considered marine if it is obtained from marine or brackish water and it can grow on media containing 35 ‰ (parts per thousand) of such salts as occur in ocean water." In 1961 this definition was expanded to include those fungi that had been exposed either continually or intermittently to seawater, but were still able to sporulate after exposure.[32] The effect of salinity on fungal growth has been considered by many groups,[44] and it was later found that most terrestrial fungi are much less tolerant of variations in salinity than their marine counterparts.[45] Wood[46] suggested that a requirement for ions present only in seawater may also help to establish if the fungus in question is marine or terrestrial.

Jones argued that repeated isolation of any given fungal species from the marine environment was a good indicator that the fungus was of marine origin.[47] Pugh further suggested that the pattern of physiological behaviour of the fungus in varying concentrations of sea water, such as growth and morphological changes, could also be

used for classification.[48] It was found that marine fungi developed better in seawater media than on media prepared with distilled water[49] and Ravishankar *et al* showed that enzyme activity in the marine fungus *Cirrenalia pygmea* increased with salinities close to that found in natural seawater.[50] Some marine fungi have also been shown to produce a nitrate reductase, a capability not detected in terrestrial fungi.[51]

Further suggestions proposed include that resistance to lysis by marine microflora,[52] or characteristically high moisture requirements,[53] might both be an indicator of obligate marine fungi.

Kohlmeyer and Kohlmeyer[54] considered fungi to be marine if they grew and sporulated in a marine environment, then further divided the marine fungi into two distinct groups, obligate and facultative. Obligate marine fungi were those only found in the marine environment and facultative marine fungi were those found in both terrestrial and marine habitats, but they maintained that a fungus was only marine if the development and reproduction took place in seawater.

By 1979 this definition was modified slightly[55] to take into account Kirk's[56] postulation that restricting the definition of a marine fungus to those that only grow and sporulate in the marine environment would exclude those facultative species that might grow well, but not sporulate in the marine environment. It read as follows, "Obligate marine fungi are those that grow or sporulate exclusively in a marine or estuarine habitat, whereas the facultative marine fungi originate from freshwater or terrestrial environments and are able to grow in saltwater".

At present there are 444 species of marine fungi known, with numerous more species awaiting description.[57] Early estimates put the total number of marine fungi at 6,000 species or more,[55] however the latest estimates have been downscaled to 1,500 species.[56] To date, most of the obligate marine fungi isolated belong to the more evolved groups such as Ascomycotina, whereas filamentous fungi with flagellated spores, ideal for preventing sedimentation in the water column, represent less than 15% of the total strains currently isolated. However, this could be the result of selective searching, specifically looking for the more evolved fungi, such as those that produce macroscopic structures, or by using selective isolation techniques.

1.5.2 Morphology of marine fungi

Many fungi exhibit a distinct morphology having specifically adapted to their environment. Fungi found in the marine environment are typically microscopic, existing as single cells or short hyphal filaments. The fruiting bodies of these fungi are of necessity very small, with the largest of these no more than 4 mm in diameter. Marine fungi do not develop larger fruiting bodies, unlike terrestrial fungi, as they are exposed to constant movement and abrasion by water and suspended particles, like sand. Those fungi that do sporulate in the marine habitat typically only do so in sheltered areas such as cracks in wood, or rocks, or other sheltered areas.[55]

1.5.3 Natural products from marine fungi

Most research on marine micro-organisms has targeted marine bacteria,[58, 59] however recent studies have begun to examine fungi isolated from the marine environment.[60-63] These studies indicate that marine fungi are an excellent source of bioactive secondary metabolites.

Marine fungi represent a large amount of biomass in the marine environment. They typically live on high energy substrates, and contribute significantly to biological turnover. Because marine fungi are in a highly competitive environment and have no physical means of defence, it was theorised that they might produce a plethora of new and potentially useful compounds.[64]

The number of metabolites isolated from marine fungi to date is small in comparison to those from other marine organisms.[16] Compounds isolated from marine fungi are predominantly antimicrobial or cytotoxic, which is not surprising considering most isolation work done on marine fungi is through bioassay guided fractionation. The first compound isolated from a marine fungus was cephalosporin C (**2**),[65] and this is the only compound at this stage that has been used as a pharmaceutical. It was not until about 40 years later that the first novel compound, leptosphaerin (**33**), was isolated from a marine fungus.[66]

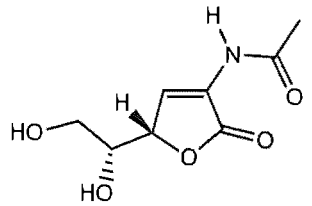

33

Terrestrial bacteria and fungi are the prime sources of bioactive compounds used in medicine today. Similar roles were expected from their marine counterparts, which has since been proved many times.

A strain of *Aspergillus fumigatus*, cultured from the intestinal tract of the saltwater fish *Pseudolabrus japonicus* produced two compounds, fumiquinazolines A (**34**) and B (**35**), with moderate cytotoxic activity against the P388 murine leukaemia cell line.[31]

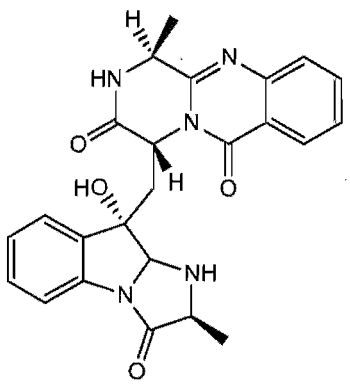

34

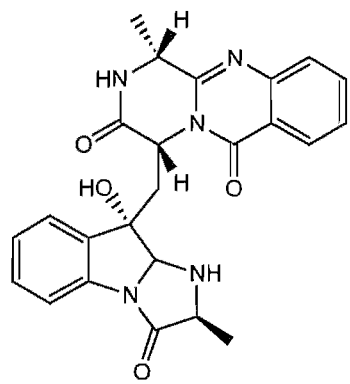

35

An extremely diverse range of compounds have been isolated from fungi cultured from the marine environment. Table 1.4 shows some compounds recently isolated from marine fungi.

Source Organism	*Metabolites Isolated*	*Activity*
Fusarium sp	Halymecin A (**36**)[67] Halymecin B (**37**) Halymecin C (**38**)	Antimicroalgal
Acremonium sp	Halymecin D (**39**)[67] Halymecin E (**40**)	Antimicroalgal
Aspergillus insulicola	Insulicolide A (**41**)[68]	Antitumour
Microascus longirostris	Cathestatin C (**42**)[69]	Cysteine Protease Inhibitor
Kallichroma tethys	Isoculmorin (**43**)[70]	Antitumour
Penicillium sp	NI15501A (**44**)[71]	Antimicrobial
Scytalidium sp	Exumolide A (**45**)[72] Exumolide B (**46**)	Antimicroalgal
Aspergillus niger	Asperazine (**47**)[73]	Cytotoxic
Ascochyta salicorniae	Ascosalipyrrolidinone A (**48**)[74] Ascosalipyrrolidinone B (**49**)	Antimicrobial
Gymnasella dankaliensis	Gymnastatin A (**50**)[75] Gymnastatin B(**51**) Gymnastatin C(**52**)	Cytotoxic
Phomopsis sp	Phomopsidin (**53**)[76] MK8383 (**54**)	Microtubule Assembly Inhibitor
Unidentified fungus	*Iso*-cladospolide B (**55**)[77] *Seco*-patulolide C (**56**) Pandangolide 1 (**57**) Pandangolide 2 (**58**)	Not Tested
Fusarium sp	Neomangicol A (**59**)[78]	Cytotoxic
	Neomangicol B (**60**)	Antibacterial
	Neomangicol C (**61**)	Cytotoxic
Fusarium sp	Sansalvamide (**62**)[79]	Cytotoxic
Trichoderma longibrachiatum	Epoxysorbicillinol (**63**)[80]	Cytotoxic
Aspergillus sp	Aspergillamide A (**64**)[81] Aspergillamide B (**65**)	Cytotoxic
Emericella unguis	Guisinol (**66**)[82]	Antibacterial

Table 1.4: Metabolites recently isolated from marine fungi

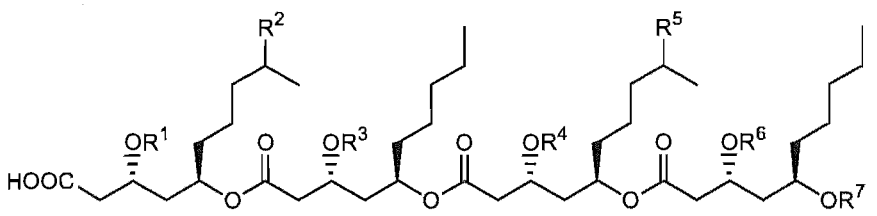

36 R^1=H, R^2=H, R^3=Ac, R^4=H, R^5=H, R^6=H, R^7=H
37 R^1=H, R^2=H, R^3=Ac, R^4=Ac, R^5=H, R^6=Ac, R^7=Ac
39 R^1=H, R^2=OH, R^3=H, R^4=H, R^5=OH, R^6=H, R^7=H

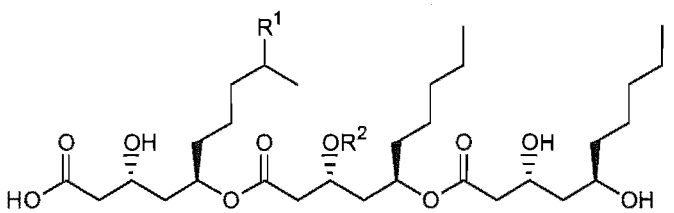

38 R^1=H, R^2=Ac
40 R^1=OH, R^2=H

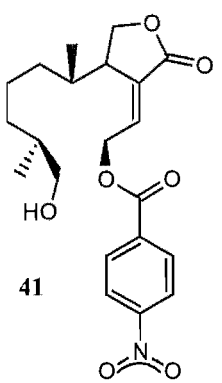

41

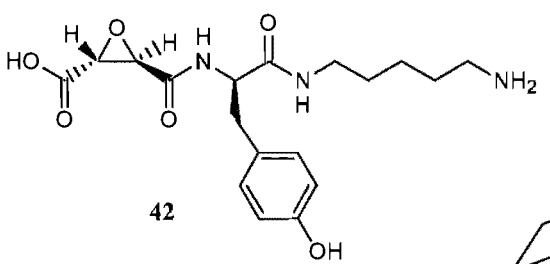

42

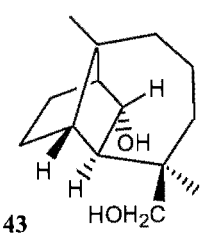

43

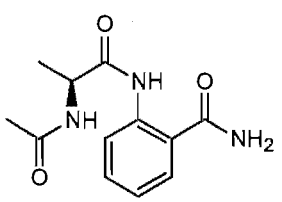

44

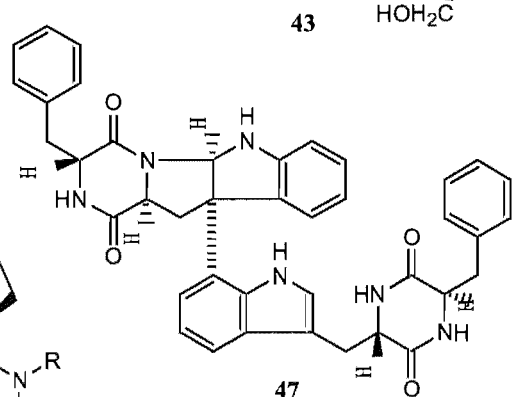

47

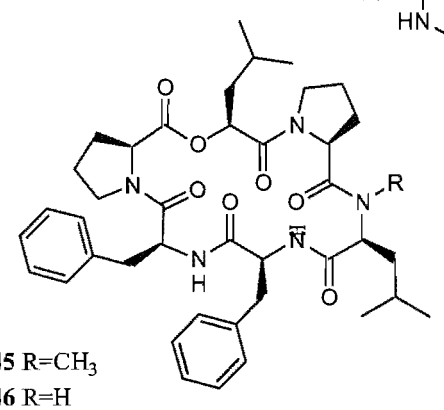

45 R=CH_3
46 R=H

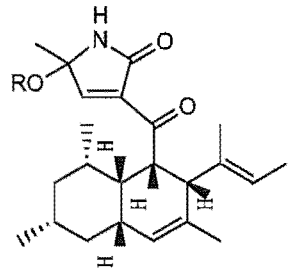

48 R=$CH_2CH_2CH_2CH_3$
49 R=CH_3

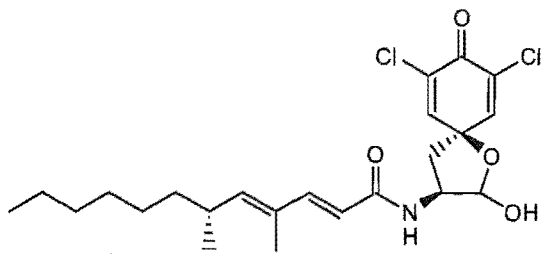

50

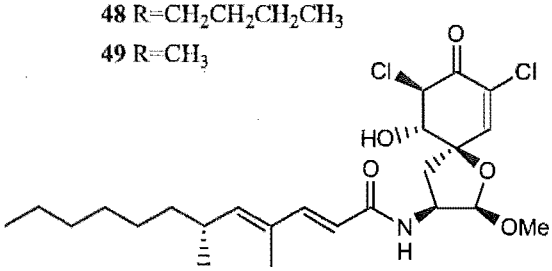

51

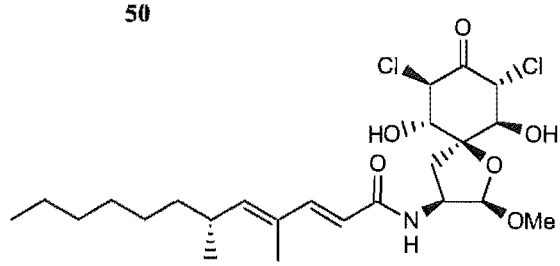

52

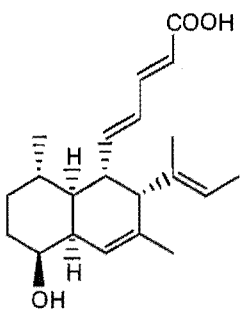

53

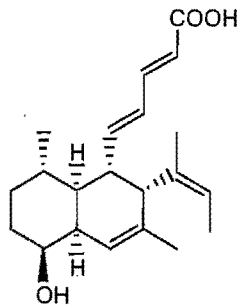

54

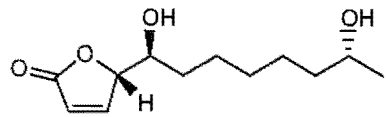

55

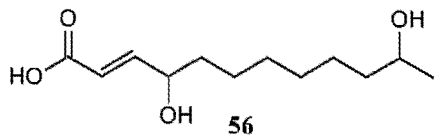

56

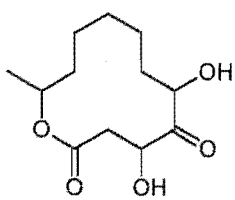

57

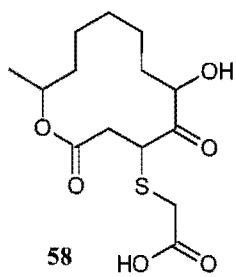

58

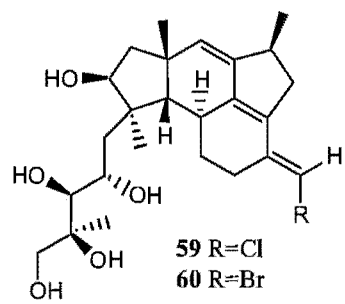

59 R=Cl
60 R=Br

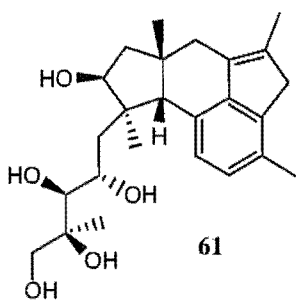

61

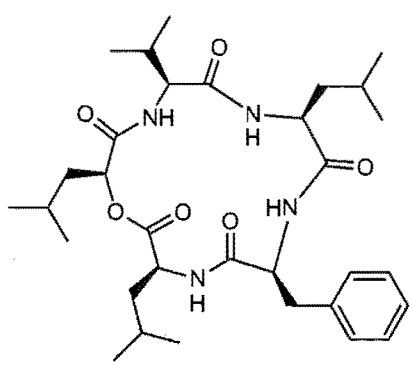

62

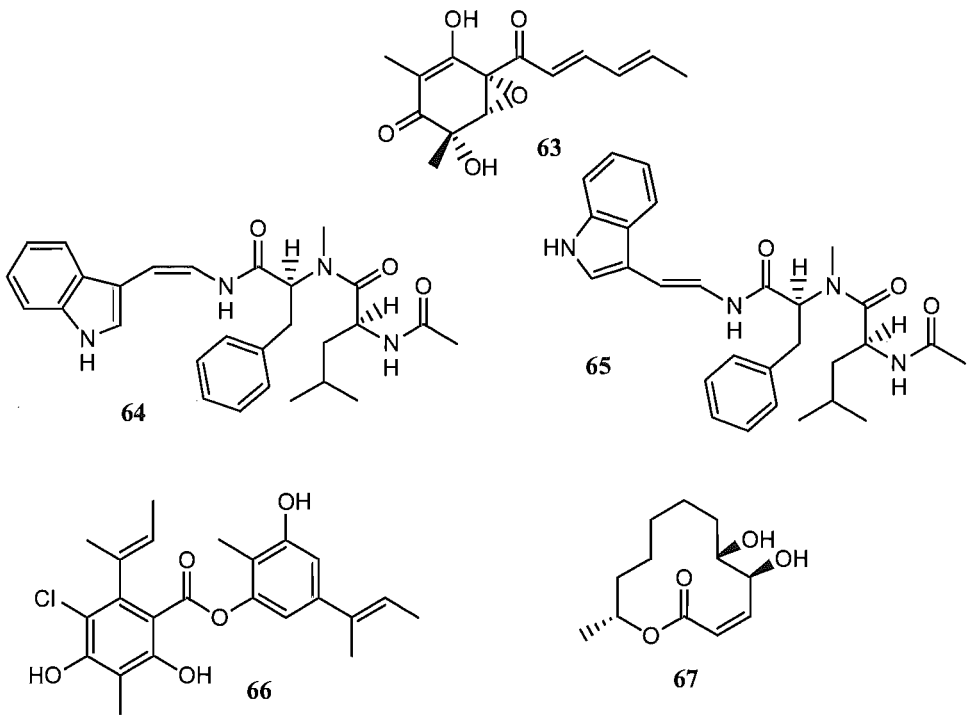

Similarities can be seen between some of these marine metabolites and other metabolites from various terrestrial micro-organisms, such as pandangolide 1 (**57**), isolated from a species of marine fungus, and the known terrestrial metabolite cladospolide B (**67**).[77]

Terrestrial fungi have been shown to produce a wide variety of interesting compounds with an extremely diverse range of bioactivities. Many of these compounds are either in use as pharmaceuticals, have been in use in the past, or were 'lead' compounds for those that are.

Both novel marine compounds and compounds previously isolated from terrestrial fungi have been found in marine fungi,[83] suggesting some similarities between their respective biochemical pathways. Marine fungi are believed to have evolved from terrestrial fungi,[43, 51] however they have evolved in a much more stressful environment which may have led to significant variations in the biochemical pathways, enabling unusual modifications to terrestrial fungal metabolites.

In addition to filamentous fungi a large number of yeasts are found in the marine environment. Even though the number of yeasts isolated is much higher than filamentous fungi the number of novel biologically active compounds isolated from these yeasts is extremely low.

1.6 Aims of this research

Terrestrial organisms have long been a rich source of bioactive metabolites. Organisms from the marine environment have also yielded a number of bioactive metabolites. Even though a large number of bioactive metabolites have been isolated from marine organisms, when compared with those from terrestrial organisms, only a few are close to clinical use. Indeed one of these, Ziconotide (**11**) is expected to be approved for use in 2002.[27] Most of the marine organisms investigated for biological activity are macro-organisms, such as sponges. Until recently little attention had been paid to compounds produced by marine fungi which therefore make the marine fungi an excellent target for chemical investigation.

One of the primary aims of this study was to isolate a number of fungi from marine substrates collected from various sites around the South Island of New Zealand. This involved the isolation, culture and tentative identification of isolates.

Fungi and actinomycetes for chemical characterization would be selected initially on morphology and cultural characteristics, and later on those cultures whose extracts showed cytotoxicity in the microassay (Section 2.3). Once purified the structural elucidation of any components would be undertaken using a variety of spectroscopic techniques such as NMR spectroscopy and mass spectrometry.

CHAPTER TWO

ISOLATION, SCREENING AND DEREPLICATION

2.1 Introduction

There are two main methods for isolating fungi and actinomycetes from the marine environment. The first is through direct examination of marine material for microbial structures and the second is by indirect examination, incubating material in the laboratory. The former method is preferable as it indicates that the micro-organism is active in the marine environment and can therefore be considered marine. The indirect method was used since few microbial structures were observed on any of the marine substrates that were collected at any of the sites investigated.

Microbial cultures were initially selected for chemical examination based on apparent uncommon morphology, but as the number of cultures being isolated increased the feasibility of this method decreased significantly. As a result a small scale culturing system was developed to enable rapid identification of those micro-organisms possessing some cytotoxicity in their extracts (Section 2.3).
A database containing details on the various microbial isolates, including pictures of the individual micro-organisms was also created (Section 2.3.2).

2.2 Origin of macro-algal and driftwood substrates

All micro-organisms investigated in this study were isolated from macro-algae or driftwood. Macro-algal samples were collected from the intertidal zone of several sites on the east coast of the South Island of New Zealand between Kaikoura and Dunedin (Kaikoura, Lyttelton, Taylors Mistake, Moeraki and Macrocarpa Point). Driftwood and the remaining macro-algal samples were collected from a number of locations between Hokitika and Haast on the Westcoast of the South Island of New Zealand, (Hokitika River mouth, Tauronga Bay, Fox River, Punakaiki, Grey River, Cook Beach, Okarito, Ship Creek, Jackson Bay, Waiho River mouth, Okuru Beach, Whakapohai River, Bruce Bay, Hunts Beach, Gillespies Beach and Haast Spit).
All macro-algal samples were stored in seawater at 4°C and plated out within four days of collection. Driftwood samples were stored in sterile plastic bags and examined within seven days of collection.

2.2.1 Taxonomy of macro-algae

Voucher samples of the macro-algae were created to aid in identification. Voucher specimens of the filamentous or thin macro-algae were made by pressing in a plant press as described in Seaweeds of New Zealand.[84]
Thick or woody macro-algae were initially washed with distilled water to remove excess salt and then dried with blotting paper. Once dry the macro-algae were freeze dried then placed in a sealed container with desiccant. After the voucher specimens

were created the macro-algae were identified using Seaweeds of New Zealand as a guide.[84] Any macro-algae for which the identity was ambiguous or unknown were identified by Dr Murray Parsons at Landcare Research, Lincoln, New Zealand.

2.2.2 Classification of micro-organisms

Isolated micro-organisms were classified as terrestrial, facultative marine or obligate marine based on an arbitrary system dependent on their growth on two media. The first medium was prepared with seawater and the second prepared with distilled water. A precise designation of obligate marine fungi is difficult to give, but for the purpose of this research those that grew exclusively on seawater media were considered obligate. Those growing preferentially in seawater media, but also in distilled water media were considered facultative and those growing preferentially on distilled water media were considered terrestrial.

Approximately 1400 microbial strains were isolated which included 167 obligate marine, 591 facultative marine and 241 terrestrial micro-organisms, most of which were filamentous fungi. A further 401 isolates with no obvious preference for seawater or freshwater media were also isolated. Of the total microbial strains isolated about 50 % showed morphologies similar to each other which indicated repeat isolations of the same micro-organisms.

2.2.3 Database

Each micro-organism was given a unique identification number. This number consisted of a three letter acronym derived from the name of the collection site (e.g. Fox - Fox River), a number for the substrate (1-50) followed by a number for the collection from that site (1-3) and finally a number for the microbial culture isolated from the particular substrate. An extensive interactive database was constructed using Microsoft® Access and lists details about the micro-organisms isolated in the first round of collections. Together with details about growth rate and fungal type the database also contains

photographs showing the crude colony characteristics of each fungal isolate. This database is searchable and able to be easily updated (see include compact disc).

2.3 Microassay screening

Since the number of micro-organisms isolated was extremely high a rapid, miniaturised method for assessment of biological activity was developed. To this end micro-organisms were cultured in 1 mL of appropriate broth in 24-well microtitre plates. Incubation time was arbitrarily determined based on the growth rate of the microbes on solid agar plates as shown in Table 2.1.

Growth rate on agar	*Incubation time*
4 cm / week	14 days
3 cm / week	17 days
2 cm / week	21 days
1 cm / week	24 days
0.5 cm / week	30 days
< 0.5 cm / week	40 days

Table 2.1: Micro-organism growth rate vs. microassay incubation time.

After the appropriate incubation period had elapsed the cultures were homogenized with an Ultra-Turrax® (Janke & Kunkle) *in situ* and extracted overnight with an equal volume of EtOAc. The resulting EtOAc extract was then assayed for cytotoxicity with a single point assay against the P388 murine leukemia cancer cell line. Table 2.2 shows microbial extracts displaying significant cytotoxicity in this assay.
This method may not detect all potentially cytotoxic micro-organisms, but did provide valuable insights as to which micro-organisms should be further investigated.

2.3.1 Results

Of the approximately 800 isolates examined in the microassay almost ten percent (75 isolates) showed significant cytotoxicity against the P388 cell line (> 90 % cell

inhibition compared to the cell control). A further twenty percent showed mild cytotoxicity with > 50 % cell inhibition.

Microbial isolate	Cell inhibition (% of control)	Microbial isolate	Cell inhibition (% of control)	Microbial isolate	Cell inhibition (% of control)
Bru 1-1-2	89.3	Fox 18-2-19	95.8	Kai 25-2-1	88.9
Bru 11-1-2	95.2	Fox 22-2-3	100	Kai 32-2-1	95.9
Coo 1-1-3	94.4	Fox 23-2-4	88.1	Kai 33-2-1	95.6
Coo 6-1-1	95.1	Fox 23-2-6	100	Kai 38-2-5	100
Fox 2-2-8	100	Fox 27-2-16	94.7	Kai 41-2-1	94.5
Fox 4-2-10	100	Fox 29-2-1	95.2	Kai 41-2-3	100
Fox 4-2-13	94.5	Fox 29-2-5	94.8	Kai 51-2-1	100
Fox 4-2-14	88.1	Fox 29-2-7	100	Kai 51-2-2	100
Fox 4-2-15	94.8	Fox 34-3-34	100	Kai 58-2-1	100
Fox 4-2-21	96.8	Fox 35-2-5	91.6	Kai 58-2-2	97.2
Fox 4-2-23	95.5	Fox 37-2-2	100	Kai 65-2-1	100
Fox 4-2-37	94.3	Fox 38-2-13	95.9	Kai 65-2-3	100
Fox 4-2-37	97.2	Fox 38-2-16	97.2	Kai 65-2-5	98.3
Fox 4-2-6	92.4	Fox 39-2-2	96.9	Moe 2-2-1	93.4
Fox 6-2-21	95.3	Hok 9-1-2	92.2	Mpt 8-2-4	91.2
Fox 8-2-18	100	Kai 18-1-2c	95.2	Mpt 16-2-2	97.5
Fox 9-2-14	97.2	Kai 1-2-3	95.8	Mpt 71-2-12	94.6
Fox 13-2-10	97.7	Kai 2-2-3	100	Mpt 73-2-5	95.9
Fox 13-2-6	95.8	Kai 4-2-1	95.8	Mpt 80-2-1	98.3
Fox 15-2-11	97.5	Kai 5-2-2	89.6	Tay 1-3-2	97.5
Fox 15-2-11	94.8	Kai 5-2-3	97.0	Tay 1-3-3	98.9
Fox 15-2-2	94.8	Kai 6-2-2	96.4	Tay 8-3-3	99.1
Fox 16-2-10	96.4	Kai 6-2-4	100	Tay 9-3-2	98.0
Fox 16-2-11	100	Kai 11-2-1	92.9	Tay 18-3-2	98.2
Fox 17-2-4	100	Kai 18-2-1	99.7	Wai 7-1-1	96.4

Table 2.2: % Cell inhibition for microbial isolates showing cytotoxicity in the microassay.

Key for Table 2.2.

Abbreviation	Location	Abbreviation	Location
Bru	Bruce Bay	Mpt	Macrocarpa Point
Coo	Cook Beach	Moe	Moeraki
Fox	Fox River	Tay	Taylors Mistake
Hok	Hokitika River	Wai	Waiho River
Kai	Kaikoura		

2.4 Dereplication

Even though marine derived fungi have not been examined as extensively for biologically active compounds as terrestrial fungi there was a strong likelihood that at least some of the metabolites produced by the micro-organisms isolated in this study would already be known. To limit the amount of time spent isolating metabolites that were already known, all bioactive small scale extracts were subjected to a dereplication step prior to culturing on a larger scale.

The dereplication procedure involved partially purifying a small scale crude extract (typically < 50 mg) with solid phase extraction enabling the polarity, charge and approximate size of the bioactive component(s) to be determined.

A MeOH solution (50mg/mL) was prepared and an aliquot (200 µL) loaded onto a C_{18} cartridge followed by 200 µL H_2O. Three fractions were collected using a stepped gradient system of 1:1 MeOH/H_2O, MeOH and 1:1 MeOH/DCM. A second aliquot (200 µL) was loaded onto a CBA cartridge. Three fractions were also collected from this cartridge using a gradient system of 3:2 MeOH/0.05M CH_3CONH_2, 3:2 MeOH/2% NH_3 and 4:1 MeOH/0.05% TFA. A third aliquot (200 µL) was loaded onto LH20 (1.5 g) and eluted with MeOH. Depending on the sample under examination four to six fractions were collected (3.3 mL, 1 mL, 4 mL and 4 mL).

Active fractions from the solid phase extractions were then examined further by reverse phase C18 analytical HPLC. The eluant from the HPLC was collected in 96 well microtitre plates and the region of cytotoxicity determined by P388 assay (Section 8.1.6). The region of cytotoxicity can be directly related back to the analytical HPLC trace thereby highlighting the bioactive peak and enabling the UV chromophore to be determined. Potential molecular ions for the cytotoxic compounds can also be obtained by examining wells in the 'master' microtitre plate which corresponded to the region of cytotoxicity with ESI-MS. This procedure generally provides enough information to search available databases. If either a large number of matches or no matches were found the microbial isolate was cultured on a much larger scale and the cytotoxic compound determined. Whereas if only one or two matches were found no further work was performed, unless other discrepancies were noted.

To this end a number of small scale extracts were not investigated further due to the presence of various known compounds, such as mycophenolic acid (7), penicillic acid (**68**) and patulin (**69**) to name but a few.

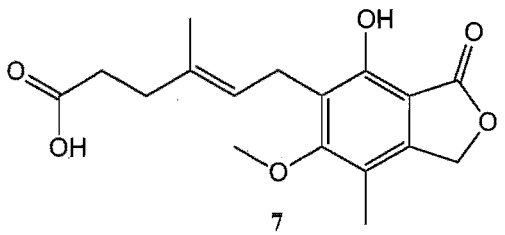

7

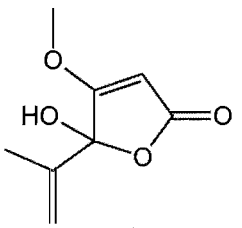

68

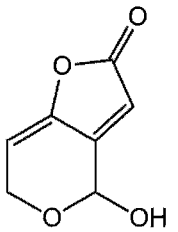

69

A good example of the dereplication procedure can be seen with cephalochromin (**119**) in Chapter 4. The initial chemical screen and subsequent HPLC microtitre plates (Figure 4.3) clearly showed which peak in the HPLC trace was responsible for the observed cytotoxicity. This peak also displayed a very distinctive UV chromophore (Figure 4.4). A mass of 519 Da (MH^+) was obtained from the mass spectrum of compounds in the bioactive wells and a search in the Berdy Natural Products Database (BNPD) on the molecular mass and UV chromophore found two compounds with identical masses and UV chromophores which were atropisomers of each other.

2.5 Discussion

The large number of micro-organisms isolated from marine substrates in this study suggests that the marine environment is a prolific source of micro-organisms. The number of microbes isolated however, does not distinguish between those actively growing in the marine environment or those that were present as resistant spores waiting for conditions to become conducive for germination. The simple classification system used (Section 2.2.2) to distinguish obligate marine micro-organisms from the rest provided an indication of those micro-organisms which were possibly active in the marine environment. However, without further studies into their growth requirements these micro-organisms might still have arisen from resistant spores.

Approximately ten percent of the organisms screened in the microassay displayed significant cytotoxicity with a further twenty percent showing slight cytotoxicity. Time

constraints prevented an in depth investigation of most of the microbial isolates possessing cytotoxicity in the microassay. Furthermore, the microbial extracts produced for the microassay were tested for cytotoxicity only and it could be that the non-cytotoxic extracts possessed other forms of biological activity such as antimicrobial or antiviral activities. The mass of extract produced in the microassay however, was so low that the other biological activities were unable to be determined.

As can be seen in the following chapters the marine derived micro-organisms are capable of yielding both novel and known compounds. Thus marine derived micro-organisms could be capable of producing a plethora of potentially useful bioactive compounds.

CHAPTER THREE

OKA 2-1-1 ~ *FUSARIUM* SP

3.1 Introduction

Broth extracts from Oka 2-1-1, a *Fusarium* sp isolated from driftwood collected from Okarito Lagoon, showed significant cytotoxicity towards the P388 cell line (941 ng/mL). This fungal isolate was targeted for further chemical investigation because it produced unusual orange nodules when grown on agar plates. Preliminary investigations (Section 3.2.1) of the crude extract showed that the antitumour activity was centred on a series of small peaks in a moderately complex HPLC chromatogram (Figure 3.2). Two pale yellow compounds with excellent cytotoxicity against the P388 cell line (**104**, 23 ng/mL and **109**, 99 ng/mL) were isolated and purified from culture extracts. The chromatography of these compounds is discussed in Section 3.3 and the structural elucidation described in Sections 3.4 and 3.5 of this chapter.

3.1.1 Importance of *Fusarium* toxins

The genus *Fusarium* is extremely important as various members of this genus are responsible for considerable crop losses worldwide either through infection of host plants or, contamination of badly stored grains. Even if fungal contamination is not observed, mycotoxins may still be present and can enter the food chain through feedstuffs.

Fusarium mycotoxins have been shown to be the causative agent of many diseases in both humans and animals.[85] In the late 1970's horses in the United States suffered from a sickness called equine leukoencephalomalacia, thought to be caused by the fumonisin toxins from *Fusarium moniliforme* J. Sheld.[86] Since the early 19th century thousands of people have suffered from the potentially fatal syndrome, alimentary toxic aleukia (ATA), caused by ingestion of trichothecene metabolites from *Fusarium* contaminated grain.[87]

Most of the major biosynthetic classes from isoprenoids to polyketides and peptide derivatives, as well as numerous mixed class compounds have representatives amongst the *Fusarium* mycotoxins. The most toxic *Fusarium* metabolites include the trichothecenes, zearalenone, the fumonisins, the fusarins and the cyclic enniatins.[88]

3.1.2 Toxins from *Fusarium*

3.1.2.1 Polyketides

A great variety of polyketide derivatives have been isolated from a vast array of *Fusarium* spp, including zearalenone (**70**), moniliformin (**71**), chlamydosporol[89] (**72**), various fumonisins, such as fumonisin B1 (**73**) and some fusarins (**74**).

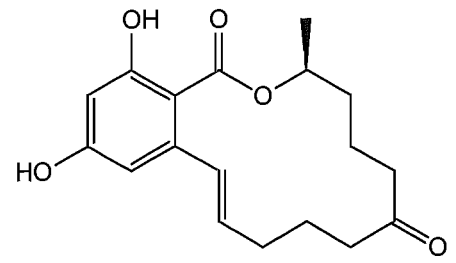

70

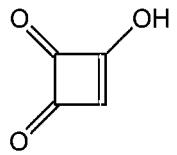

71

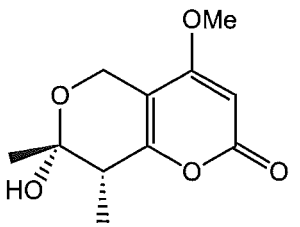

72

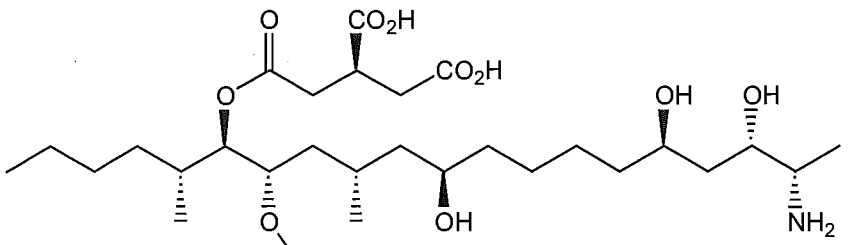

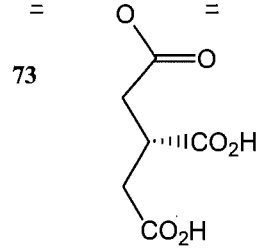

73

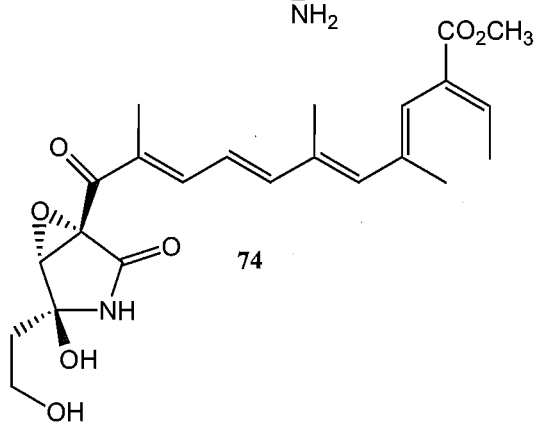

74

Polyketide secondary metabolites in *Fusarium* are not as common as the trichodienoids, but are responsible for a number of toxic effects.

Zearalenone

Zearalenone (**70**) is a member of a small group of compounds known as the undecyl resorcylic acid derivatives, which include radicicol (**75**) from *Monosporium bonorden*[90] and *Nectria radicicola*,[91] and hypothemycin (**76**) from *Hypomyces trichothecoides*.[92] The structural similarities seen between radicicol and zearalenone are not completely unexpected as many *Fusarium* spp are anamorphs of *Nectria* spp.

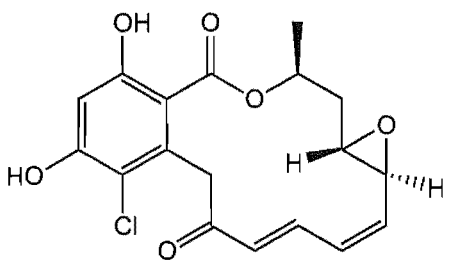

75

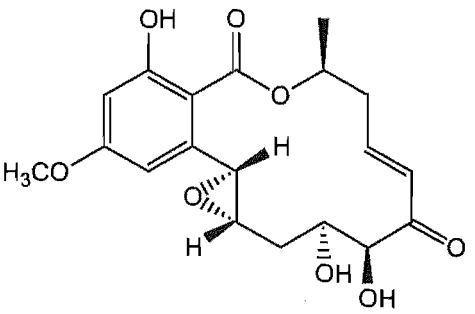

76

Zearalenone is produced by a number of different *Fusarium* spp and displays an oestrogenic effect on animals.[93] This compound is not generally considered toxic as oral doses in excess of 10 g/kg were non-lethal in mice and rats.[94] However, the oestrogenic effect of zearalenone in young animals can cause harmful physiological changes.[85] The naturally occurring hydroxy derivative of zearalenone, α-zearalenol (77) is ten times more active than zearalenone. Since many zearalenone reductases have been found in animal tissue α-zearalenol is thought to be the active form of zearalenone.[85]

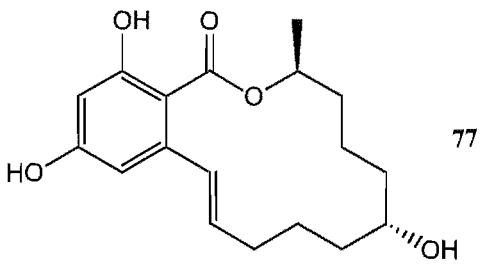

77

Although zearalenone itself is non-lethal it is generally an indicator that other more toxic compounds from *Fusarium* spp are present such as trichothecenes.[93] Along with oestrogenic effects, zearalenone has also been shown to be highly phytotoxic at low concentrations ranging from 10^{-5} - 10^{-6} M.[95]

Moniliformin

Moniliformin (71) was originally isolated from *Fusarium moniliforme*[96] and displayed significant biological activity towards animals and plants.[97] Even though the structure of moniliformin was very simple its biosynthetic origins were not immediately apparent. Several different biosynthetic pathways were proposed to explain the production of

moniliformin and ^{13}C labeling experiments showed that it was formed via the condensation of two acetate units.[98]

Fumonisins

The fumonisins were originally discovered from an isolate of *Fusarium moniliforme* implicated in many horse deaths from equine leukoencephalomalacia,[99] a disease causing extensive degeneration of brain tissue.[100] Three types of fumonisin have been isolated, A, B and C. The A type (**78**) differs from the B type (**79**) by acylation of the secondary amino group attached at C^2, while the C type (**80**) lacks the C^1 methyl group.[101] The A and B type fumonisins have only been isolated from *F. moniliforme* and *F. proliferatum*, with the C type fumonisins only isolated from *F. oxysporum*.[102]

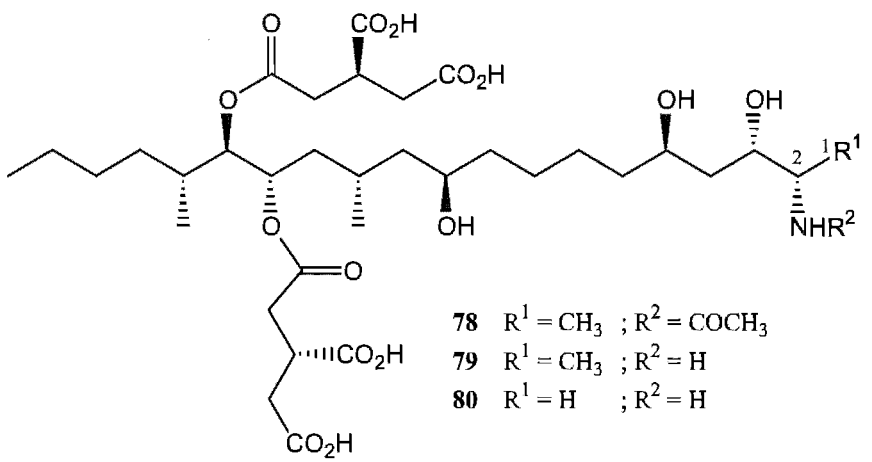

78 $R^1 = CH_3$; $R^2 = COCH_3$
79 $R^1 = CH_3$; $R^2 = H$
80 $R^1 = H$; $R^2 = H$

Similar structural features are seen between the fumonisins and sphingosine (**81**), a sphingolipid found in the cell membranes of brain and nerve tissue and implicated in cell-cell interactions. This similarity could explain the extensive degeneration of brain tissue seen in horses affected by fumonisin toxins.[103]

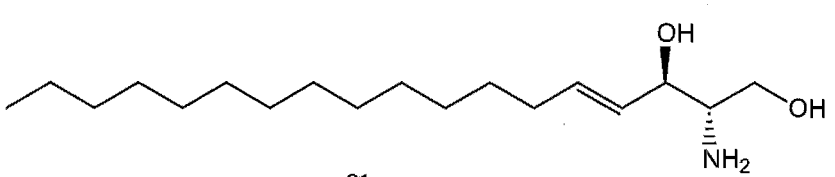

81

Fusarins

Five fusarins are currently known (A, C, D,[104] E and F[105]) as well as various isomers.[102] Of these compounds only fusarin C (**74**) was shown to possess any biological activity and was highly mutagenic in the Ames test against *Salmonella*.[106] The fact that none of the other fusarins show biological activity indicates that the epoxide / lactam ring system is essential for this activity as no other fusarins contain this lactam system.

3.1.2.2 Amino acid derivatives

Enniatins

The enniatins (**82**) are cyclic depsipeptides comprised of three α-hydroxy acids and three amino acids. The three α-hydroxy acids are always α-hydroxy isovaleric acid and the amino acids are either of *N*-methyl-isoleucine, *N*-methyl-leucine, *N*-methyl-valine or valine.[103] They were initially investigated because of their anti-microbial activity, but they have since shown to be slightly phytotoxic[107] and to possess insecticidal properties against adult blowflies and mosquito larvae.[108]

82

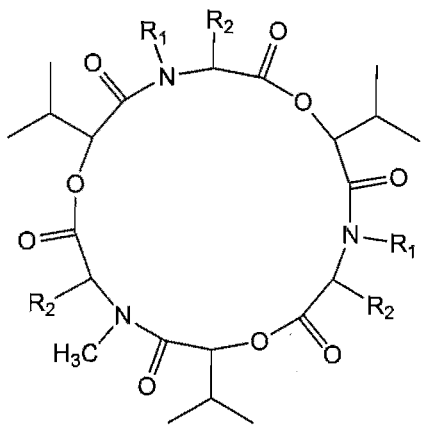

R_1 = H or CH_3

R_2 = 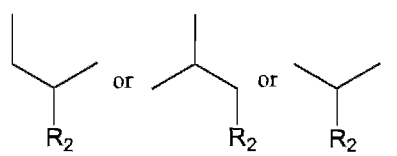

The enniatins have been shown to fuse with cell walls, interfering with the functioning of Na^+ pumps resulting in a disruption of the ionic balances within the affected cells and causing swelling and subsequent rupture.[103] The more active enniatins are those containing *N*-methyl groups, as these would greatly increase the lipophilicity of the enniatins, enabling better cell wall interactions.[100]

3.1.2.3 Isoprenoids

The greatest variety of *Fusarium* mycotoxins arise from a common precursor, trichodiene (**83**), derived from the common metabolite, farnesol (**84**). The trichodiene precursor can subsequently be modified into one of five structural classes, sambucinic acid (**85**), sambucoin (**86**), the trichothecenes (**87**), sambucinol (**88**) and the apotrichothecenes (**89**). To date all of the known trichodienoids are derived from one of these five skeletons.[100]

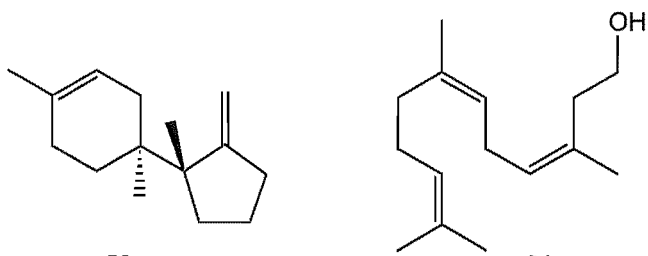

83

84

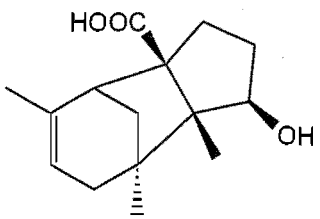

85

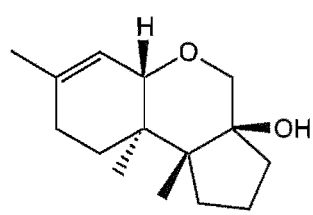

86

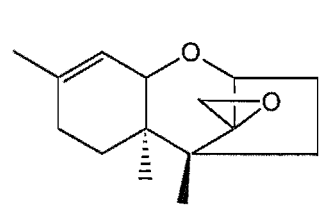

87

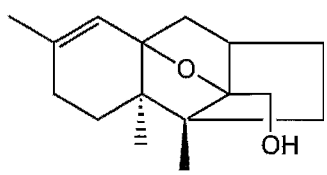

88

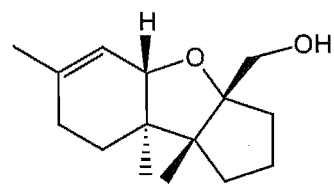

89

After the initial rearrangement of trichodiene to one the five structural classes (**85-89**), a great many more rearrangements and oxidations may occur within the molecule which can give rise to highly oxygenated compounds such as gramilaurone (**90**).[109]

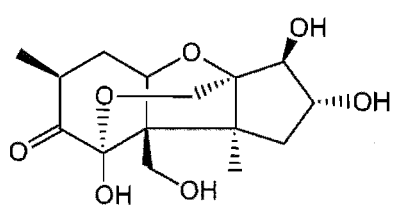

90

The trichodiene derivatives are not the only sesquiterpenes isolated from *Fusarium* spp. Other sesquiterpenes have also been isolated such as the tricyclic culmorins (**91**)[86] and the cyclonerols, such as cyclonerodiol (**92**).[100] Like trichodiene, the culmorins are also derived from farnesol. However, the cyclisation pattern is slightly different, whereas the cyclonerols are derived from nerolidol (**93**).

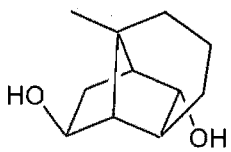

91

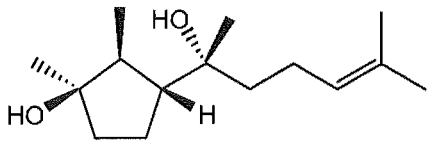

92

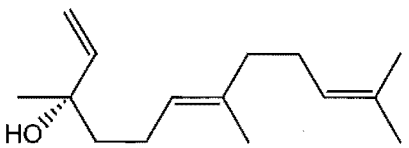

93

Trichothecenes

The trichothecenes are produced by members of a number of fungal genera including *Acremonium*, *Myrothecium*, *Stachybotrys* and *Trichoderma*. However, the largest variety of trichothecenes are produced by *Fusarium*. The trichothecenes have been divided into 4 classes, A-D, based on modifications made to the carbon skeleton common to all trichothecenes (Figure 3.1).

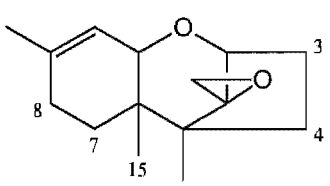

Figure 3.1: Carbon skeleton common to the trichothecenes

In type A trichothecenes, positions 3, 4, 7, 8 and 15 can be substituted with hydroxyl groups which may in turn be esterified. Type B trichothecenes show the same substitution as type A but position 8 is always a carbonyl group. Type C contains a

second epoxide group between positions 7 and 8, and in type D positions 4 and 15 are linked by a series of ester groups.[85] Only type A and B have been isolated from *Fusarium*. Trichothecenes are well known inhibitors of protein synthesis in mammalian cells,[110] have been shown to be immunotoxic[111] and have been responsible for, or implicated in many diseases such as alimentary toxic aleukia, through ingestion of contaminated grain.[112]

Even though a vast array of mycotoxins are produced by various *Fusarium* spp when cultured in the laboratory, there is little evidence to suggest that most of these compounds are produced in the environment from which the fungi are originally isolated.[93] In the case of the trichothecenes where over 150 different variations are known,[102] only five have been regularly isolated directly from the source of the contamination.[88, 97] These five trichothecenes are T-2 toxin (**94**), diacetoxyscirpenol (**95**), nivalenol (**96**), deoxynivalenol (**97**), and neosolaniol (**98**).[113]

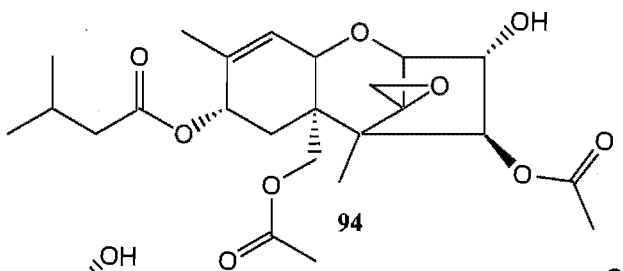

94

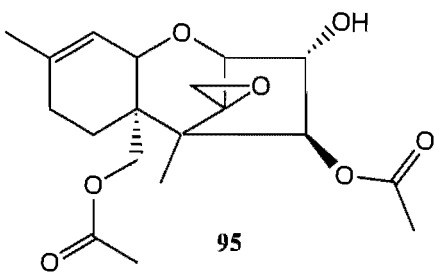

95

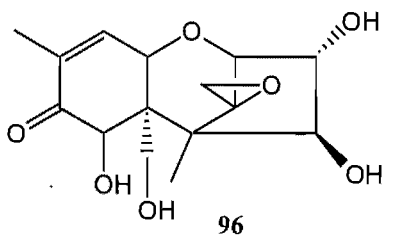

96

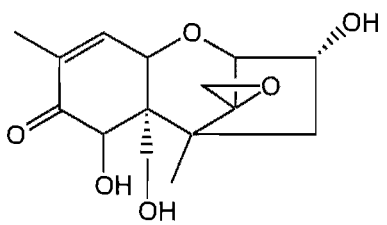

97

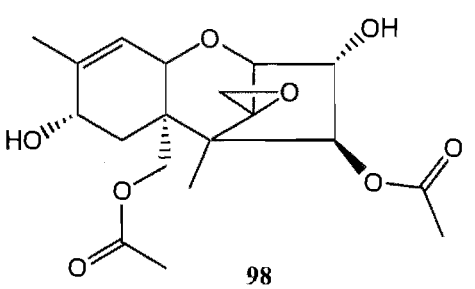

98

3.1.3 Toxins from marine derived *Fusarium* spp

To date no obligate marine *Fusarium* spp have been described,[57] although a few *Fusarium* spp have been isolated from the marine environment in the past.[32] The first novel metabolites reported from a marine derived *Fusarium* were the neomangicols (**59-61**)[78] followed closely by the mangicols (**99**),[114] sansalvamide (**62**)[79] and *N*-methylsansalvamide (**100**).[115]

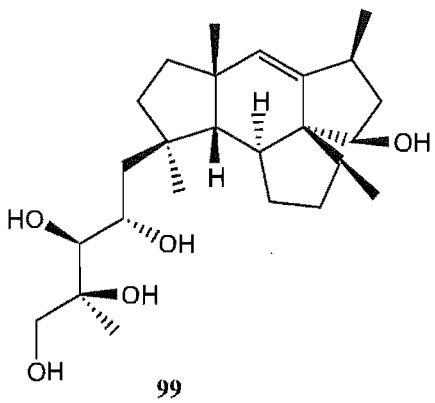

99

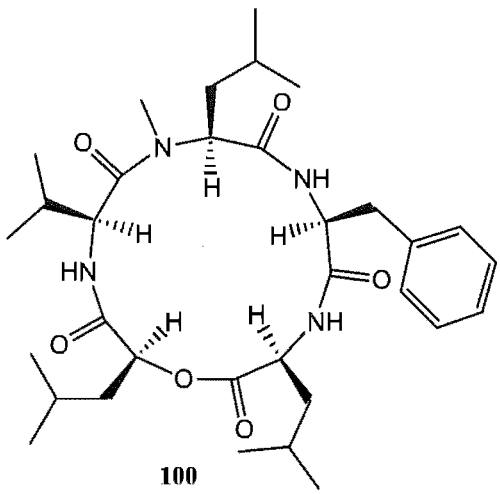

100

Recently, three new macrocyclic trichothecenes (**101-103**) were isolated from a *Fusarium* spp derived from a marine sponge, *Dictyoceratide* sp.[116] This was the first report of any trichothecene metabolite from a marine derived fungus.

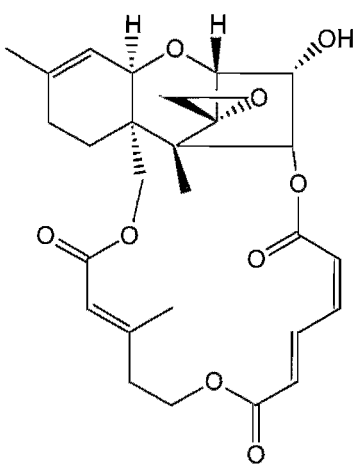

101

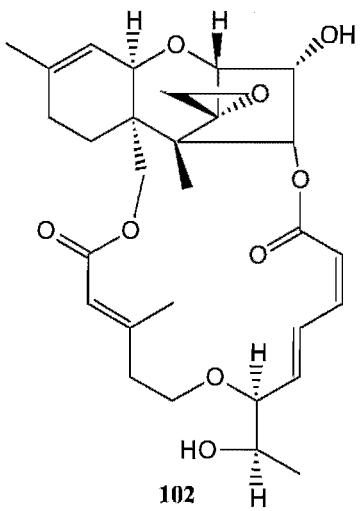

102

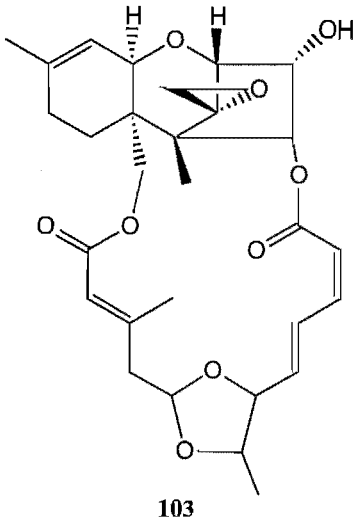

103

Until the discovery of these three macrocyclic trichothecenes no common *Fusarium* metabolites had been isolated from marine derived fungi, with the exception of isoculmorin (**43**) from the marine fungus *Kallichroma tethys*.[70]

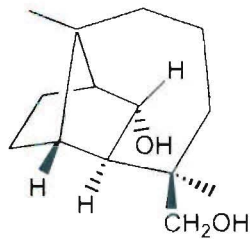

43

3.2 Culturing and extraction of Oka 2-1-1

3.2.1 Preliminary investigations

The fungal culture Oka 2-1-1, a *Fusarium* spp, was isolated from driftwood collected at the low tide zone of Okarito Lagoon on the West Coast of the South Island of New Zealand in February 1999. This isolate produced some unusual orange nodules which slowly turned brown on solid media (Figure 3.2) and as such was examined for biological activity. The fungus was cultured in 250 mL PDB broth in the dark at 26°C for one month. Extraction of this broth culture with EtOAc and subsequent concentration under vacuum yielded a light purple solid with significant cytotoxicity (941 ng/mL).

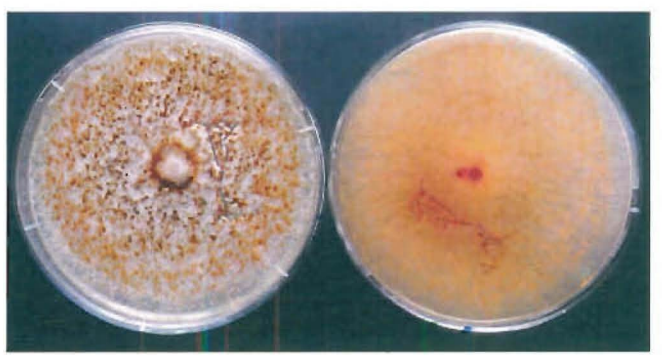

Figure 3.2: Fungal isolate Oka 2-1-1 (*Fusarium* sp) grown on a PDA plate.

3.2.1.1 Chemical screening

The initial extract of Oka 2-1-1 was examined with a technique known as "chemical screening", whereby a MeOH solution (50 mg/mL) is prepared and aliquots chromatographed on C_{18}, LH20 and CBA cartridges (Section 2.4).

Chromatography on C_{18} concentrated the cytotoxicity in the MeOH fraction, with less activity seen in the preceding methanol-water fraction and no activity in the DCM fraction, indicating that the cytotoxic compounds were of medium polarity. Significant cytotoxicity was observed in the first fraction eluted from the CBA cartridge, and from the last fraction from the LH20 cartridge. This indicated that the compound(s) responsible for bioactivity were uncharged and with a molecular weight less than 500 Da.

3.2.1.2 HPLC microtitre plate screening

To determine the peak responsible for bioactivity an aliquot of the crude extract was chromatographed on reverse phase C_{18} HPLC, with fractions collected into a 96 well microtitre plate. The microtitre plate was then assayed for cytotoxicity against the P388 cell line. The major region of bioactivity in this extract was centred on 3 small peaks in the HPLC chromatogram, eluting at approximately 13.5 minutes (Figure 3.3), with a minor region of bioactivity eluting approximately 2 minutes earlier. The weak cytotoxicity seen eluting at 11.5 minutes was initially assumed to be a single point variation in the biological assay, but subsequent purification of a large scale extract showed that the cytotoxicity was due to the presence of another bioactive compound. The UV-visible spectrum of these peaks displayed only end absorbance at 190 nm.

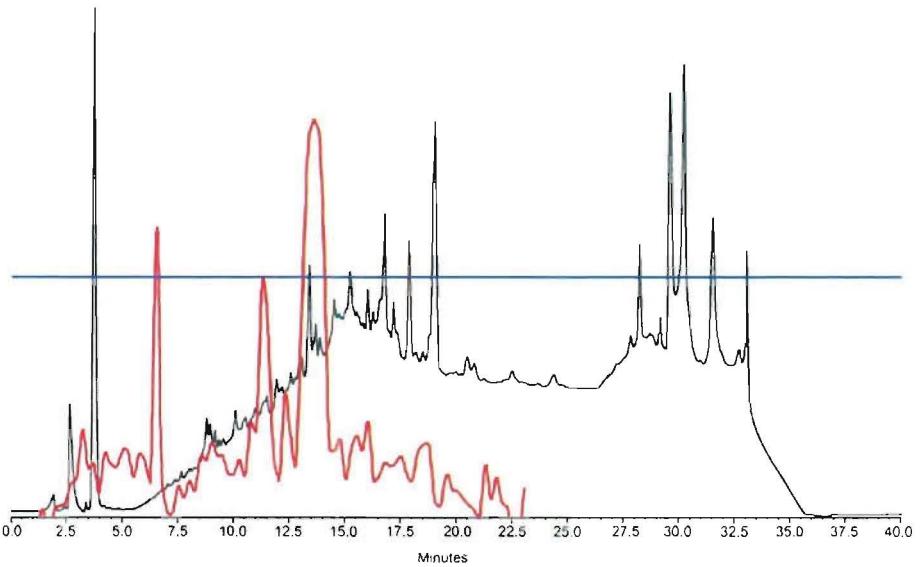

Figure 3.3: Spectrum max plot[1] HPLC trace (black) and bioactivity data (red) of Oka 2-1-1 extract showing region of biological activity (the blue line represents 50% cell death).

The lack of a distinct chromophore for these compounds hindered determination of the class of compounds responsible for the biological activity. ESI-MS of the bioactive wells from the microtitre plate provided no information regarding possible parent ions of the compound as the peaks observed varied significantly between adjacent wells. A search on the UV maximum and the physical properties (approximate size, polarity and charge) in available databases found over 100 possible matches. Because it was impossible to narrow the search parameters further, this extract was purified to obtain the bioactive compounds. During the preliminary investigations (Section 3.2.1) it was observed that the biological activity of this extract was concentrated into the second fraction from the C_{18} cartridge whilst most of the mass was retained until the third. It was therefore decided to use reverse phase C_{18} for the initial chromatographic step.

3.2.2 Large scale culturing and extraction

Very little mass was left from the small scale extract after chemical screening, therefore Oka 2-1-1 was cultured in a further 4 L of half strength PDB under the same conditions

[1] A spectrum max plot is a chromatogram with each point plotted at its maximum absorbance over a given wavelength range and combined into a single HPLC trace. The plot indicates what the chromatogram would look like when the wavelengths are optimized for each peak. The spectrum max plots of the HPLC traces depicted in this work were calculated over the wavelength range 190 - 600 nm.

as described in Section 3.2.1. Repeated extraction of this culture with distilled EtOAc, followed by solvent removal under vacuum yielded a deep purple oily solid (405.1 mg) with an HPLC and bioactive profile almost identical to that of the small scale extract (Figure 3.3).

3.3 Chromatography

The chromatographic steps for the large scale extract of Oka 2-1-1 are shown in Scheme 3.1. A more detailed description of the chromatographic steps carried out on this extract can be found in the Experimental Section.

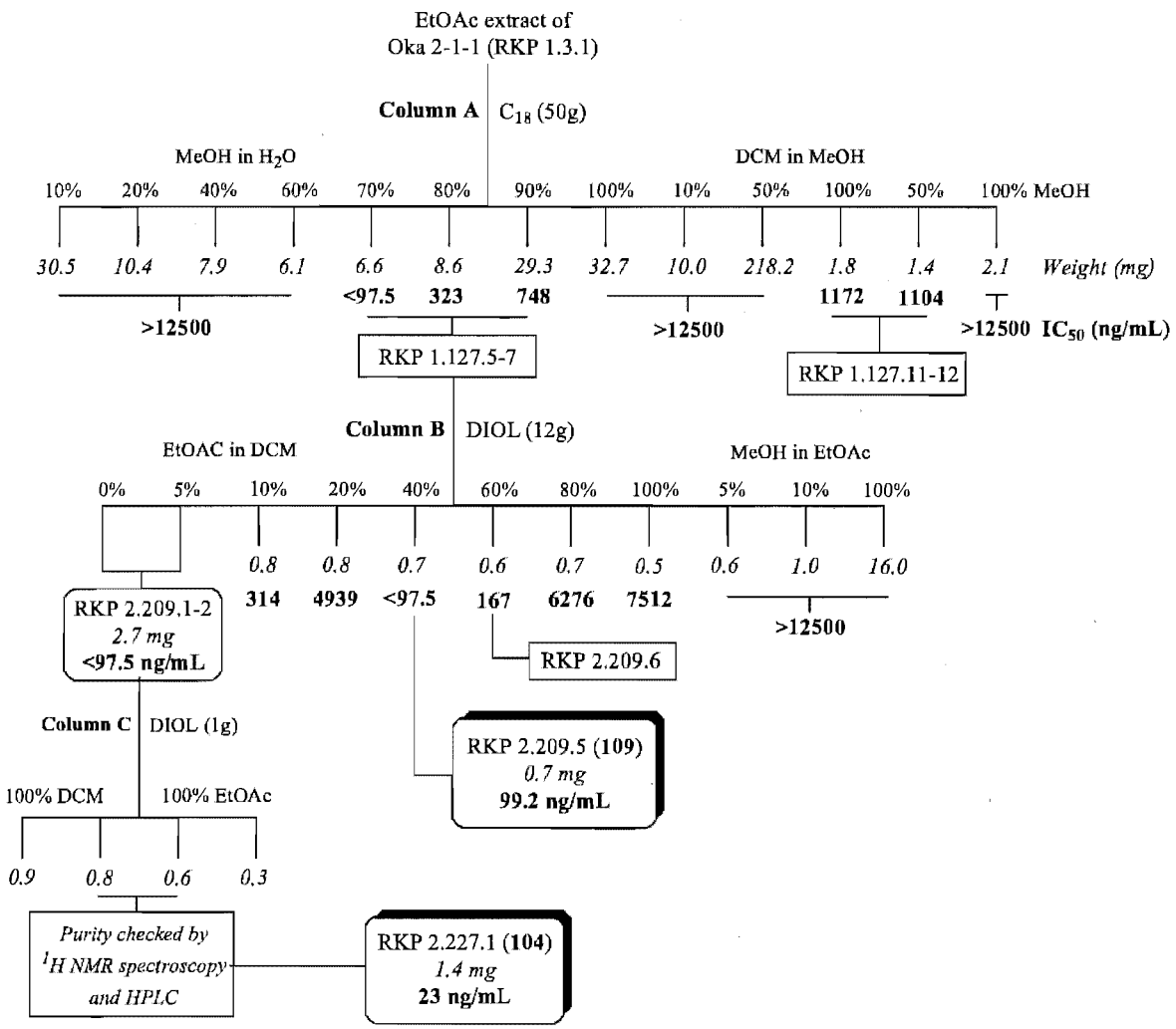

Scheme 3.1: Purification flow chart of an extract prepared from the fungal isolate Oka 2-1-1.

The large scale culture extract (405.1 mg) was initially fractionated on reverse-phase C_{18} (column A), using a stepped gradient solvent system for elution. The elution profile started at 10% H_2O in MeOH and increased to 100 % MeOH then changed to DCM in MeOH followed by a final MeOH wash. The three fractions (44.5 mg) that eluted between 70 and 90% MeOH/H_2O (RKP 1.127.5-7) showed the highest cytotoxicity towards the P388 cell line with IC_{50} values ranging from < 97.5 ng/mL through to 748 ng/mL. Although two late eluting fractions, RKP 1.127.11-12 also displayed cytotoxicity (1100 ng/mL), further work on these two fractions was not performed because very little sample was recovered for each fraction (3.2 mg total). Analytical HPLC of these two compounds highlighted multiple impurities and the ^{1}H NMR spectrum only showed signals indicative of triglycerides. Analysis of fractions RKP 1.127.5-7 by reverse-phase HPLC (Figure 3.4) showed many impurities and ESI MS results from these fractions were unable to be reconciled, as no matching peaks or peak patterns ($+Na^+$, $+K^+$) were seen between the three fractions.

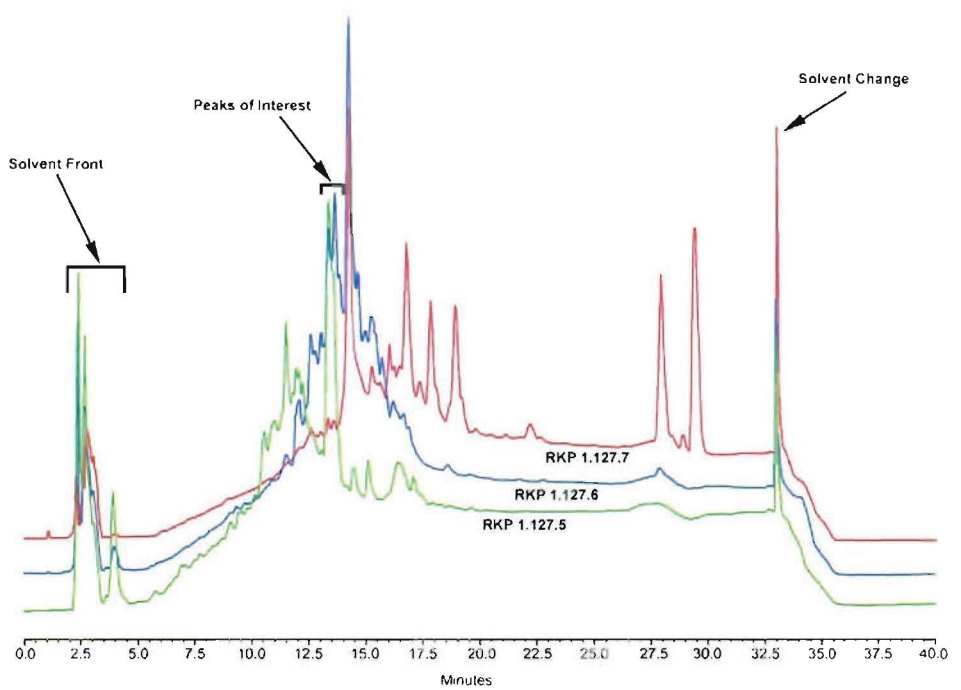

Figure 3.4: HPLC chromatogram of RKP 1.127.5-7

Based upon analytical HPLC, bioassay and ^{1}H NMR data, fractions 5, 6 and 7 were combined and further purified by normal phase chromatography on DIOL (column B). The combined bioactive fractions (RKP 1.127.5-7) were eluted off column B using a stepped gradient system starting at 100 % DCM, through EtOAc and then to MeOH,

collecting 11 fractions in total. Two bands of cytotoxicity eluted off column B, the first eluted between 0 and 10 % EtOAc in DCM (RKP 2.209.1-2), and the second eluted between 40 and 60 % (RKP 2.209.5-6), with moderate cytotoxicity seen in the side fractions (RKP 2.209.3,4 and 7).

RKP 2.209.1-2

Analytical HPLC (Figure 3.5) and the ^{1}H NMR spectrum (Figure 3.6) of RKP 2.209.1 confirmed the presence of **104**, but highlighted many impurities in the sample. However HPLC (Figure 3.5) and the ^{1}H NMR spectrum (Figure 3.7) of the second fraction (RKP 2.209.2) showed a very high degree of purity.

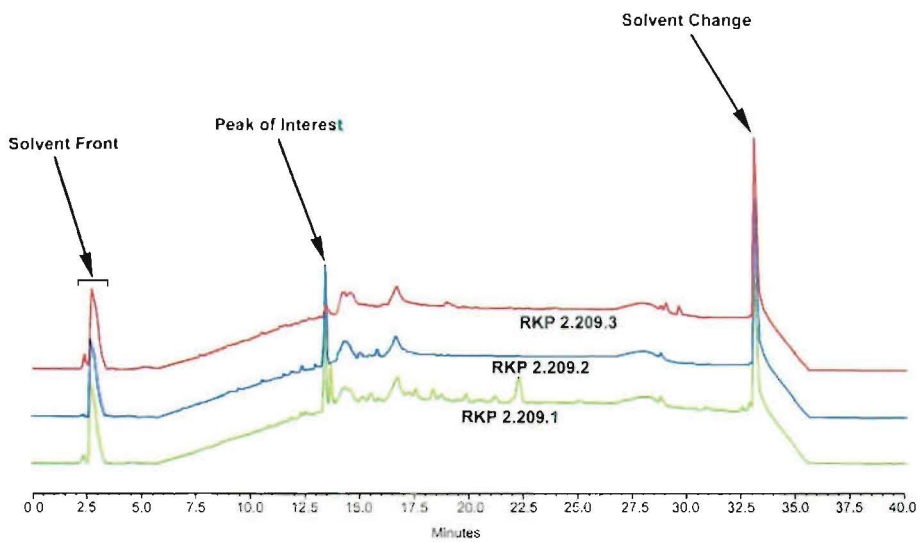

Figure 3.5: HPLC chromatogram of RKP 2.209.1-3

As the recovered mass of RKP 2.209.2 was relatively low (< 1 mg), it was combined with RKP 2.209.1 and further purified using a small scale (1 g) normal phase DIOL column (column C).

Column C was eluted with two column volumes of 100 % DCM then washed with a further two column volumes of 100% EtOAc, collecting four fractions in total. To save both time and sample the presence of **104** in these fractions was determined by analytical HPLC rather than biological assay, with relative purity examined by ^{1}H NMR spectroscopy. HPLC analysis of the four fractions from column C located compound

104 in the last two fractions (RKP 2.226.3-4), with the ^{1}H NMR spectrum indicating a very high degree of purity for both fractions. These fractions were subsequently combined (RKP 2.227.1) and examined by 1D and 2D NMR spectroscopy. The structural elucidation of **104** is discussed in Section 3.4.

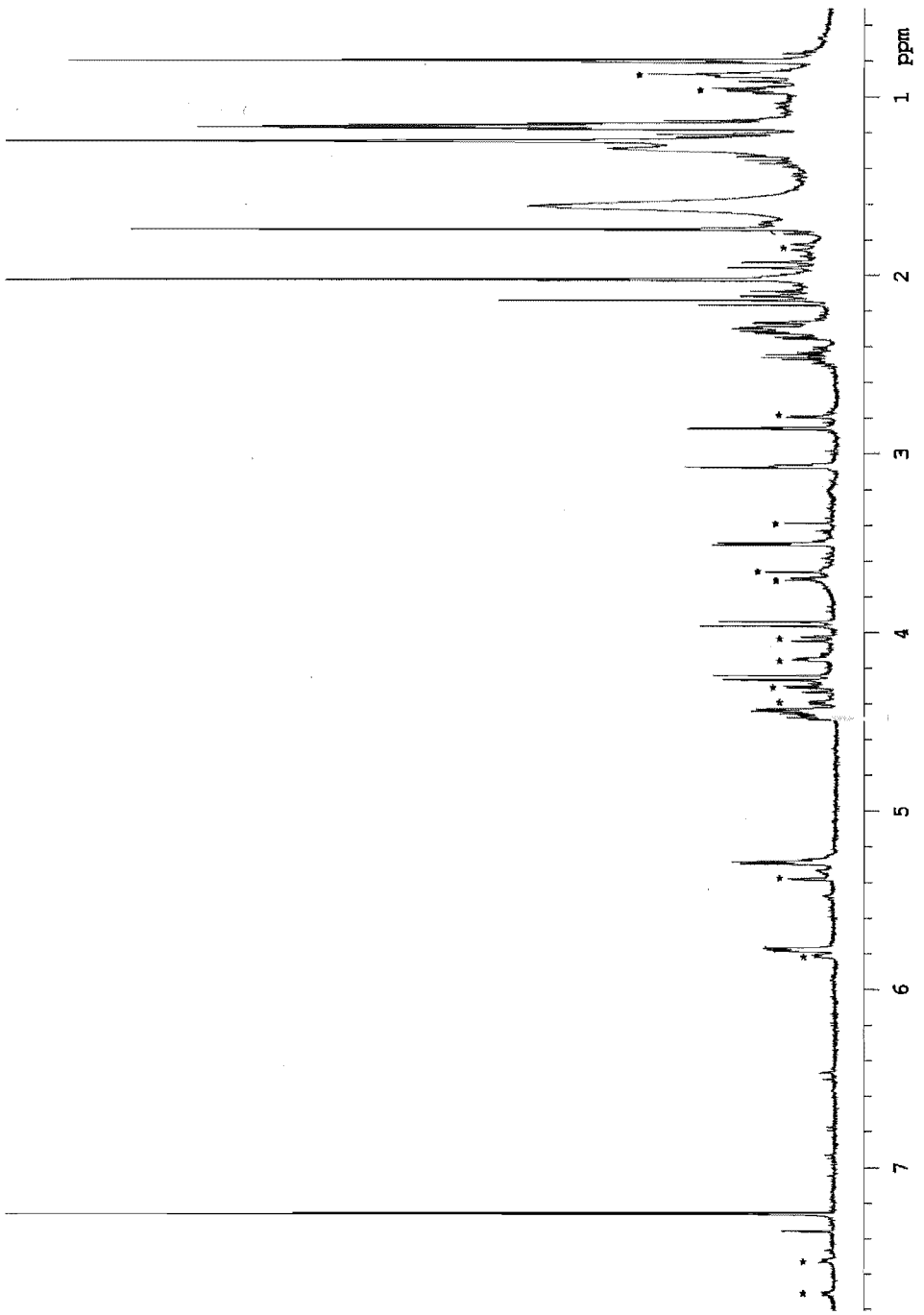

Figure 3.6: ^{1}H NMR spectrum of RKP 2.209.1 in $CDCl_3$. (* = peaks from impurities).

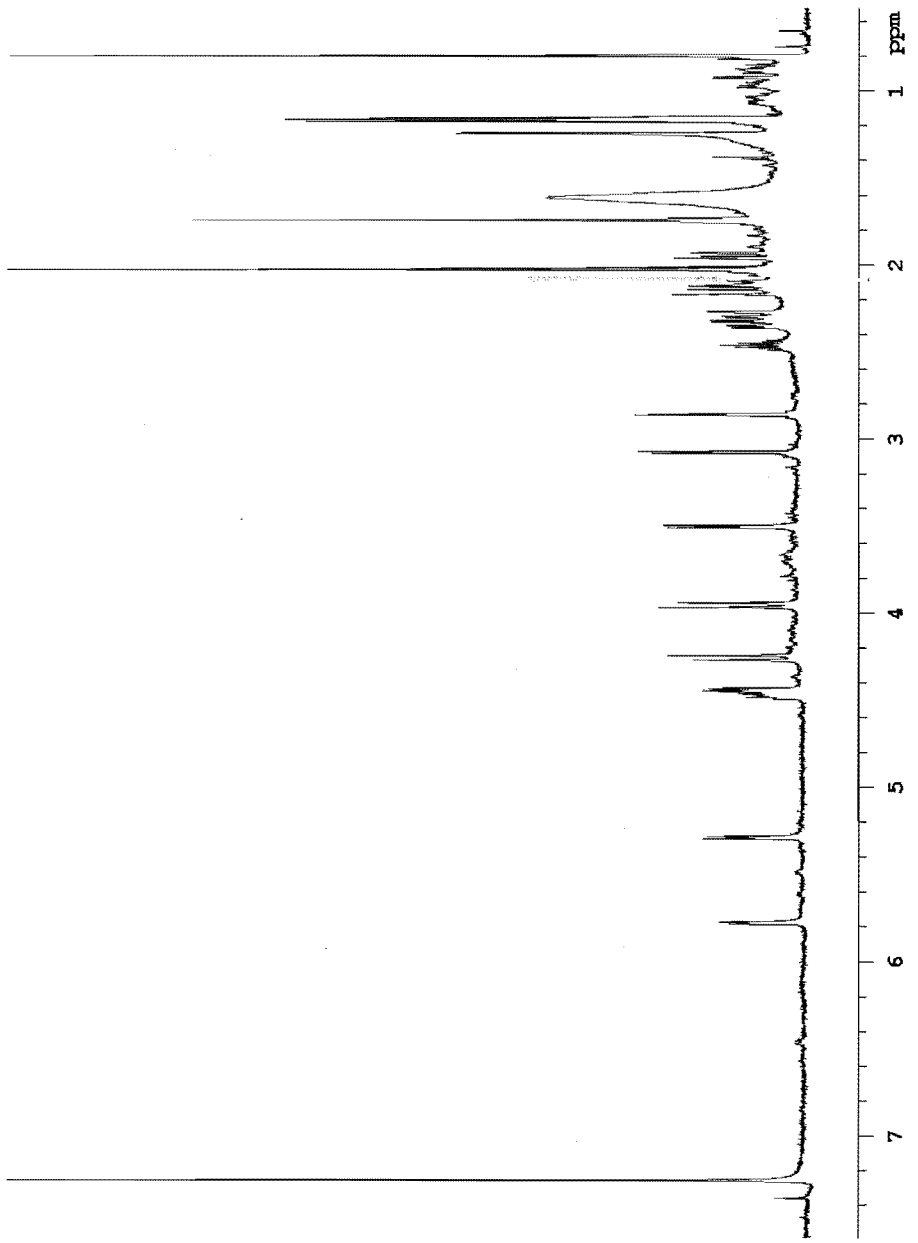

Figure 3.7: ^{1}H NMR spectrum of RKP 2.209.2 in $CDCl_3$

RKP 2.209.5-6

The two later eluting fractions from DIOL column B (RKP 2.209.5-6) which also displayed excellent cytotoxicity were examined by analytical HPLC (Figure 3.8) and ^{1}H NMR spectroscopy. The analytical HPLC chromatogram and ^{1}H NMR spectra of RKP 2.209.5 and 6 showed that RKP 2.209.5 was reasonably pure, but not RKP 2.209.6.

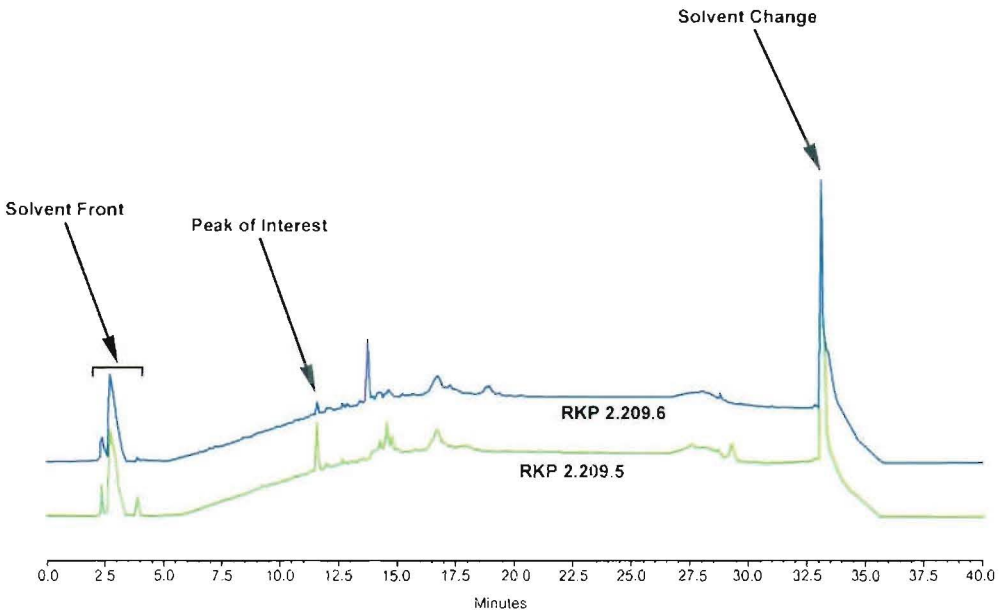

Figure 3.8: HPLC chromatogram of RKP 2.209.5-6

The ^{1}H NMR spectrum of RKP 2.209.5 (Figure 3.9) indicated that it was also a member of the trichothecene family. Even though some impurities were still present in RKP 2.209.5 further 1D and 2D NMR experiments were performed on the fraction as the initial ^{1}H NMR spectrum displayed sharp, well defined signals. The structural elucidation of **109** is discussed in Section 3.5.

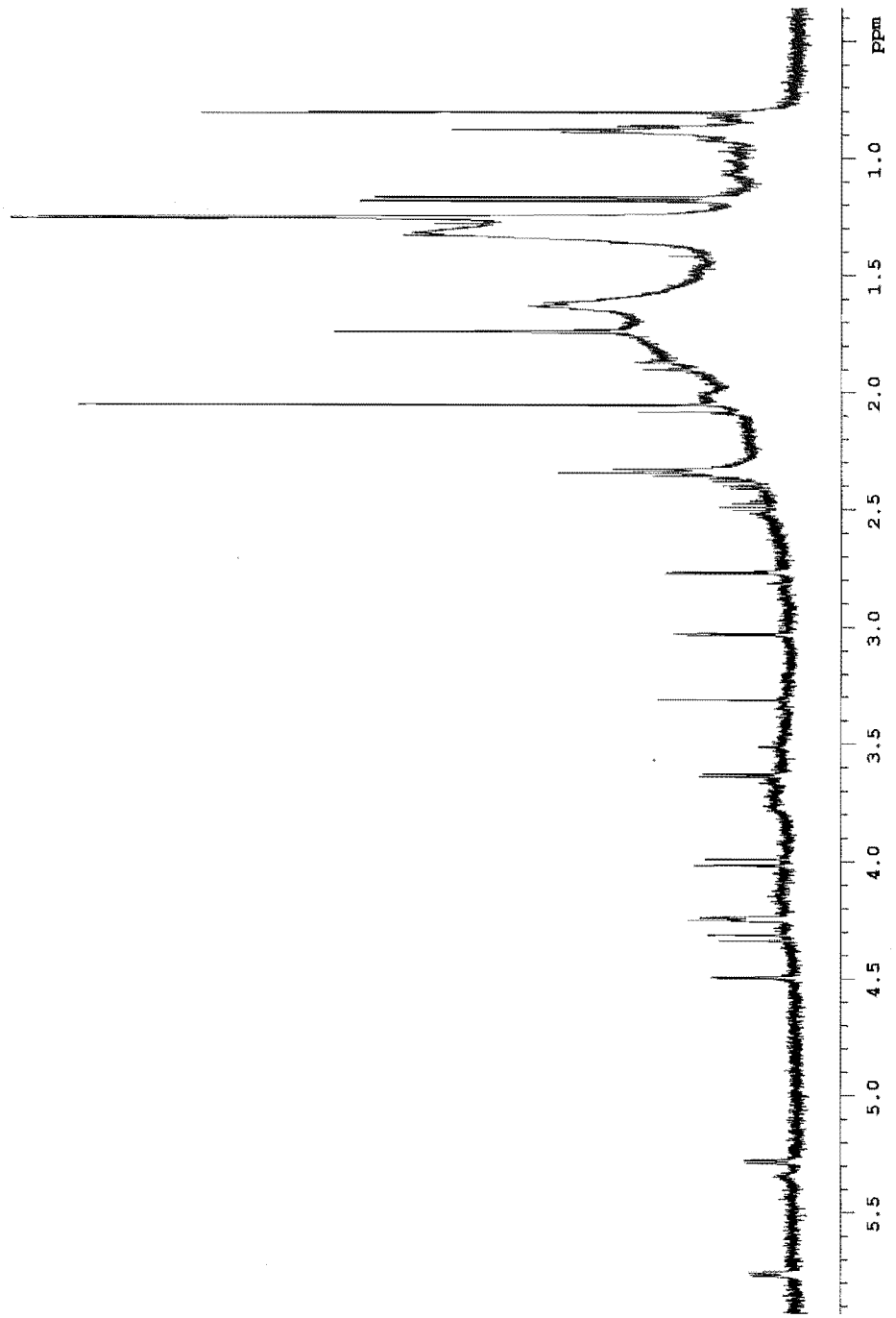

Figure 3.9: ^{1}H NMR spectrum of RKP 2.209.5 in $CDCl_3$.

3.4 Structural elucidation of 104

During the purification of **104** numerous attempts to obtain the molecular mass and molecular formula were made. However, all attempts were relatively unsuccessful as ESI-MS data varied between injections. After purification of **104** and re-analysis by positive and negative ion ESI-MS, the molecular ion peaks were then readily detected. Positive ion ESI-MS with formic acid displayed two small signals at 395 (MH^+) and 417 (MNa^+). Negative ion ESI-MS showed an intense signal at 393 (MH^-), and a weaker signal at 375 (MH^- -18), equivalent to the loss of water. The signals observed for both positive and negative ion ESI-MS indicated that the molecular mass of **104** was 394 Da. High resolution ESI-MS on the cesium adduct indicated a molecular formula for **104** of $C_{21}H_{30}O_7$ (seven double bond equivalents).

The ^1H NMR spectrum (Figure 3.10) of **104** was relatively simple, with a large number of well separated doublets and multiplets. Three methyl singlets were observed at δ_H 0.8, 1.74 and 2.05, with a further two methyl doublets at δ_H 1.17 and 1.16. All the other signals were due to methine groups, with no signals above δ_H 6.0 being observed. A ^{13}C APT spectrum was obtained for this sample and showed 19 signals (Figure 3.11). However, the molecular formula indicated that there were actually 21 carbons present in the molecule. The APT spectrum showed signals corresponding to a quaternary carbon at δ_C 136.2 and a tertiary carbon at δ_C 124.1 indicating a trisubstituted double bond. It also displayed four tertiary and two secondary carbon resonances at δ_C 79.6, 69.0, 68.5, 67.7 and δ_C 65.4, 64.9 respectively. A further five secondary or quaternary carbon peaks were observed at δ_C 48.6, 45.5, 42.1, 41.7 and 27.5. The APT spectrum also confirmed the presence of the methyl signals observed in the ^1H NMR spectrum. A further two quaternary signals were observed in the CIGAR spectrum at δ_C 170.4 and 176.7, indicative of two carbonyl groups, to bring the total number of observed carbon resonances to 21, as required by the molecular formula.

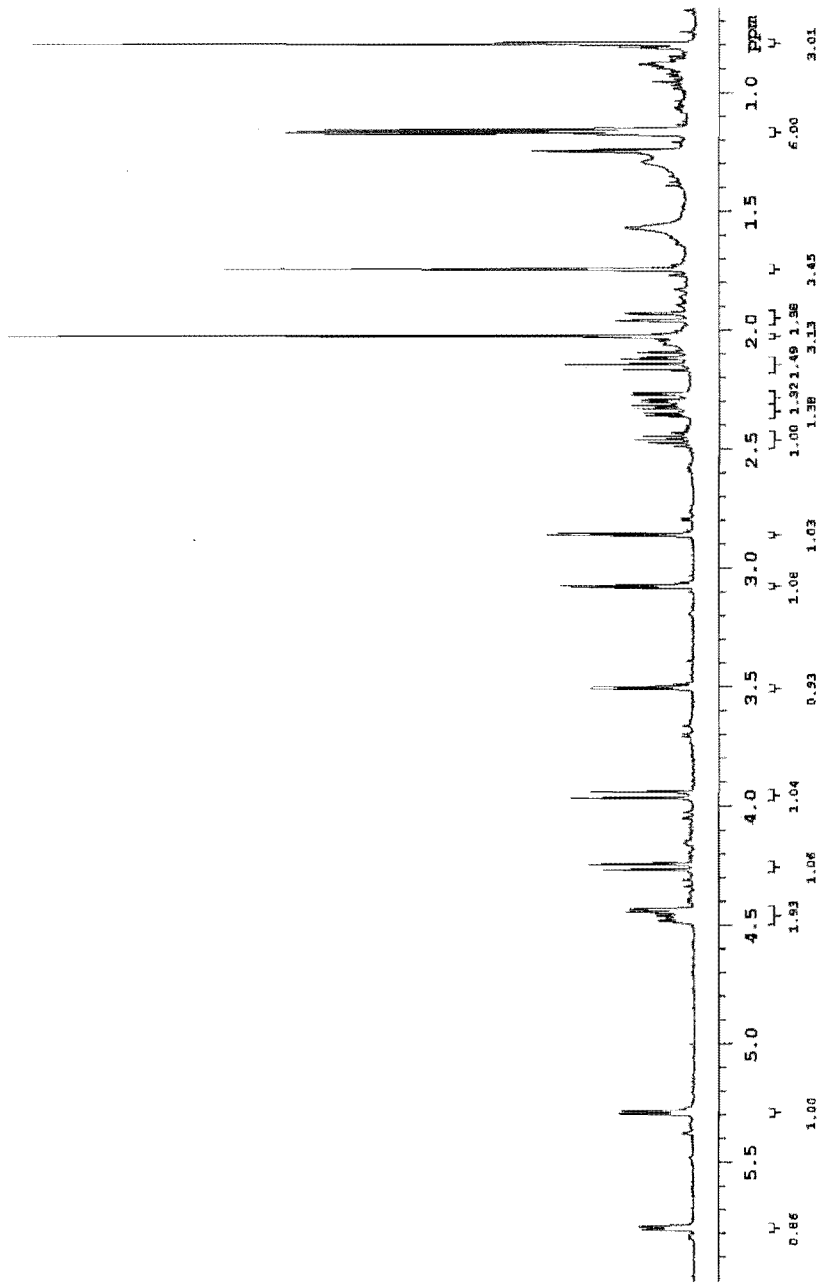

Figure 3.10: ^{1}H NMR spectrum of **104** in $CDCl_3$

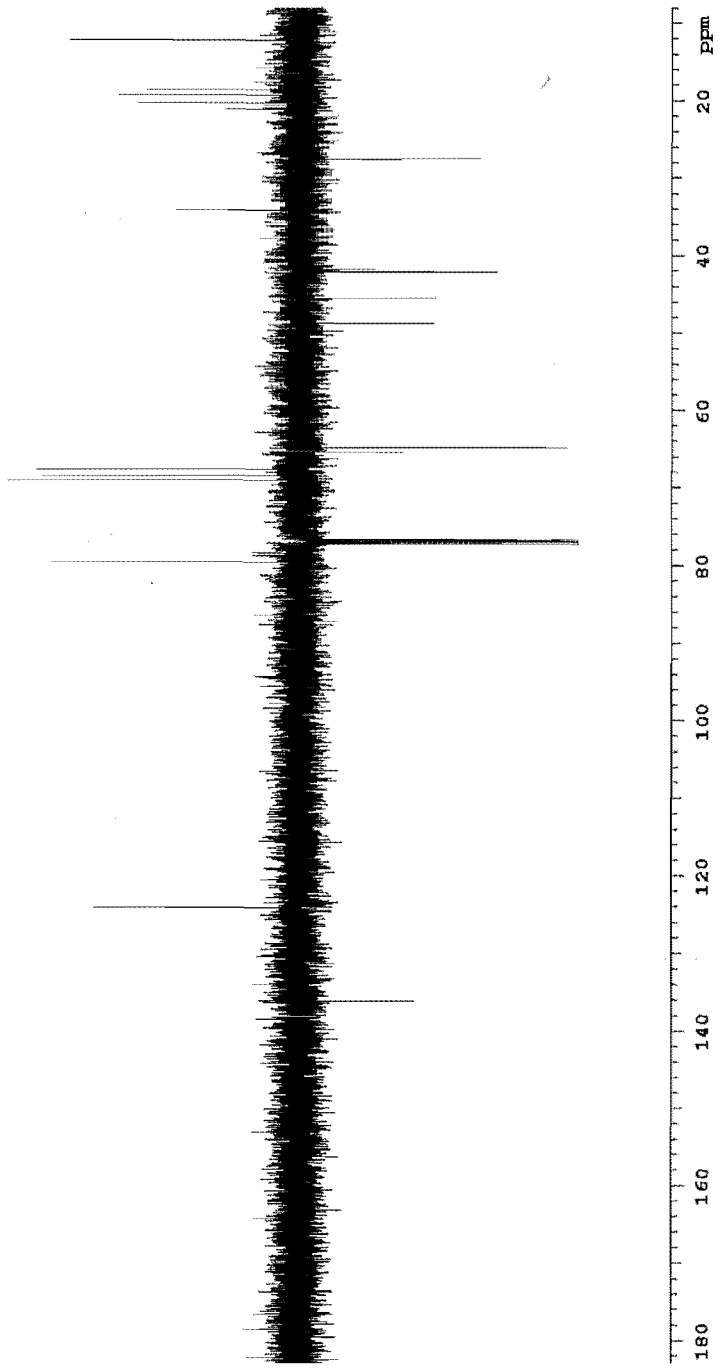

Figure 3.11: ^{13}C APT spectrum of **104** in $CDCl_3$

From COSY, TOCSY and HSQC experiments (Figures 3.28 - 3.30) six different spin systems were deduced. Long range coupling was observed between a methyl signal at δ_H 1.74 and a proton resonance at δ_H 5.79, which was in turn further coupled to a signal at δ_H 4.43. The chemical shift of the signal at δ_H 5.79 suggested that it was a vinyl proton which was confirmed with a $^1J_{CH}$ correlation to a carbon at δ_C 124.1 (Figure 3.12a). The methyl signals at δ_H 1.17 and δ_H 1.16 were both coupled to a multiplet signal at δ_H 2.45 (Figure 3.12b). The proton resonance at δ_H 5.28 showed correlations to two proton signals at δ_H 2.34 and δ_H 1.95. The two protons at δ_H 2.34 and δ_H 1.95 both showed $^1J_{CH}$ correlations to the same carbon signal at δ_C 27.5 (Figure 3.12c). The fourth spin system contained four proton signals at δ_H 4.47, 3.50, 2.27 and δ_H 2.14, with the HSQC spectrum indicating that the signals at δ_H 2.27 and δ_H 2.14 were on the same carbon (Figure 3.12d). The final two spin systems (Figure 3.12e-f) each contained two proton signals with the HSQC experiment showing that both systems were CH_2 groups.

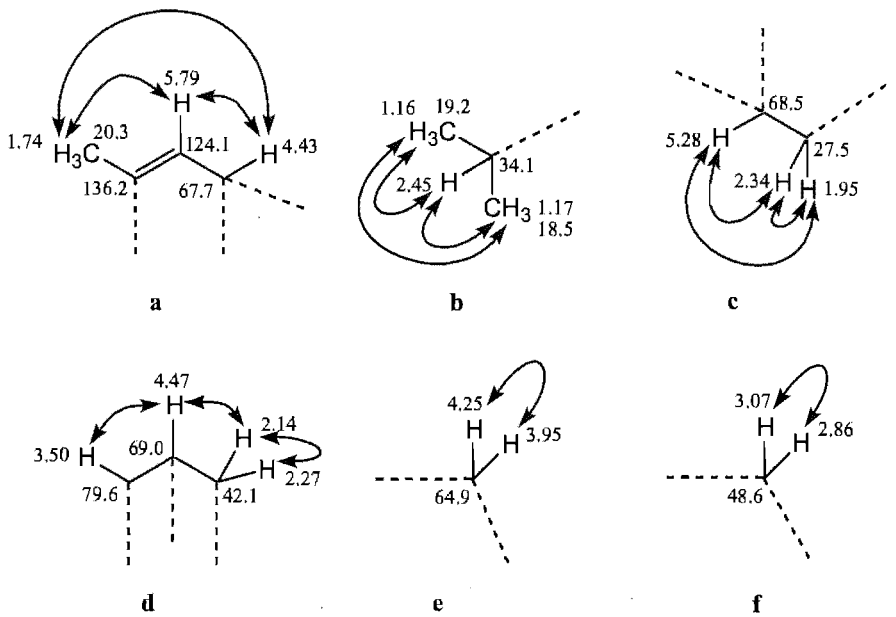

Figure 3.12a-f: Spin systems of **104** obtained from COSY, TOCSY and HSQC correlations

Two further methyl groups at δ_H 2.05 and δ_H 0.80 showed $^1J_{CH}$ correlations to carbons at δ_C 21.1 and δ_C 12.1 respectively. The chemical shift of the carbons observed in the HSQC spectrum allowed for five oxygen atoms to be included in the various fragments. These oxygen atoms were attached to the carbons at δ_C 67.7, 68.5, 79.6, 69.0 and δ_C 64.9 (Figure 3.13a-d).

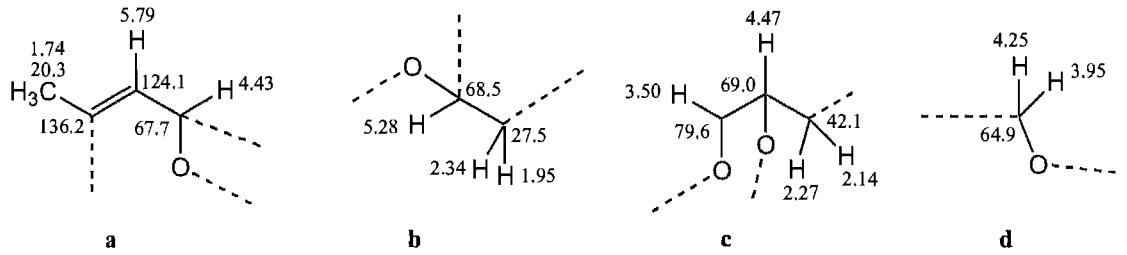

Figure 3.13a-d: Oxygenation pattern of fragments a, c, d and e in Figure 3.11

Correlations from the 2D CIGAR spectrum (Figure 3.31) enabled a full structural assignment. The proton signals in Figure 3.12b all showed correlations to a carbonyl group at δ_C 176.7 indicating an isobutyryl ester (Figure 3.14a). The proton signal at δ_H 5.28 showed correlations to the same carbonyl at δ_C 176.7, as well as two vinyl carbons at δ_C 136.2 and 124.1, a vinyl methyl at δ_C 20.3 and quaternary carbon at δ_C 41.7 (Figure 3.14b).

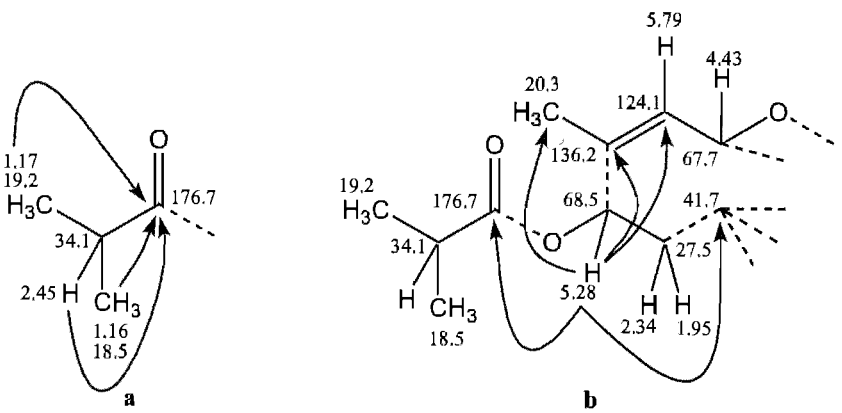

Figure 3.14a-b: CIGAR correlations for δ_H 5.28, 2.45, 1.17 and δ_H 1.16

The vinyl proton at δ_H 5.79 showed correlations to carbons at δ_C 68.5, 67.7, 41.7 and 20.3 confirming the partial structure seen in Figure 3.14b and enabling ring closure between the carbons at δ_C 67.7 and δ_C 41.7.

The proton signals at δ_H 2.34 and δ_H 1.95 showed $^3J_{CH}$ correlations to a secondary carbon at δ_C 64.9 and a quaternary carbon at δ_C 45.5 to further expand the fragment seen in Figure 3.13b (Figure 3.15).

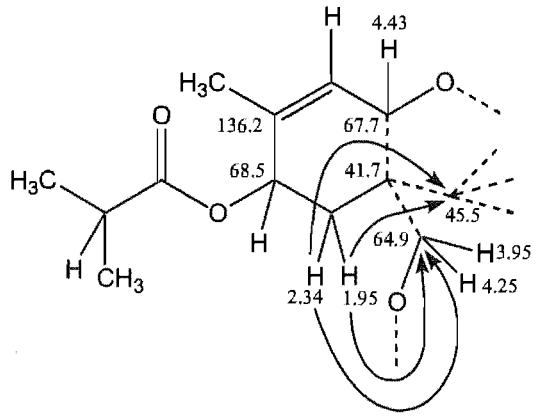

Figure 3.15: CIGAR correlations for δ_H 2.34 and δ_H 1.95

The proton pair at δ_H 4.25 / 3.95 and the methyl singlet at δ_H 2.05 all showed $^3J_{CH}$ correlations to a quaternary carbonyl δ_C 170.4 (Figure 3.16).

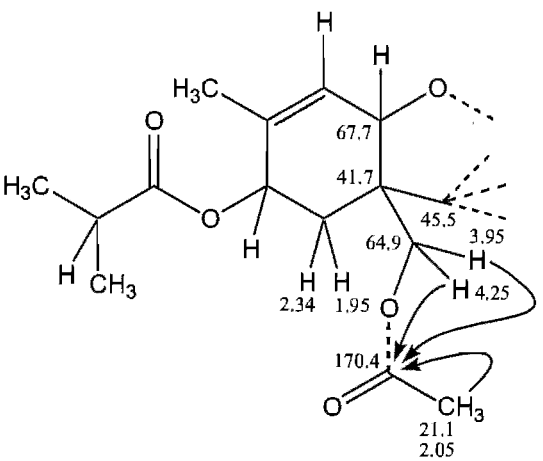

Figure 3.16: CIGAR correlations for δ_H 4.25, 3.95 and δ_H 2.05

A singlet methyl signal at δ_H 0.80 showed correlations to carbons at δ_C 65.4, 45.5, 42.1 and δ_C 41.7. This placed the methyl signal at δ_H 0.80 next to the quaternary carbon signal at δ_C 45.5 (Figure 3.17).

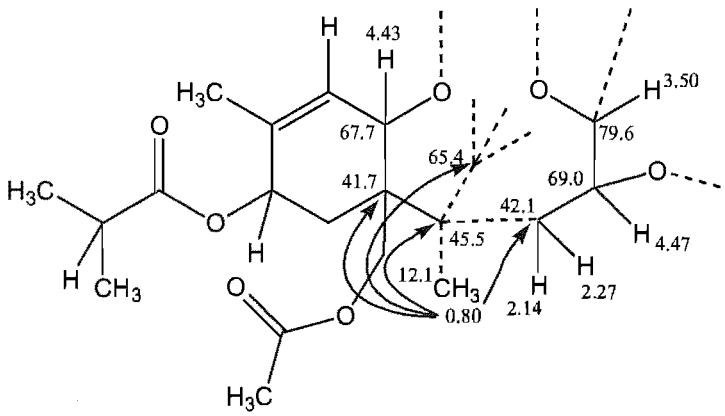

Figure 3.17: CIGAR correlations for the methyl signal at δ_H 0.80.

The proton signal at δ_H 3.50 showed correlations to carbon signals at δ_C 67.7, 65.4, 45.5 and δ_C 42.1 to give a five and a six membered ring (Figure 3.18).

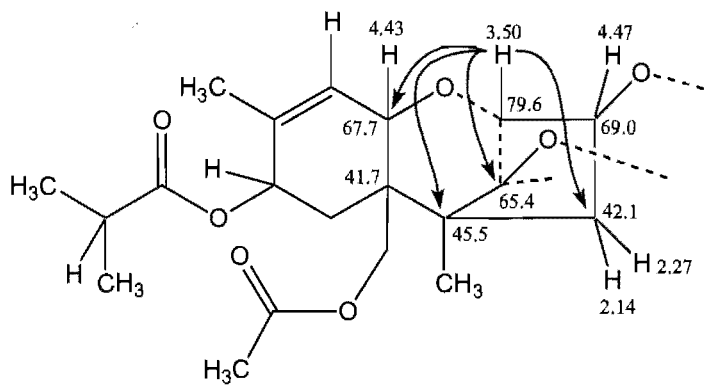

Figure 3.18: CIGAR correlations observed for the proton signal at δ_H 3.50.

The chemical shift of the quaternary carbon at δ_C 65.4 indicated the presence of an oxygen atom, which left 15 Da (CH_2 and H) unaccounted for in the molecular formula. No CIGAR correlations were observed either to the carbon at δ_C 48.6 or from the protons at δ_H 3.07 and δ_H 2.86. However, ROESY correlations were seen between the protons at δ_H 3.50 and δ_H 3.07 and between δ_H 2.86 and δ_H 0.80 (Figure 3.19).

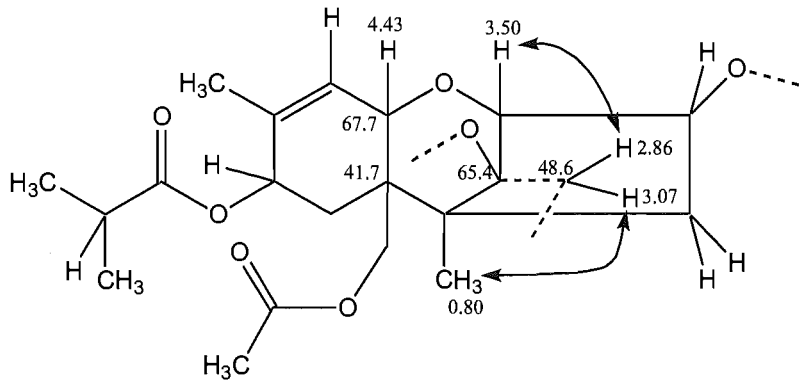

Figure 3.19: ROESY correlations for δ_H 3.50 and δ_H 0.80.

At this point all the atoms from the molecular formula $C_{21}H_{30}O_7$, except for a single proton had been assigned. However, only six of the double bond equivalents had been accounted for. The final double bond equivalent was postulated to arise from an epoxide ring between the carbon at δ_C 48.6 and the oxygen attached to the carbon at δ_C 65.4. The final proton was then assigned as part of a hydroxyl group at position 3 (Figure 3.20). The relative stereochemistry of **104** is discussed in Section 3.4.1.

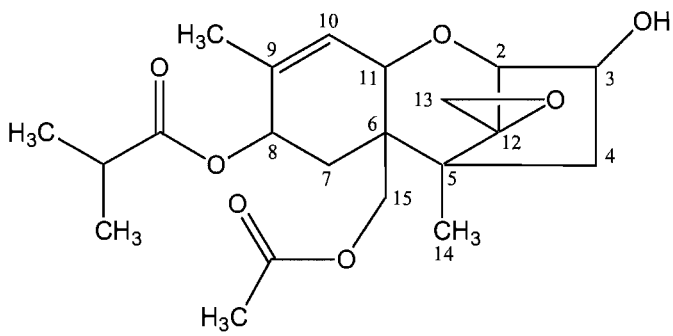

Figure 3.20: Numbering system used for trichothecenes

3.4.1 Relative stereochemistry of 104

The relative stereochemistry of **104** was determined from a 2D ROESY spectrum (Figure 3.32) which also enabled the connectivity of the CH_2 group at δ_C 48.6 to be determined.

The majority of previously reported trichothecenes put the proton at δ_H 5.28 in the β position. The only observable coupling for the proton at δ_H 1.95 was a $^2J_{HH}$ of 15 Hz. Thus the expected $^3J_{HH}$ coupling to δ_H 5.28 must be small indicating a dihedral angle close to 90°. This places the proton at δ_H 1.95 in an equatorial position. ROESY correlations were seen from the proton signal at δ_H 1.95 to the quaternary methyl at δ_H 0.8. This methyl group showed a correlation to an epoxide proton at δ_H 2.87 which turn showed a correlation to the proton at δ_H 2.34. The proton at δ_H 3.50 showed correlations to the second epoxide proton at δ_H 3.07 and another proton at δ_H 4.47. The proton at δ_H 2.14 showed ROESY correlations to the proton at δ_H 4.47 and the methyl at δ_H 0.8 as shown in Figure 3.21.

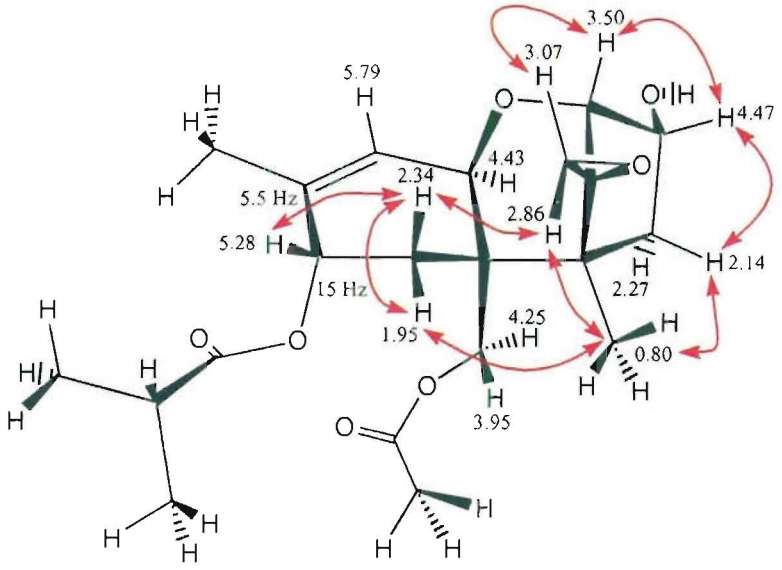

Figure 3.21: Important ROESY correlations and J_{HH} coupling constants for **104**.

Further ROESY correlations were seen from δ_H 4.43 to δ_H 4.25, δ_H 4.25 to δ_H 2.27 and δ_H 3.95 to δ_H 0.80 (Figure 3.22). These correlations provided confirmation of the relative stereochemistry of **104**.

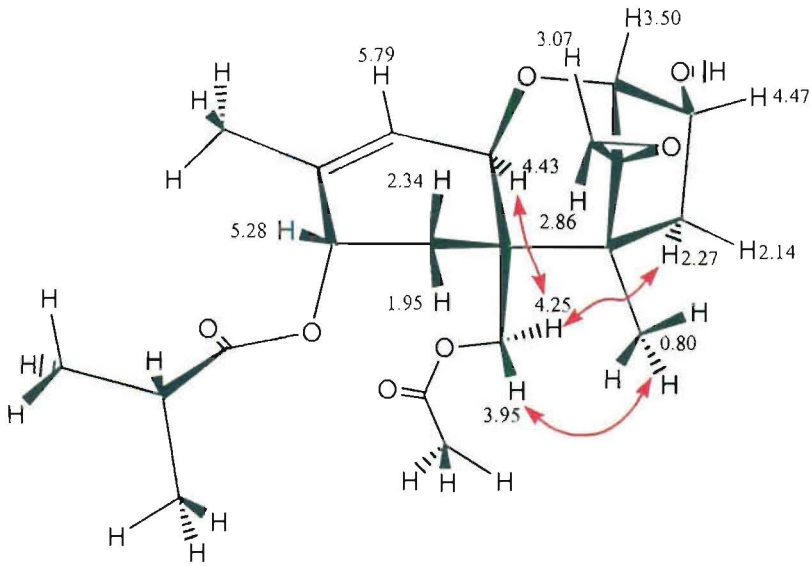

Figure 3.22: Additional ROESY correlations observed in **104**.

The epoxide ring could be in two different configurations, but the correlation seen between δ_H 2.34 and 2.86 proved that the configuration seen in Figure 3.23b was the only possible one. If the configuration proposed in Figure 3.23a was the preferred one the correlation between δ_H 2.34 and δ_H 2.86 would not have been observed. Furthermore the configuration in Figure 3.23a would show additional ROESY correlations between the protons at δ_H 3.07 and δ_H 4.47 as well as δ_H 2.86 and δ_H 2.14.

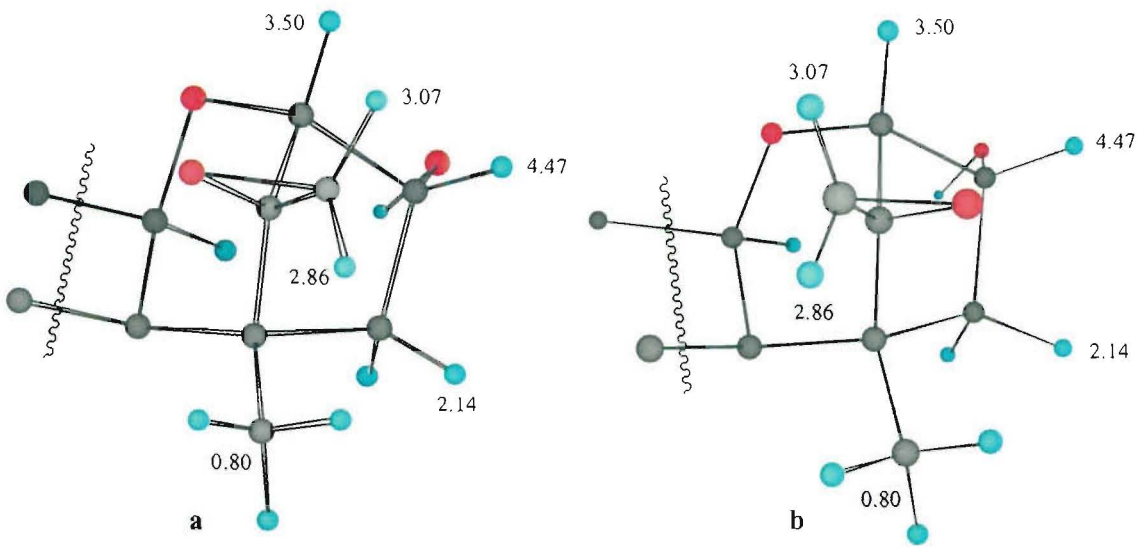

Figure 3.23a-b: Possible epoxide ring configurations for **104**.

An extensive search of numerous databases found only four trichothecenes with a similar oxygenation pattern at C^3, C^8 and C^{15}, and no oxygenation at C^4. Of these, three were calonectrin derivatives, such as 8-hydroxycalonectrin (**105**) and one was sporotrichiol (**106**).[102] Compound **104** also showed structural similarities to various T-2 derivatives, such as 4-deacetoxy-T-2 Toxin (**107**) and some neosolaniol derivatives,[117] such as 8-isobutyrylneosolaniol (**108**). However, no absolute matches for this structure were found. Compound **104** was therefore considered novel and as such, was called 4-deacetoxy-8-isobutyrylneosolaniol or, 3-hydroxy-8-isobutyryl-15-acetyl-12,13-epoxytrichothec-9-ene.

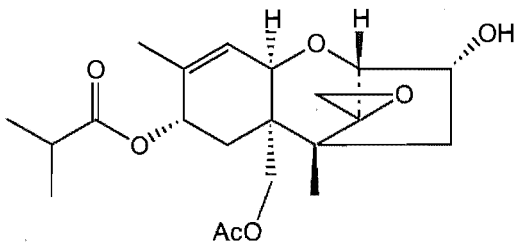

104

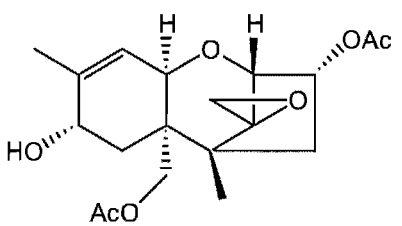

105

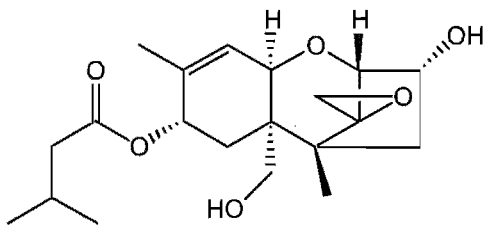

106

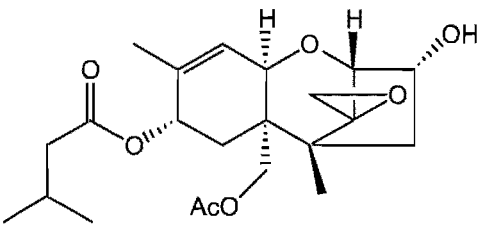

107

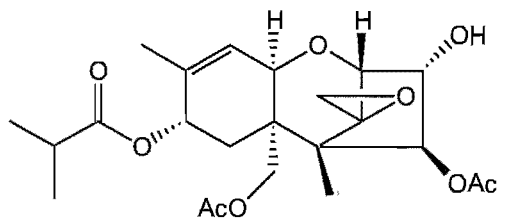

108

3.5 Structural elucidation of 109

The ^{1}H NMR spectrum of **109** showed a high degree of similarity to that of **104**, with a few notable differences. The proton signals at δ_H 4.47 and δ_H 4.43 seen in the ^{1}H NMR spectrum of **104** were absent while two new signals were observed at δ_H 4.49 and δ_H 4.24 with the signal at δ_H 4.24 integrating for two protons. Correlations in the COSY and HSQC spectra indicated that the same six fragments observed for **104** were also present in **109**, with the exception of the fragment in Figure 3.24d. The CH_2 resonances seen in Figure 3.13d were replaced with a proton resonating at δ_H 4.47 with a $^1J_{CH}$ to a carbon at δ_C 81.7 (Figure 3.24d) indicating that this centre was now oxygenated.

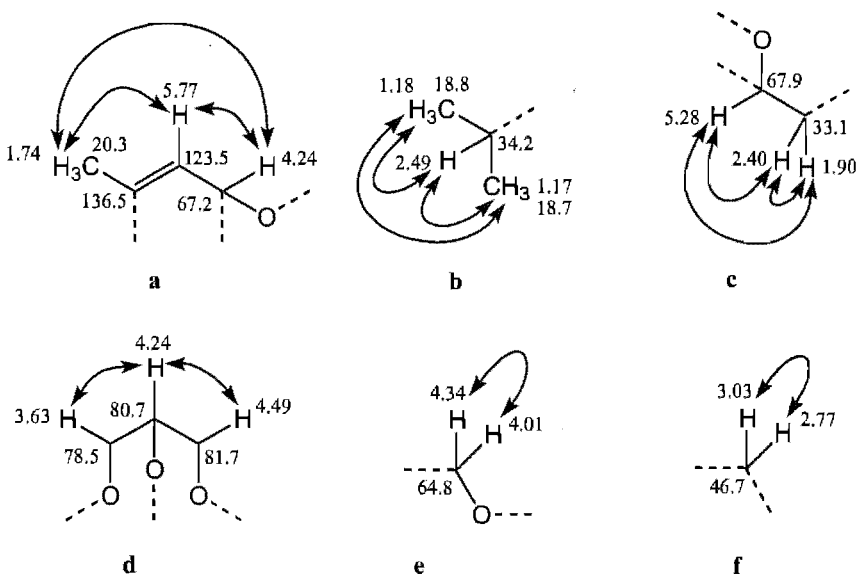

Figure 3.24a-f: Fragments of **109** deduced from COSY, TOCSY and HSQC correlations.

Even though the recovered mass of **109** was very small (< 1 mg) the CIGAR correlations seen from the five methyl groups were sufficient to allow assembly of the fragments in Figure 3.24 to give **109**, an analogue of **104** oxygenated at position 4. The methyl signal at δ_H 0.80 showed correlations to 4 carbons at δ_C 81.7, 64.5, 48.7 and 42.3. The methyl group at δ_H 1.74 showed correlations to carbons at δ_C 136.5, 123.5 and 67.9. Two weak $^3J_{CH}$ correlations were seen from the proton at δ_H 3.63 to two

carbons at δ_C 81.7 and 67.2. The protons at δ_H 4.01 and 4.34 both showed very weak correlations to a carbon at δ_C 48.7, with the proton at δ_H 4.34 also showing a correlation to a carbon at δ_C 67.2. As with compound **104** no correlations were observed either to the carbon at δ_C 46.7, or from the protons at δ_H 3.03 or δ_H 2.77. However, NOESY correlations enabled these protons to be assigned as part of the epoxide (Figure 3.25).

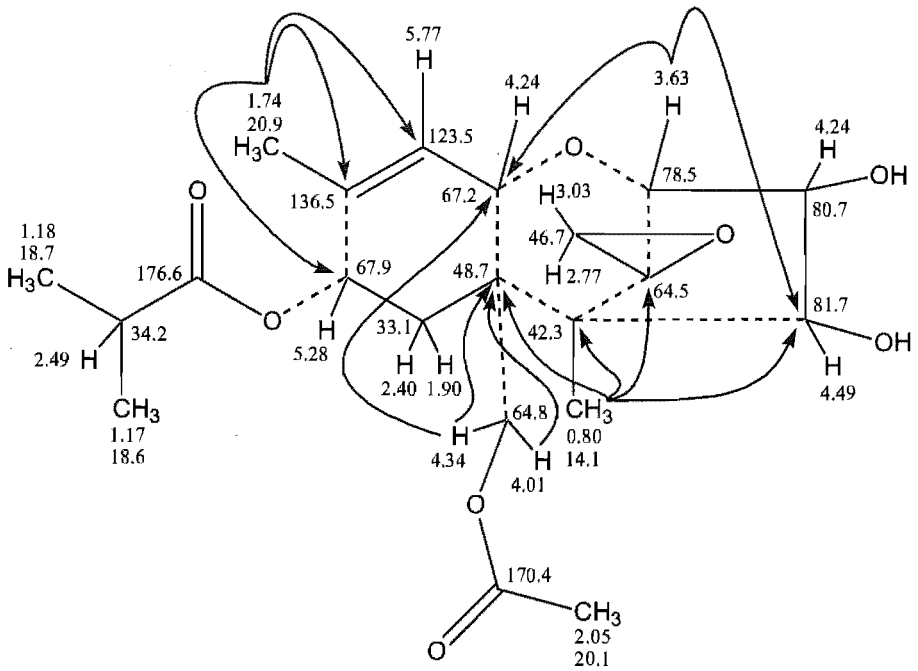

Figure 3.25: CIGAR correlations observed for **109**.

High resolution ESI MS on the sodium adduct of **109** showed an MNa^+ at 433.1849 Da corresponding to a molecular formula of $C_{21}H_{30}O_8Na$, lending further support for the structure in Figure 3.25. The relative stereochemistry seen in **109** is discussed below in Section 3.5.1.

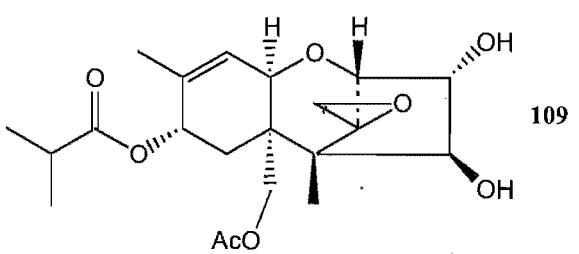

109

3.5.1 Relative stereochemistry of 109

The same relative stereochemistry seen in compound **104** was also observed for **109** except that an extra stereocentre is present in **109** at C^4. The stereochemistry at this centre was unable to be determined via the coupling constant between the protons at δ_H 4.49 and 4.24 as the signal at δ_H 4.24 is coincident with another signal. NOESY correlations were seen from the proton signal at δ_H 4.49 to the proton signals at δ_H 4.24 and δ_H 4.34, but the correlation to δ_H 4.24 could have been due to the protons attached at either C^3 or C^{11}. However, a correlation from the proton signal at δ_H 4.49 to the proton signal at δ_H 4.34 indicated that the stereochemistry at C^4 was opposite to that at C^3. A Chem3D (Cambridge software) energy minimisation using MM2 parameters on the rigid ring system of compound **109** placed the proton at δ_H 4.49 within 2.3 Å of both protons at δ_H 4.24 (Figure 3.26) further supporting the proposed stereochemistry at C^3 and C^4 respectively.

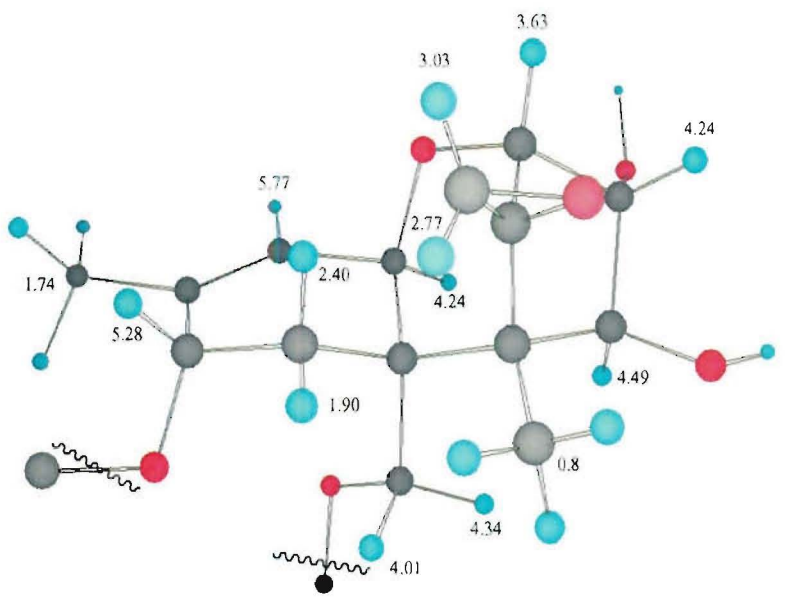

Figure 3.26: Energy minimised Chem3D structure of **109** using MM2 parameters

All previously reported trichothecenes with similar substitutions at C^3 and C^4 display the same stereochemistry as that shown in Figure 3.26 at these two stereogenic

centres.[102] Exhaustive searches on all available databases eventually found a single compound[118] with proton chemical shifts identical to **109**. However, this compound was not isolated from a natural source but rather, was the result of semi-synthetic modifications to neosolaniol (**98**). A comparison of the experimental and literature ^{1}H NMR data for **109** can be found in Table 3.2

3.6 Discussion

Purification of an extract from a *Fusarium* sp yielded two trichothecene derivatives, each with significant biological activity against the P388 murine leukaemia cell line. A literature search on the first of these, compound **104**, found no matches and was subsequently identified as a novel trichothecene called 4-deacetoxy-8-isobutyrylneosolaniol. As previously described in Section 3.5.1 the second compound (**109**) had been reported in 1987,[118] but had not previously been isolated as a natural compound.

Experimental ^{1}H and ^{13}C data in $CDCl_3$ for compounds **104** and **109** are shown in Tables 3.1 and 3.2 respectively. The literature ^{1}H NMR data for **109** in $CDCl_3$ are also shown in Table 3.2.

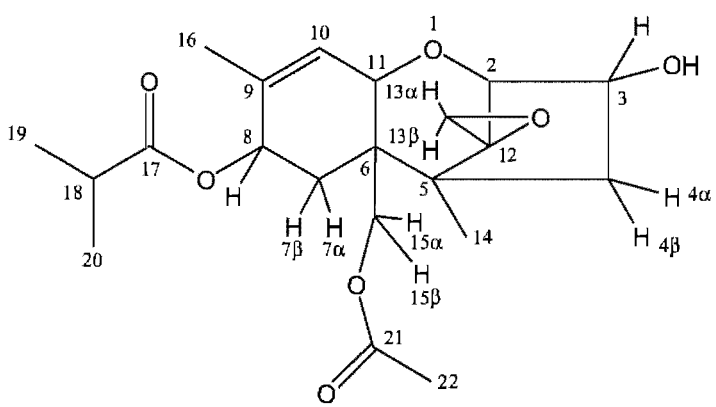

Figure 3.27: Trichothecene numbering system for Tables 3.1 and 3.2.

Table 3.1: ^{1}H and ^{13}C NMR data for **104** in $CDCl_3$

Number	^{1}H, multiplicity, (J_{HH} Hz)	COSY	TOCSY	HSQC / APT	CIGAR	ROESY
2	3.50 d (4.5)	4.47	4.47 , 2.27 , 2.14	79.6	67.7 , 65.4 , 45.5 , 42.1	4.47 , 3.07
3	4.47 dt (5, 12)	3.50 , 2.14	3.50 , 2.27 , 2.14	69.0	-	3.50 , 2.30 , 2.13
4 α	2.27 dd (3.5, 14.5)	4.47 , 2.14	4.47 , 3.50 , 2.14	42.1	69.0 , 45.5 , 41.7	4.47 , 4.25 , 2.14
4 β	2.14 dd (14.5, 3.5)	4.47 , 2.27	4.47 , 3.50 , 2.27	42.1	79.6 , 69.0 , 12.1	4.47 , 2.27 , 0.8
5	-	-	-	45.5	-	-
6	-	-	-	41.7	-	-
7 α	1.95 d (15)	2.34	5.28 , 2.34	27.5	136.2 , 68.5 , 67.7 , 64.9 , 41.7	2.34 , 0.8
7 β	2.34 dd (5.5, 15)	5.28 , 1.95	5.28 , 1.95	27.5	67.7 , 64.9 , 45.5 , 41.7	5.28 , 2.86 , 1.95
8	5.28 d (5.5)	2.34	2.34 , 1.95	68.5	176.7 , 136.2 , 124.1 , 67.7 , 41.7 , 20.3	2.34 , 1.95 , 1.74
9	-	-	-	136.2	-	-
10	5.79 d (5.5)	4.43 , 1.74	4.43 , 1.74	124.1	68.5 , 67.7 , 41.7 , 20.3	4.43 , 1.74
11	4.43 d (6)	5.79	5.79 , 1.74	67.7	138.2 , 124.1 , 64.9 , 27.5	5.79 , 4.25
12	-	-	-	65.4	-	-
13 α	3.07 d (4)	2.86	2.86	48.6	-	3.50 , 2.86
13 β	2.86 d (4)	3.07	3.07	48.6	-	3.07 , 2.34 , 0.8
14	0.80 s	-	-	12.1	65.4 , 45.5 , 42.1 , 41.7	3.95 , 2.86 , 2.14 , 1.95
15 α	4.25 d (12.5)	3.95	3.95	64.9	170.4 , 67.7 , 45.5 , 41.7 , 27.5	4.43 , 3.95 , 2.27
15 β	3.95 d (12.5)	4.25	4.25	64.9	170.4 , 67.7 , 45.5 , 41.7	4.25 , 0.8
16	1.74 s	5.79	5.79 , 4.43	20.3	136.2 , 124.1 , 68.5	5.79 , 5.28
17	-	-	-	176.7	-	-
18	2.45 m (6.5)	1.17 , 1.16	1.17 , 1.16	34.1	176.7 , 19.2 , 18.5	1.17 , 1.16
19	1.17 d (7)	2.45	2.45	19.2	176.7 , 34.1 , 18.5	2.45
20	1.16 d (7)	2.45	2.45	18.5	176.7 , 34.1 , 19.2	2.45
21	-	-	-	170.4	-	-
22	2.05 s	-	-	21.1	170.4	-

Literature ^{1}H, multiplicity, (J_{HH} Hz)	Number	Experimental ^{1}H, multiplicity, (J_{HH} Hz)	COSY	HSQC	CIGAR	NOESY
3.61 d (4.9)	2	3.63 d (5)	4.25	78.5	81.7 , 67.2	4.24 , 3.03
4.22 dd (4.9, 3)	3	4.24 d (5.5)	3.36	80.7	-	4.49
4.45 d (3)	4	4.49 d (2.5)	4.24	81.7	-	4.34 , 4.24
1.88 dt (15, 1.5)	7	1.90 d (15.5)	2.40	33.1	-	5.28 , 2.40 , 0.80
2.36 dd (15, 5.5)	7	2.40 dd (14.5, 5.5)	5.28 , 1.90	33.1	-	5.28 , 2.77 , 1.90
5.26 br d (5)	8	5.28 d (5.5)	2.40	687.9	-	2.40 , 1.90 , 1.74
5.74 br d (6)	10	5.77 d (5.5)	4.24 , 1.74	123.5	-	4.24 , 1.74
4.22 d (6)	11	4.24 d (5.5)	5.77	67.2	-	5.77 , 4.34
2.75 d (4)	13	3.03 d (4)	2.77	46.7	-	3.63 , 2.77
3.01 d (4)	13	2.77 d (4)	3.03	46.7	-	3.03 , 2.40 , 0.80
0.78 s	14	0.80 s	-	14.1	81.7 , 64.5 , 48.7 , 42.3	4.01 , 2.77 , 1.90
3.97 d (12.5)	15	4.34 d (13)	4.01	64.8	48.7	4.49 , 4.01
4.32 d (12.5)	15	4.01 d (13.5)	4.34	64.8	81.7 , 67.2	4.34 , 0.80
1.72 br s	16	1.74 s	5.77	20.9	136.5 , 123.5 , 67.9	5.77 , 5.28
2.46 m (7)	18	2.49 m (7)	1.18 , 1.17	34.2	-	1.18 , 1.17
1.15 d (7)	19	1.18 d (7)	2.49	18.7	176.6 , 34.2 , 18.6	2.49
1.16 d (7)	20	1.17 d (7)	2.49	18.7	176.6 , 34.2 , 18.7	2.49
2.03 s	22	2.05 s	-	20.1	170.4	-

Table 3.2: Literature[118] and experimental NMR data for **109** in $CDCl_3$

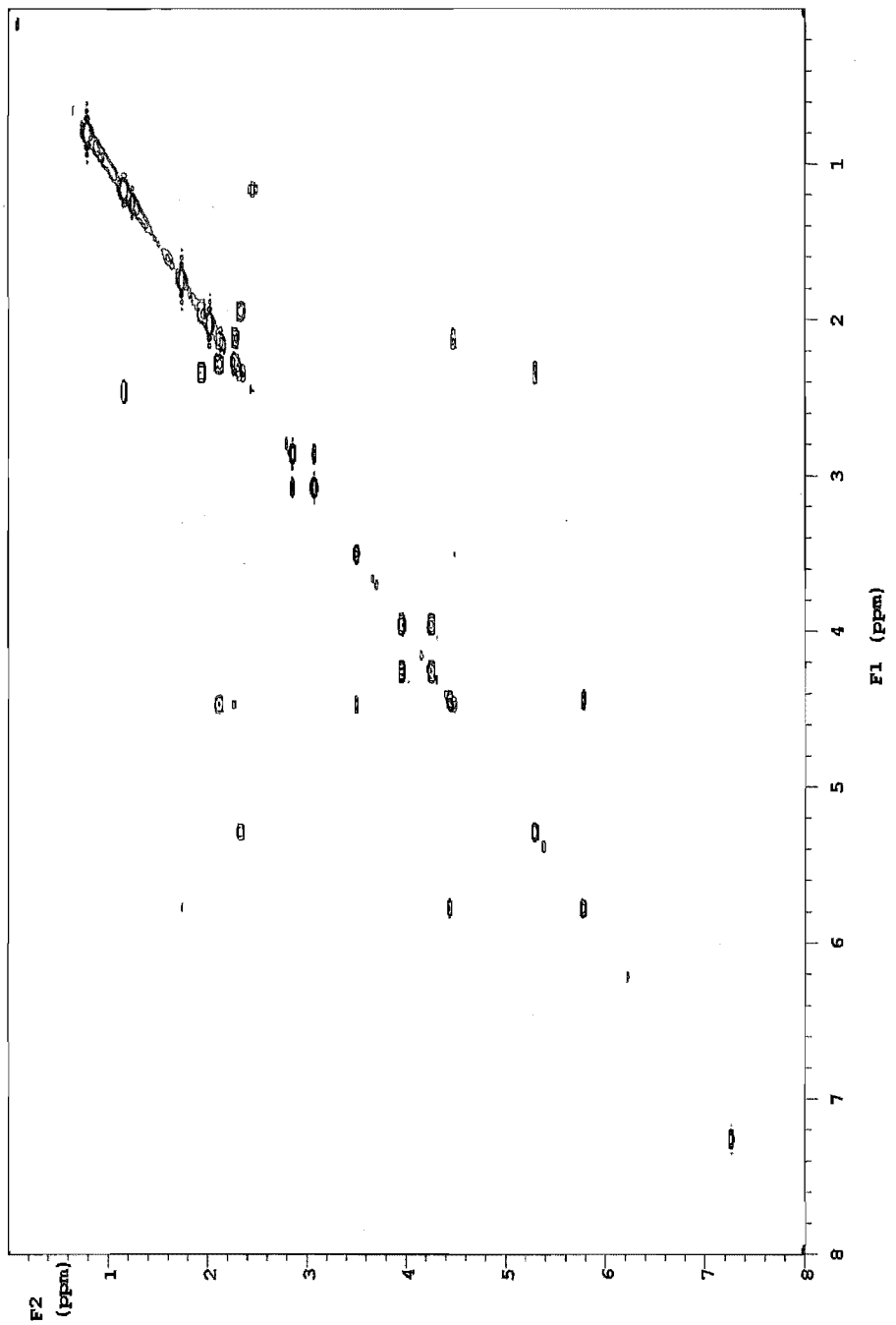

Figure 3.28: COSY spectrum of **104** in $CDCl_3$

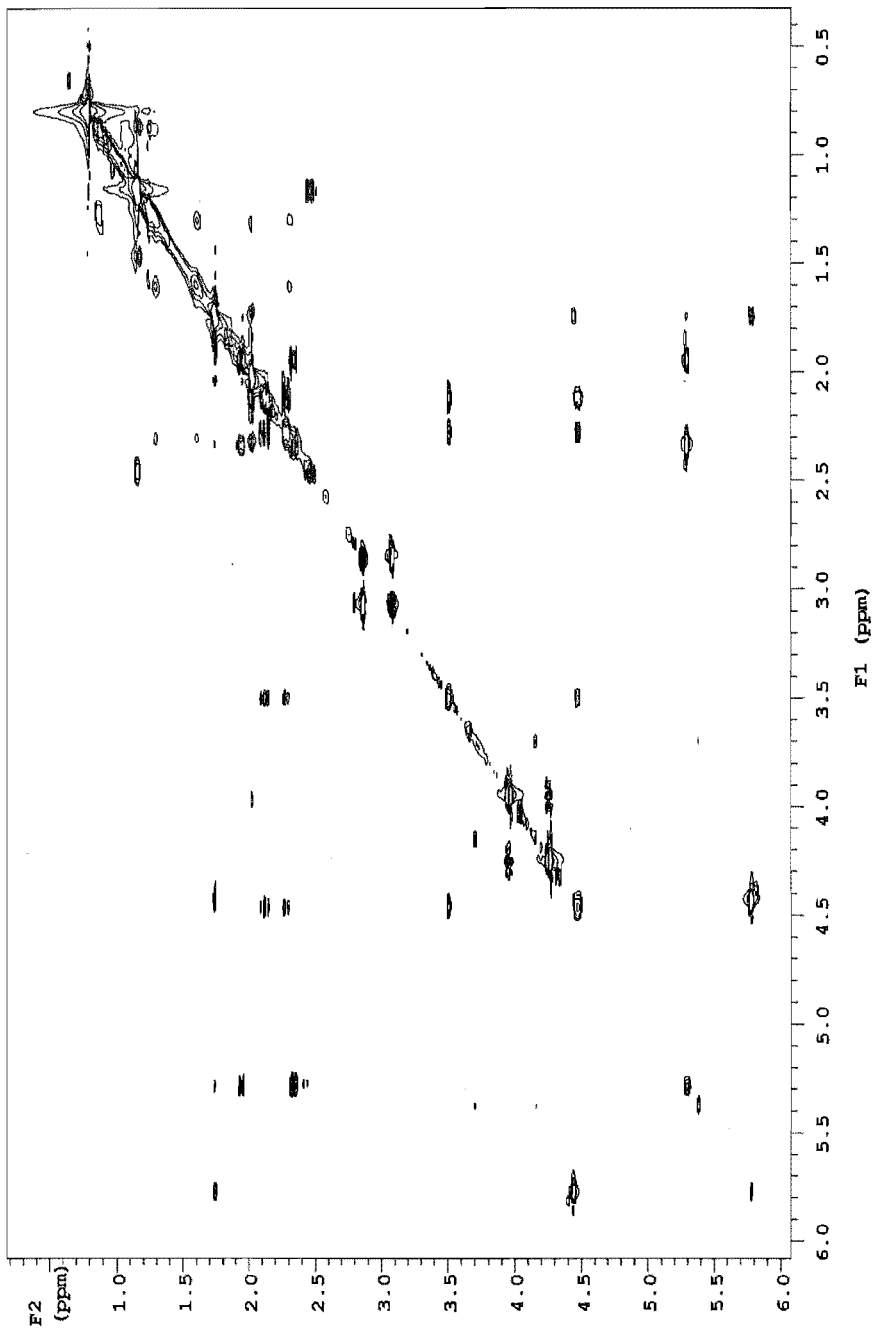

Figure 3.29: TOCSY spectrum of **104** in $CDCl_3$

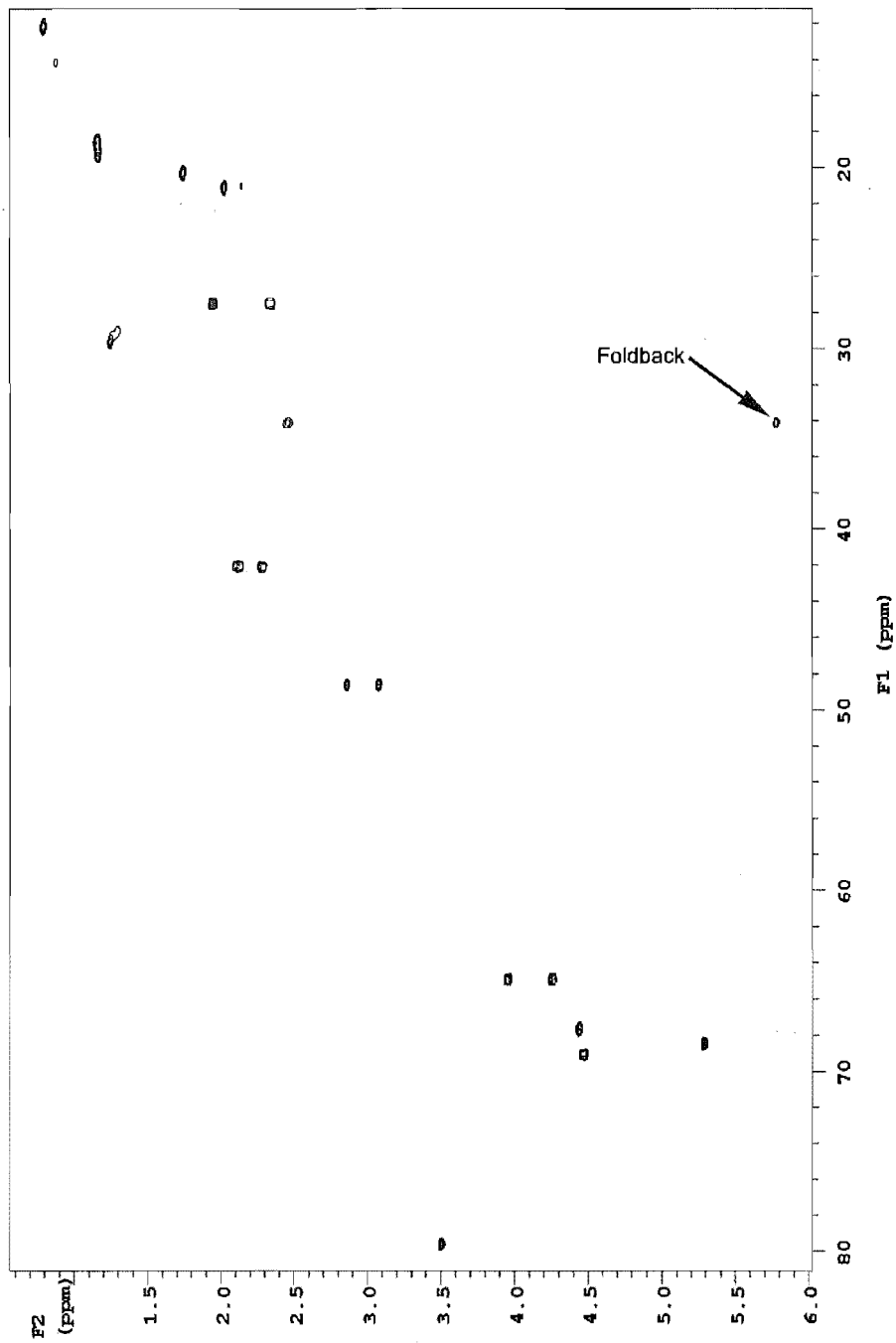

Figure 3.30: HSQC spectrum of **104** in $CDCl_3$

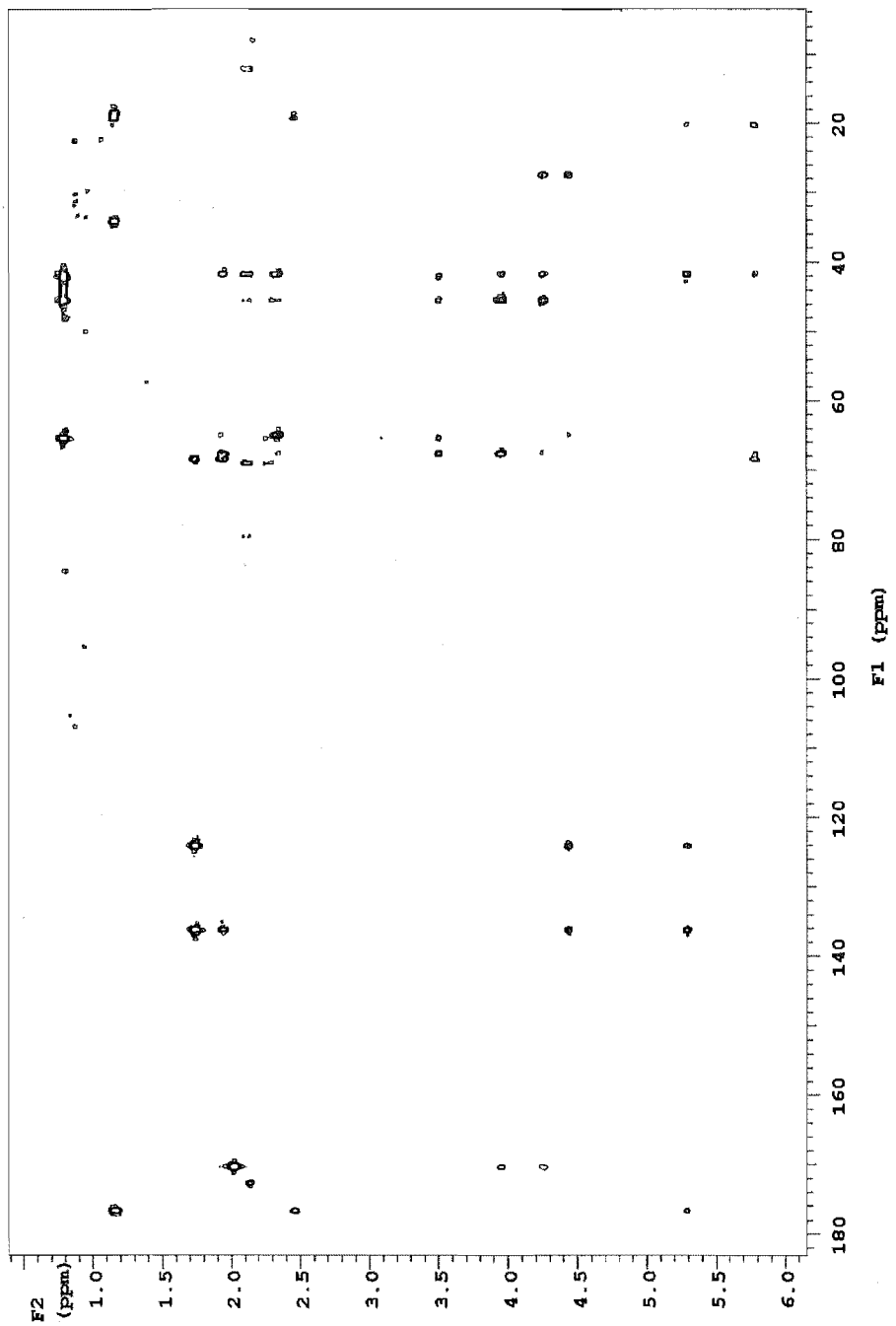

Figure 3.31: CIGAR spectrum of **104** in $CDCl_3$

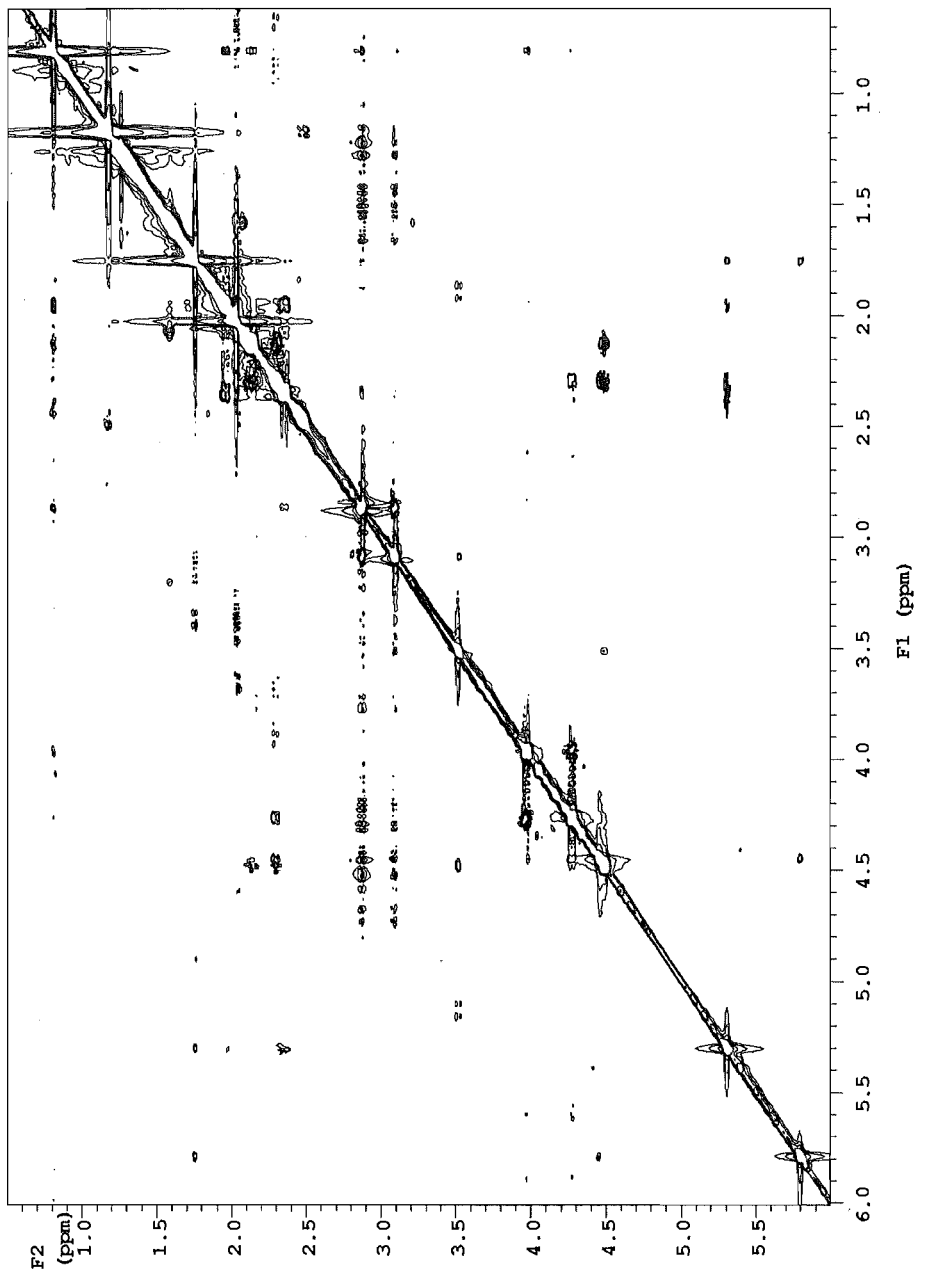

Figure 3.32: ROESY spectrum of **104** in $CDCl_3$

CHAPTER FOUR

WAI 7-1-1 & FOX 35-2-5 ~ UNIDENTIFIED *CEPHALOSPORIUM*-LIKE HYPHOMYCETES

4.1 Introduction.

Broth extracts from two apparently identical fungi (Wai 7-1-1 and Fox 35-2-5), cultured from driftwood collected near the mouth of the Waiho and Fox Rivers respectively, showed moderate cytotoxicity towards the P388 cell line (1498 ng/mL). Initial investigations (Section 4.2.1) of the crude extracts showed that the cytotoxic activities were centred on a single peak of moderately complex HPLC chromatograms (Figure 4.3). An intense yellow-green bis(naphtho-γ-pyrone) with excellent cytotoxicity against the P388 cell line (**116**, 774 ng/mL) was isolated and purified from culture extracts. The chromatography of this compound is discussed in Section 4.3 and the structural elucidation described in Section 4.4 of this chapter.

4.1.1 *Naphtho-γ-pyrones*

Naphtho-γ-pyrones are a large class of polyketide compounds with examples found in both marine and terrestrial organisms. Naphtho-γ-pyrones from the marine environment include **110** and **111**, both isolated from different species of crinoid.[119, 120] Naphtho-γ-pyrones from the terrestrial environment include **112** from the terrestrial plant *Cassia pudibunda*[121] and **113** - **114** from the fungi *Gaunomyces polythrix*[122, 123] and *Aspergillus parasiticus*.[124]

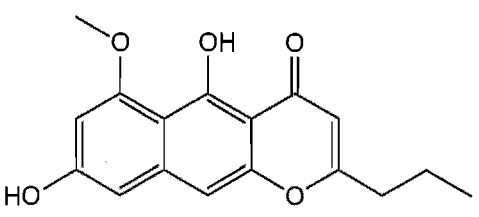

110

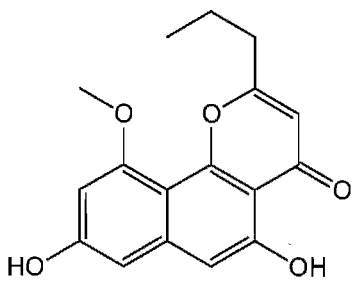

111

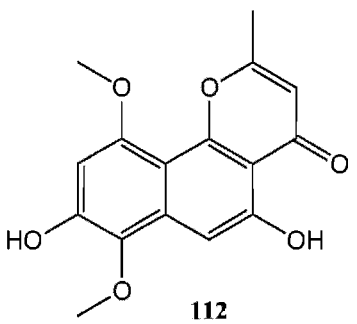

112

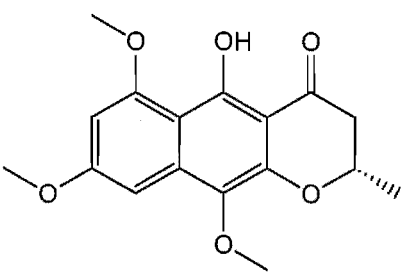

113

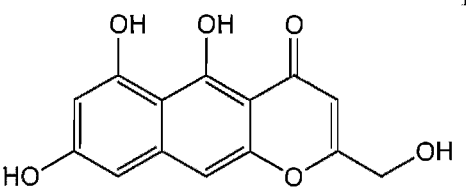

114

4.1.2 *Bis(naphtho-γ-pyrones)*

Bis(naphtho-γ-pyrones) consist of a naphthopyrone unit like those of **110** - **114** linked to a second naphtho-γ-pyrone unit through C^7, C^9 or C^{10} (Figure 4.1).

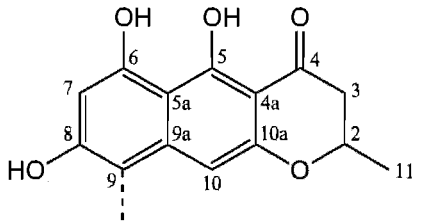

Figure 4.1: Numbering system for naphthopyrone derivatives

The bis(naphtho-γ-pyrones) include a number of different compounds such as chaetochromin D (**115**),[125] cephalochromin (**116**)[126] and fonsecinone C (**117**).[127]

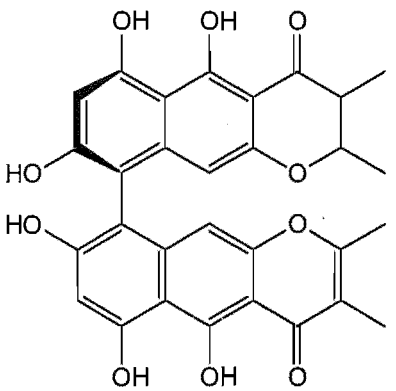

115

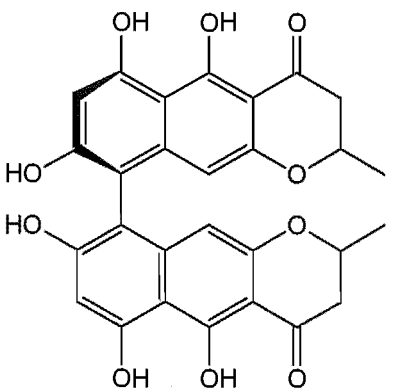

116

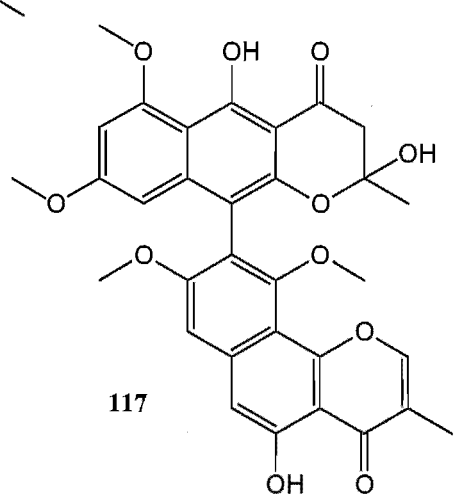

117

The occurrence of the bis(naphtho-γ-pyrones) appears to be limited to filamentous fungi such as *Aspergillus* spp, *Verticillium* spp, *Chaetomium* spp, *Cephalosporium* spp, *Nectria* spp and *Acremonium* spp.[102] The bis(naphtho-γ-pyrones) show a wide range of biological activities including cytotoxicity[128] and enzyme inhibition.[129]

4.2 Culturing and Extraction of Wai 7-1-1

4.2.1 Preliminary investigations

A *Cephalosporium*-like unidentified fungus, Wai 7-1-1, was isolated from driftwood collected at the low tide zone near the mouth of the Waiho River on the West Coast of the South Island of New Zealand in February 1999. This isolate produced an unusual green-brown pigment that was excreted into the medium (Figure 4.2) and also showed sporing characteristics similar to that of the *Cephalosporium* complex.

An EtOAc extract from a 1 mL broth culture of Wai 7-1-1 showed moderate cytotoxicity which, in association with its affiliation to a creative group of fungi made it an excellent candidate for chemical investigation. For the initial investigation the isolate was cultured in 500 mL PDB broth at 26°C for four weeks. Extraction of this broth culture with EtOAc and subsequent concentration under vacuum yielded a deep green-brown solid with significant cytotoxicity (1498 ng/mL).

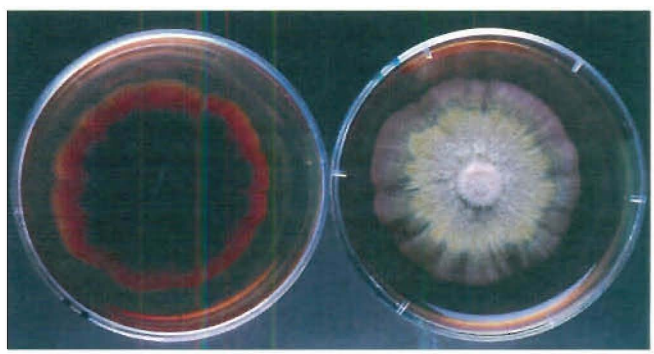

Figure 4.2: Fungal isolate Wai 7-1-1 grown on a seawater PDA plate.

4.2.1.1 Chemical screening

The small scale EtOAc extract was chromatographed on CBA, C_{18} and LH20 cartridges as in Section 3.2.1.1. Chromatography on C_{18} concentrated the cytotoxicity into the second fraction with significant carry over to the third fraction. Elution of the extract from the CBA cartridge also concentrated the bioactivity into the second fraction with a low level of activity eluting in the preceding fraction. This suggested that the compound(s) of interest were of medium to low polarity and positively charged.

Whilst fractionating the crude extract on an LH20 cartridge it was noted that a great deal of colour was retained on the column after the three initial fractions had been collected and even though colour intensity is not always attributable to the amount of material present, a further three fractions were collected. Biological activity was detected in fractions two to five from the LH20 cartridge with the cytotoxicity concentrated in fraction four. This suggested that the compound(s) of interest were either extremely small, being retained for a long time on the LH20 column, or they were interacting with the LH20 in some other fashion than just size exclusion.

4.2.1.2 HPLC bioassay

To obtain a chemical profile of the compound(s) responsible for the bioactivity of this extract an aliquot of the crude extract was chromatographed by reverse phase C_{18} HPLC as before in Section 3.2.1.2. The major region of bioactivity in this extract was centred on a single large peak in the HPLC chromatogram, eluting at approximately 16.5 minutes (Figure 4.3), which showed a very distinct spectrum with multiple UV absorption maxima (Figure 4.4).

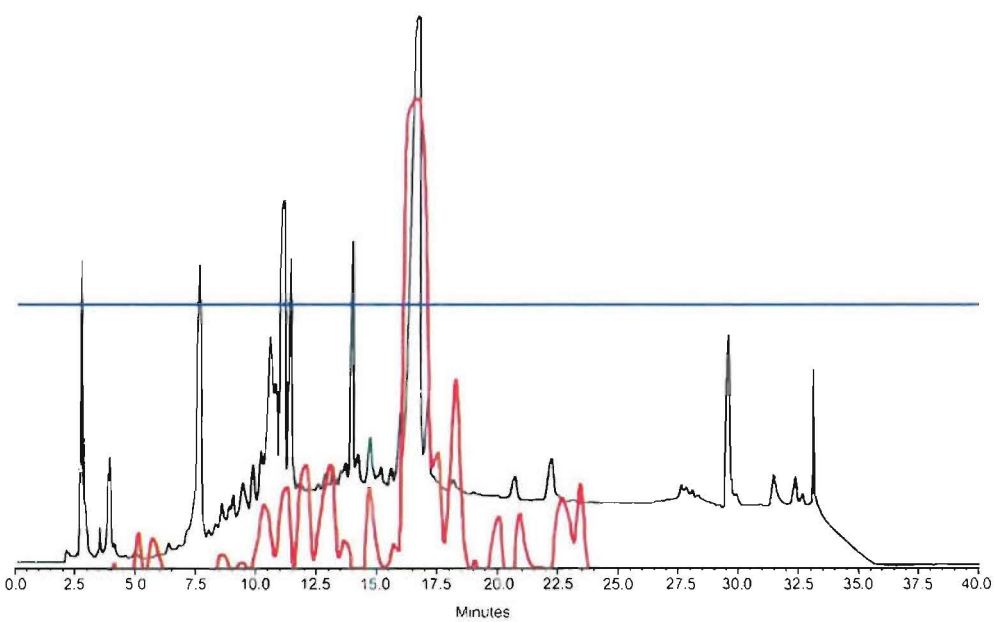

Figure 4.3: Spectrum max plot HPLC trace (black) and bioactivity data (red) of Wai 7-1-1 extract showing region of biological activity (the blue line represents 50% cell death).

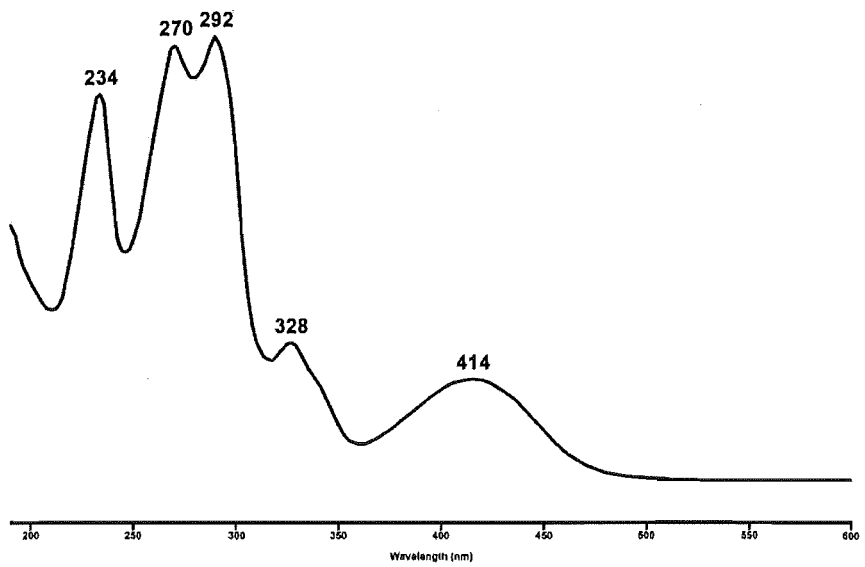

Figure 4.4: UV profile of bioactive peak from HPLC trace (16.5 minutes) as determined by microtitre plate assay

ESI-MS of the bioactive wells from the microtitre plate showed a very intense molecular ion at 519 Da (MH^+), although the elution profile from the LH20 cartridge had suggested that the mass was actually a lot smaller. A search in the Berdy Natural Products Database (BNPD) for a compound with similar UV maxima and a possible mass of 518 Da found two matches, cephalochromin (**116**)[129, 130] and ustilaginoidin F (**118**).[131, 132] These two compounds are atropisomers of each other.

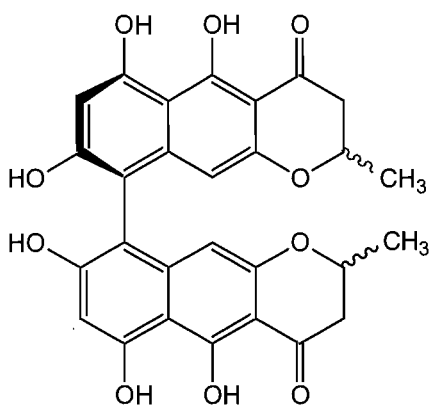

116

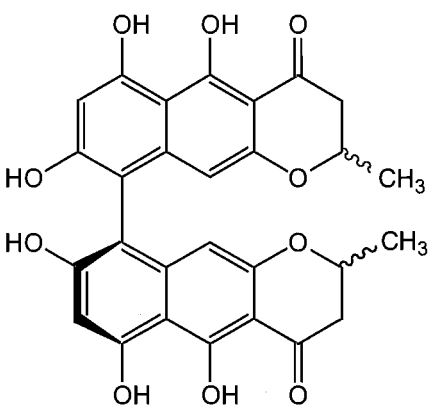

118

At this point a very limited amount of mass was available. To unambiguously assign the bioactive compound present in extracts of Wai 7-1-1 as either **116** or **118** a larger quantity of purified compound was required to obtain ^1H and ^{13}C NMR spectra for

comparison to the literature data.[126, 129, 131, 133] To this end a large scale extract was prepared.

4.2.2 Large scale culturing and extraction

To obtain adequate mass for an accurate identification of the active component, the fungal isolate Wai 7-1-1 was cultured in a further 4 L of half strength PDB under the same conditions as described in Section 4.2.1. Repeated extraction of this culture with distilled EtOAc, followed by solvent removal under vacuum yielded a deep brown-green solid (550.4 mg) with a similar bioactive profile to that of the small scale extract.

4.3 Chromatography of Wai 7-1-1

The chromatographic steps for the large scale extract of Wai 7-1-1 are shown in Scheme 4.1. A more detailed description of the chromatographic steps carried out on this extract can be found in the Experimental Section.

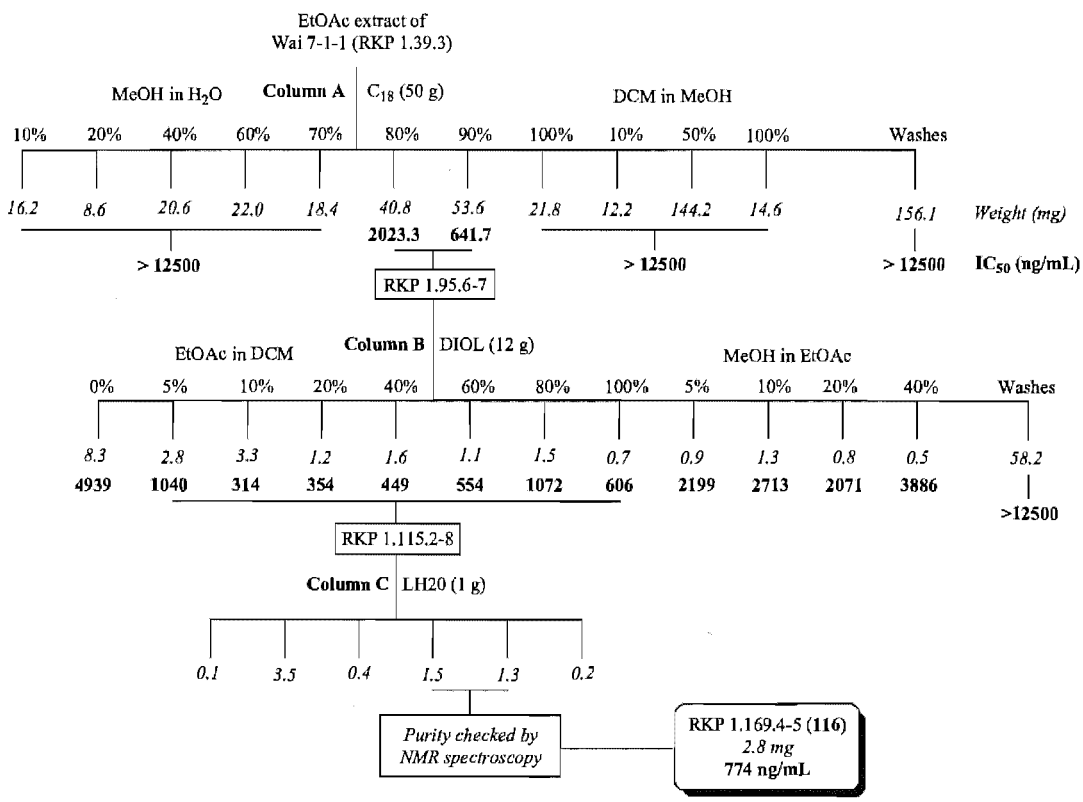

Scheme 4.1: Purification flow chart of an extract prepared from the fungal isolate Wai 7-1-1.

The large scale culture extract (550.4 mg) was initially fractionated on reverse-phase C_{18} (column A), using a stepped gradient solvent system for elution. The elution profile started at 10% H_2O in MeOH and increased to 100 % MeOH then changed to DCM in MeOH followed by a DCM wash. However, after eluting with 100 % DCM it was noted that a large amount of material was still retained on the column. To recover this extra material from the column it was washed three times with 0.05 % TFA in varying percentages of MeOH/DCM, then washed a further three times with 0.1 % NH_3 in MeOH/DCM. The two fractions (94.4 mg) that eluted between 80 and 90% MeOH/H_2O (RKP 1.95.6-7) were the only ones to show any cytotoxicity, 2023 and 641 ng/mL respectively. Analysis of these two fractions (RKP 1.95.6-7) and the two side fractions (RKP 1.95.5 and 8) by reverse-phase HPLC (Figure 4.5) showed that the active component of Wai 7-1-1 was only present in fractions 6 and 7, with ESI MS results also showing a large signal at 519 Da (MH^+) in these two fractions. ^1H NMR spectra of these two fractions indicated that they were not sufficiently pure for comparison to the literature NMR data of **116** and **118**.

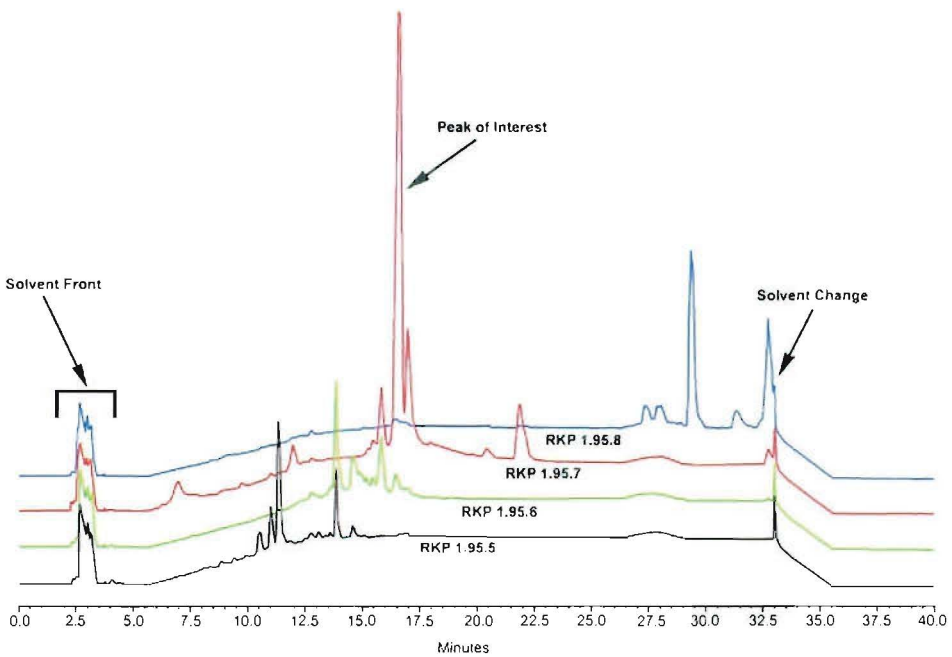

Figure 4.5: HPLC chromatogram of RKP 1.95.5-8

Based on analytical HPLC and bioassay data fractions 6 and 7 were combined and further purified by normal phase chromatography on DIOL (column B). The combined

bioactive fractions (RKP 1.95.6-7) were eluted off column B with a stepped gradient system similar to that for column B in Section 3.3. The gradient elution profile started at 100 % DCM, moved through to 100 % EtOAc and then to 100 % MeOH, collecting 15 fractions in total. However, after completion only half the total mass from RKP 1.95.6 and 7 had been recovered. The material retained on column B was recovered by eluting with MeOH in EtOAc and EtOAc in DCM, both with 0.05 % TFA with a further six fractions collected. Significant biological activity was detected from fractions 2 to 8, with moderate activity in fractions 1 and 9 to 12 and no activity in the late eluting fractions (13-21). At this point it was noted that the solubility of the biologically active fractions in MeOH was decreasing and as a result the purity of these fractions was subsequently determined by ^{1}H NMR spectroscopy rather than by analytical HPLC. The ^{1}H NMR spectra of fractions RKP 1.115.2-8 showed the same series of peaks in each fraction, but they also indicated the presence of a phthalate plasticizer. Based on the similarities in the ^{1}H NMR spectra and the similar biological activities these seven fractions were combined then further purified on a 1 g Sephadex LH20 column (column C). RKP 1.115.2-8 was eluted from column C with 100 % MeOH with six fractions collected in total. ^{1}H NMR spectroscopy of these six fractions located the bioactive component of Wai 7-1-1 in RKP 1.169.4 and 5 in a very high degree of purity. These fractions were combined and examined further with available NMR techniques.

4.3.1 Chromatography of Fox 35-2-5

The principal bioactive component of a small 1 mL extract from a second *Cephalosporium*-like fungus, Fox 35-2-5 was also thought to be the same as the bioactive component of Wai 7-1-1, but it was not until extraction and purification of the large scale extract that this was confirmed. Fox 35-2-5 was isolated from a section of driftwood collected in the water below the low tide zone at the Fox River mouth on the West Coast of the South Island of New Zealand in October 1998. This isolate was cultured in 4 L half strength PDB in the dark at 26°C for four weeks. However, after this time very little growth was observed so the cultures were left for a further four weeks, after which time subsequent extraction yielded a deep green solid (280 mg).

Earlier work on the extracts of Wai 7-1-1 showed that the bioactive component was strongly retained on Sephadex LH20 whilst allowing most of the inactive fungal metabolites to pass through. With this in mind a small amount (5 x 10 mg) of the extract was initially fractionated on a small scale 1 g Sephadex LH20 column (Scheme 4.2).

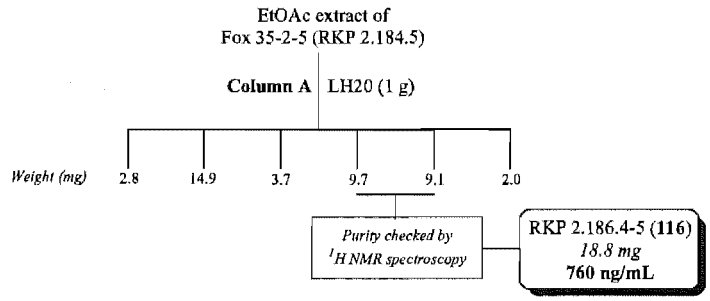

Scheme 4.2: Purification flow chart of an EtOAc extract of Fox 35-2-5.

The EtOAc extract of Fox 35-2-5 was eluted from the Sephadex LH20 column with 100 % MeOH, collecting a total of six 1 mL fractions. After 50 mg had been processed the purity of the fractions was determined by ^{1}H NMR spectroscopy, which indicated that the bioactive component of Wai 7-1-1 was present in fractions four and five in excess of 90 % purity, thus these two fractions were combined and examined further with available NMR techniques.

4.4 Structural elucidation of Fox 35-2-5

The NMR spectra were obtained in DMSO-d_6 rather than $CDCl_3$ due to solubility problems in the latter solvent. The ^{1}H NMR spectrum of the bioactive component of Fox 35-2-5 in DMSO-d_6 (Figure 4.6) revealed a methyl signal at δ_H 1.37, five proton signals at δ_H 2.77, 2.92, 4.55, 5.72, 6.52 and three phenolic hydroxyl signals at δ_H 9.9, 10.1 and δ_H 15.1. The ^{13}C APT spectrum (Figure 4.7) showed eight quaternary carbon resonances at δ_C 101.7, 104.3, 107.2, 141.6, 155.0, 158.7, 160.1, 164.9 and a carbonyl peak at δ_C 198.2. It also showed three tertiary carbon signals at δ_C 100.1, 98.6 and δ_C 73.0, a secondary carbon resonance at δ_C 42.8 and a primary carbon signal at δ_C 20.6.

A comparison of the experimental ^{1}H and ^{13}C NMR data for the bioactive component of Fox 35-2-5 with the literature data for **116** and **118** is shown in Table 4.1. The numbering system for the bis(naphtho-γ-pyrones) can be seen in Figure 4.1.

Number	Experimental NMR data of Fox 35-2-5		Literature NMR data for 116[131]		Literature NMR data for 118[131]	
	^{1}H, (J_{HH} Hz)	^{13}C	^{1}H, (J_{HH} Hz)	^{13}C	^{1}H, (J_{HH} Hz)	^{13}C
2 H	4.55 (3, 6, 12.5)	73.0	4.47 (7.3, 6.1)	73.3	4.43 (4.1, 5.9, 11.2)	73.3
3α H	2.77 (3, 17.5)	42.8	2.66 (7.3)	43.1	2.68 (4.1, 17.6)	43.1
3β H	2.92 (12.5, 17.5)	42.8	2.66 (7.3)	43.1	2.75 (11.2, 17.6)	43.1
4		198.2		198.4		198.2
4a		101.7		102.2		101.9
5 OH	15.1	164.9	14.9	164.4	15.16	164.6
5a		104.3		105.4		105.5
6 OH	10.1	158.7	9.6	160.1	9.74	160.2
7 H	6.52	100.1	6.49	100.1	6.55	100.1
8 OH	9.9	160.1	5.90	160.7	5.55	161.1
9 Dimer		107.2		102.4		102.4
9a		141.6		142.1		141.9
10 H	5.72	98.6	6.16	99.6	5.95	99.4
10a		155.0		156.3		156.2
11 CH_3	1.37 (6)	20.6	1.39 (6.1)	20.9	1.41 (5.9)	20.9

Table 4.1: Experimental NMR data in DMSO-d_6 for the bioactive component of Fox 35-2-5 and literature NMR data for **116** and **118** in $CDCl_3$.

As shown in Table 4.1 the carbon shifts for the experimental and two literature compounds are almost identical. However, the ^{1}H NMR data show a number of discrepancies (shown in red) between the experimental and literature values. This indicated that the bioactive compound in extracts of Wai 7-1-1 and Fox 35-2-5 was ustilaginoidin F (**118**) rather than cephalochromin (**116**). However, subsequent circular dichroism (CD) experiments suggested otherwise.

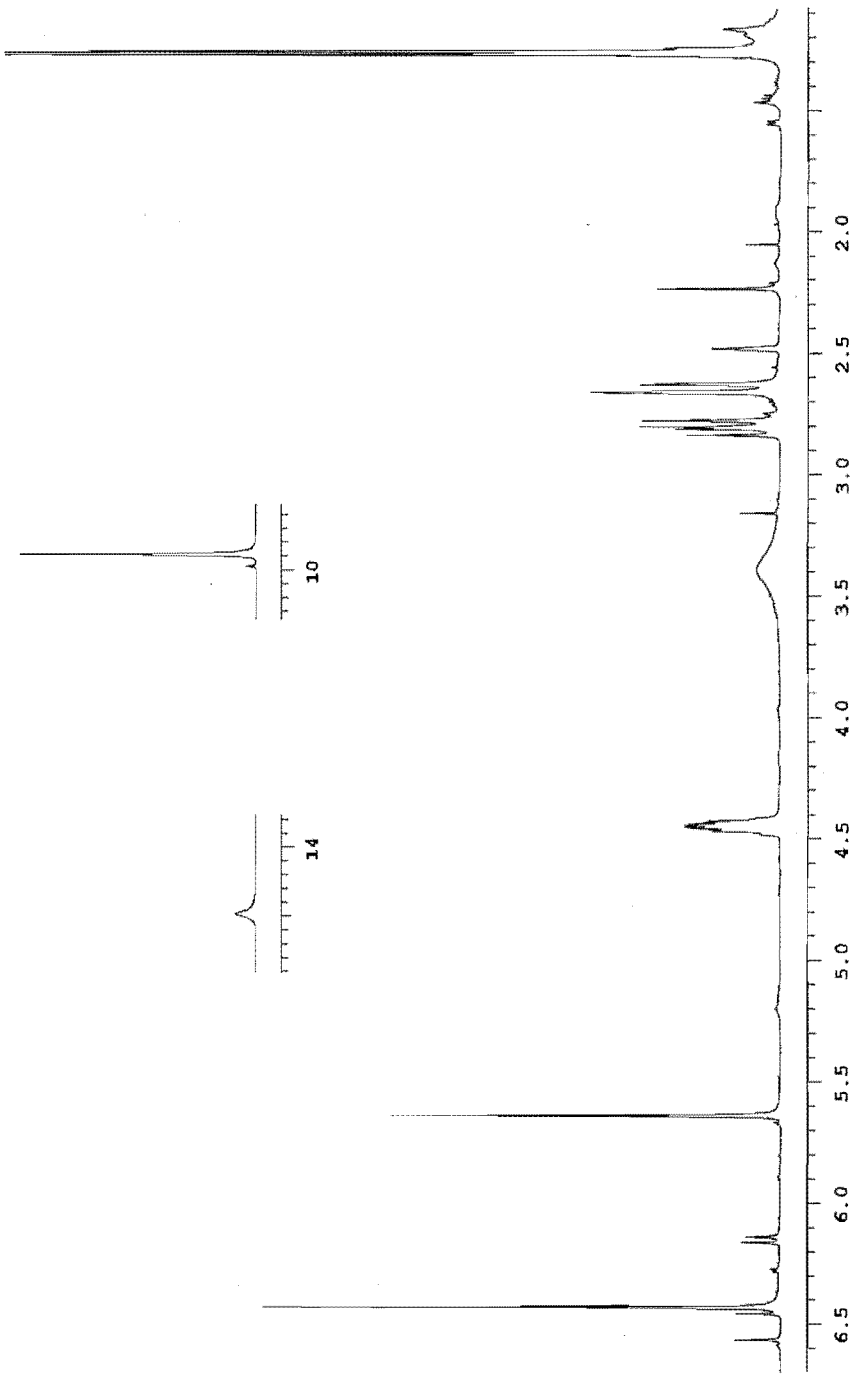

Figure 4.6: ^{1}H NMR spectrum of the active compound in Fox 35-2-5 extracts in DMSO-d_6

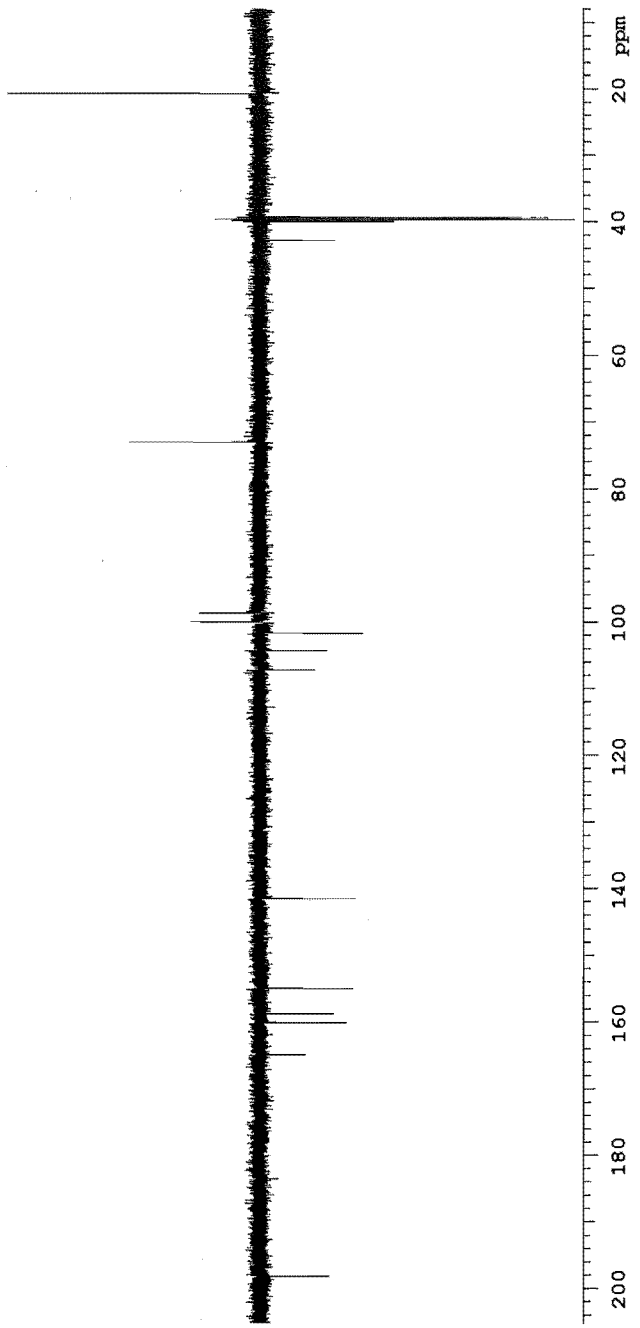

Figure 4.7: ^{13}C APT spectrum of the active compound in Fox 35-2-5 extracts in DMSO-d_6

4.4.1 Circular Dichroism of the active compound from extracts of Wai 7-1-1 and Fox 35-2-5

The absolute stereochemistry of chaetochromin A (**119**), a bis(naphtho-γ-pyrone) related to **116** and **118**, had previously been determined by x-ray crystallography.[133]

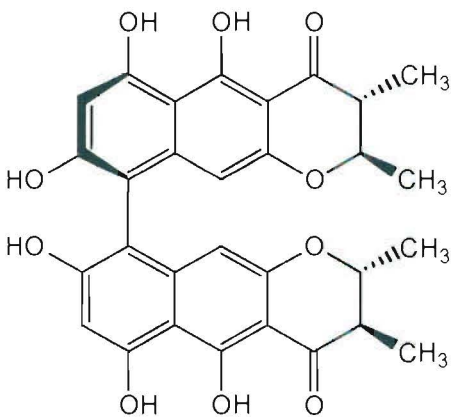

119

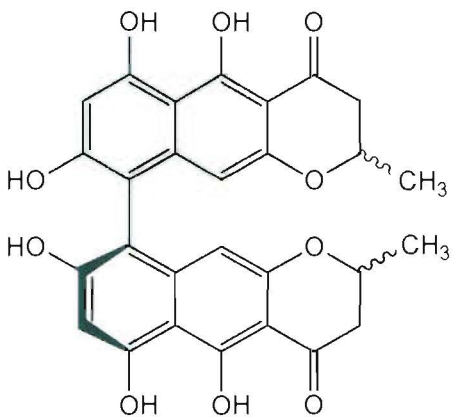

118

The CD spectra of chaetochromin A and cephalochromin have previously been shown to be the same.[132, 133] Figure 4.8a shows the literature CD spectra for chaetochromin A, cephalochromin and ustilaginoidin F. The experimental CD spectra for the bioactive compound in extracts of Wai 7-1-1 and Fox 35-2-5 in MeOH is shown is Figure 4.8b.

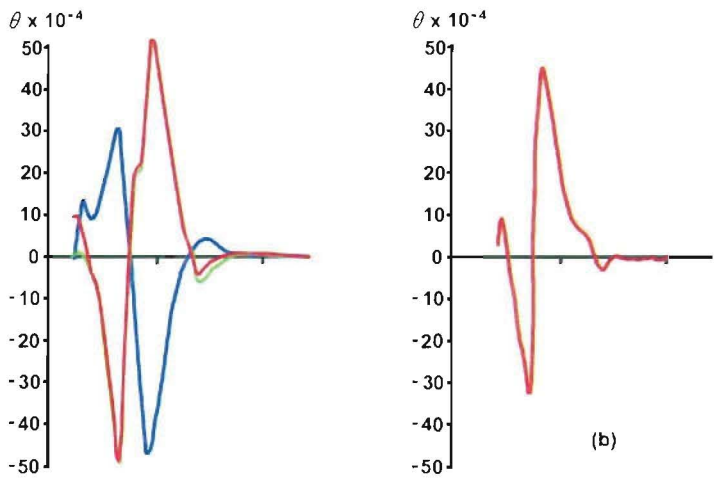

Figure 4.8: Literature CD spectra (a) for cephalochromin (red), chaetochromin A (green) and ustilaginoidin F (blue) in dioxane[132, 133] and experimental (b) CD spectra for the bioactive compound isolated from extracts of Wai 7-1-1 and Fox 35-2-5 in MeOH

Thus the correct stereochemistry around the C^{9}-$C^{9'}$ bond was able to be determined by comparison of the CD spectrum of the bioactive compound in extracts of Wai 7-1-1 and Fox 35-2-5 with those of **116** and **118**. It has been shown that a positive Cotton effect at

294 nm arises from the long axes about the C^9-$C^{9'}$ bond being twisted in a clockwise manner. The reverse is true for a negative Cotton effect.[133] The active compound of extracts of Wai 7-1-1 and Fox 35-2-5 showed positive first (θ 45 x 10^4 (294 nm)) and negative second (θ -35 x 10^4 (266 nm)) Cotton effects (Figure 4.8b) which were almost identical to that for **116** (Figure 4.8a).[132, 133] The slight differences between the two CD spectra were attributed to the different solvent systems in use.

The differences between the ^{1}H NMR spectra of **116** and the active compound in extracts of Wai 7-1-1 and Fox 35-2-5 were attributed to the use of a different solvent while obtaining the ^{1}H NMR spectrum. To confirm this a ^{1}H NMR spectrum of the active compound from extracts of Fox 35-2-5 in $CDCl_3$ was obtained and showed that the signals for the two protons on C^3 were replaced with a resonance at δ_H 2.74. Thus the active compound in extracts of Wai 7-1-1 and Fox 35-2-5 was identified as cephalochromin (**116**).[131]

4.5 Summary

An intense yellow-green pigment was purified from culture extracts of two *Cephalosporium*-like fungal isolates and identified using spectroscopic methods as cephalochromin (**116**). Table 4.2 shows experimental ^{1}H and ^{13}C data in DMSO-d_6 for **116**.

Number	^{1}H, multiplicity, (J_{HH} Hz)	HSQC/APT	CIGAR	NOESY
2 H	4.55 ddq (3, 6, 12.5)	73.0		2.93 , 2.74 , 1.37
3α H	2.77 dd (3, 17.5)	42.8	198.2 , 101.7	4.56 , 2.93 , 1.37
3β H	2.92 dd (12.5, 17.5)	42.8	198.2 , 73.0 , 20.6	4.56 , 2.74 , 1.37
4		198.2		
4a		101.7		
5 OH	15.1	164.9		10.06 , 9.88
5a		104.3		
6 OH	10.1	158.7		15.08 , 9.88
7 H	6.52 s	100.1	160.1 , 158.7 , 107.2 , 104.3	9.88
8 OH	9.9	160.1	160.1 , 107.2 , 100.1	15.08 , 10.06 , 6.55
9 Dimer		107.2		
9a		141.6		
10 H	5.72 s	98.6	155.0 , 107.2 , 104.3 , 101.7	
10a		155.0		
11 CH_3	1.37 d (6)	20.6	73.0 , 42.8	4.56 , 2.93 , 2.74

Table 4.2: ^{1}H and ^{13}C NMR data for the bioactive component of an extract of Fox 35-2-5 in DMSO-d_6

CHAPTER FIVE

GIL 12-1-3 ~ *ALTERNARIA* SP

5.1 Introduction

Broth extracts from Gil 12-1-3, an *Alternaria* sp cultured from driftwood collected below low tide at Gilespies Beach, showed moderate cytotoxicity against the P388 cell line (9.7 μg/mL) but no antimicrobial or antiviral activity. This fungal isolate was targeted for further chemical investigation because preliminary investigations (Section 5.2.1) of the crude extract showed that the cytotoxicity was centred on a single peak in a very complex HPLC chromatogram (Figure 5.2). An intense yellow pigment (**141**) with significant cytotoxicity against the P388 cell line (0.68 μg/mL) was isolated and purified from extracts of this fungus. The chromatography of this compound is discussed in Section 5.3 and the structural elucidation described in Section 5.4 of this chapter.

5.1.1 Economic importance of *Alternaria* spp

Many *Alternaria* spp are responsible for major crop losses worldwide, through either plant diseases or contamination of animal feed. Diseases caused by *Alternaria* spp include early blight of potato and tomato by *Alternaria solani*,[134] black spot of onion by *A. porri*[135] and wheat by *A. alternata* and *A. triticina*.[136] The degree of pathogenicity by *Alternaria* spp varies depending on the type of toxin the pathogen produces. These are either host specific (HS) or non-specific toxins.

5.1.2 HS Toxins from *Alternaria* spp

HS toxins are highly toxic to a specific plant species or cultivar that serves as a host for the fungus, and are generally required for fungal pathogenesis to occur. Other plant species, or resistant cultivars, can tolerate a much higher dosage of the same toxin that would generally kill a susceptible plant. All HS toxin producing *Alternaria* strains are extremely pathogenic towards their hosts. However, strains that are unable to produce HS toxins are not pathogenic.[136] Several HS toxins have been isolated, for example maculosin (**120**) and destruxin B (**121**). A fuller list is given in Table 5.1.

Fungal Species	*Toxin*	*Host plant*
Alternaria alternata	Maculosin (**120**)[137]	*Centaurea maculosa* Lam. (Spotted Knapweed)
A. brassicae	Destruxin B (**121**)[138]	Rapeseed
A. mali	AM Toxin (**122**)[139]	Apple, Pear
A. citri	ACTG Toxin (**123**)[139]	Citrus (Dancy Tangerine)
A. citri	ACRL Toxin (**124**)[139]	Citrus (Rough Lemon)
A. kikuchiana	AK Toxin (**125**)[139]	Japanese Pear
A. kikuchiana	AF Toxin (**126**)[139]	Japanese Pear, Strawberry
A. alternata f. sp. *lycopersici*	AAL Toxin TA1 (**127**)[139]	Tomato

Table 5.1: HS toxins isolated from species of *Alternaria*.

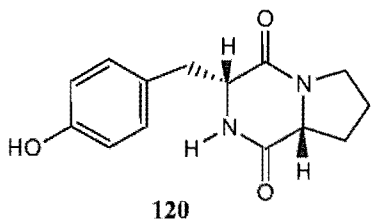

120

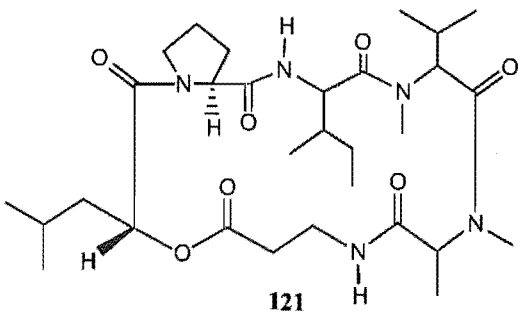

121

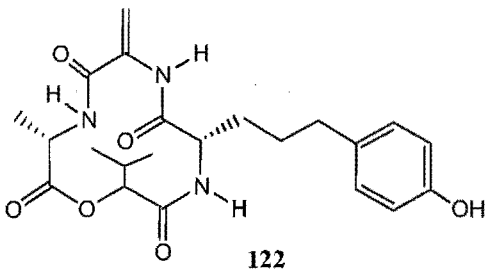

122

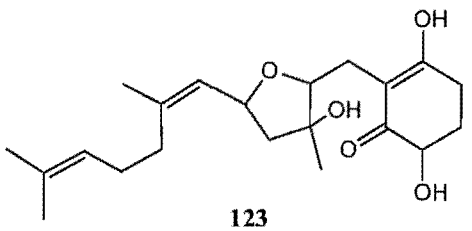

123

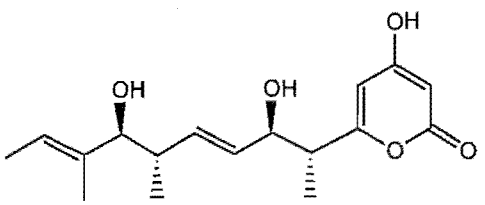

124

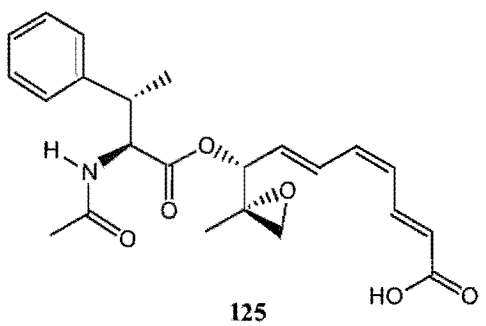

125

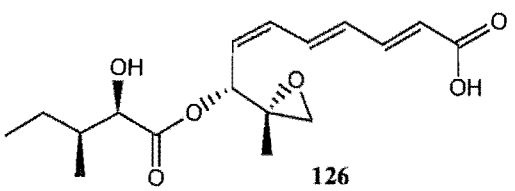

126

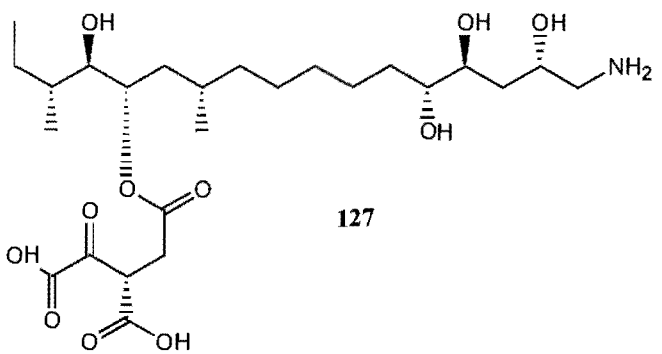

127

5.1.3 Non-specific toxins from *Alternaria* spp

Non-specific toxins are typically less damaging to host plants and a large number of these toxins have been isolated from *Alternaria* spp. A small proportion of this total are listed in Table 5.2.

Fungal Species	*Toxin*
Alternaria solani	Altersolanol A (**128**)[140]
Alternaria solani	Hydroxybostrycin (**129**)[141]
Alternaria tagetica	Zinniol (**130**)[142]
Alternaria porri	Alterporriol A (**131**)[143]
Alternaria solani	Tetrahydroaltersolanol B (**132**)[144]
Alternaria porri	Macrosporin (**133**)[145]
Alternaria alternata	Altertoxin I (**134**)[146]
Alternaria tenuis	Alternariol (**135**)[147]
Alternaria kikuchiana	Tenauzonic Acid (**136**)[147]

Table 5.2: Some non-specific toxins isolated from *Alternaria* spp.

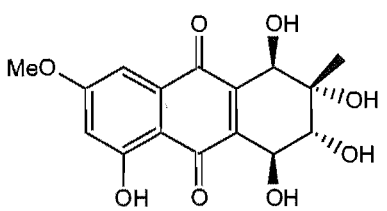

128

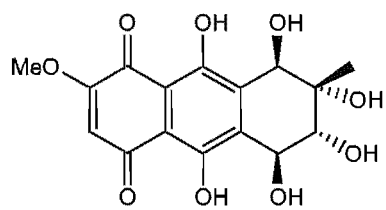

129

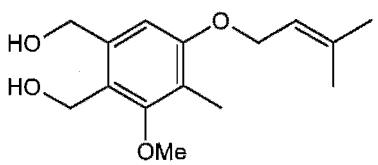

130

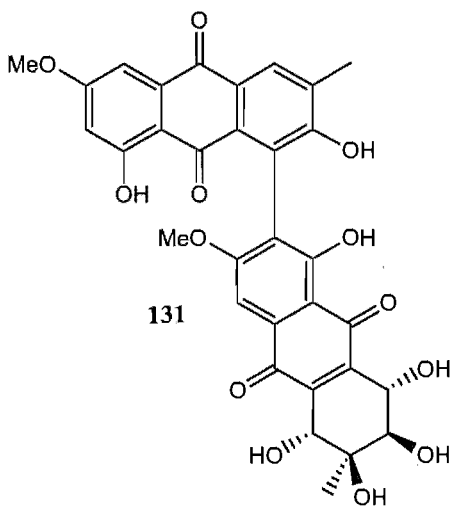

131

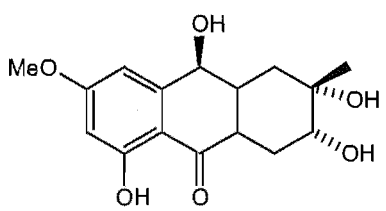

132

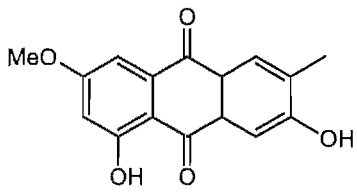

133

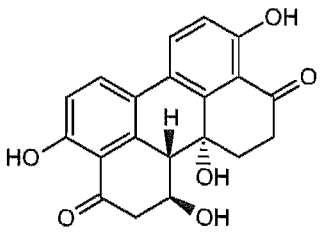

134

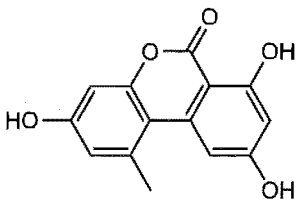

135

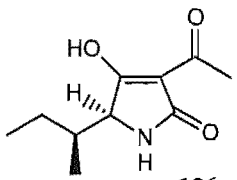

136

Many of these compounds, such as altersolanol A (**128**)[148] and zinniol (**130**),[142] have also been reported as dimers.[135, 143] All of these compounds have been shown to be phytotoxic, however some also show additional biological activities. Altersolanols A-C are both antibacterial[140] and cytotoxic.[145, 147, 149] The altertoxins (**134**) are weakly mutagenic in the Ames *Salmonella typhimurium* assay,[146] and both tenauzonic acid (**136**) and the dibenzo-α-pyrones, such as alternariol (**135**), are also cytotoxic. These last two compounds have been repeatedly isolated from *Alternaria* strains commonly found contaminating feedstuffs and as such are considered a major class of *Alternaria* toxins.[147] Although many *Alternaria* spp have been isolated from the marine environment only one, *Alternaria maritima*, was ever considered as of marine origin.[32] Doubt was later cast on this identification by Kohlmeyer and Kohlmeyer, due in part to a lack of fungal material available for confirmation of identity.[55]

5.2 Culturing and extraction of Gil 12-1-3

5.2.1 Preliminary investigations

Gil 12-1-3 was isolated from driftwood collected at the intertidal zone of Gillespies Beach on the West Coast of the South Island of New Zealand in February 1999. After purification, the isolate was cultured in 250 mL PDB broth for 28 days, at 26°C in the

dark. Extraction with EtOAc and subsequent concentration under vacuum yielded a dark brown oily solid showing moderate cytotoxicity (9.7 µg/mL).

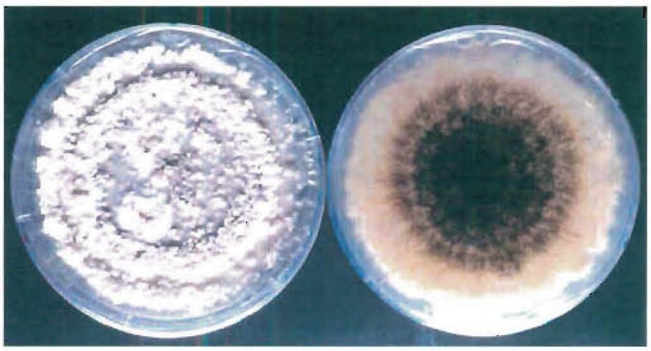

Figure 5.1: Fungal isolate Gil 12-1-3, an *Alternaria* sp, grown on seawater PDA plates.

5.2.1.1 Chemical screening

The chemical properties (polarity, charge and size) of the small scale extract of Gil 12-1-3 were examined by "chemical screening" as in Section 3.2.1.1.

Chromatography on C_{18} concentrated the cytotoxicity to the MeOH/water fraction, with slight carry over into the MeOH fraction, indicating that the cytotoxic compounds were of high to medium polarity. The highest degree of cytotoxicity eluting from the LH20 cartridge was seen in the last fraction, indicating that the bioactive compound(s) were small to medium in size (< 500 Da). The highest level of cytotoxicity seen from CBA was in the first fraction, signifying that the compound(s) of interest were uncharged.

5.2.1.2 HPLC Microtitre plate screening

To obtain a chemical profile of the compounds responsible for the bioactivity an aliquot of the crude extract was chromatographed with reverse phase C_{18} HPLC as before in Section 3.2.1.2. The microtitre plate was then assayed for cytotoxicity against the P388 cell line. The cytotoxicity of this extract was concentrated to a single peak in the HPLC chromatogram, which eluted at 8.5 minutes (Figure 5.2) and displayed a very distinct UV spectrum (Figure 5.3).

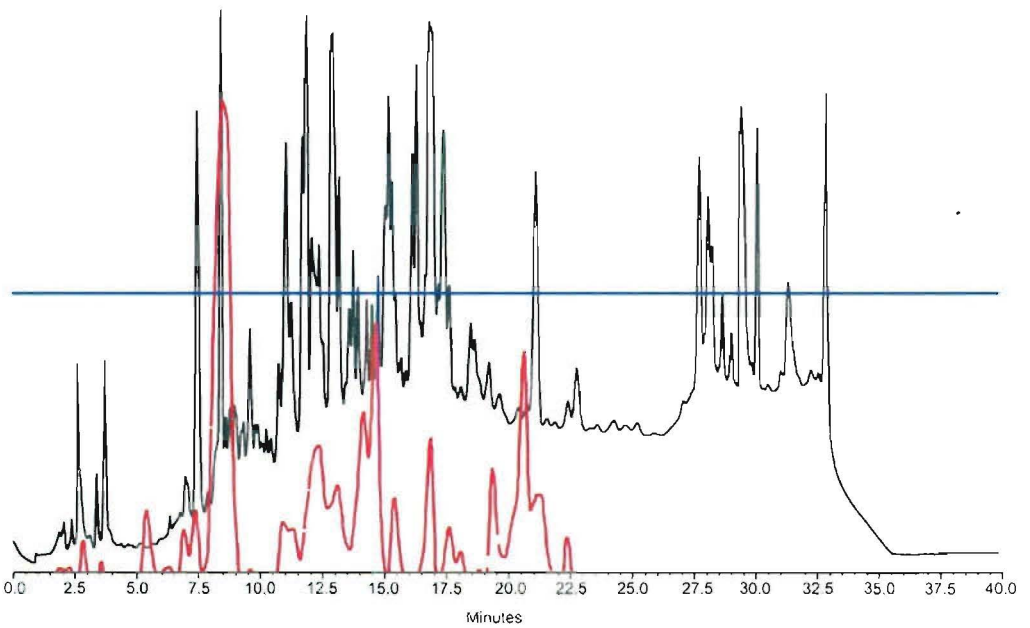

Figure 5.2: Spectrum max plot HPLC trace (black) and bioactivity data (red) of Gil 12-1-3 with region of biological activity at 8.5 minutes (The blue line represents 50% cell death).

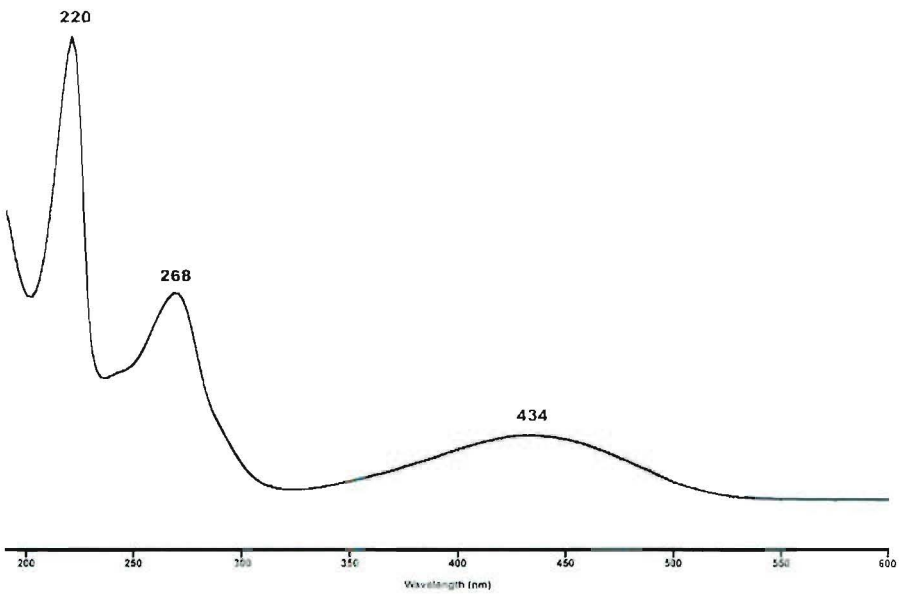

Figure 5.3: UV profile of bioactive peak from HPLC trace (8.5 minutes) as obtained from microtitre plate fraction

Based on the HPLC microtitre plate assay the following assumptions regarding this compound were made: first, the intense yellow colour and the UV-visible spectrum indicated that the compound of interest contained a highly conjugated system, and the

peaks at 220 and 268 nm in the UV-visible chromophore were also characteristic of a quinone moiety (**137**).[140]

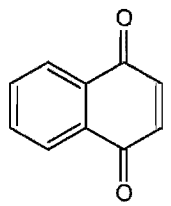

137

Secondly, initial positive ESI-MS results from selected bioactive wells of the microtitre plate showed an intense signal at 338 Da (MH^+) which suggested the presence of a nitrogen atom. A search in both MarinLit and Antibase with these parameters found no matches, therefore further work was deemed necessary.

Based on the observations from chemical screening and the HPLC microtitre plate this sample was initially separated using reverse-phase chromatography on C_{18}.

5.2.2 Large scale culturing and extraction

As the initial small scale extract displayed significant biological activity, Gil 12-1-3 was cultured in a further 2 L of half strength PDB broth under the same conditions as described previously (Section 5.2.1). Repeated extraction of this culture with distilled EtOAc, followed by solvent removal under vacuum, resulted in a deep brown oil (149.2 mg) displaying a bioactivity profile similar to that seen in the original extract (Figure 5.2).

5.3 Chromatography of Gil 12-1-3 extracts

5.3.1 Chromatography of the large scale extract

The chromatographic steps for the large scale extract of Gil 12-1-3 are given in Scheme 5.1. A more detailed description of chromatographic steps is given in the Experimental Section.

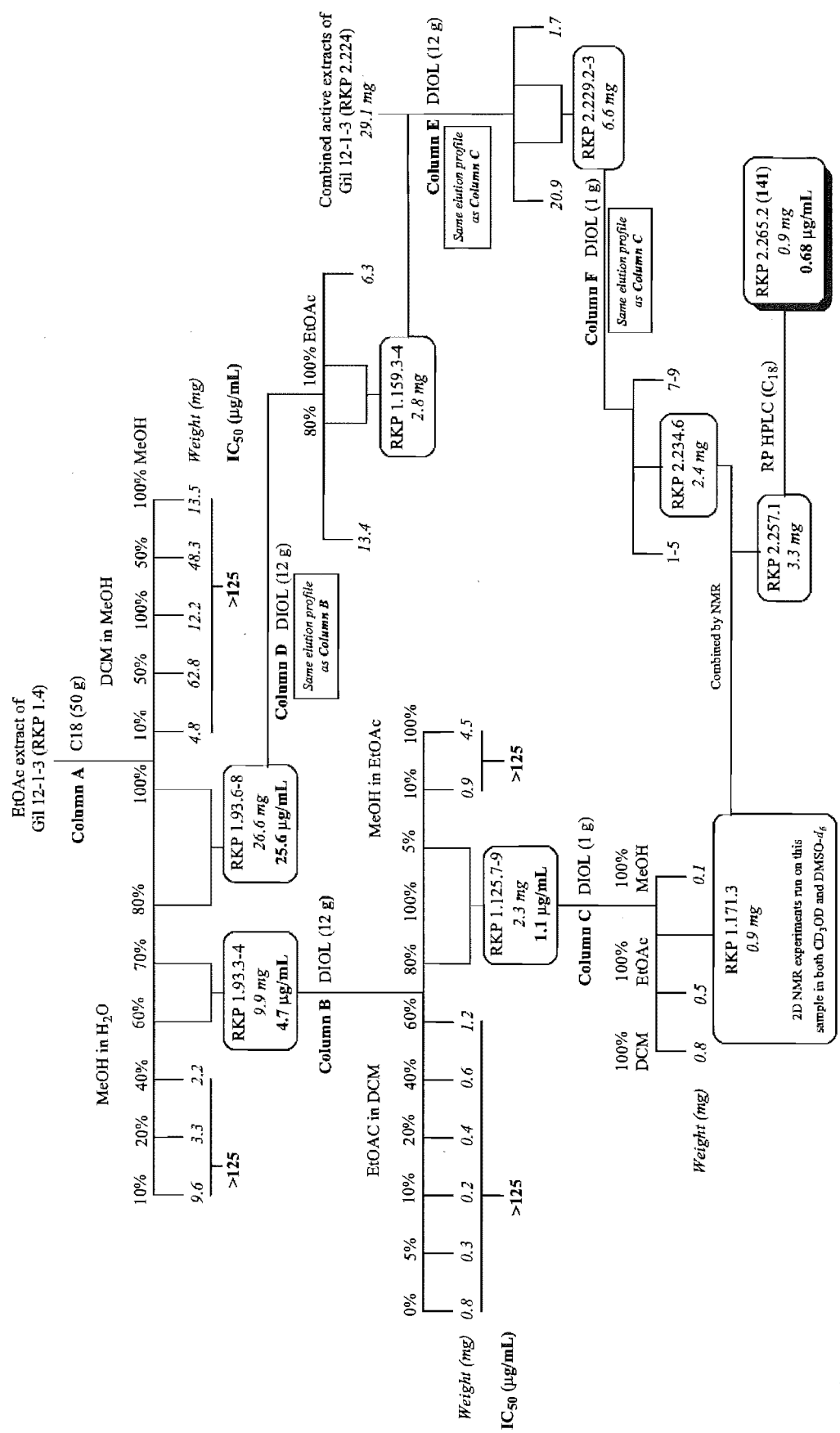

Scheme 5.1: Purification flow chart of extracts prepared from fungal isolate Gil 12-1-3.

The complete large scale culture extract (149.2 mg) was initially purified by reverse-phase C_{18} (column A). A stepped gradient solvent system was used for sample elution, ranging from 10% H_2O in MeOH to 100 % MeOH, through to DCM and followed by a final MeOH wash. The fractions (9.9 mg) that eluted between 60 and 70% MeOH/H_2O (RKP 1.93.4-5) were the most active against P388 with IC_{50} values of 4.7 µg/mL and 9.7 µg/mL respectively. Purity analysis by reverse-phase HPLC (Figure 5.4) showed that these fractions contained a number of compounds, including the compound of interest, as determined earlier from the HPLC microtitre plate (Section 5.2.1.2).

Based upon analytical HPLC, assay and mass spectrometry data, fractions 4 and 5 were combined and further purified with normal phase chromatography on DIOL (column B). RKP 1.93.4 and 5 were eluted off DIOL column B using a stepped gradient from DCM through to EtOAc, then MeOH, collecting a total of 12 fractions. Cytotoxicity was seen in fractions that eluted between 20 % DCM and 100 % EtOAc (RKP 1.125.7-8). Analysis of these fractions by HPLC showed a higher degree of purity (Figure 5.5), but ^{1}H NMR spectroscopy indicated the presence of a phthalate plasticizer in the sample, so a further purification step on normal phase DIOL was performed (column C). Six fractions were collected, with the coloured compound being present in only one of these, RKP 1.171.3 (0.9 mg).

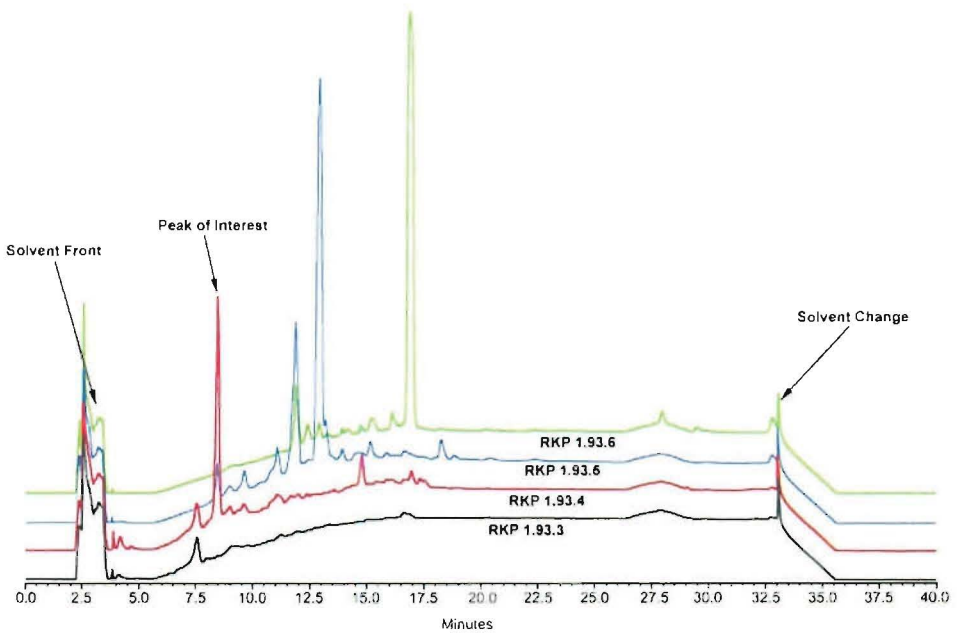

Figure 5.4: Analytical reverse-phase HPLC of fractions RKP 1.93.3 to RKP 1.93.6.

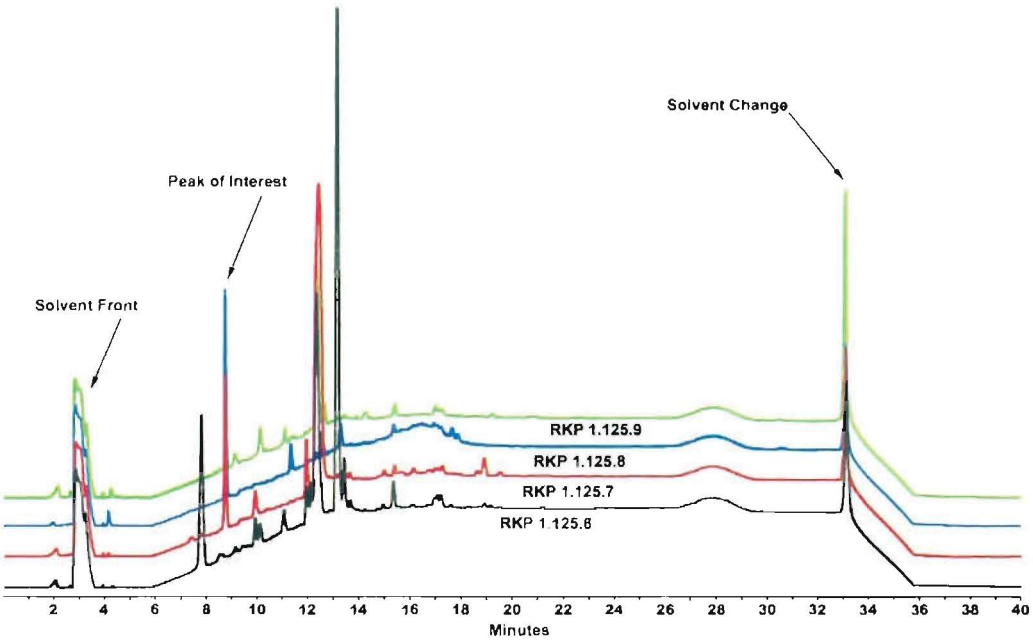

Figure 5.5: Analytical reverse-phase HPLC of fractions RKP 1.125.6 to RKP 1.125.9.

Due to the low mass recovered from column C, and as the compound of interest was highly coloured, the presence of **141** was henceforth determined by analytical HPLC, rather than by its biological activity. Although only approximately 0.9 mg of **141** was recovered, RKP 1.171.3 was examined by 1D and 2D NMR, with the structural elucidation of **141** described in Section 5.4.

5.3.1.1 Chromatography of the combined fractions

The recovered mass of **141** was very low (< 1 mg) and thought to be insufficient for a full structural identification. As a result attempts were made to re-culture the isolate Gil 12-1-3. Revival attempts from storage on agar slopes, the original isolation plate, or from cold storage at -80°C all failed. It was therefore decided to combine all bioactive fractions from the chemical screening and the side fractions from columns A and B.

The combined fractions (26.6 mg) were chromatographed on DIOL (column D) using a stepped gradient system from DCM to EtOAc to MeOH, with the yellow compound eluting at 100 % EtOAc, fractions RKP 1.159.3 and 4 (1.1 mg and 1.7 mg respectively). Analysis of these fractions by HPLC indicated the presence of numerous impurities and

as a result fractions RKP 1.159.3 and 4 were purified further on normal phase DIOL (column E) using a similar elution profile to that of column D. Both HPLC and ^{1}H NMR spectroscopy (CD_3OD) of fraction six (RKP 2.234.6) from this DIOL column showed a high degree of purity and as a result was combined with RKP 1.171.3 to give 3.2 mg. A ^{1}H NMR spectrum of the combined fraction (RKP 2.257.1) in CD_3OD initially showed a high degree of purity but after transfer to DMSO-d_6 multiple new signals were observed. When this fraction was re-analysed by analytical reverse phase HPLC multiple new peaks were seen in the HPLC trace. As a result RKP 2.257.1 underwent a final purification step by analytical reverse phase HPLC, with the yellow compound collected as it eluted off the column, RKP 2.265.2 (1.0 mg). As the mass recovered for this sample was similar to that obtained during initial chromatographic steps further 1D and 2D NMR experiments were deemed unnecessary.

5.4 Structural elucidation of 141

Attempts to obtain the molecular mass and molecular formula of compound **141** were relatively unsuccessful, as ESI-MS data varied between injections, which indicated that the sample did not ionise well in either positive or negative ion modes in relation to sample contaminants. This compound was also analysed using alternative methods of ionisation (EI and LC-APcI) but the results obtained could not be rationalised. EI-MS suggested the parent ion to be 335 Da, but LC-APcI suggested a mass of 291 (MH^-) in negative ion mode and 261 (MH^+) in positive ion mode. The difference of 32 Da between positive and negative ion modes was attributed to the loss of a methoxyl group, hence the molecular ion was postulated to be 292 Da. It was not until the structure of **141** had been proposed from the NMR data that the mass data were able to be rationalised. Re-examination of the ESI-MS data (Figure 5.6) from active wells of the microtitre plate (Section 5.2.1.2) showed intense signals at 359 and 695 Da in positive ion mode (MNa^+ and M_2H^+ respectively), and a very weak signal at 337 (MH^+). A negative ion ESI-MS of purified **141** showed a single intense signal at 335 (MH^-) and, when coupled to the data from positive mode ESI-MS, indicated that the mass of compound **141** was 336 Da. The difference of 1 mass unit between the mass used for

the initial search in Antibase (MH^+ 338 Da) and the mass obtained after purification (MH^+ 337 Da) was attributed to variations in the calibration of the instrument.

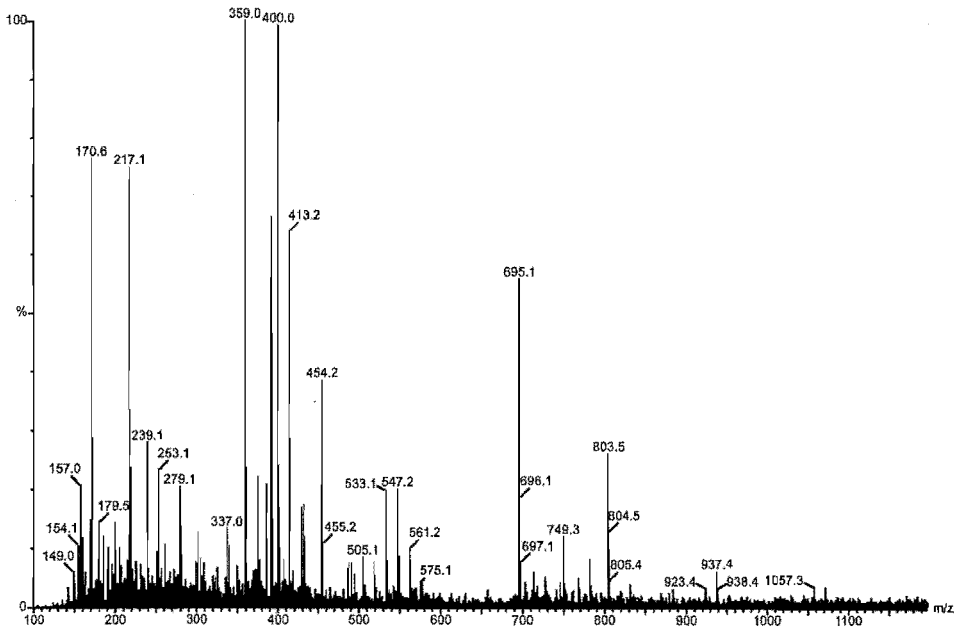

Figure 5.6: Low resolution ESI-MS of active wells from a microtitre plate assay.

The ^1H NMR spectrum (Figure 5.7) of **141** (CD_3OD) was very simple showing only eight signals, a methyl singlet (δ_H 1.42), an *O*-methyl (δ_H 3.91), a pair of aromatic proton signals (δ_H 7.15 and 6.74) and three methine signals (δ_H 3.84, 4.51 and 4.73). A small coupling constant of 2.5 Hz was seen between the aromatic signals at δ_H 7.15 and 6.74 which indicated a 1,3 relationship. The 2D NMR experiments, including HSQC (Figure 5.16) and CIGAR (Figure 5.17) carried out on this sample in CD_3OD were insufficiently definitive to allow total structural assignment of **141**.

During purification it had been noted that this sample was very polar and therefore assumed to be highly oxygenated. If the oxygen atoms were present as hydroxyl groups then some signals might not be observed in the ^1H NMR spectrum when dissolved in CD_3OD due to deuterium exchange. Thus **141** was re-examined in DMSO-d_6, which revealed five new signals in the ^1H NMR spectrum (Figure 5.8). As a result further HSQC and CIGAR experiments were performed on this sample in DMSO-d_6.

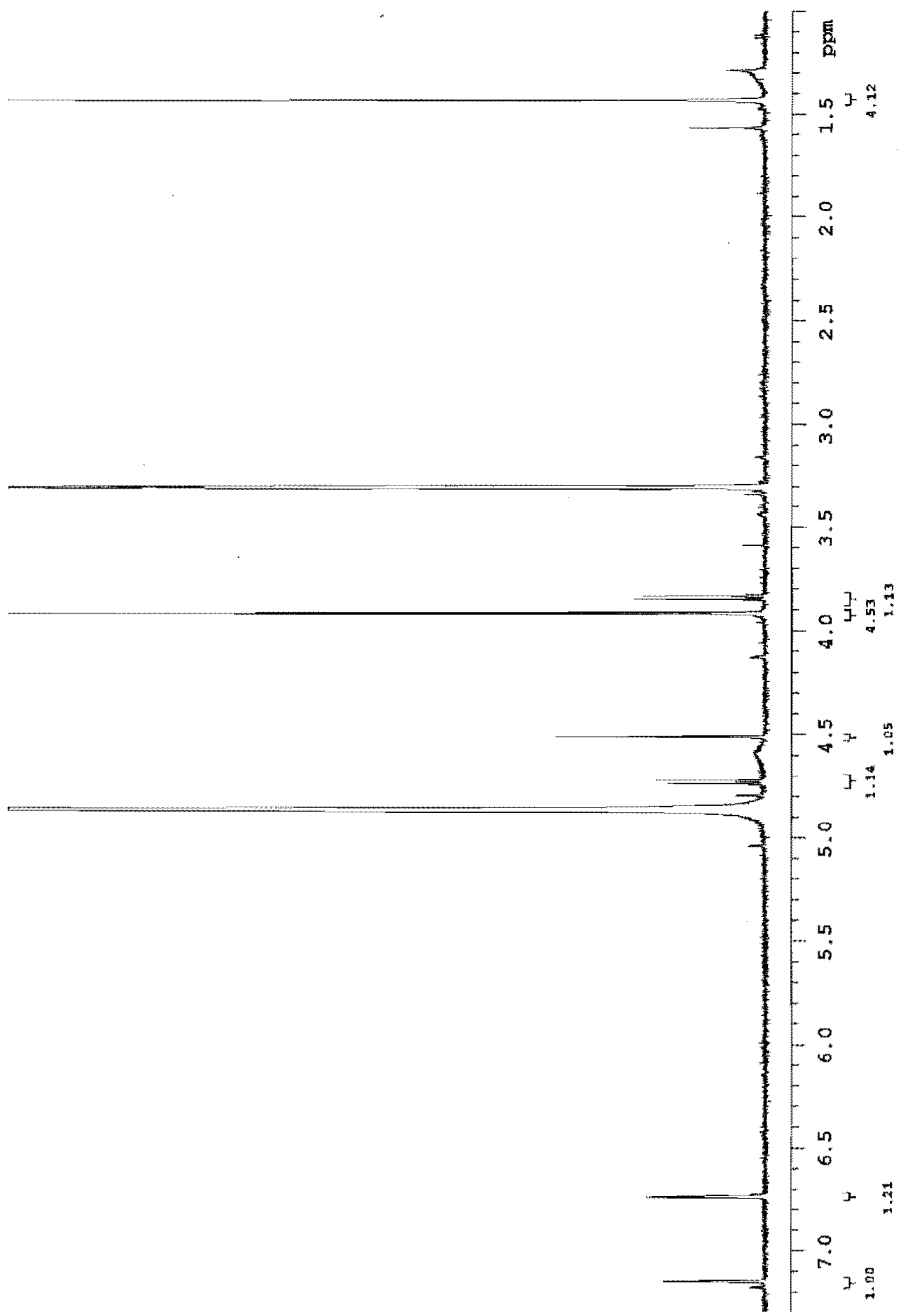

Figure 5.7: ^{1}H NMR spectrum of **141** in CD_3OD.

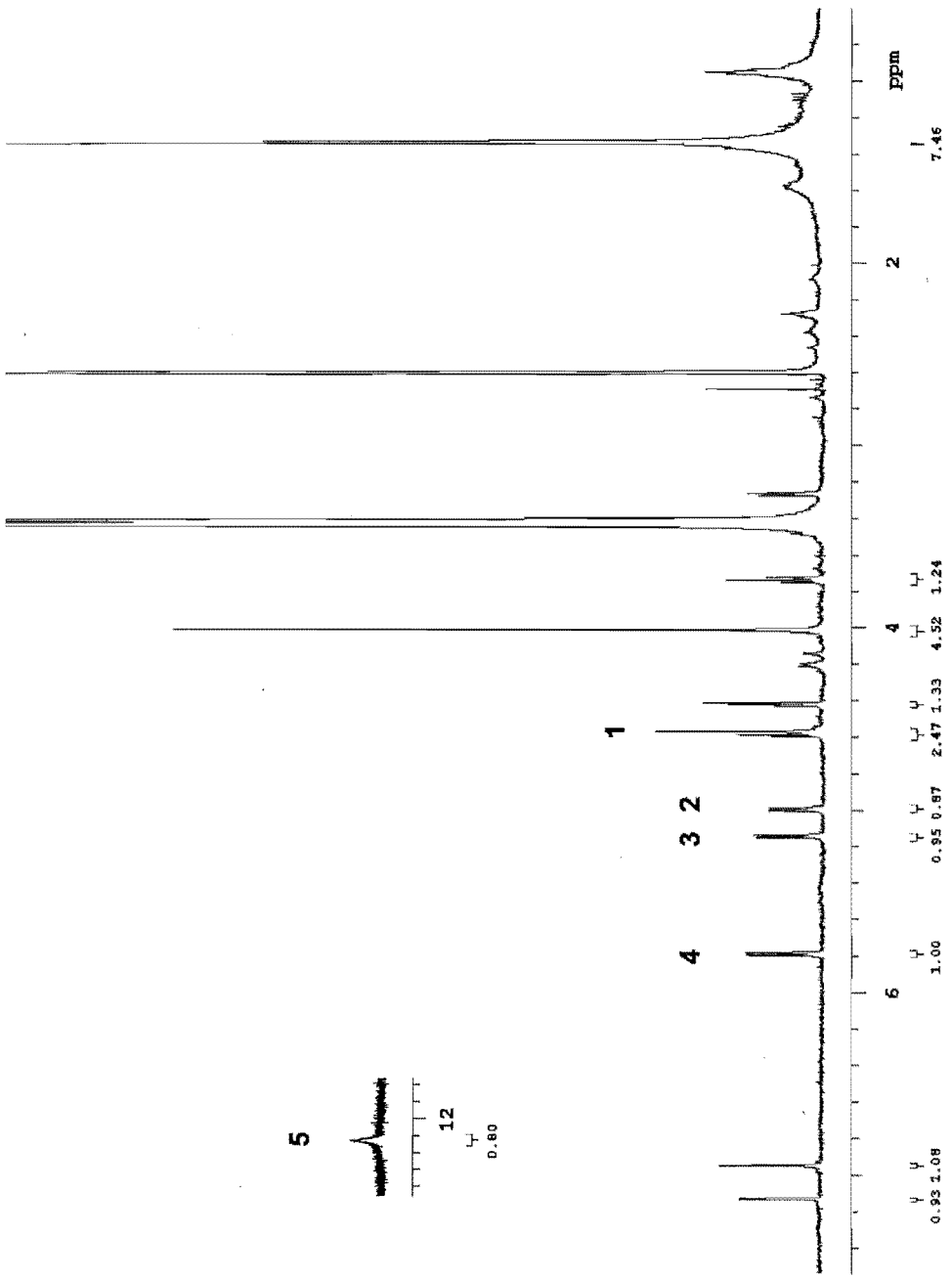

Figure 5.8: ^{1}H NMR spectrum of **141** in DMSO-d_6, new signals are marked 1-5.

As the mass recovered of **141** was low no direct carbon observations were possible so all ^{13}C NMR resonances were obtained by HSQC (Figure 5.16), $^{1}J_{CH}$ connectivities, and CIGAR experiments (Figures 5.17 and 5.19), $^{n}J_{CH}$ connectivities. CIGAR experiments were also initially run in CD_3OD but were re-run in DMSO-d_6 to determine if there

were any long range $^{n}J_{CH}$ correlations from the hydroxyl protons. As stated previously the aromatic protons at δ_H 7.12 and 6.94 (DMSO-d_6) showed coupling distinctive to a 1,3 arrangement, and from HSQC experiments were attached to carbons at δ_C 107.7 and δ_C 107.0 (DMSO-d_6) respectively. Both of these protons showed CIGAR correlations to the carbons of each other (δ_C 107.7, 107.0) and to a third quaternary carbon at δ_C 109.9. In aromatic systems $^{3}J_{CH}$ correlations are often stronger than the corresponding $^{2}J_{CH}$ correlations[150] therefore the carbon at δ_C 109.9 was placed in position 5 in a 1,3,5 arrangement. Because the δ_C of the aromatic carbons were high field, coupled with the aromatic nature of the protons resonating at δ_H 7.12 and 6.94, it was concluded that the aromatic portion of the molecule was at least 1,3-dioxygenated (Figure 5.9).

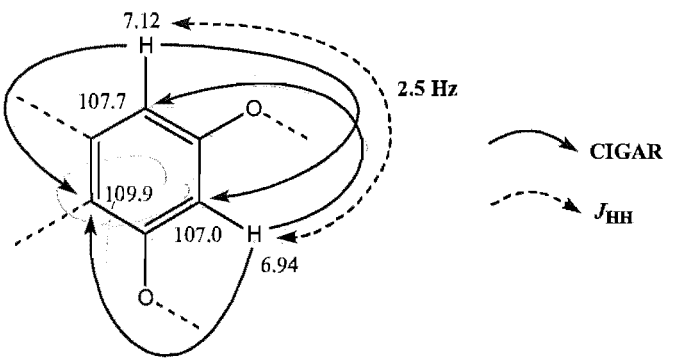

Figure 5.9: CIGAR correlations and $^{4}J_{HH}$ coupling constants for at δ_H 7.12 and 6.94.

All other proton signals were assigned to respective carbons by HSQC experiments, which were then connected via COSY (Figure 5.18) and 2D-TOCSY experiments (Figure 5.10a-d).

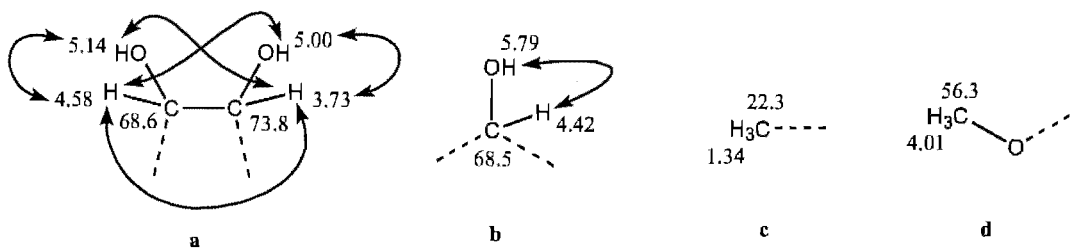

Figure 5.10a-d: Fragments deduced from COSY, TOCSY and HSQC (DMSO-d_6) correlations for **141**.

The low field proton resonance at δ_H 4.01 integrated for 3 protons which indicated an *O*-methyl group connected to either a double bond or a carbonyl group. This was confirmed by CIGAR experiments which showed a single intense $^{3}J_{CH}$ correlation to a quaternary carbon at δ_C 165.4 (Figure 5.11c). Of the hydroxyl protons, only δ_H 5.79

showed any CIGAR correlations, and this was to a quaternary carbon at δ_C 142.1. Two further quaternary carbons were observed by CIGAR experiments, at δ_C 72.9 and 144.6. The chemical shift of the carbon at δ_C 72.9 suggested a C-O group and those at δ_C 142.1 and 144.6 suggested that they were part of an aromatic or conjugated double bond system. Further CIGAR correlations allowed the connectivity of the fragments in Figure 5.11 to be determined.

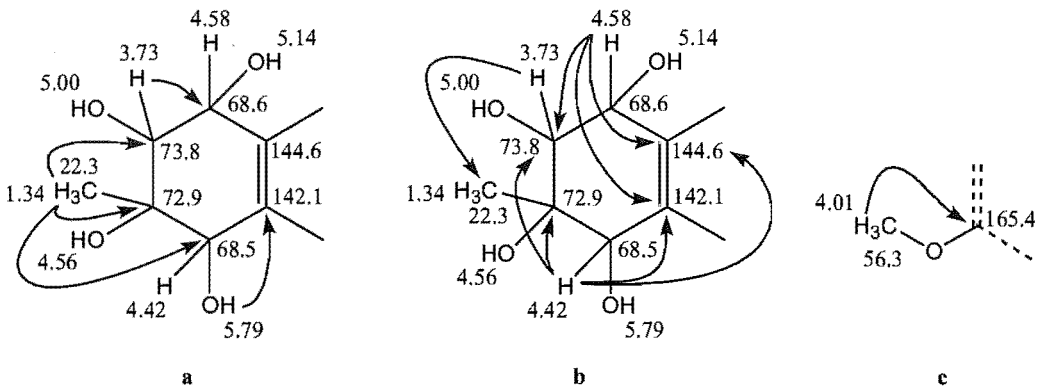

Figure 5.11a-c: CIGAR correlations (DMSO-d_6) observed for **141**.

The chemical shift of the quaternary carbon at δ_C 165.4 (Figure 5.11c) was suggestive of an oxygenated aromatic carbon rather than a carbonyl group thus the *O*-methyl group was placed on the aromatic ring between the protons at δ_H 7.12 and δ_H 6.94. The phenolic proton resonance at δ_H 12.12 was attached to the other oxygenated position on the aromatic ring (Figure 5.12a). An important CIGAR correlation was seen from a proton resonating at δ_H 4.42 to a quaternary carbon at δ_C 184.0. The chemical shift of this carbon suggested that it was a carbonyl group (Figure 5.12b).

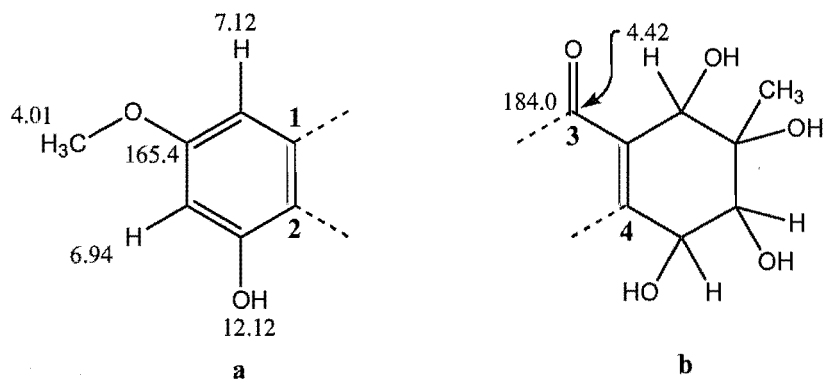

Figure 5.12a-b: An important CIGAR correlation for δ_H 4.42.

The fragments in Figure 5.12a-b were still 28 Da short of the postulated mass of 336 Da. However, as stated previously, the purified sample was intensely coloured and thus to fulfil the required mass, conjugation and quinone nature of the molecule another carbonyl group was placed adjacent to position 4 in Figure 5.12b. The two carbonyl groups were then attached to the fragment in Figure 5.12a, at positions 1 and 2, to give structure **138**.

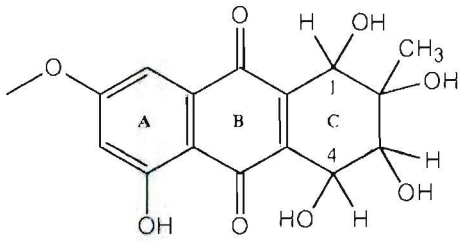

138

This structure was confirmed with high resolution mass spectrometry on the MNa^+ ion rather than the weak MH^+ ion. The calculated and experimental mass for this sample were identical, at 359.0743 Da. Structure **138** satisfies the mass, conjugation and the absorptions in the UV region characteristic of quinone moieties.[140]

A search for similar compounds in various databases found **138** to be a member of the altersolanols.

5.4.1 Relative stereochemistry of 141

Although the carbon experimental data were identical to those previously reported for altersolanol A,[134] discrepancies were seen between the experimental and previously reported proton data[140, 141] (Table 5.3).

Proton Number	*Altersolanol A*	*Experimental (DMSO-d_6)*	*Altersolanol F*
H-C1-OH	4.38, 5.30 (4 Hz)	4.42 , 5.79 (6.5 Hz)	4.10 , 5.06 (7 Hz)
Me-C2-OH	1.24 , 4.48	1.34 , 4.56	1.14 , 4.84
H-C3-OH	3.64 , 5.00 (7 Hz)	3.73 , 5.00 (7 Hz)	3.61 , 4.30 (7 Hz)
H-C4-OH	4.54 , 5.71 (7 Hz)	4.58 , 5.14 (7 Hz)	4.45 , 5.67 (7 Hz)
5-OH	12.15	12.12	-
H-C6	6.72 (2.5 Hz)	6.94 (2.5 Hz)	6.93
7	3.90	4.01	3.69
H-C8	6.93 (2.5 Hz)	7.12 (2.5 Hz)	6.93

Table 5.3: Comparison of proton (^1H) signals and $^3J_{HH}$ (Hz) in DMSO-d_6 of two altersolanols and experimental data for **141**; differences are highlighted in red.[140]

Two discrepancies involved the inversion of hydroxyl proton signals at C^1 and C^4, with a third being a difference in proton coupling between H-C-OH at C^1. The differences in hydroxyl proton assignment could be due to a reporting error, but the third difference was attributed to an alternate stereochemistry. To confirm this, 1D NOESY experiments were carried out on signals at δ_H 1.34, 4.01, 6.94 and 7.12. Unfortunately due to an extremely low sample mass (< 0.4 mg) no NOESY correlations were observed.

There are four carbon centres in altersolanol A at which the stereochemistry can vary and two where regioisomers are possible. The four stereocentres are C^1-C^4, with the possibility of regioisomers centred on C^5 and C^7. The functional groups at C^1-C^4 can exist in two conformations, pseudo-axial or pseudo-equatorial, which would display differing J_{HH} for each proton pair at each stereocentre. Therefore an examination of the coupling constants for these stereocentres was warranted. The *O*-methyl at δ_H 4.01 could be attached at either C^7 or C^5 as in altersolanol A (**139**) or F (**140**) respectively.

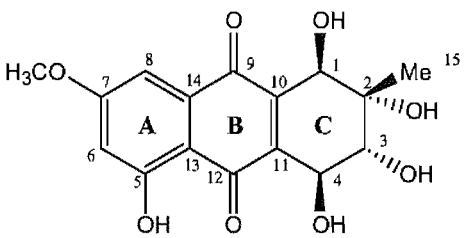

139

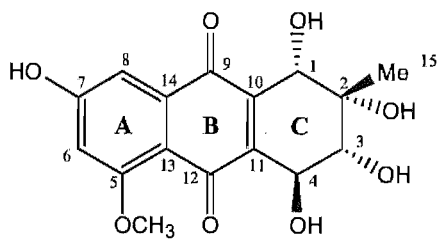

140

A comparison of the reported ^1H signals in the A ring,[140] showed the experimental values (Table 5.3) to be almost identical with those of altersolanol A (**139**), which indicated that the *O*-methyl group was attached at C^7 and the phenolic hydroxyl attached at C^5, rather than the other way around as in altersolanol F (**140**). However, the $^3J_{HH}$ coupling constant of 4 Hz between the proton signal at δ_H 4.42 and the hydroxyl proton signal at δ_H 5.79 on C^1 for altersolanol A did not agree with the experimental value of 6.5 Hz. Of the fourteen altersolanols reported only altersolanol F has a coupling constant close to 6.5 Hz at C^1, with the reported value being 7 Hz.[140] This indicates that **141** has the same relative stereochemistry for all the hydroxyl groups around the C ring as that seen in altersolanol F (Figure 5.13).

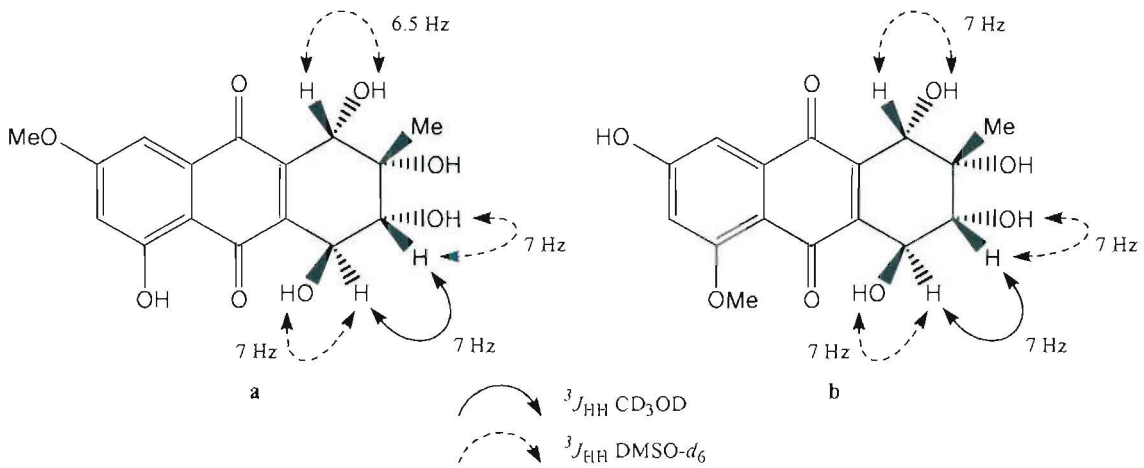

Figure 5.13: Experimental $^3J_{HH}$ coupling constants for **141** (a) and literature coupling constants for altersolanol F[140] (b).

The final position at which a variation in stereochemistry can occur is at C^2. Since a methyl group is attached at this centre, no coupling is seen for the hydroxyl signal. However, all previously reported altersolanols[102] have the same stereochemistry at C^2 as shown in Figure 5.13. Energy minimisation of the structure represented in Figure 5.13 using MM2 minimisation parameters in Chem3D (Cambridge software) indicated two possible conformations (Figure 5.14a-b). There are unfavourable dipole interactions in Figure 5.14a between the hydroxyl groups at C^1 and C^2, C^1 and C^3, and a third interaction between the methyl and hydroxyl groups attached at C^2 and C^4. In Figure 5.14b the only unfavourable interaction is between the hydroxyl groups of C^3 and C^4, thus suggesting that Figure 5.14b is the preferred conformation.

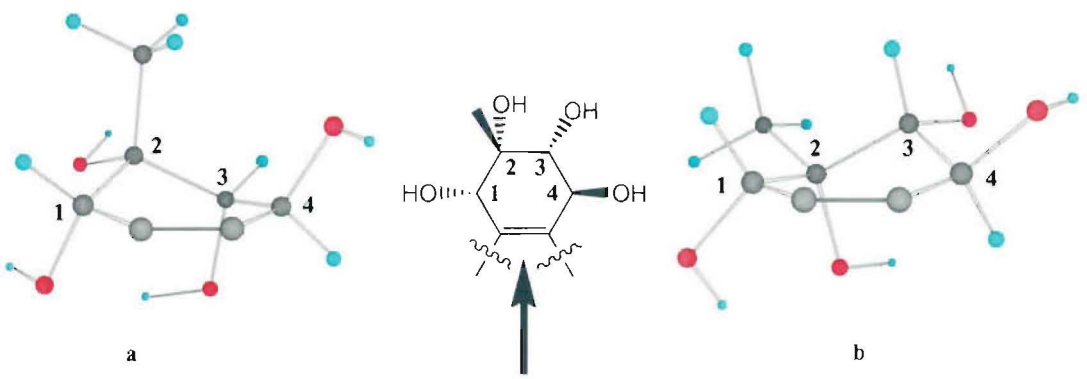

Figure 5.14a-b: Energy minimised diagrams for the two possible conformations of the C-ring of **141**.

The dihedral angles between the protons attached at C^3 and C^4 (δ_H 3.73 and δ_H 4.58) were -80.4° (Figure 5.14a) and -159.8° (Figure 5.14b). Calculation of the coupling constants with the Karplus equation[151] for these two conformations gave $^3J_{HH}$ couplings of 1.1 and 7.7 Hz respectively, thus the observed coupling of 6.5 Hz between these two protons further indicates that Figure 5.14b is the favoured conformation to give **141**.

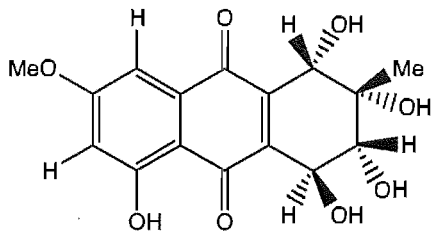

141

5.5 Discussion

An extract from an *Alternaria* sp was found to possess mild cytotoxicity against the P388 cell line. The cytotoxic component was purified and assigned as a new member of the altersolanols, tentatively called altersolanol J.

As this fungal culture was unable to be revived, future work on **141** would require a re-isolation of *Alternaria* spp from substrates collected from the initial sampling site. If any extracts from these *Alternaria* spp were found to produce the yellow pigment, large scale culture and subsequent purification could enable the stereochemistry of **141** to be definitively assigned by either further NOESY experiments or X-ray crystallography.

Experimental ^{1}H and ^{13}C NMR data for compound **141** are shown in Tables 5.4 and 5.5, in CD_3OD and DMSO-d_6 respectively.

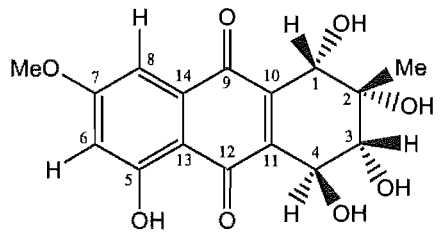

Figure 5.15: Altersolanol numbering system for Tables 5.4 and 5.5

Number	^{1}H, multiplicity, (J_{HH} Hz)	HSQC	CIGAR
1 H	4.51 s	69.1	184.0 , 144.1 , 142.4 , 74.2 , 73.6
2 Me	1.42 s	21.1	74.2 , 73.6 , 69.1
3 H	3.84 d (7)	74.2	69.6
4 H	4.73 d (7)	69.6	144.1 , 142.4 , 74.2
6 H	6.74 d (2.5)	105.8	110.0 , 107.5
7 OMe	3.91 s	55.6	166.7
8 H	7.15 d (2.5)	107.5	110.0 , 105.8

Table 5.4: ^{1}H and ^{13}C NMR data for **141** in CD_3OD.

Number	^{1}H, multiplicity, (J_{HH} Hz)	COSY	TOCSY	HSQC	CIGAR
1-H	4.42 d (6.5)	5.79	5.79	68.5	184.0 , 144.6 , 142.1 , 73.8 , 72.9
1-OH	5.79 d (6.5)	4.42	4.42		142.1
2-Me	1.34 s			22.3	73.8 , 72.9 , 68.5
2-OH	4.56s				68.5
3-H	3.73 t (6.5 , 7)	5.00 , 4.58	5.14 , 5.00 , 4.58	73.8	68.6 , 22.3
3-OH	5.00 d (7)	3.73	5.14 , 4.58 , 3.73		
4-H	4.58 t (6.5 , 7)	5.14 , 3.73	5.14 , 5.00 , 3.73	68.6	144.6 , 142.1 , 73.8
4-OH	5.14 d (6)	4.58	5.00 , 4.58 , 3.73		
5-OH	12.12 br s				
6-H	6.94 d (2.5)	7.12	7.12	107.0	109.9
7-OMe	4.01 s			56.3	165.4
8-H	7.12 d (2)	6.94	6.94	107.7	109.9

Table 5.5: ^{1}H and ^{13}C NMR data for **141** in DMSO-d_6.

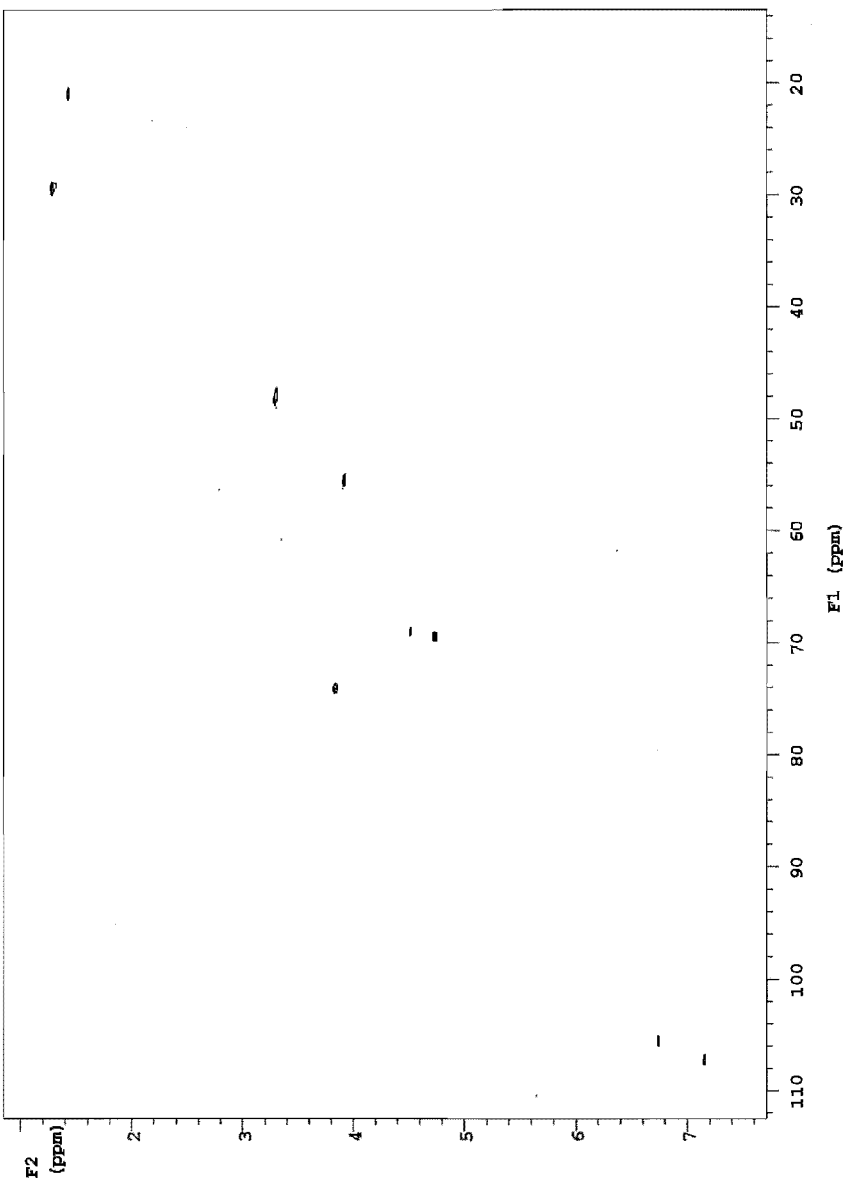

Figure 5.16: HSQC spectrum of **141** in CD_3OD

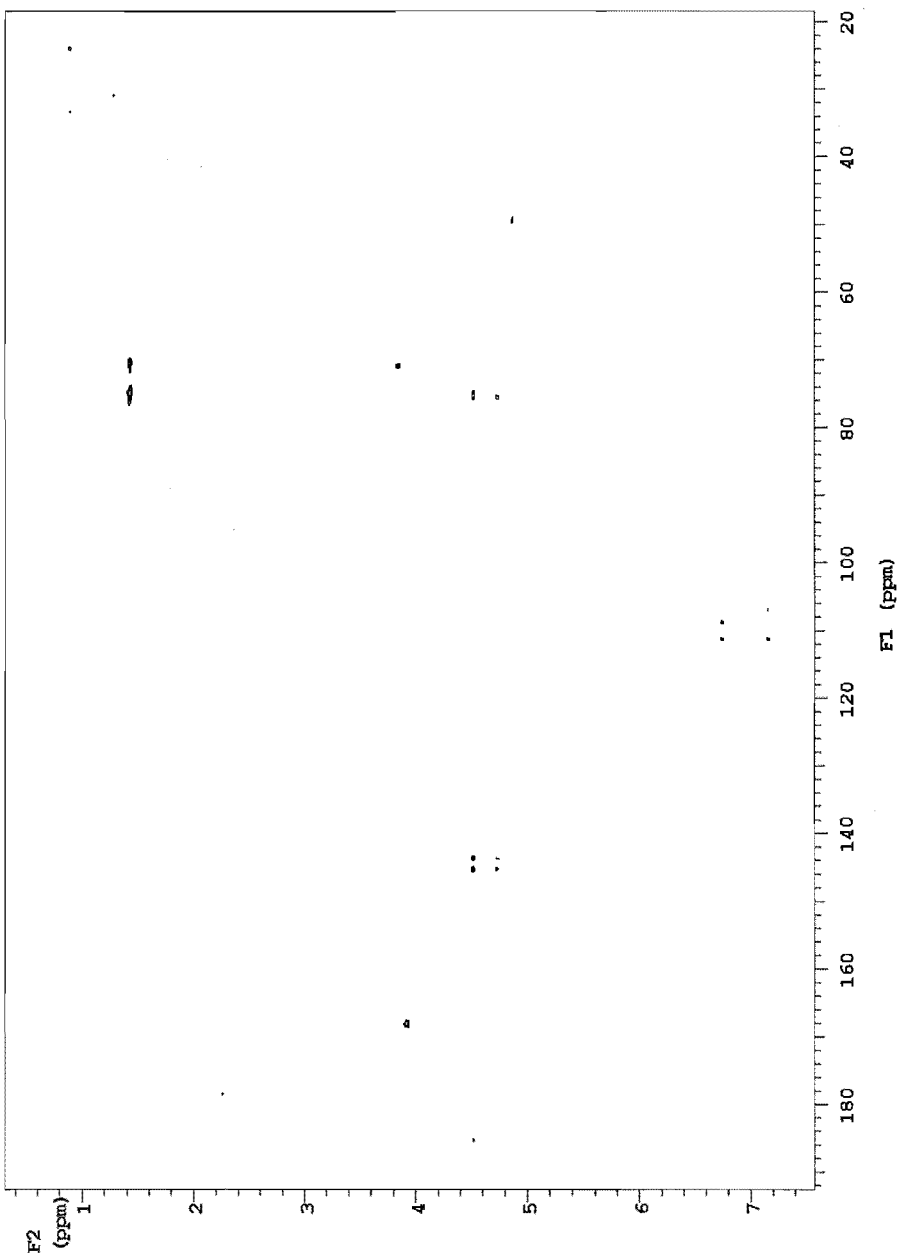

Figure 5.17: CIGAR spectrum of **141** in CD_3OD

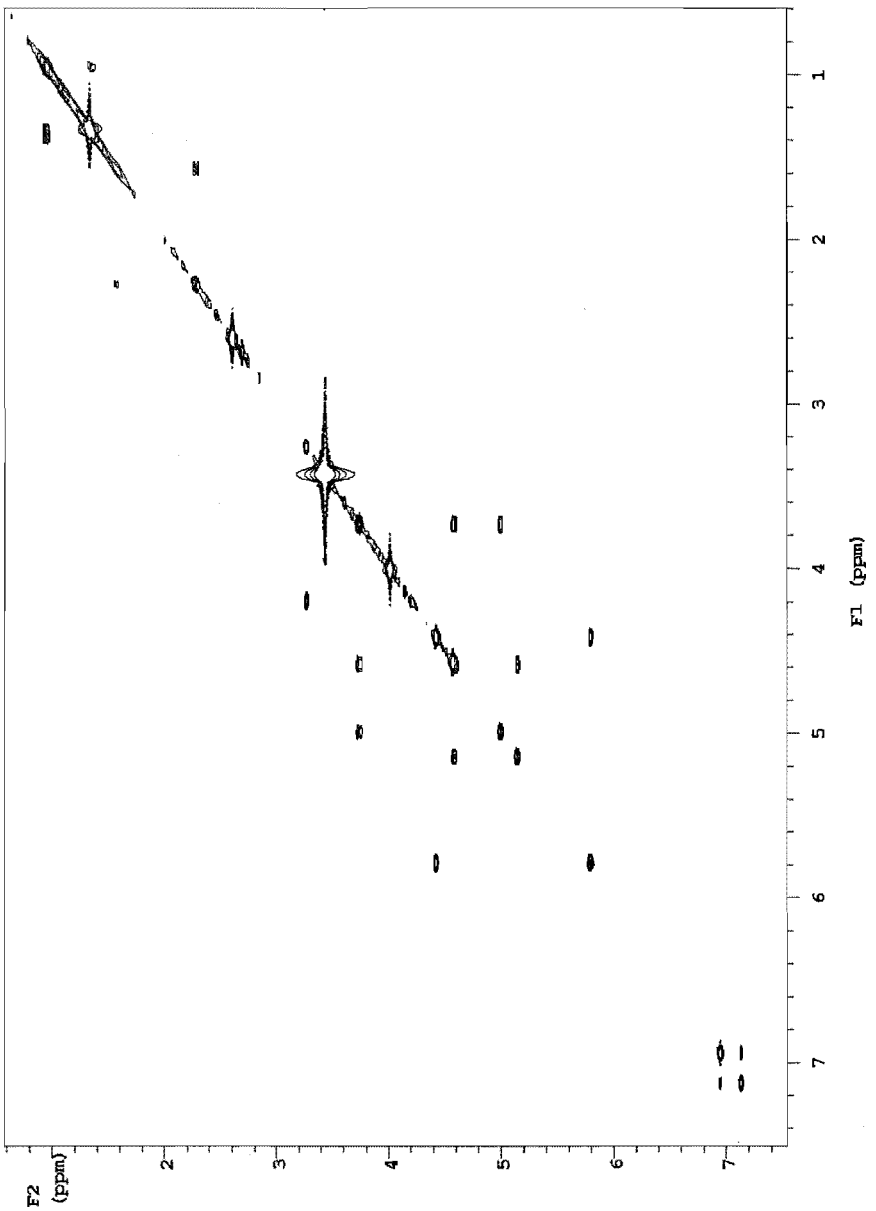

Figure 5.18: COSY spectrum of **141** in DMSO-d_6

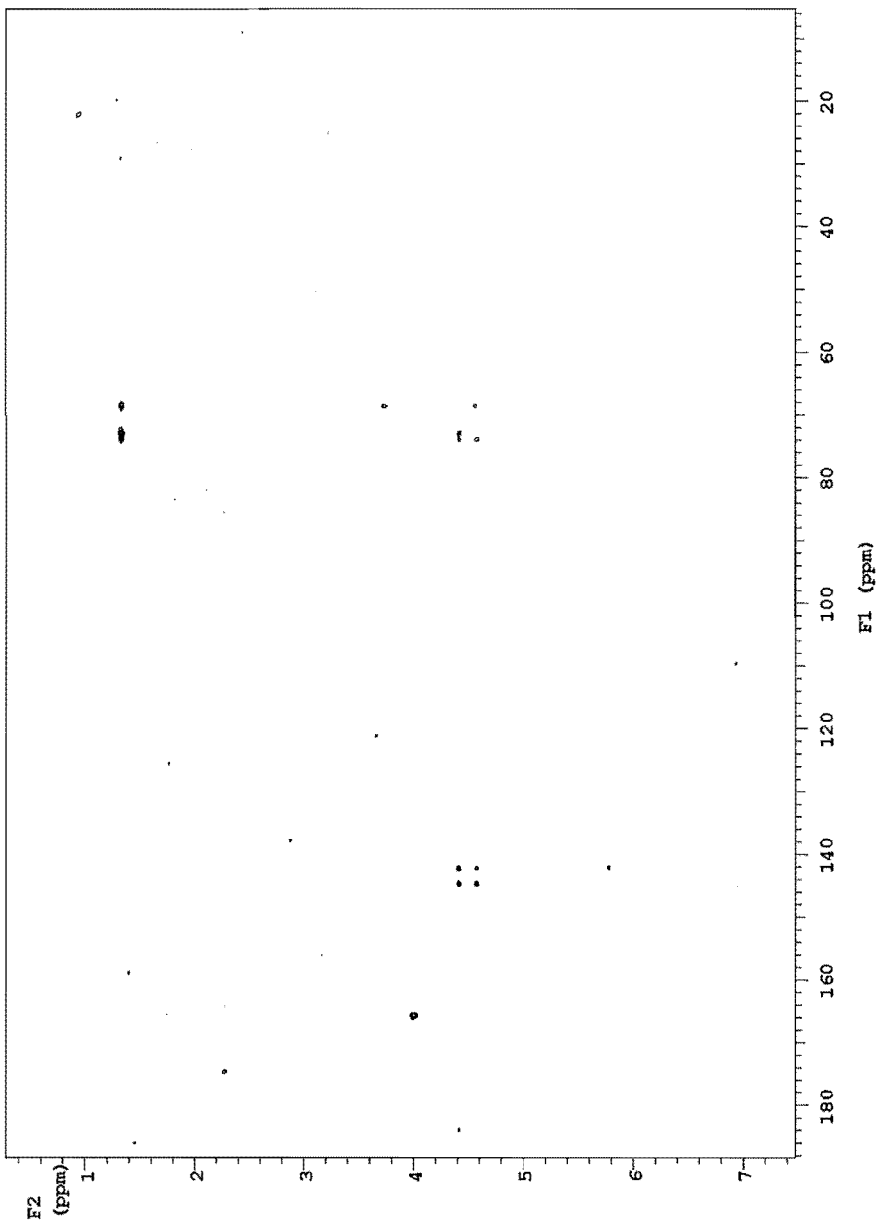

Figure 5.19: CIGAR spectrum of **141** in DMSO-d_6

CHAPTER SIX

FOX 21-2-6a ~ *STREPTOMYCES* SP

6.1 Introduction

Broth extracts from Fox 21-2-6a, a *Streptomyces* sp isolated from driftwood collected near the mouth of the Fox River, showed excellent cytotoxicity towards the P388 cell line (< 97.5 ng/mL). This microbial isolate was targeted for chemical investigation because it showed large zones of inhibition against some filamentous fungi when grown together on agar plates. Investigations (Section 6.2.1) into the small scale crude extract showed that the cytotoxicity was centered on a series of small peaks in a relatively simple HPLC chromatogram (Figure 6.2). Six intense red antibiotics (**154** - **159**), all with excellent cytotoxicity against the P388 cell line (378 - 65 ng/mL respectively) were purified from culture extracts. The chromatography of these compounds is discussed in Section 6.3 and the structural elucidations described in Sections 6.4 and 6.5 of this chapter.

6.1.1 Antibiotics

Almost all the compounds produced by actinomycetes are termed antibiotics. The vast majority of antibiotics are of microbial origin and can inhibit the growth of other organisms, but not the antibiotic producer. The first known antibiotic was mycophenolic acid (**7**) originally described in 1896 and was followed closely by penicillic acid (**68**) in 1913[152] and penicillin in 1928.

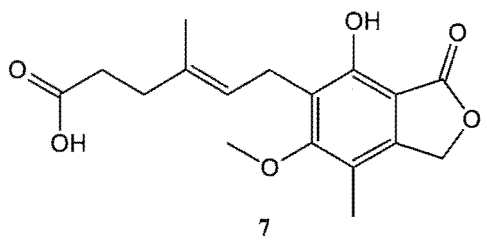

7

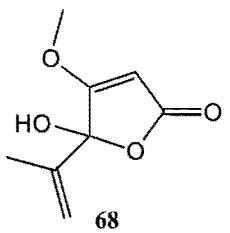

68

Sporadic discoveries of various antibiotics, including penicillin, were made until the early 1940's when the number discovered started to increase significantly. The discovery of the actinomycins from various *Streptomyces* spp in 1940 by Waksman and Woodruff[153] was followed closely by streptomycin from *Streptomyces griseus* in 1943.[154] In fact all of the antibiotics used in human and veterinary medicine in the 1950's except for penicillin were derived from actinomycetes.[152] Actinomycetes are still the most prolific source of antibiotics with approximately 4600 compounds isolated by 1998 followed by fungi (1600 compounds) and other bacteria (960 compounds).[1]

6.1.1.1 Antibiotic compounds from actinomycetes

A vast number of antibiotics that have been isolated from actinomycetes possess an extremely diverse range of biological activities including antitumour and immunogenic compounds. Some of the best known antitumour compounds include the mitomycins such as mitomycin C (**142**), various actinomycins and the aclacinomycins, such as aclacinomycin A (**143**), which is also known to act as an immunomodulator.

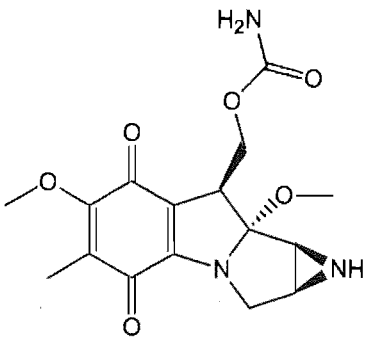

142

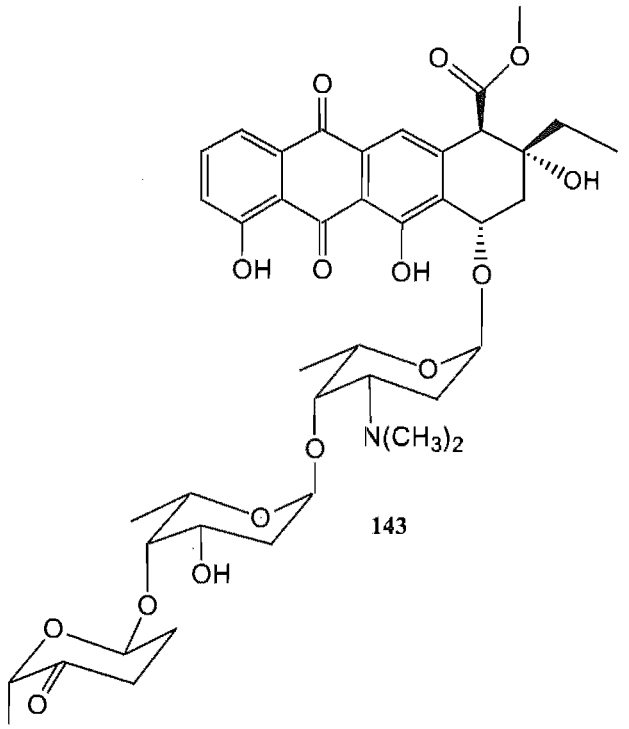

143

Although antibiotics can possess very complex structures they are still biosynthesized from simple building blocks such as acetate, sugars and amino acids.

6.1.1.2 Peptide derived antibiotics from actinomycetes

Perhaps one of the most important peptide derived antibiotics from *Streptomyces* spp is clavulanic acid (**144**), a member of the β-lactam family of antibiotics.[155] Although clavulanic acid is a weak antibiotic it was found to be an irreversible inhibitor of many β-lactamases This prompted interest in the development of semi-synthetic penicillin analogues that were also capable of β-lactamase inhibition.[156]

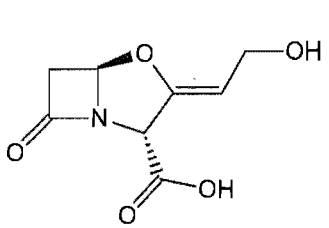

144

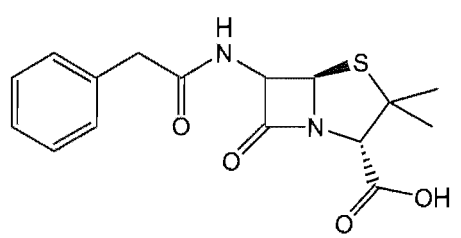

1

The major difference between clavulanic acid (**144**) and penicillin G (**1**) is replacement of the sulphur atom in the five membered ring with an oxygen atom.

Another well known peptide antibiotic is vancomycin (**145**), from *Amycolotopsis orientalis*, which has been widely used in medicine especially against β-lactam resistant bacteria.[157]

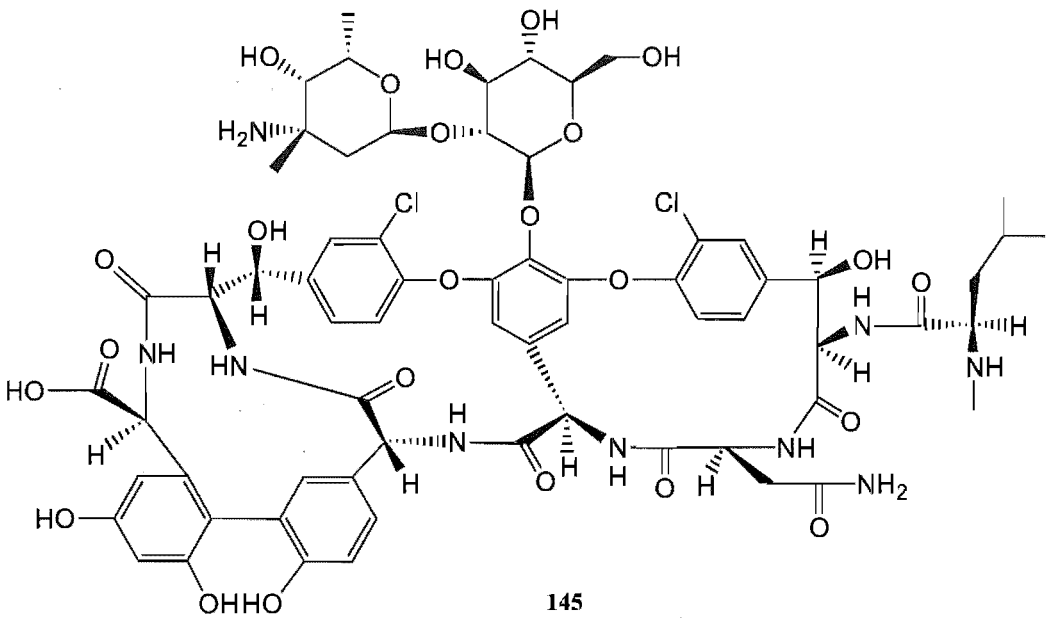

145

6.1.1.3 Polyketide derived antibiotics from actinomycetes

Some of the best known polyketide antibiotics include the tetracyclines, the anthracyclines and the nystatins. Tetracyclines, such as chlortetracycline (**146**), are widely used both in veterinary and human medicine and show a broad spectrum of activity against both Gram-positive and Gram-negative bacteria. However, their use is limited as they also display significant toxicity towards humans.[156]

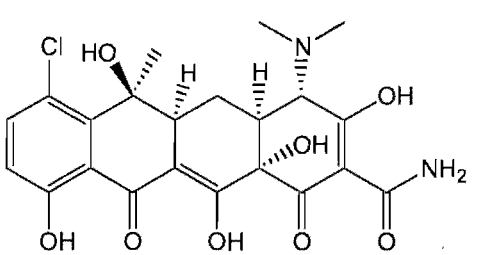

146

The anthracycline group of antibiotics, such as doxorubicin (**147**), are synthesized in a similar way to that of the tetracyclines, but normally contain one or more sugar residues. Doxorubicin and the related anthracycline daunorubicin (**148**) are both used for the treatment of various solid tumours. Once again however, these antibiotics are relatively toxic at high doses.[156]

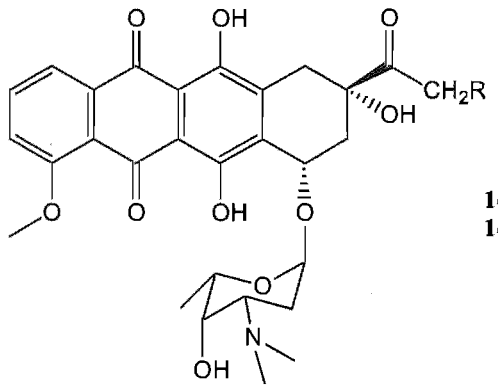

147 R = OH
148 R = H

The third class of compounds which include the antifungal nystatins are the macrolides which contain a lactone ring and at least one sugar residue. The macrolides can be split further into those compounds with 12 - 16 atoms forming the lactone ring, such as erythromycin A (**149**),[158] and those with 26 - 38 atoms in the macro lactone ring including two to seven unsaturated bonds such as nystatin A_1 (**150**).[159]

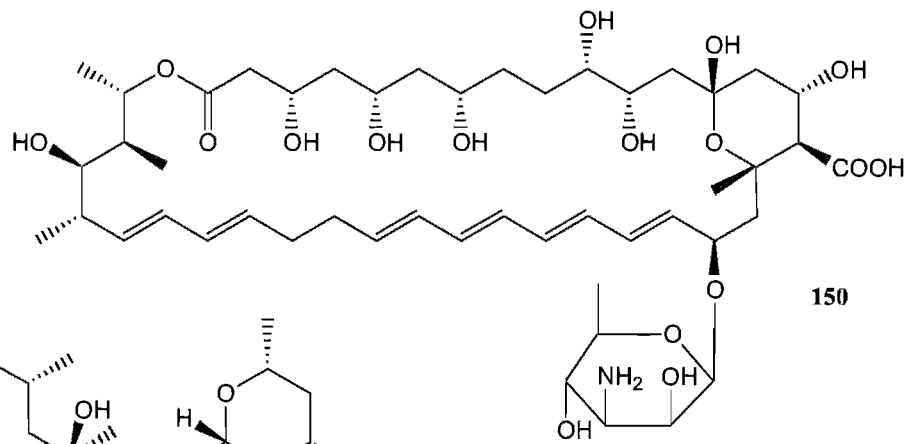

150

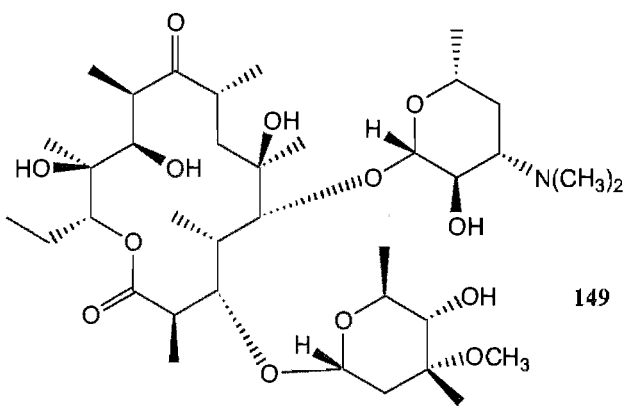

149

Another unusual but well known group of macrolides are the antihelminthic avermectins which include the ivermectins (**151**).[160] These compounds contain a 16 - membered lactone ring and possesses very potent anti-nematode activity with little or no side effects which make them ideal for the control of nematodes in farm animals.

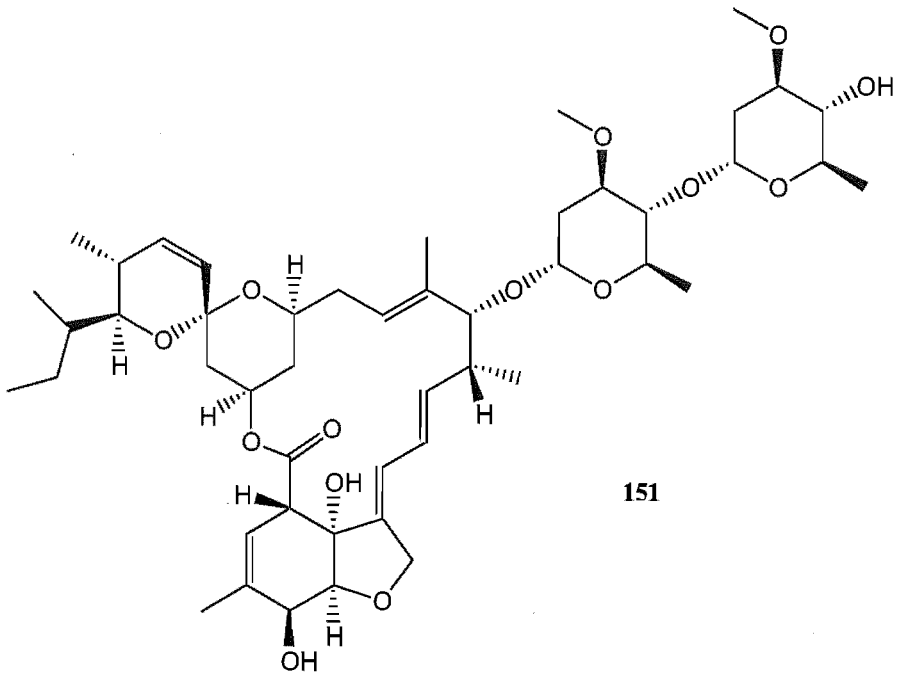

151

6.1.1.4 Miscellaneous antibiotics from actinomycetes

The antimicrobial antibiotic chloramphenicol (**152**) was initially isolated from the actinomycete *Streptomyces venezuelae*.[161] It possesses a broad spectrum of antibacterial activity and works by inhibiting bacterial protein synthesis. Soon after the discovery of chloramphenicol it was able to be synthesized in the laboratory from *p*-nitroacetophenone[162] and is currently produced commercially via a fully synthetic process.[156]

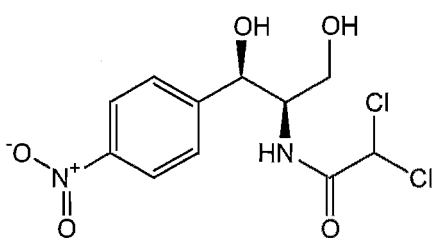

152

Another very well known antimicrobial antibiotic, streptomycin (**153**), is also produced by various *Streptomyces* sp and was first discovered in 1944 by Schatz *et al.*[154]

153

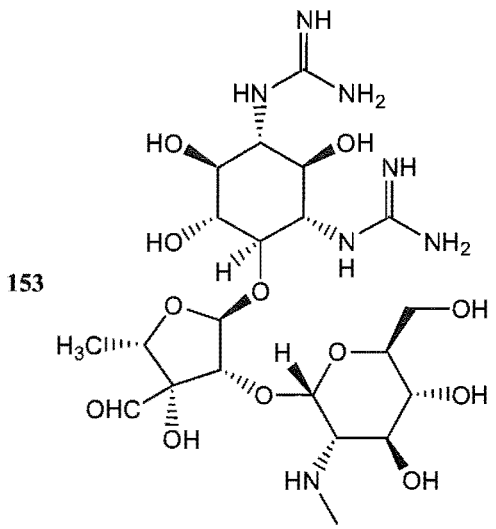

Streptomycin, an unusual trisaccharide, functions by selectively inhibiting cell wall biosynthesis in Gram-positive bacteria ultimately causing bacterial lysis and cell death.
All of the antibiotics that have been isolated to date have been classified by Berdy[163] based on their carbon skeletons into nine major groups. This classification system is open ended which enables newly discovered compounds with slightly different or previously unknown carbon skeletons to be easily integrated in the classification system without disrupting the numbering system in use.

6.2 Culturing and extraction of Fox 21-2-6a

6.2.1 Preliminary investigations

Actinomycete isolate, Fox 21-2-6a, a *Streptomyces* sp, was isolated from a section of driftwood collected in the water below the low tide zone at the mouth of the Fox River on the West Coast of the South Island of New Zealand in October 1998.
A small scale extract prepared from a culture grown in 250 mL starch casein broth showed significant cytotoxicity towards the P388 cell line (< 97.5 ng/mL) and as such was selected for chemical investigation.

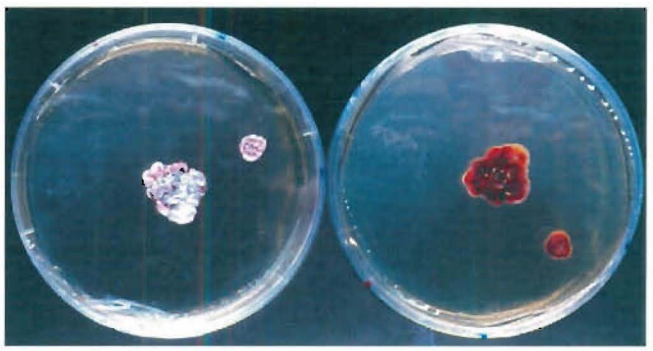

Figure 6.1: Isolate Fox 21-2-6a (*Streptomyces* sp) grown on a starch-casein plate.

6.2.1.1 Chemical screening

The small scale EtOAc extract was chromatographed on CBA, C_{18} and LH20 cartridges (Section 3.2.1.1).

Chromatography on CBA concentrated the cytotoxicity into the first two fractions with limited carry over to the third fraction. The second and third fractions from the LH20 cartridge both showed activity with the highest level of cytotoxicity seen in the third fraction and chromatography on C_{18} concentrated the activity into the third fraction. Thus the compound(s) responsible for the cytotoxicity were thought to be of medium size, non-polar and neutral to positively charged. After sample elution from the C_{18} cartridge it was noted that a large amount of colour was retained. However, as the biological activity had eluted from the cartridge this was not considered a significant problem.

6.2.1.2 HPLC Microtitre plate screening

The biological profile of this extract showed that the bioactivity was centred on four small peaks eluting between 10 and 12 minutes in the HPLC chromatogram (Figure 6.2) and which all showed the same very distinctive UV spectrum (Figure 6.3). The UV spectra of the bioactive compounds in this extract were similar to the UV spectrum of **141** (Figure 5.3) suggesting that the bioactive components of this extract contained a similar chromophore. However, as the bioactive components of Fox 21-2-6a absorbed at a longer wavelength in the UV spectrum (492 nm rather than 434 nm) it was postulated that the chromophoric group of the bioactive compounds from Fox 21-2-6a was more extensively conjugated.

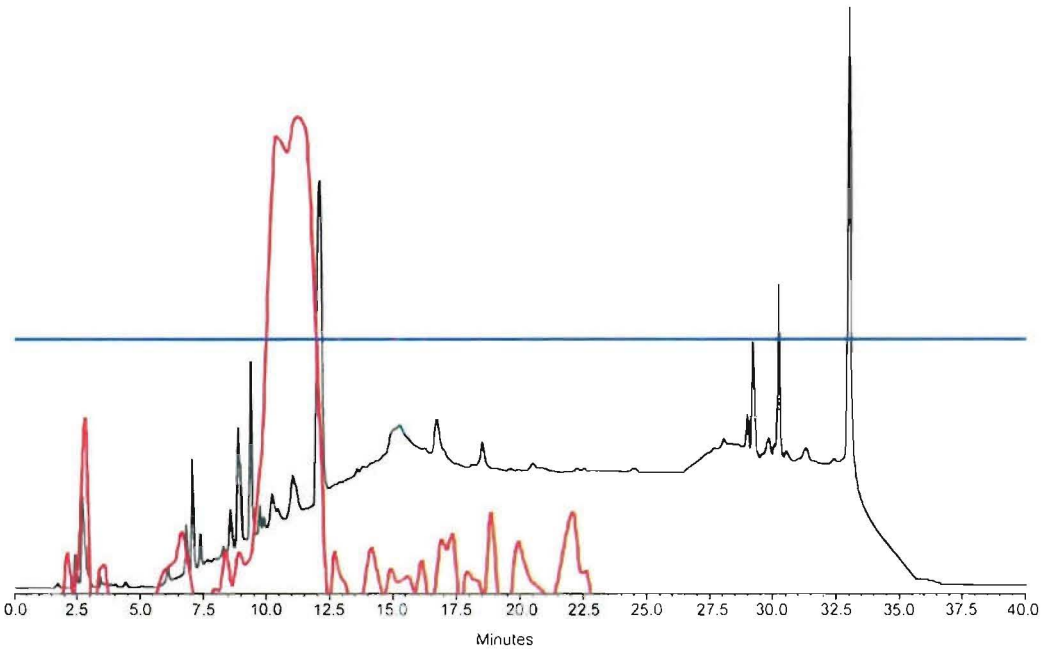

Figure 6.2: Spectrum max plot HPLC trace (black) and bioactivity data (red) of a Fox 21-2-6a extract showing region of biological activity (the blue line represents 50% cell death).

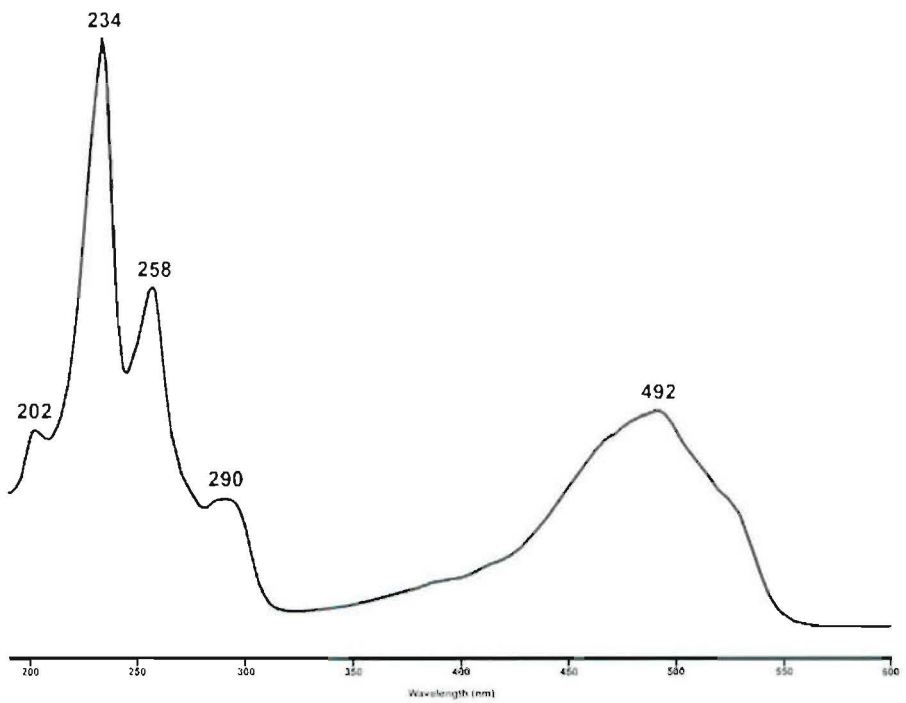

Figure 6.3: UV spectrum of bioactive peaks from HPLC trace (10 - 12 minutes) as determined by the microtitre plate assay

ESI-MS of the bioactive wells from the microtitre plate showed a series of small peaks (< 10 % peak intensity) between 500 - 560 Da and 800 - 860 Da with two large peaks at 810.4 Da and 826.4 Da. The mass spectrum from the active microtitre plate wells and the UV spectrum from the HPLC trace indicated that the compounds most likely responsible for the biological activity of this extract were analogues of the aclacinomycins, a group of anthraquinone glycosides with an intense red/orange colour. A subsequent search in Antibase with the UV maxima found four matches with a molecular mass of 810 Da and a further twelve matches with a mass of 826 Da. So to identify which aclacinomycins the bioactive components were, the extract was further purified.

6.2.2 Large scale culturing and extraction

To obtain enough sample for purification the microbial isolate Fox 21-2-6a was cultured twice in starch casein broth under similar conditions as described in Section 6.2.1. The first large scale culture was prepared in 4 L broth for 30 days and the second in 10 L broth for 18 days. Repeated extraction of these cultures with distilled EtOAc, followed by removal of the solvent under vacuum yielded a deep red solid for the first extract (420.5 mg) and a viscous red/purple oil for the second extract (7 mL). The first extract showed cytotoxicity towards the P388 cell line on a par with that of the small scale extract used for the preliminary investigations (Section 6.2.1). However, the second extract showed a decrease in observed cytotoxicity thought to be due to the large volume of oily material present in the extract.

6.3 Chromatography of Fox 21-2-6a extracts

6.3.1 Chromatography the first Fox 21-2-6a extract

The chromatographic steps for the first large scale extract of Fox 21-2-6a are shown in Scheme 6.1. A more detailed description of the chromatographic steps carried out on this extract can be found in the Experimental Section.

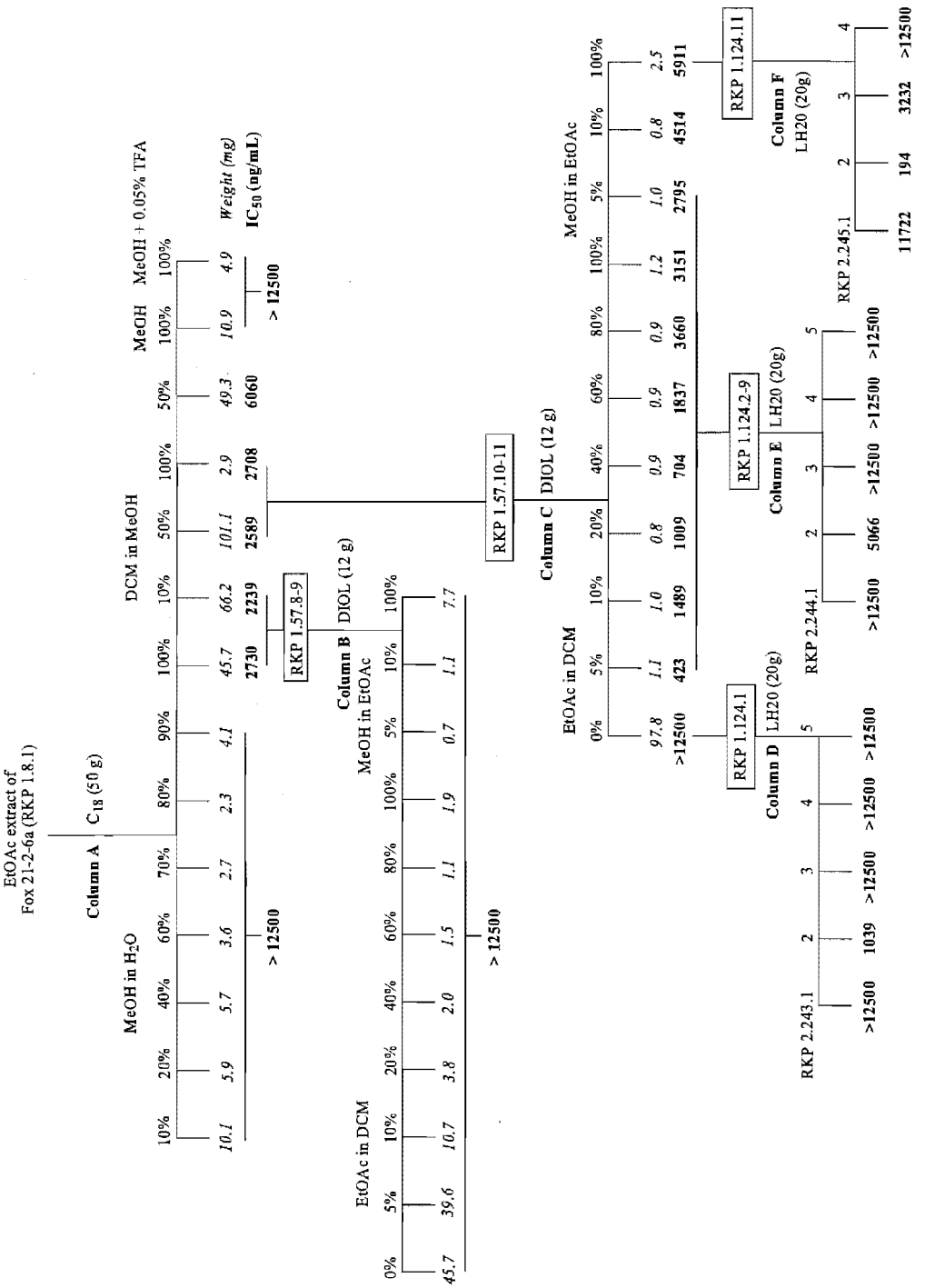

Scheme 6.1: Purification flow chart of an extract prepared from the microbial isolate Fox 21-2-6a

The first large scale culture extract (420.5 mg) was initially fractionated by reverse-phase C_{18} (column A), using a similar stepped gradient solvent system to that used for the elution of compound **141**. The only region of activity seen to elute from the C_{18} column was between 100 % MeOH and 100 % DCM with a much lower level of activity seen in the second 50 % MeOH wash. However, the overall bioactivity of the

four most active fractions (RKP 1.57.8-11, ~ 2000 ng/mL) was actually much lower than that seen in the crude extract (167 ng/mL). As these four fractions were very oily in nature the observed decrease of biological activity was thought to be due to the presence of a large amount of fatty acid/triglyceride material. A similar group of peaks was observed in the HPLC trace and the ESI-MS spectra for fractions RKP 1.57.8 and 9 as was also the case for fractions RKP 1.57.10 and 11. Based upon these results RKP 1.57.8 and 9 were combined as were RKP 1.57.10 and 11 and both subsequent fractions were further purified by normal phase chromatography on DIOL (columns B and C) using the same stepped gradient system that was used for column B in compound **141**.

None of the fractions of RKP 1.57.8-9 from column B showed any biological activity. However, a large quantity of material eluted from this column in the first three fractions and after solvent removal, these three fractions proved to be very oily. These three fractions were an intense red colour, and as previously indicated from the HPLC microtitre plate this colour was indicative of the compound(s) thought to be responsible for the cytotoxicity of this extract. However, further attempts to remove the oily material were unsuccessful suggesting that the oily material was attached to the chromophoric group.

A similar mass elution profile was seen for the second set of combined fractions (RKP 1.57.10-11) when subjected to normal phase chromatography with DIOL (column C). In this case however, cytotoxicity ranging from 423 ng/mL to almost 6000 ng/mL was observed in almost all of the fractions (RKP 1.124.2-11). The middle fractions (RKP 1.124.2-9) all showed similar HPLC profiles with three peaks of varying intensities eluting between 12 and 14 minutes and as such these eight fractions were recombined and subjected to a further chromatographic step on Sephadex LH-20, as was the case with the first (RKP 1.124.1) and last (RKP 1.124.11) fractions that eluted from DIOL column C. Columns D and E of RKP 1.124.1 and RKP 1.124.2-9 respectively both showed a similar mass - elution profile with biological activity detected only in the second fractions (RKP 2.243.2 and RKP 2.244.2 respectively). Both of these fractions comprised an intense red oil which only showed cytotoxicity at very high concentrations. This indicated that the compound(s) of interest were present only in very low concentrations, but once again attempts to remove the oily material were unsuccessful. The third LH20 column (column F) also showed the highest level of cytotoxicity in the second fraction (RKP 2.245.2) with moderate activity seen in the two

side fractions. HPLC analysis of these three fractions all showed a similar series of peaks between 11 and 14 minutes (Figure 6.4).

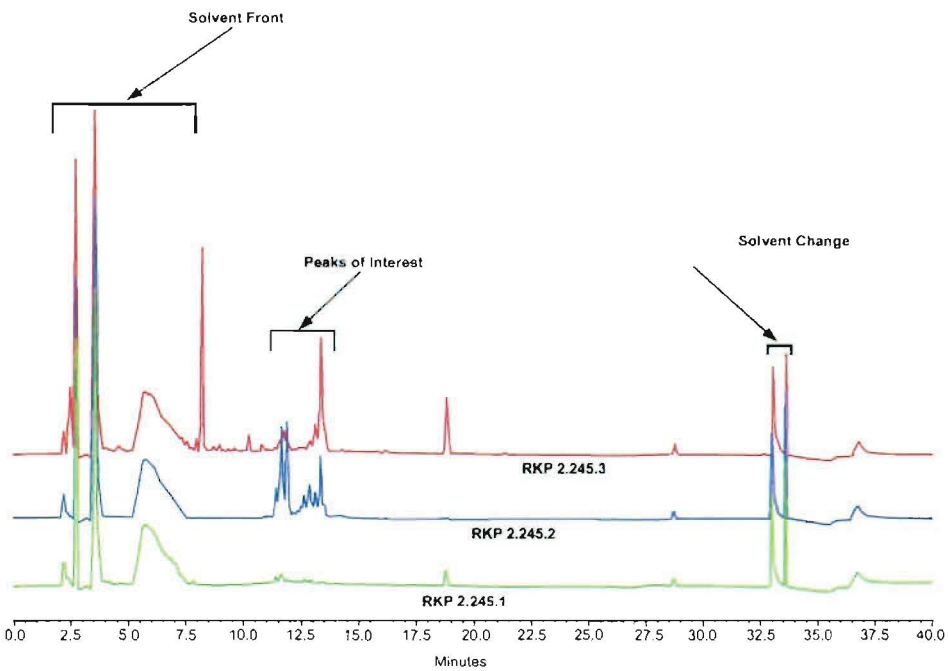

Figure 6.4: HPLC chromatogram of RKP 2.245.1-3

The ^{1}H NMR spectrum of RKP 2.245.2 (Figure 6.5) showed three low field phenolic protons between δ_H 12.0 and δ_H 13.0, some aromatic signals between δ_H 7.0 and δ_H 8.0, and some possible anomeric signals between δ_H 5.0 and δ_H 6.0. A low sample mass and the presence of multiple impurities within this fraction prevented further work on this extract and because of this a second extract was prepared from 10 L of starch casein broth. As stated previously this extract was cultured for only 18 days rather than 30 days with the ensuing extract unable to be completely dried to a powder due to the high volume of oily material present in the extract. The chromatography of this second extract is detailed in Section 6.3.2.

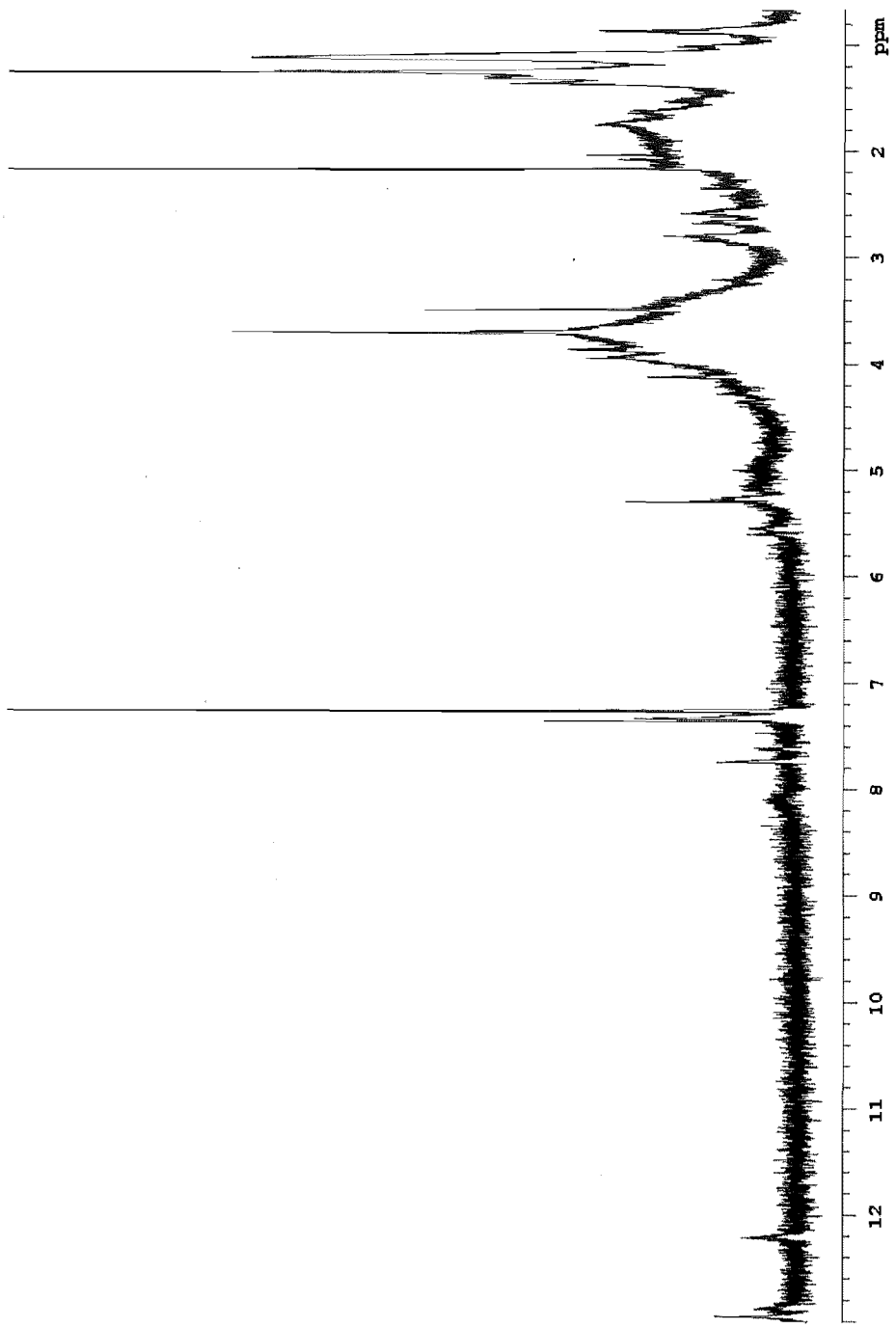

Figure 6.5: ^{1}H NMR spectrum of RKP 2.245.2 in $CDCl_3$

6.3.2 Chromatography of the second Fox 21-2-6a extract

The high volume of oily material suggested that a slightly different approach be used for purification of this extract. The chromatographic steps for this second extract are shown in Scheme 6.2 with a more detailed description of the chromatographic steps carried out on this extract found in the Experimental Section.

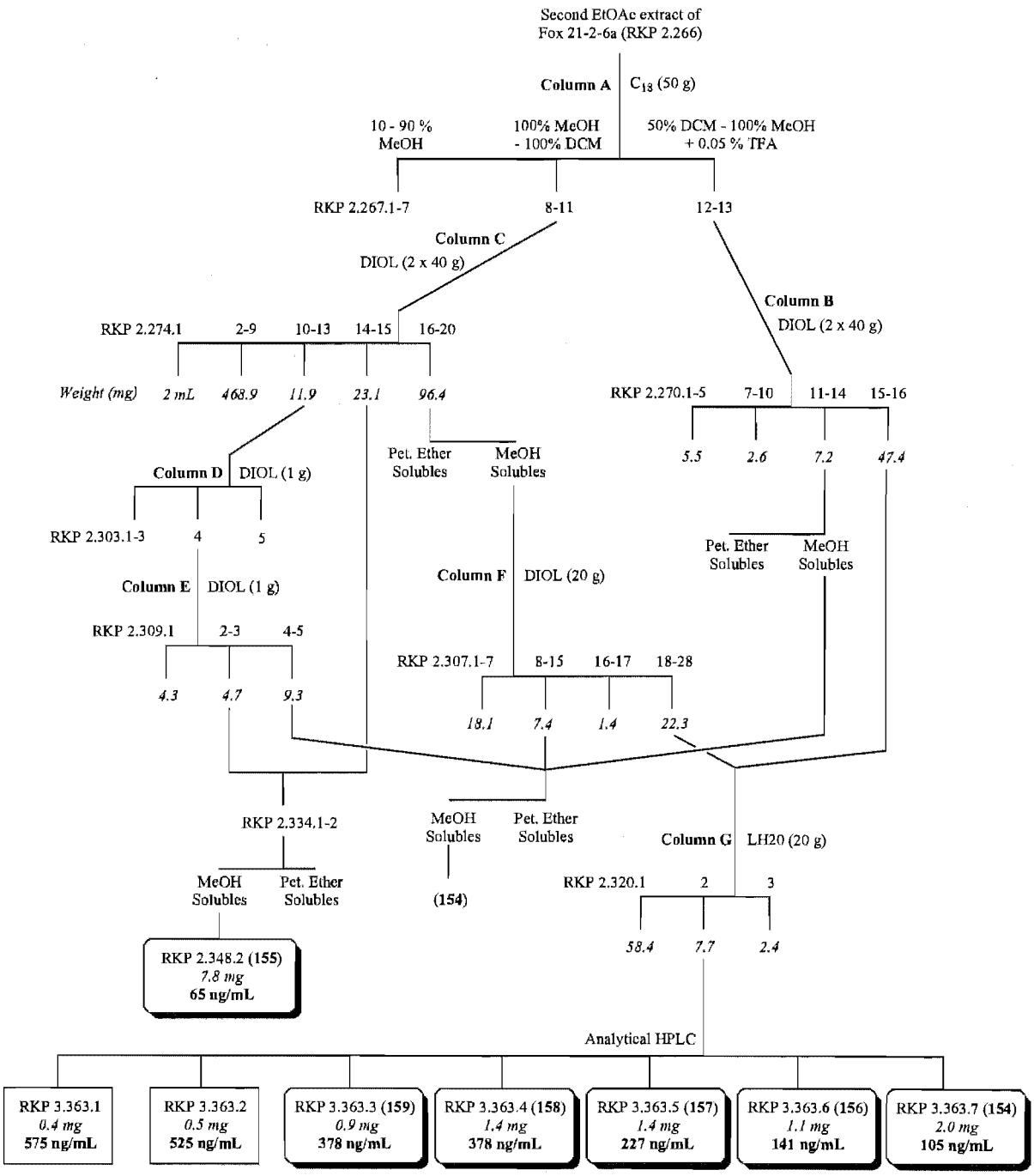

Scheme 6.2: Purification flow chart of the second extract of the microbial isolate Fox 21-2-6a

The second crude extract of Fox 21-2-6a was initially fractionated on C_{18} with the same method as used for column A in Scheme 6.1. However, because the bioactivity profile was expected to be similar to the first extract the various fractions were collected together based on colour differences in the various fractions. RKP 2.267.1-7 were all yellow in colour and RKP 2.267.8-13 were all deep red. The last two of these fractions (RKP 2.267.12-13) required 0.05 % TFA in the mobile phase to elute off the column and as such were kept separate from the other four red fractions (RKP 2.267.8-11). The cytotoxicity of RKP 2.267.8-11 and RKP 2.267.12-13 was unable to be determined due to the high volume of oily material present in the fractions. However, RKP 2.267.1-7 showed no cytotoxicity towards the P388 cell line.

RKP 2.267.12-13

In an attempt to remove the excess oil from this combined fraction a slightly different elution profile with normal phase chromatography on DIOL was devised. The high mass of this fraction meant that it needed to be split into two then run in series. RKP 2.267.12-13 was eluted from normal phase DIOL (column B) with a stepwise gradient starting at Pet. Ether (bp 40 - 60°C) through to DCM, then EtOAc and finally MeOH collecting 16 fractions in total. No cytotoxicity was observed in the first five fractions, but all subsequent fractions displayed excellent cytotoxicity. Analysis of fractions RKP 2.270.7 - 10 by reverse phase C_{18} HPLC showed that all four fractions contained similar components but were still relatively complex however, this complexity combined with the low mass recovery in these four fractions prevented further investigations. Analysis of the next four fractions (RKP 2.270.11-14) by reverse phase HPLC indicated that these fractions all contained the same major principle and were relatively pure and as such were combined. A ^{1}H NMR spectrum in $CDCl_3$ of the combined fractions showed a number of peaks arising from fatty acid contamination thus this combined fraction was washed with Pet. Ether which left less than 1 mg of active principle. Another ^{1}H NMR spectrum in CD_3OD indicated that the residue of this fraction was relatively pure but the low mass prevented further investigation of this fraction. The same ^{1}H NMR spectrum was also obtained from a later series of fractions (RKP 2.307.8-15).

The final two fractions from column B (RKP 2.270.15-16) both displayed relatively complex HPLC traces. As with the previous four fractions the ^{1}H NMR spectra

highlighted the presence of large amounts of contaminating fatty acid material, thus both fractions were combined and washed with Pet. Ether to remove the fats to leave less than 2 mg of sample. As with RKP 2.270.11-14 both the complexity of the ^{1}H NMR spectrum and the low sample mass prevented further investigations. These two fractions (RKP 2.270.15-16) were later combined with fractions RKP 2.307.18-28 for which the HPLC traces were virtually identical.

RKP 2.267.8-11

The same elution profile on normal phase DIOL for RKP 2.267.12-13 was also adopted for RKP 2.267.8-11 but with 20 fractions collected rather than 16. The first eight fractions from this round of chromatography (column C) showed no cytotoxicity and were very oily. However, all the subsequent fractions showed excellent cytotoxicity (< 97.5 ng/mL). Reverse phase C_{18} HPLC analysis of the cytotoxic fractions showed that RKP 2.274.10 - 13 were identical to each other and as such were combined. This was also the case in fractions RKP 2.274.14 and 15 which were also combined. The last five fractions (RKP 2.274.16 - 20) all contained over eight related compounds eluting between 11 and 15 minutes in the HPLC trace and as such these fractions were also combined. The first combined fractions (RKP 2.274.10 - 13) showed a number of peaks in the ^{1}H NMR spectrum typical of triglycerides thus a further purification step with normal phase chromatography on DIOL (column D) was done. The fraction was eluted from column D with a steep stepped gradient starting at 100 % Pet. Ether, through to DCM and finally to MeOH collecting bands of colour as they eluted. Only the second (RKP 2.303.2) and fourth (RKP 2.303.4) fractions from this column were red in colour. The second fraction (RKP 2.303.2) however, was also very oily which prevented further work on this sample. Both the ^{1}H NMR spectrum and the ESI-MS spectrum of the fourth fraction (RKP 2.303.4) indicated the presence of at least two different compounds thus this fraction was subjected to another purification step with normal phase chromatography on DIOL (column E). As the fats and oils had already been removed from RKP 2.303.4 this fraction was eluted from column E with a stepped gradient starting at DCM, into EtOAc and finally MeOH again collecting the coloured bands as they eluted. As with column D the coloured bands eluted in the second (RKP

2.309.2) and fourth (RKP 2.309.4) fractions. Reverse phase C_{18} HPLC and ^1H NMR spectroscopy showed that fraction RKP 2.309.2 was identical to an earlier fraction (RKP 2.274.14-15) and as such these two samples were combined then washed with Pet. Ether to give 7.8 mg of **155**. The structural elucidation for **155** is discussed in Section 6.5.

The ^1H NMR spectra for the last two fractions from column E (RKP 2.309.4 -5) were identical to those of RKP 2.270.11-14, RKP 2.307.8-15 and RKP 3.363.7. However, only the last of these fractions (RKP 2.363.7) was examined fully by NMR spectroscopy. The structural elucidation of the compound in this fraction (**154**) is discussed in Section 6.4.

RKP 2.274.16-20

The last of the fractions from column C (RKP 2.274.16-20) were combined and purified on a long thin normal phase DIOL column (1000mm x 5 mm). A stepped gradient solvent system starting at 100 % Pet. Ether, through to DCM, EtOAc and on to MeOH was used for sample elution. The ^1H NMR spectra of the first seven fractions from this column indicated that they contained high levels of triglycerides with very low levels of the compounds of interest which were characterised by low field phenolic protons between δ_H 12.0 - 13.0, aromatic signals between δ_H 7.0 and δ_H 8.0, anomeric signals between δ_H 5.0 and δ_H 6.0 and an *O*-methyl resonance between δ_H 3.6-3.9. The ^1H NMR spectra for the remaining fractions showed signals comparable to those of the cytotoxic components. Fractions RKP 2.307.8 - 15 showed identical signals in the respective ^1H NMR spectra and a similar trend was also seen in the reverse phase C_{18} HPLC traces, thus these eight fractions were combined. Subsequent investigation of this combined fraction by NMR spectroscopy indicated that the major component was identical to **154**.

Fractions RKP 2.307.18 - 28 all showed a series of peaks in the reverse phase C_{18} HPLC traces that eluted between four and seven minutes which was identical to that of a pair of earlier eluting fractions (RKP 2.270.15 - 16) from column B. These thirteen fractions were subsequently combined, and subjected to size exclusion chromatography on Sephadex LH20 (column G). Although only one band of colour eluted from column

G (RKP 2.320.2) most of the mass eluted in the preceding fraction (RKP 2.320.1). Analytical reverse phase C_{18} HPLC of the red fraction (RKP 2.320.2) indicated that there were at least five components in this fraction, all with the same UV spectrum and all eluting within two minutes of each other thus the final purification steps were carried out by HPLC. A 32 % ACN/H_2O isocratic solvent system was used to separate the individual components of RKP 2.320.2 by analytical reverse phase C_{18} HPLC (Figure 6.6). However, the relatively high mass of RKP 2.320.2 indicated that it would be easier to process this fraction by semi-preparative C_{18} HPLC. Attempts to purify this fraction by semi-preparative HPLC were not successful as the samples were either retained on the column too long (approximately 2 hours) or only eluted with 100 % MeOH with no separation of the individual components. Compounds **154**, **156** - **159** were therefore purified from RKP 2.320.2 by analytical C_{18} HPLC, collecting the fractions as shown in Figure 6.6.

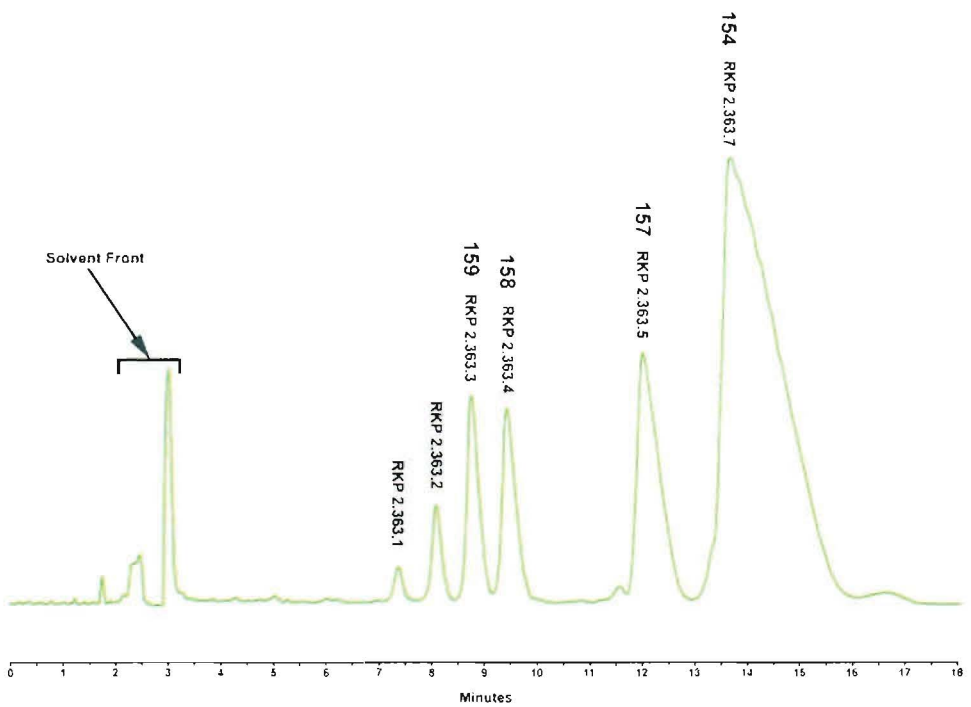

Figure 6.6: HPLC chromatogram for RKP 2.320.2

A further three fractions (RKP 2.307.16 - 17 and RKP 2.320.3) were subsequently processed to increase the yield of the compounds of interest. However, these two fractions also contained a seventh peak (RKP 2.363.6) located between RKP 2.363.5 and RKP 2.363.7. All of these compounds displayed identical UV spectra suggesting

that they were derivatives of each other. Not enough mass was recovered for the first two fractions from the analytical HPLC collections thus only RKP 2.363.3 - RKP 2.363.7 were examined by NMR spectroscopy and the structural elucidations for these five compounds (**154**, **156** - **159**) are discussed in Section 6.4

6.4 Structural elucidation

6.4.1 Structural elucidation of 154 (RKP 2.363.7)

High resolution ESI-MS indicated a mass of 585.2280 Da and a molecular formula of $C_{30}H_{35}NO_{11}$ (14 double bond equivalents). The high number of double bond equivalents coupled with an absorbance in the red region of the UV-visible spectrum suggested that **154** contained a highly conjugated aromatic system. The UV-visible spectrum also showed absorbances in the ultraviolet region similar to that seen for **141**, suggesting that the chromophoric group of this compound was similar to that seen in quinones (**137**). However, the UV spectrum for **154** also showed a third intense peak in the ultraviolet region of the spectrum suggesting the presence of a third aromatic ring system attached to the quinone system, similar to that seen in **160**.

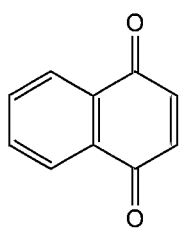

137

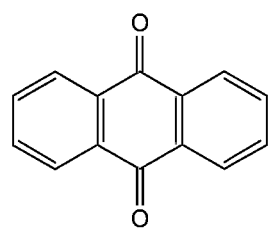

160

The ^1H NMR spectrum in CD_3OD (Figure 6.7) showed 19 signals including two aromatic signals at δ_H 7.5110 and δ_H 7.08, an anomeric proton signal at δ_H 5.56, a low field proton resonance at δ_H 5.10, an *O*-Methyl signal at δ_H 3.75, two *N*-methyl peaks at δ_H 2.87 and two methyl signals at δ_H 1.33 and δ_H 1.11 and many other signals between δ_H 4.4 and δ_H 1.4.

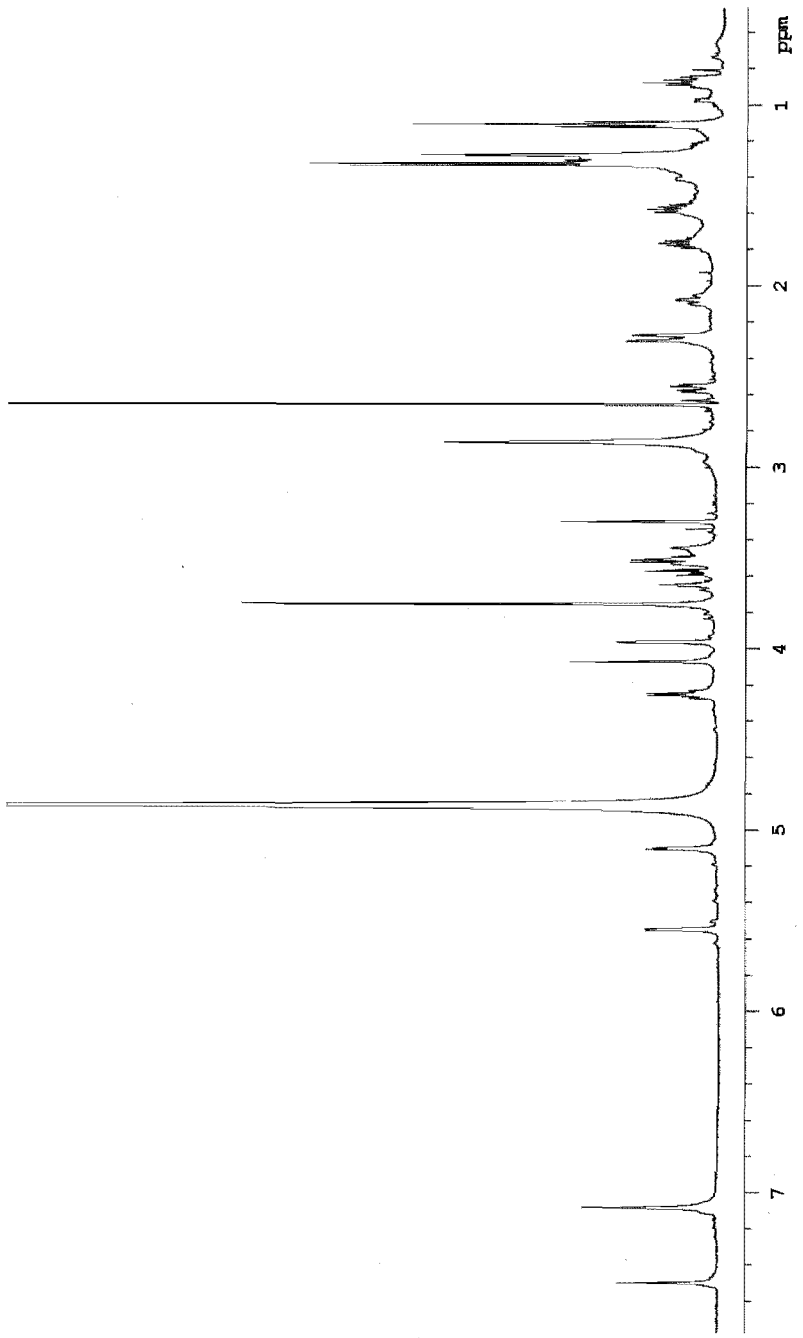

Figure 6.7: ^{1}H NMR spectrum of **154** in CD_3OD

A ^{13}C spectrum was obtained for this sample and showed 33 signals (Figure 6.8) but the molecular formula indicated that there were only 30 carbons present in the molecule. Three of the signals however, were of a much lower intensity that those next to them.

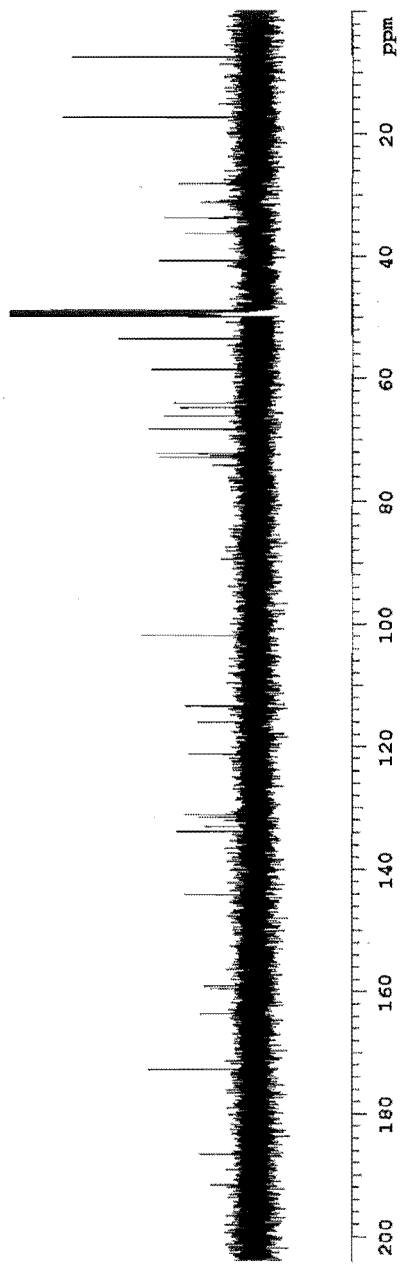

Figure 6.8: ^{13}C NMR spectrum of **154** in CD_3OD

The signals between δ_C 191.6 and δ_C 113.4 suggested that the postulated aromatic anthraquinone structure was highly oxygenated and this was further borne out by a ^1H NMR spectrum of **154** in $CDCl_3$ which showed three phenolic signals below δ_H 12.0. COSY (Figure 6.35), TOCSY and HSQC (Figure 6.36) experiments enabled seven different spin systems to be determined (Figure 6.9a - d and Figure 6.10a - c). The first of these spin systems showed correlations from the proton at δ_H 5.1 to a pair of CH_2 protons at δ_H 2.56 and δ_H 2.28 with the proton at δ_H 5.1 showing a $^1J_{CH}$ correlation to a carbon at δ_C 72.9 which indicated the presence of an oxygen atom on this carbon (Figure 6.9a). The second spin system was an ethyl group with correlations from a methyl triplet at δ_H 1.11 to two proton multiplets at δ_H 1.76 and δ_H 1.56 (Figure 6.9b). The third and fourth spin systems were both part of an aromatic system. The first aromatic proton signal at δ_H 7.08 integrated for two protons and showed two $^1J_{CH}$ correlations in the HSQC spectrum to carbons with almost identical chemical shifts (Figure 6.9c). The second aromatic signal at δ_H 7.51 showed a $^1J_{CH}$ correlation to a carbon at δ_C 121.2 (Figure 6.9d).

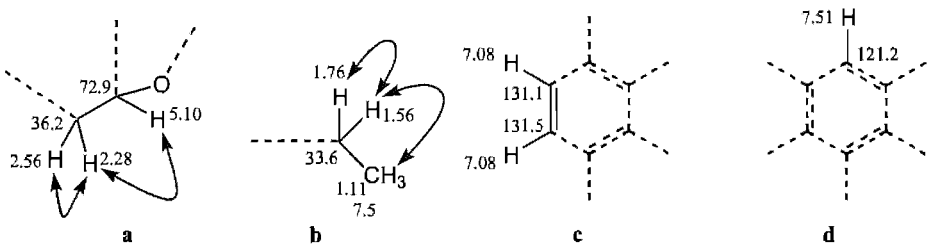

Figure 6.9a-d: Fragments from correlations seen in COSY, TOCSY and HSQC experiments for **154**.

The proton in the fifth fragment at δ_H 4.07 showed a single $^1J_{CH}$ correlation to a carbon at δ_C 58.5 (Figure 6.10a). The sixth fragment was relatively complex compared to those already assembled. The signal at δ_H 5.56 was suggestive of an anomeric proton and showed correlations to proton resonances at δ_H 2.28 and δ_H 2.08. The two signals at δ_H 2.28 and δ_H 2.08 showed $^1J_{CH}$ correlations to a carbon at δ_C 28.1. The proton signal at δ_H 3.52 showed correlations to proton signals at δ_H 2.28, 2.08 and δ_H 3.96. The proton resonance at δ_H 4.26 showed correlations to the proton signal at δ_H 3.96 and a methyl signal at δ_H 1.33. The $^1J_{CH}$ correlations for the protons at δ_H 3.96 and δ_H 4.26 to carbon signals at δ_C 66.1 and δ_C 68.2 respectively were both indicative of an oxygen atom present on these two carbons. The $^1J_{CH}$ correlation for the proton at δ_H 5.56 to a carbon

signal δ_C 101.9 suggested the presence of two oxygen atoms on this carbon (Figure 6.10b). One *O*-methyl and two *N*-methyl resonances were also seen. The two *N*-methyl groups showed the same ^1H and ^{13}C chemical shifts. They were thought to be in a similar environment thus were placed on the same nitrogen atom (Figure 6.10c).

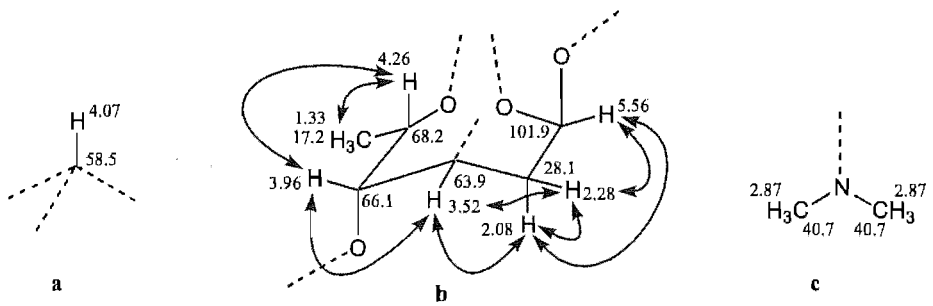

Figure 6.10a-c: Fragments from correlations seen in COSY, TOCSY and HSQC experiments for **154**.

Correlations in the CIGAR spectrum (Figure 6.37) enabled a full structural assignment of the non aromatic portion of **154**. However, due to the high number of spectroscopically silent centres in the aromatic portion a full assignment was not possible by NMR spectroscopy alone. The proton at δ_H 5.10 showed correlations to three aromatic carbons at δ_C 163.6, 144.1 and δ_C 133.1, an oxygenated quaternary carbon at δ_C 72.2 and the anomeric carbon at δ_C 101.9. The CH_2 protons at δ_H 2.56 and δ_H 2.28 (Figure 6.9a) also showed correlations to an aromatic carbon at δ_C 133.1, the oxygenated quaternary carbon at δ_C 72.2 and the methine carbon at δ_C 58.5 which enabled the connection of Figures 6.9a, 6.9d and 6.10b (Figure 6.11).

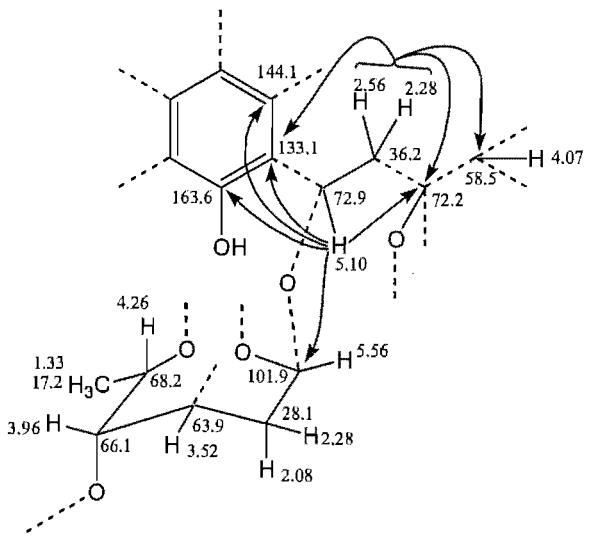

Figure 6.11: CIGAR correlations observed for the protons at δ_H 5.10, 2.56 and δ_H 2.28.

The proton at δ_H 4.07 showed correlations to a carbonyl group at δ_C 172.8, three aromatic carbons at δ_C 144.1, 133.1 and 121.2, the oxygenated quaternary carbon atom at δ_C 72.2 and the CH_2 group at δ_C 36.2 (Figure 6.12).

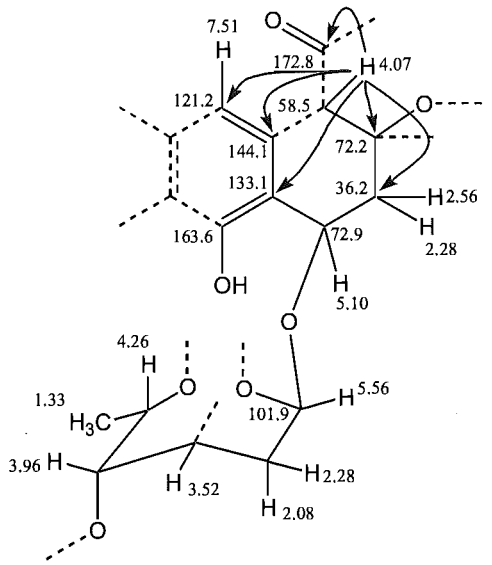

Figure 6.12: Observed CIGAR correlations for δ_H 4.10.

The aromatic proton at δ_H 7.51 showed correlations to two aromatic carbons at δ_C 133.1 and δ_C 116.0, a carbonyl at δ_C 186.7 and the tertiary carbon at δ_C 58.5. The correlations from δ_H 7.51 to δ_C 133.1 and δ_C 58.5 were both $^3J_{CH}$ correlations and as $^3J_{CH}$ correlations are often stronger in aromatic systems than the corresponding $^2J_{CH}$ correlations it also places the other two correlations from this proton to the carbons at δ_C 186.7 and δ_C 116.0 three bonds away. The low field chemical shift of the carbonyl resonance at δ_C 186.7 was suggestive of an anthraquinone moiety (Figure 6.13).

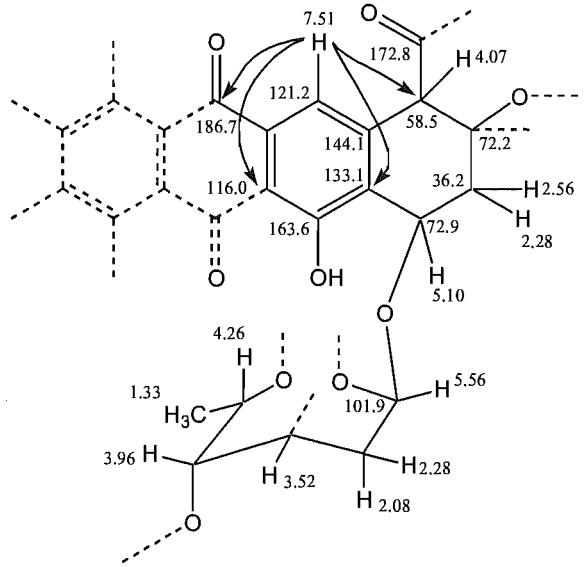

Figure 6.13: CIGAR correlations observed for δ_H 7.51.

The two aromatic protons at δ_H 7.08 showed correlations to two low field oxygenated aromatic carbon signals at δ_C 159.4 and δ_C 159.0. The two remaining phenolic signals observed in the ^1H NMR spectrum of **154** in $CDCl_3$ were attached to the to low field aromatic carbons at δ_C 159.4 and δ_C 159.0. Further correlations from the aromatic proton signals at δ_H 7.08 to carbons at δ_C 113.4 and δ_C 113.5 were also observed. The *O*-methyl resonance at δ_H 3.75 showed a single correlation to a carbonyl signal at δ_C 172.8 (Figure 6.14).

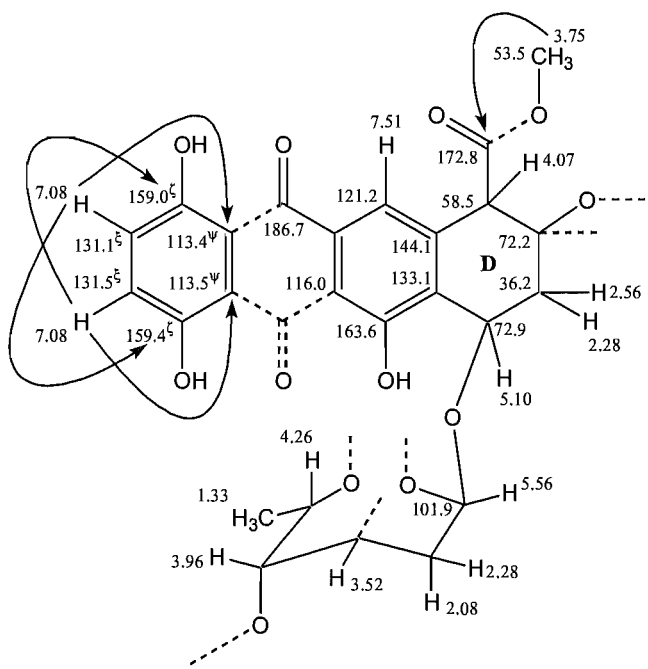

Figure 6.14: CIGAR correlations observed for δ_H 7.08 and δ_H 3.75. $^{\xi\psi\zeta}$ interchangeable signals

The methyl resonance at δ_H 1.11 showed a correlation to the oxygenated quaternary carbon at δ_C 72.2 which enabled connection of this fragment to the free position in the D- ring of the anthraquinone. This was supported with correlations from the two CH_2 protons of the ethyl group at δ_H 1.76 and δ_H 1.56 to the carbon at δ_C 72.2 as well as individual correlations to carbons at δ_C 36.2 and δ_C 58.5 respectively (Figure 6.15).

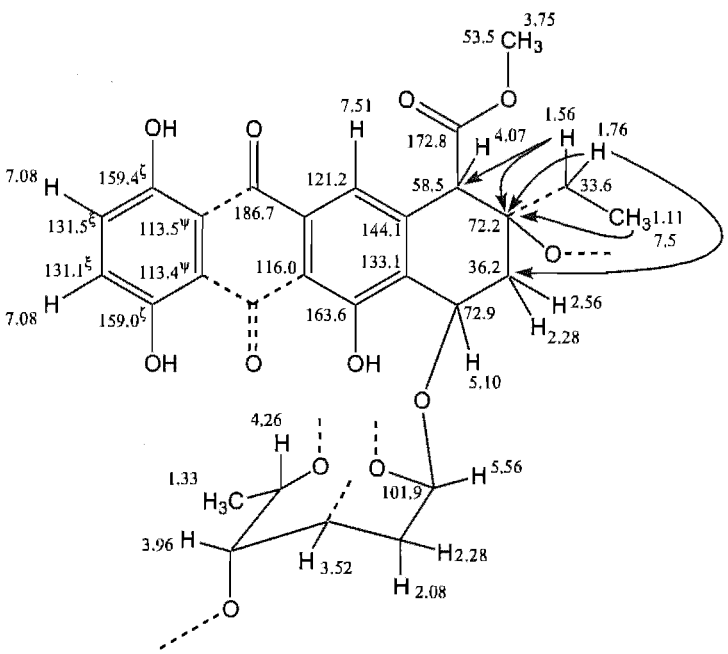

Figure 6.15: CIGAR correlations observed for δ_H 1.76, 1.56 and δ_H 1.11.

The two *N*-methyl groups at δ_H 2.87 showed a single correlation to a carbon at δ_C 63.9 and the anomeric proton at δ_H 5.56 showed an important correlation to the carbon at δ_C 68.2 which enabled closure of the sugar ring (Figure 6.16).

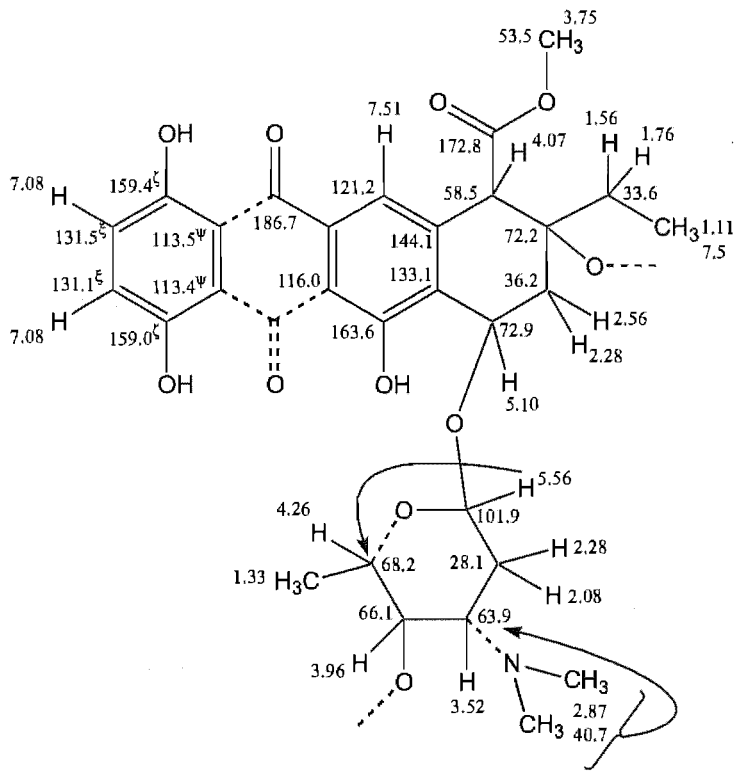

Figure 6.16: CIGAR correlations observed for δ_H 5.56 and δ_H 2.80.

The two remaining positions in the fragment in Figure 6.16 must be filled by protons as the fragment has a molecular formula of $C_{30}H_{33}NO_{11}$. This is two protons less than the molecular formula proposed from high resolution ESI-MS to give **154**. The two carbons unassigned in the anthraquinone moiety were assigned from the ^{13}C NMR spectrum with the very low field carbon signal at δ_C 191.6 assigned as the second aromatic ketone group of the quinone ring which left the signal at δ_C 133.8 to be assigned to the last available site *ortho* to the aromatic proton signal at δ_H 7.51. The relative stereochemistry seen in **154** below is discussed in Section 6.4.1.1.

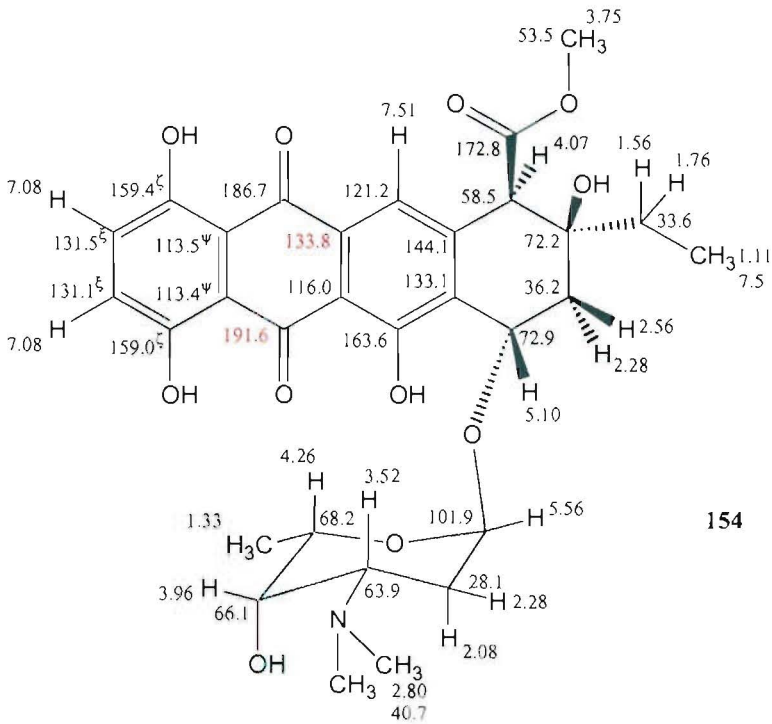

6.4.1.1 Relative stereochemistry of 154

There is one diastereotopic centre and three stereogenic centres in the D-ring (Figure 6.17) of the anthraquinone moiety with a second diastereotopic centre in the ethyl group attached to the D-ring.

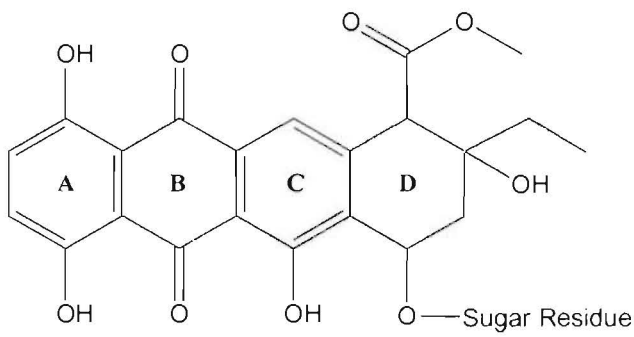

Figure 6.17: Ring labelling system for anthraquinones

A further four stereogenic centres and one diastereotopic centre are also seen in the sugar residue. The coupling constants and 1D and 2D NOESY (Figure 6.38) spectra enabled the relative stereochemistry of the anthraquinone moiety and the sugar residue to be determined.

An important NOESY correlation was seen from the proton at δ_H 4.26 to a proton at δ_H 3.52 which placed these two protons in axial positions. If one or both of these protons were in an equatorial position then NOESY correlations would not be observed. The proton at δ_H 3.52 also showed NOESY correlations to protons at δ_H 3.96 and δ_H 2.28. The final stereocentre in the rhodosamine sugar residue was at the anomeric carbon at δ_C 101.9. The $^3J_{HH}$ of 2.5 Hz for the anomeric proton at δ_H 5.56 indicated that it was in an equatorial position. The only observable coupling for the proton signal at δ_H 2.28 was a $^2J_{HH}$ of 15 Hz, thus the expected couplings to δ_H 3.52 and δ_H 5.56 must be small indicating dihedral angles approaching 90°. Figure 6.18 shows the relative stereochemistry proposed for the sugar residue.

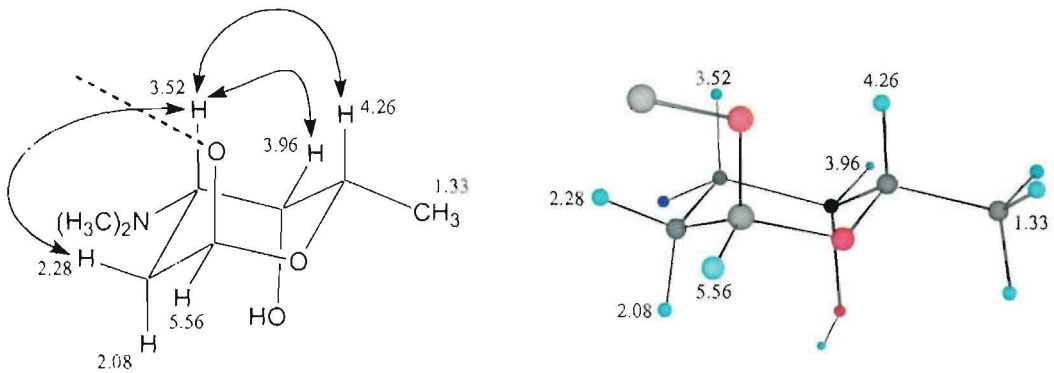

Figure 6.18: NOESY correlations observed for the sugar residue of **154**.

The relative stereochemistry proposed for the sugar residue in Figure 6.18 indicates that it is a rhodosamine residue.

The coupling constants and NOESY correlations for the proton signals of the D-ring enabled the relative stereochemistry of this ring to be assigned. The proton signal at δ_H 5.10 showed a $^3J_{HH}$ of 5 Hz, the proton peak at δ_H 2.56 showed a $^3J_{HH}$ of 5 Hz and a $^2J_{HH}$ of 15 Hz and the proton resonance at δ_H 2.28 showed a $^2J_{HH}$ of 15 Hz which placed the proton at δ_H 2.56 in the pseudo axial position. If the proton at δ_H 2.56 was in the pseudo equatorial position the resulting dihedral angle would give rise to a $^3J_{HH}$ of 8 - 10 Hz for the proton at δ_H 5.10. The other two stereogenic centres were assigned with 1D and 2D NOESY spectra. The proton signal at δ_H 2.56 showed a single NOESY correlation to the proton at δ_H 5.10 which suggested that the proton at δ_H 4.07 was in an equatorial position rather than an axial position for which a NOESY correlation would

have been expected. NOESY correlations were also observed from the protons at δ_H 4.07 and δ_H 2.28 to the ethyl protons at δ_H 1.76 and δ_H 1.56 respectively to give a final relative stereochemistry of 7*S**,9*S**,10*R** for the D-ring. This stereochemistry also allows a hydrogen bond between the OH group on C^9 and the carbonyl group at C^{10} to be formed (Figure 6.19).

Only the relative stereochemistry for the D-ring and the rhodosamine residue was able to be determined. Even if the absolute stereochemistry was known for either the D-ring or the rhodosamine residue this would be unable to be related to the other component via NMR experiments as the sugar is able to freely rotate around the anomeric bond. Thus NOESY correlations would be observed between δ_H 5.10 on the D-ring and δ_H 5.56 on the sugar no matter what the absolute stereochemistry was.

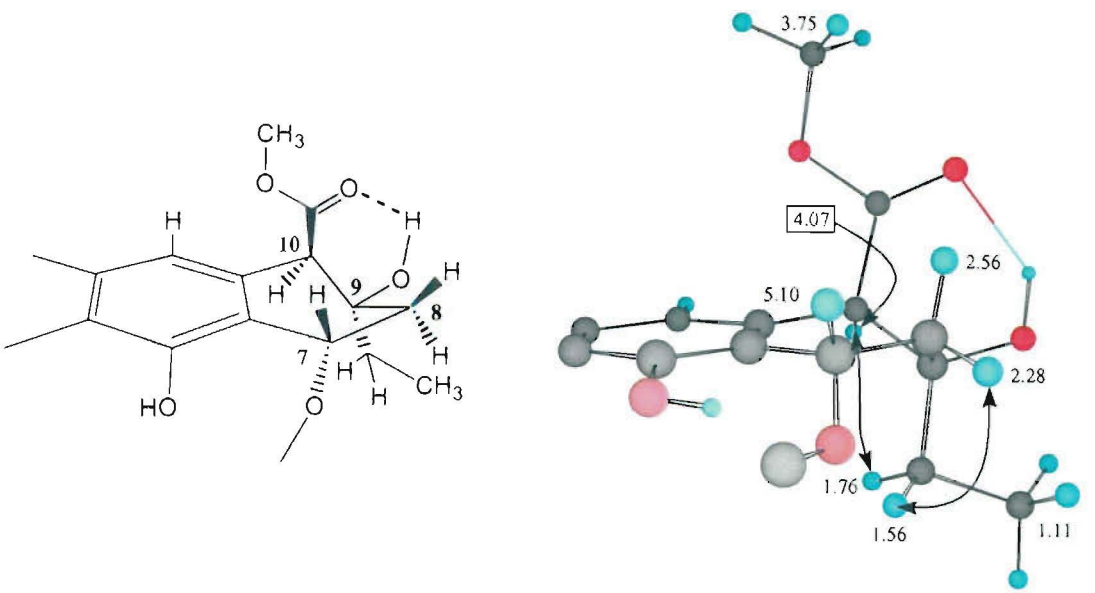

Figure 6.19: NOESY correlations observed in the anthraquinone core of **154**.

An $[\alpha]_D$ of +128° for **154** indicated that it was not a racemic mixture.

A literature search based on **154**, with no stereochemistry, indicated that **154** was a pyrromycin derivative.[102, 164, 165] However, the stereochemistry proposed for **154** had previously only been seen in one other anthraquinone, ruticulomycin B (**161**).[102, 166] Thus **154** was called (7*S**9*S**10*R**)-pyrromycin.

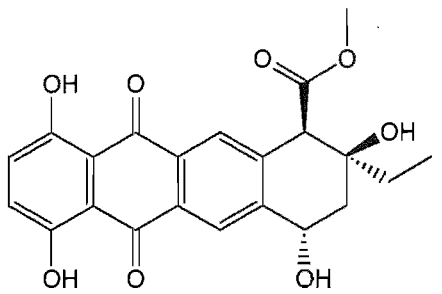

161

6.4.2 Structural elucidation of 156 (RKP 2.363.6)

The second red compound from the analytical HPLC purifications was a shoulder on the major peak (**154**) and as such contained a large amount of **154**. The high resolution ESI-MS spectrum of this fraction showed two compounds with molecular weights of 585.2283 Da and 571.2126 Da corresponding to molecular formulae of $C_{30}H_{35}NO_{11}$ and $C_{29}H_{33}NO_{11}$ respectively (both 14 double bond equivalents). The molecular weight at 586 Da was due to the presence of **154** within this fraction thus the molecular weight of the compound of interest was actually 571 Da. The UV spectrum of **156** was identical to that of **154** and therefore **156** must also contain the anthraquinone core (**160**).

The ^{1}H NMR spectrum of **156** was very similar to that of **154**. However, only one *N*-methyl group was observed and therefore **156** must be the *N*-demethyl version of **154**. The presence of only one *N*-methyl group in **156** is also consistent with the slight increase in polarity.

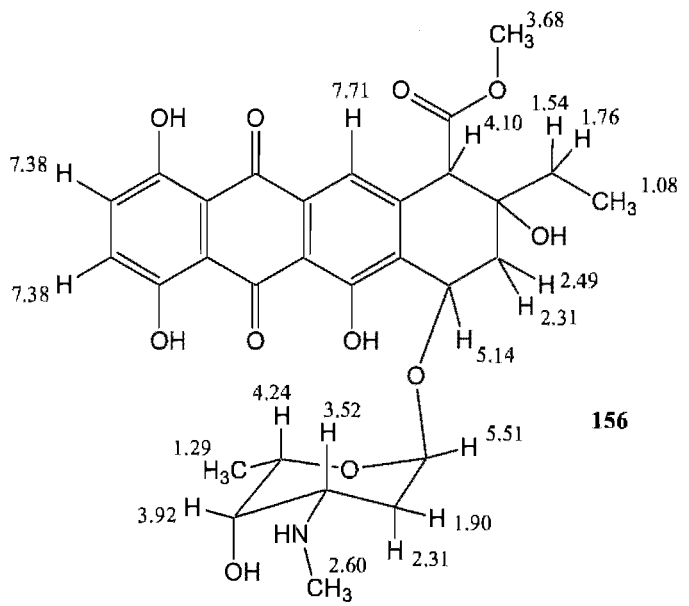

156

The low mass (1.1 mg) and presence of **154** in this fraction prevented any further work on this sample. However, a search in Antibase found two similar *N*-demethyl compounds, pyrromycin X (**162**) and *N*-demethylaklavine (**163**).[102] To confirm the proposed structure this compound would need to be re-isolated from the culture medium of the isolate Fox 21-2-6a and then analysed with further NMR spectroscopic experiments.

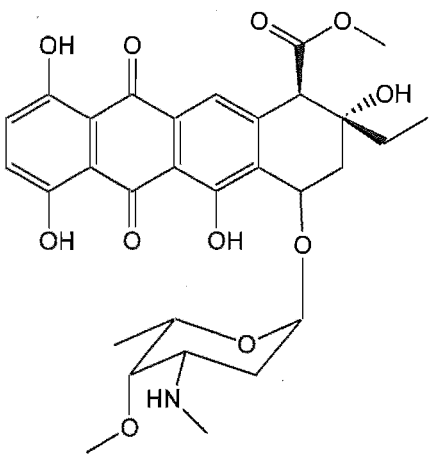

162

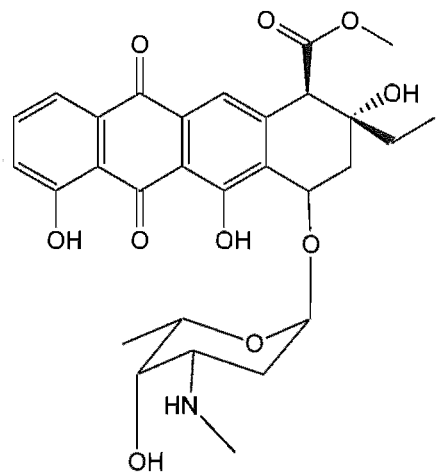

163

6.4.3 Structural elucidation of 157 (RKP 2.363.5)

High resolution ESI-MS of this fraction indicated that **156**, like **154**, also had a mass of 585.2282 Da and a molecular formula of $C_{30}H_{35}NO_{11}$ (14 double bond equivalents) with the same UV spectrum, indicative of an anthraquinone core. The ^1H NMR spectrum (Figure 6.20) of this fraction indicated that **157** was also related to **154**. However, there were significant differences in the NMR signals arising from the D-ring of the anthraquinone core. As the mass and UV chromophore of **157** and **154** were the same the difference in signal assignment must be attributed to differences in the stereochemistry.

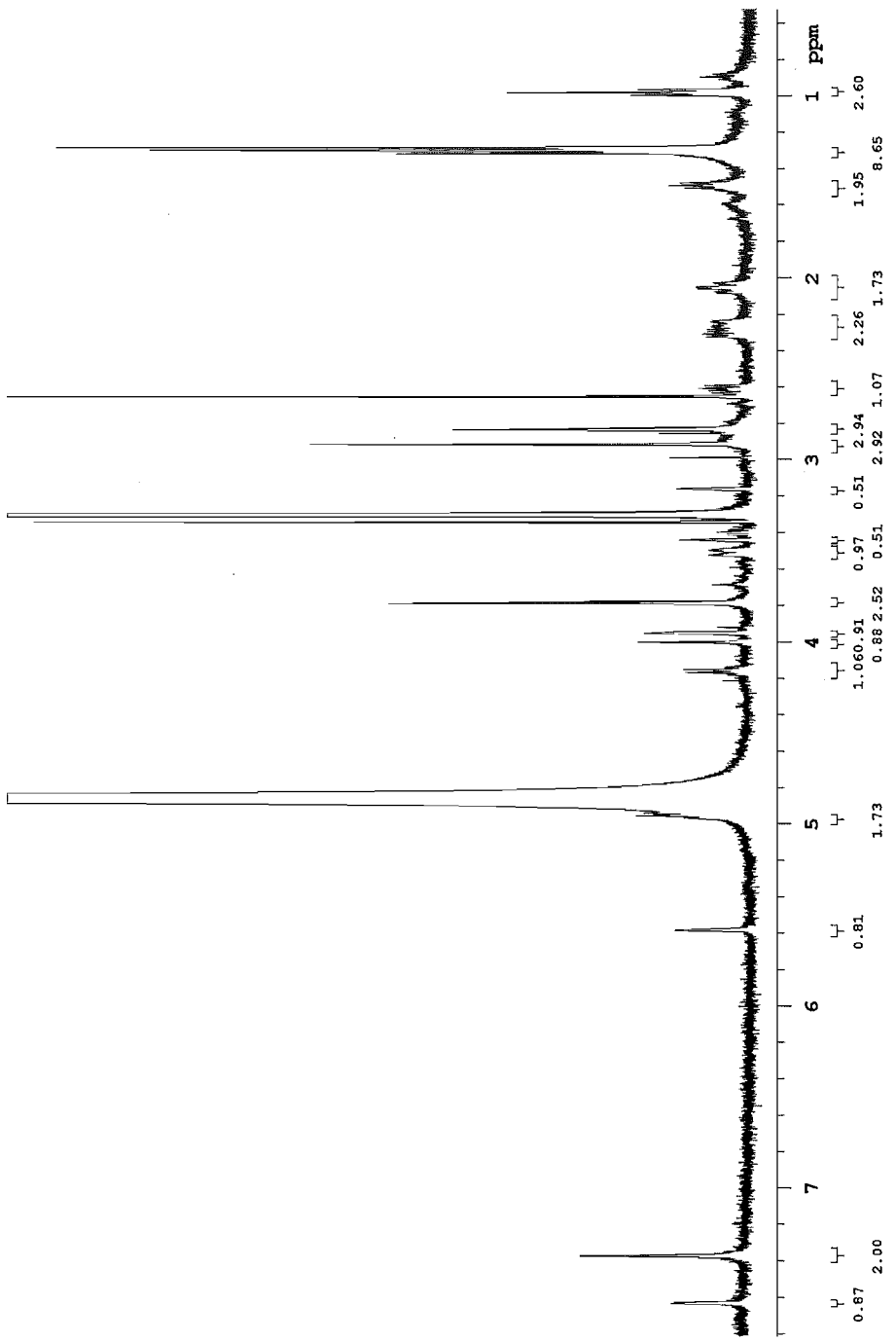

Figure 6.20: ^{1}H NMR spectrum of **157** in CD_3OD

The signals arising from the rhodosamine residue (δ_H 5.58, 4.17, 3.95, 3.52, 2.91, 2.85, 2.29, 2.06 and δ_H 1.33) were all almost identical to those seen in **154** thus the alteration in stereochemistry must be within the D-ring of the anthraquinone core. This was confirmed further as all the signals from the D-ring showed differences in the chemical shifts and the coupling constants. The signals observed for the D-ring in **154** were δ_H 5.10, 2.56, 2.28, 4.07, 1.76, 1.56 and δ_H 1.11, but in **157** the signals observed were δ_H 4.96, 2.62, 2.32, 3.99, 1.49 and δ_H 0.98 respectively.

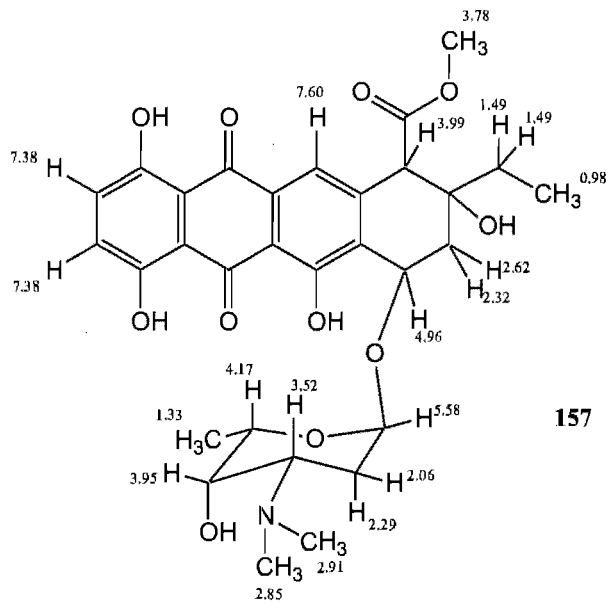

157

6.4.3.1 Relative stereochemistry of 157

The proton signal at δ_H 4.96 was now a triplet with a $^3J_{HH}$ of 6.5 Hz rather than a doublet at δ_H 5.10 with a $^3J_{HH}$ of 5 Hz. The two protons of the CH_2 group in the D-ring also showed changes in their chemical shifts and coupling constants from δ_H 2.56 with a $^3J_{HH}$ of 5.5 and a $^2J_{HH}$ of 15.5 Hz and δ_H 2.28 with a $^2J_{HH}$ of 15 Hz in **154** to δ_H 2.62 with a $^3J_{HH}$ of 7.5 and a $^2J_{HH}$ of 14 Hz and δ_H 2.32 with a $^3J_{HH}$ of 8 and a $^2J_{HH}$ of 14 Hz for **157**. The last major variations seen in the shifts of **157** were in the ethyl side chain. In **154** the two protons of the CH_2 group in the ethyl side chain resonated at δ_H 1.76 and δ_H 1.56. In **157** however, the proton signals of the CH_2 group both resonated at δ_H 1.49. This suggested that the stereochemistry of the ethyl side chain had altered from that

seen in **154**. A slight increase in the polarity of **157** over **154** was noted while purifying this compound. This increase in polarity was attributed to the lack of a hydrogen bond between the hydroxyl group at C^9 and the carbonyl group at C^{10}. To prevent the formation of the hydrogen bond the hydroxyl group at C^9 and the carbonyl group at C^{10} must both be in pseudo axial positions (Figure 6.21a - b). If these two groups were in an axial - equatorial or equatorial - equatorial conformation then hydrogen bonding between the hydroxyl group and an available oxygen could occur. This change in stereochemistry around the D-ring would also alter the coupling constants of the protons at δ_H 4.96, 2.62 and δ_H 2.32.

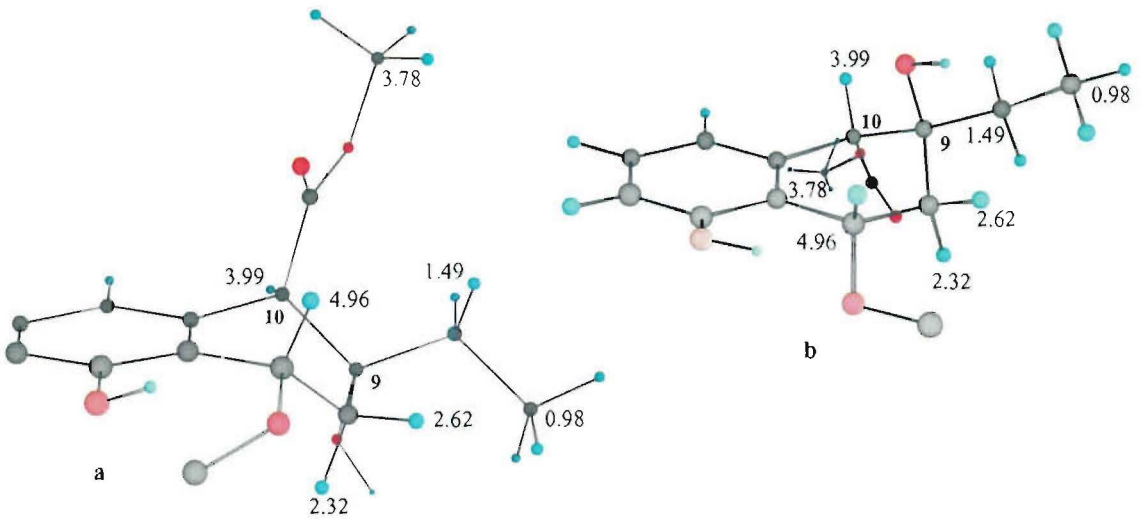

Figure 6.21a-b: Energy minimised conformations of the D ring of the anthraquinone core of **157**.

Energy minimisation using MM2 minimisation parameters in Chem3D (Cambridge software) indicated that the structure represented in Figure 6.21a contained dihedral angles between the proton at δ_H 4.96 and the CH_2 protons of 55° and 170° and that in Figure 6.21b showed dihedral angles of 33° and 145°. The Karplus equation[151] enabled an estimate of the $^3J_{HH}$ for these two conformers to be established for these protons. If Figure 6.21a was the correct conformation the expected coupling constants would be approximately $^3J_{HH}$ 4.9 and 10.9 Hz. However, if Figure 6.21b was the correct confirmation the expected $^3J_{HH}$ would be $^3J_{HH}$ 8.1 and 7.3 Hz. When compared with the experimental coupling constants of 8 and 7.5 Hz it was clear that Figure 6.21b showed the correct conformation with a 2D NOESY spectrum lending further support to

the stereochemistry of **157**. An $[\alpha]_D$ of +228° for **157** indicated that this fraction too was not a racemic mixture.

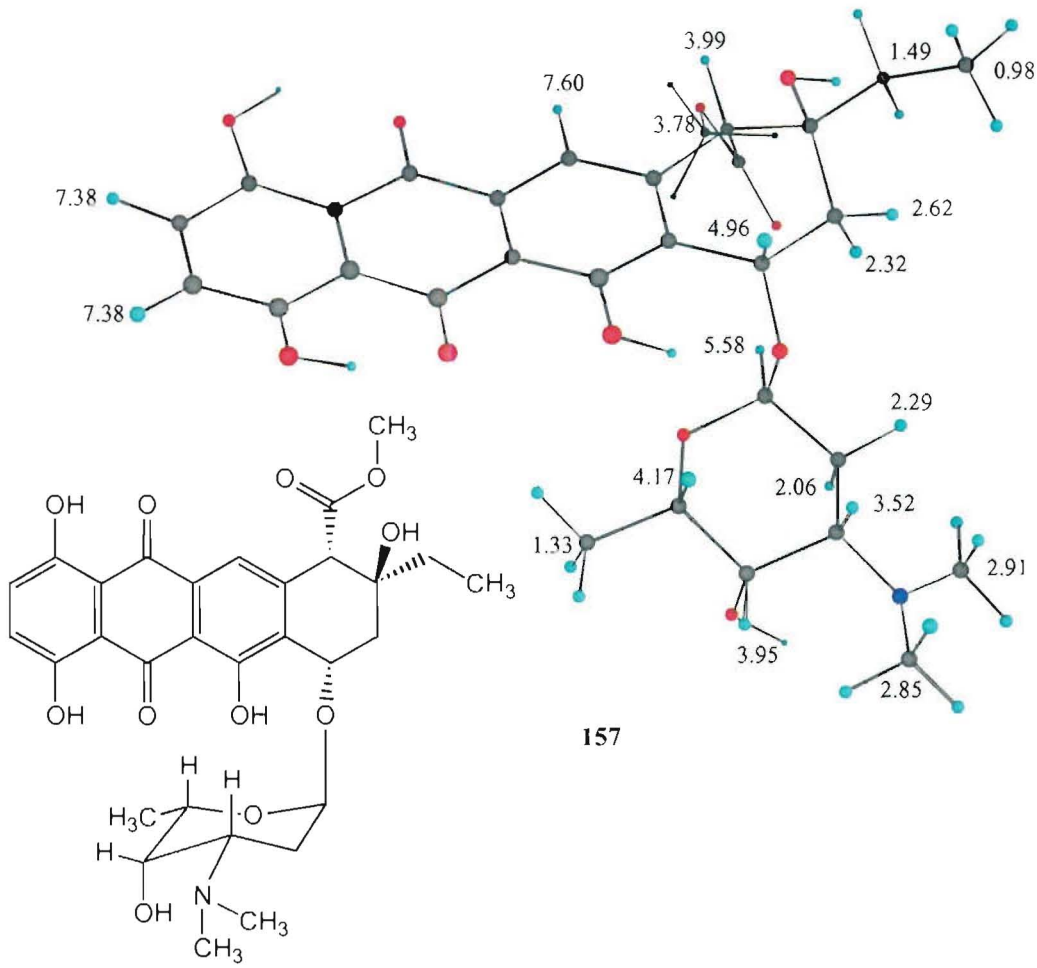

157

The stereochemistry proposed for **157** (7*R**,9*R**,10*R**) is relative, not absolute. This stereochemistry had previously only been seen in (7*R*,9*R*,10*R*)-aklavinone II (**164**).[102, 167] Thus **157** was also concluded to be a new isomer of pyrromycin and was called (7*R**9*R**10*R**)-pyrromycin.

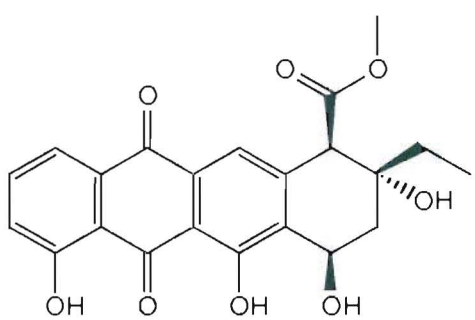

164

6.4.4 Structural elucidation of 158 (RKP 2.363.4)

A high resolution ESI-MS of the fourth fraction (RKP 2.363.4) from the analytical HPLC purification showed a mass of 572.2138 Da (MH^+) and a molecular formula of $C_{29}H_{34}NO_{11}$ (14 double bond equivalents). Once again the major compound of this fraction (**158**) contained the same UV chromophore and also showed a very similar ^1H NMR spectrum (Figure 6.22) to that of **154**. As with **157** the most significant difference between **158** and **154** was in the ethyl side chain of the D-ring. However, in this case the signals corresponding to the ethyl group (δ_H 1.76, 1.56 and δ_H 1.11) were replaced by a singlet methyl at δ_H 1.38. Therefore **158** must be the methyl version of **154** which was confirmed by HSQC and CIGAR NMR spectroscopic experiments.

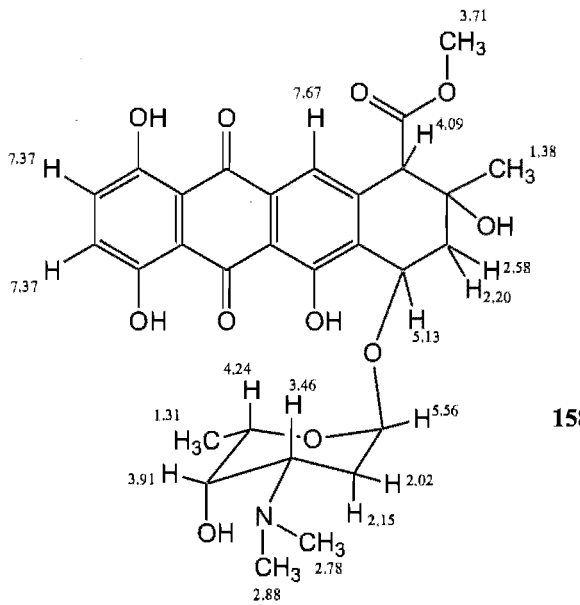

158

The coupling constants for the protons at δ_H 5.13, 2.58 and δ_H 2.20 were all similar to those observed for the equivalent protons in **154** suggesting that the stereochemistry for **158** is the same as that proposed in **154**. However, confirmation of this was not possible as the mass of **158** was insufficient for NOESY experiments.

Compounds of this type with an anthraquinone core and a methyl side chain on the D-ring are known as auramycins. Sixteen different auramycins[102] have previously been reported, but none of these had contained just one sugar residue. **158** has been tentatively named 1-hydroxyauramycin T, a name derived from the parent compound pyrromycin which is also known as 1-hydroxyaclacinomycin T.

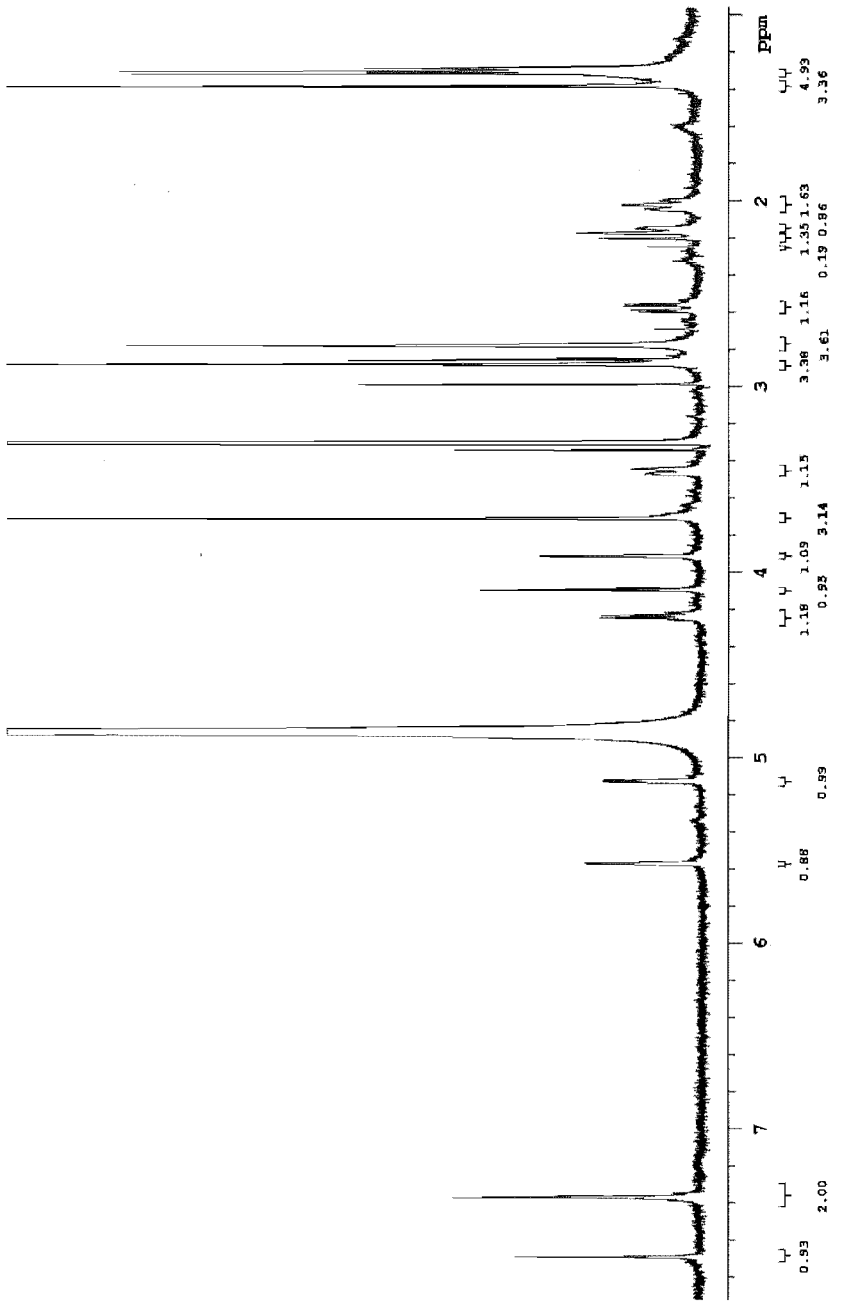

Figure 6.22: ^{1}H NMR spectrum of **158** in CD_3OD

6.4.5 Structural elucidation of 159 (RKP 2.363.3)

High resolution ESI-MS of the fifth fraction from the HPLC purification showed an increase of 28 mass units over that seen in **154** which indicated a molecular formula of $C_{31}H_{35}NO_{12}$ (15 double bond equivalents). This compound (**159**) had the same UV chromophore as **154** and also showed a very similar ^1H NMR spectrum (Figure 6.24). However, the ^1H NMR spectrum showed more differences to **154** than **156**, **157** or **158** had. The major regions of difference in the ^1H NMR spectrum were attributable to signals that arose from protons in the D-ring of the anthraquinone moiety. The signals arising from the ethyl side chain of **154** were replaced by a methyl singlet at δ_H 2.25 and a pair of isolated doublets at δ_H 3.04 and δ_H 2.66. Various other minor alterations from the ^1H NMR spectrum of **154** were also seen for the protons of the D-ring of **159** including the methine proton signal at δ_H 4.07 shifting downfield to δ_H 4.24. Because the UV spectrum and the proton signals from the sugar residue and the aromatic protons were all very similar to those of **154** it was concluded that **159** was biosynthetically related to **154**. Correlations observed in COSY and HSQC spectra confirmed the presence of the anthraquinone core and sugar but also highlighted two more fragments (Figure 6.23a-c).

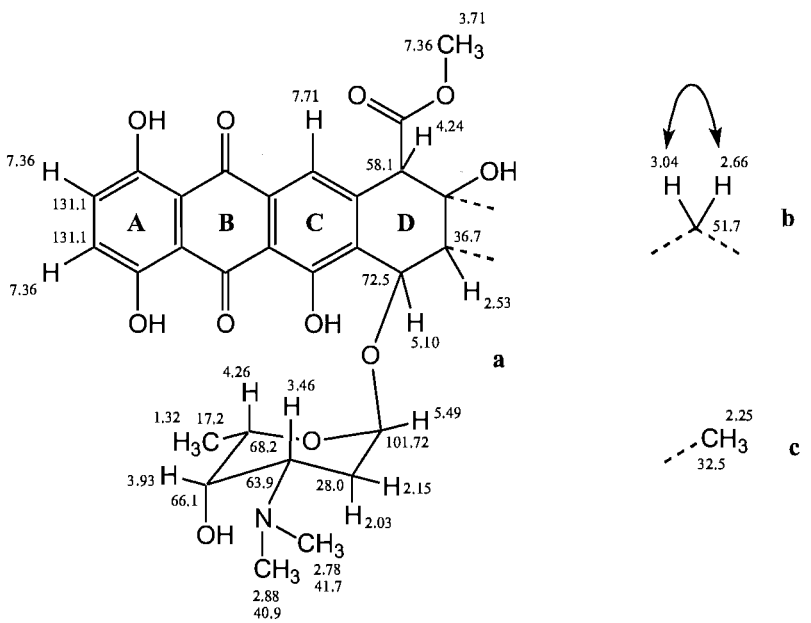

Figure 6.23a-c: Fragments of **159** deduced from ^1H, COSY, TOCSY and HSQC NMR spectra.

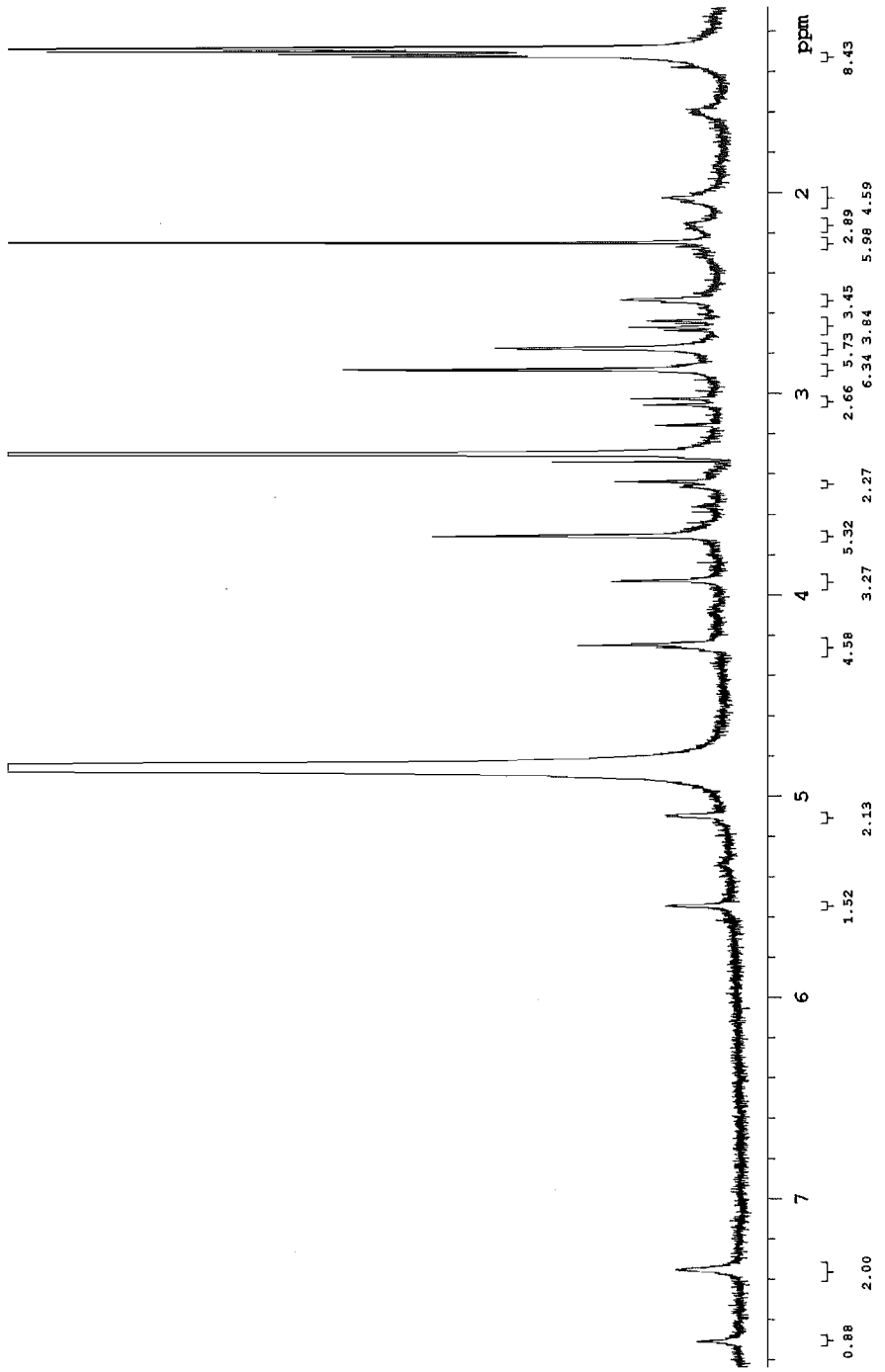

Figure 6.24: ^{1}H NMR spectrum of **159** in CD_3OD

The fragments in Figure 6.23 have a combined molecular formula of $C_{30}H_{34}NO_{11}$, 29 mass units (CHO) short of the observed mass, and also accounted for 14 of the available 15 double bond equivalents. The methyl group at δ_H 2.25 showed long range correlations in the TOCSY spectrum to the proton pair at δ_H 3.04 and δ_H 2.66 (Figure 6.25).

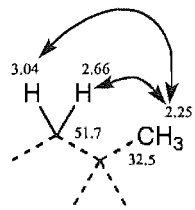

Figure 6.25: COSY correlations for the protons at δ_H 3.04, 2.66 and δ_H 2.25.

The carbon chemical shift of the methyl group at δ_H 2.25 suggested that it was next to a carbonyl group which was confirmed when a single correlation to a quaternary carbon at δ_C 210.6 was observed in the CIGAR spectrum (Figure 6.26).

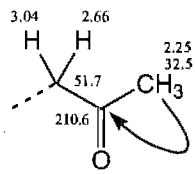

Figure 6.26: CIGAR correlation for the methyl group at δ_H 2.25.

At this point all the signals seen in the ^1H NMR spectrum had been accounted for and showed a combined molecular formula of $C_{31}H_{34}NO_{12}$ which is 1 Da short of the molecular formula proposed by high resolution ESI-MS. The fragment seen in Figure 6.26 could therefore be connected to either available position in the D-ring (Figure 6.27a and b).

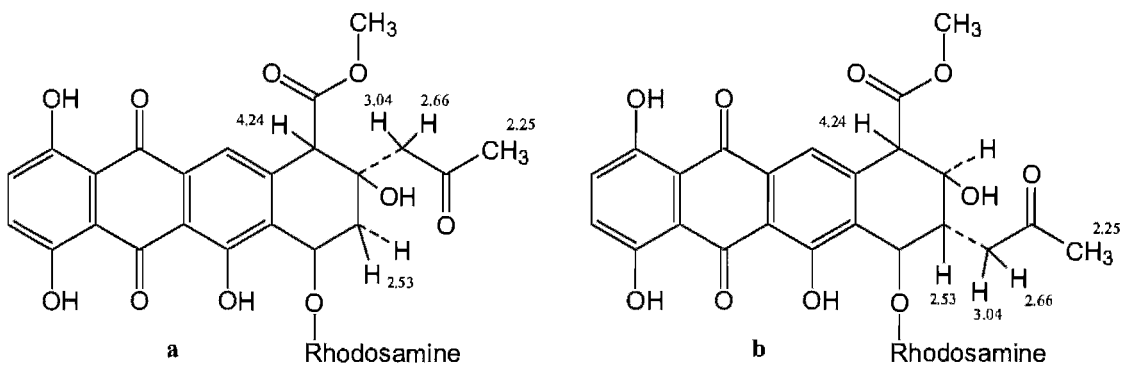

Figure 6.27a-b: Possible attachment sites of the fragment in Figure 6.25 to the anthraquinone ring.

If the structure depicted in Figure 6.27b was correct then the protons at δ_H 4.24, 3.04, 2.66 and δ_H 2.53 would all display much more complex splitting patterns in the ^1H NMR spectrum than those observed and would also show multiple correlations in a TOCSY spectrum. As well as the increase in complexity of the D-ring signals a proton at C^9 would also show a very distinct triplet between δ_H 3.5 and δ_H 5.0 in the ^1H NMR spectrum. As this is clearly not the case the structure in Figure 6.27a must be the correct one. Even though the structure in Figure 6.27a was deduced by elimination the second proton of the CH_2 group in the D-ring remained hidden either by masking from another signal or because the second proton also had a shift at δ_H 2.53. The proton at δ_H 2.53 did not show any signal splitting but rather line broadening indicating that it was at almost 90° to the proton resonating at δ_H 5.10 giving rise to an observed coupling of almost 0 Hz. If the missing proton was concealed behind another signal in the ^1H NMR spectrum then a geminal coupling of 10 - 16 Hz would be expected, but if the second proton also resonated at δ_H 2.53 then no geminal coupling would be observed. The second proton resonating at δ_H 2.53 could not also be at 90° to the proton at δ_H 5.10, but the coupling constant for the second proton signal δ_H 2.53 would also be small. This is because the second proton at δ_H 2.53 would be in a pseudo axial - pseudo equatorial arrangement with the proton at δ_H 5.10. The latter of these two possibilities is more likely as the integral for this proton was 1.75. Furthermore, the only $^1J_{CH}$ correlation seen for the carbon at δ_C 36.7 was from the proton at δ_H 2.53 and the shift for this carbon is similar to those observed for the CH_2 group in the related compounds **154** and **156 - 158**. Fujiwara *et al*[168] previously isolated various auramycins and the sulfurmycins from various *Streptomyces* spp, hydrolysed them to the parent aglycones and then obtained the ^1H NMR spectra. Comparison of the ^1H NMR spectral data of 1-hydroxysulfurmycinone (**165**) in $CDCl_3$ with the experimental data for **159** in CD_3OD showed a large number of similarities. However, the two CH_2 protons of the D-ring were at δ_H 2.42 and δ_H 2.27.

165

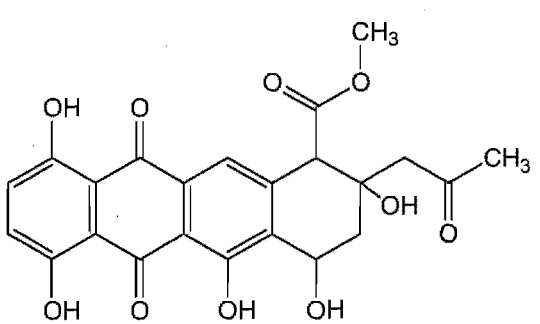

This difference could be attributable to either the solvent used to dissolve the sample for the ^{1}H NMR spectra or it could be due to differences in the stereochemistry of **159**. The latter reason is the most likely as differences in the stereochemistry of the D-ring had already been observed in the related compounds. The limited amount of mass of **159** prevented further experimental work to determine the stereochemistry from being carried out.

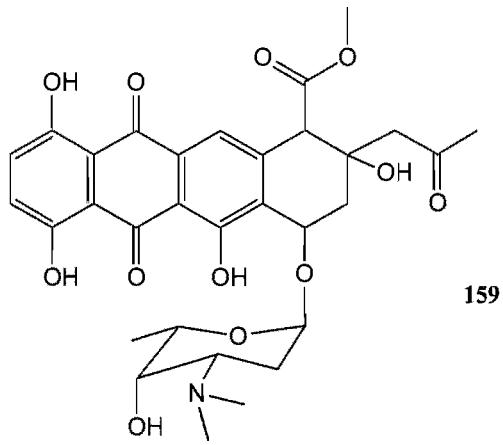

159

Anthraquinone compounds like **159** with a di-methyl ketone side chain on the D-ring are known as sulfurmycins and as with the auramycins sixteen different sulfurmycins[102] have been previously reported, but none of these sixteen contain a single sugar residue. **159** was called 1-hydroxysulfurmycin T.

6.5 Structural elucidation of 155

A high resolution ESI-MS of a sixth compound (**155**), also with the same UV spectrum as seen previously, gave a mass of 825.3287 Da which indicated a molecular formula of $C_{42}H_{51}NO_{16}$ (18 double bond equivalents). It was assumed that **155** contained the same anthraquinone moiety as that seen in the previous five compounds as the UV spectrum was the same for all these compounds and they were all isolated from the same organism. A ^{1}H NMR spectrum of **155** (Figure 6.28) showed a number of signals almost identical to those seen for the anthraquinone moiety of **154**. These signals included aromatic proton peaks at δ_H 7.70 and δ_H 7.29, an *O*-methyl signal at δ_H 3.70,

signals characteristic of an ethyl group at δ_H 1.76, 1.52 and δ_H 1.09 as well as the other signals arising from the D-ring at δ_H 4.09, 2.59, 2.28 and δ_H 5.24 (Figure 6.29).

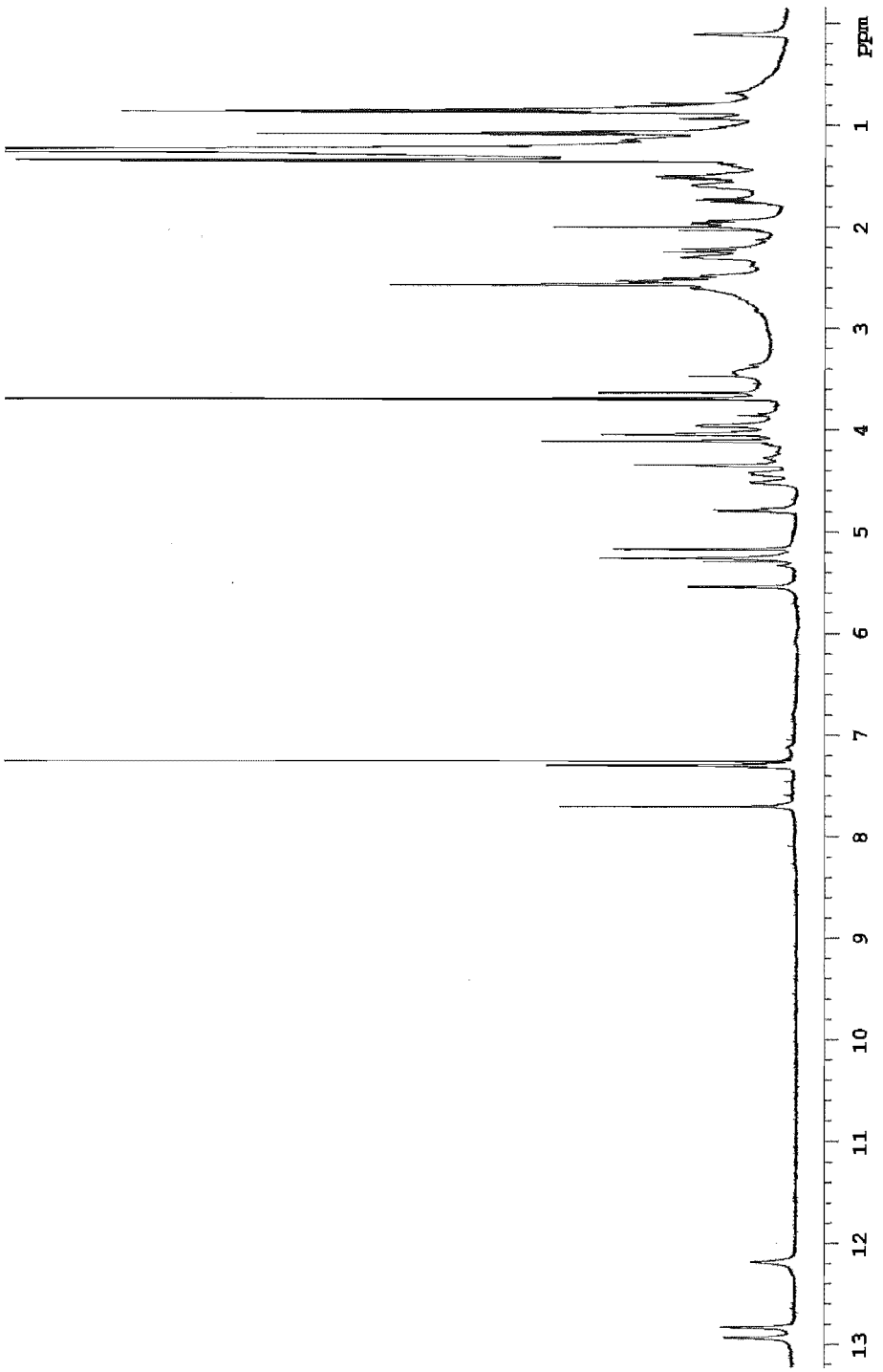

Figure 6.28: ^{1}H NMR spectrum of **155** in $CDCl_3$

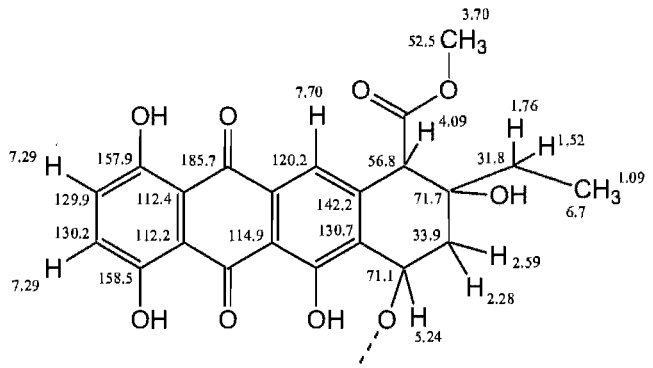

Figure 6.29: ^{1}H and ^{13}C NMR signals of **155** from the anthraquinone core.

The differences between **154** and **155** were therefore assumed to be in the sugar residues and indeed the increase in mass from 585 Da to 825 Da suggested the presence of an additional two sugar residues. A search in Antibase with the anthraquinone core and the observed mass found three compounds that matched, pyrraculomycin (**166**), 1-hydroxyaclacinomycin B (**167**) and spartanamycin-A (**168**). However, **166** contains a second chromophoric group in the third sugar residue which is known to show a strong absorbance at approximately 280 nm in the UV spectrum[169] and as **155** does not show this absorbance, **166** was discounted leaving only **167** and **168**.

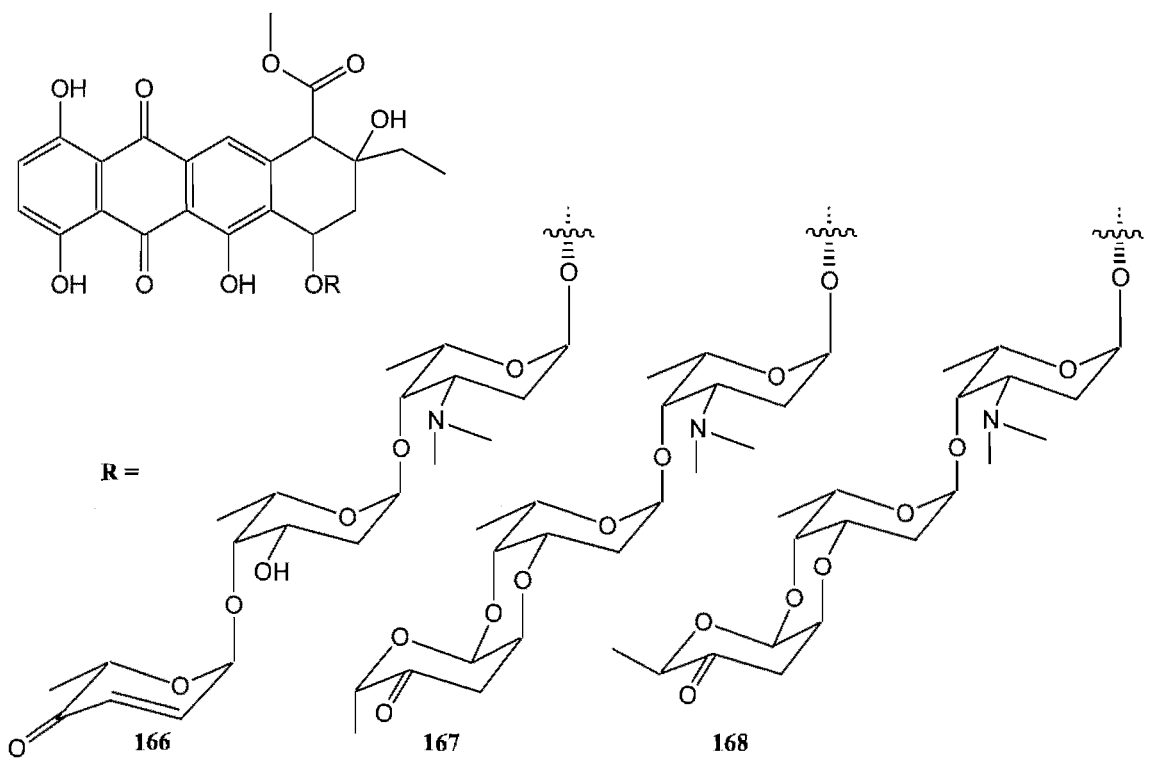

166 **167** **168**

The only difference between **167** and **168** is in the stereochemistry of the methyl group of the third sugar residue, either in an axial (**167**) or an equatorial (**168**) position. Although a reasonably high mass of **155** was recovered, the ^{1}H NMR spectrum indicated that it still contained relatively high amounts of contaminating fatty acid material which partially masked the signals arising from the sugars in **155**. This contamination was not removed by further washing with Pet. Ether as the red colour was partially soluble in the solvent.

As well as the signals arising from the anthraquinone core the ^{1}H NMR spectrum also showed a series of complex multiplets between δ_H 5.0 and δ_H 1.0 which included three anomeric proton peaks at δ_H 5.55, 5.26 and δ_H 5.16 and two methyl signals at δ_H 1.33 and δ_H 1.21. Both the molecular formula and the presence of three anomeric proton signals between δ_H 5.55 and δ_H 5.16 indicated the presence of three sugar residues. As well as the anthraquinone core COSY, TOCSY and HSQC spectra enabled four more spin systems to be determined. The first of these spin systems showed correlations from an anomeric proton at δ_H 5.55 to proton signals at δ_H 2.30 and δ_H 1.58, which in turn correlated to a proton peak at δ_H 3.48. A proton signal at δ_H 3.97 showed correlations to the signal at δ_H 3.48 as well as a signal at δ_H 4.81. The proton resonating at δ_H 4.81 correlated to a methyl signal at δ_H 1.33. The proton signals at δ_H 4.81 and δ_H 3.97 showed $^1J_{CH}$ correlations to carbons at δ_C 77.9 and 72.5 respectively. The chemical shifts of the carbon signals at δ_C 77.9 and δ_C 72.5 indicated the presence of oxygen atoms (Figure 6.30a).

The proton signals at δ_H 2.50 and δ_H 2.00 correlated to a second anomeric proton signal at δ_H 5.26 and a proton signal at δ_H 4.43. A proton resonance at δ_H 4.06 showed correlations to the proton signal at δ_H 4.43 and a second proton peak at δ_H 4.53. The proton signal at δ_H 4.53 showed a correlation to a methyl signal at δ_H 1.21. A combination of chemical shift and coupling constant data, along with the $^1J_{CH}$ correlations of δ_C 65.8, 66.2 and δ_C 66.2 for the protons at δ_H 4.53, 4.43 and δ_H 4.06 respectively allowed definition of the 2-deoxy-L-fucose sugar residue (Figure 6.30b).

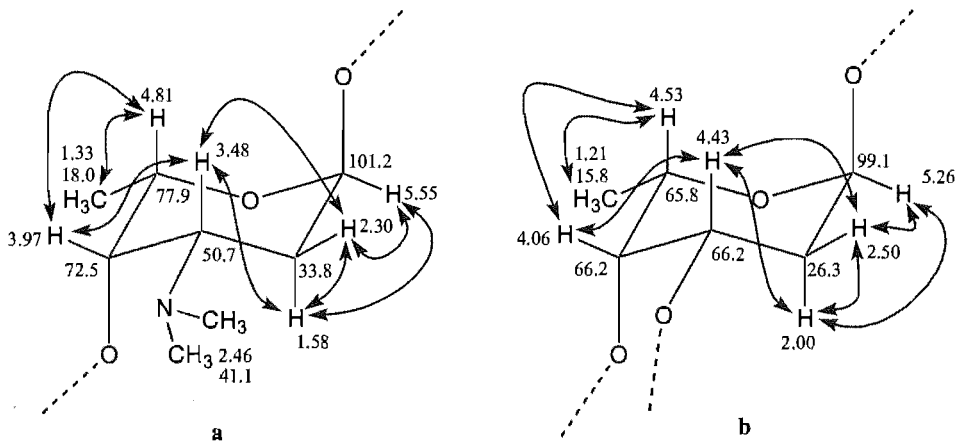

Figure 6.30a-b: COSY correlations for the rhodosamine and 2-deoxy-L-fucose sugar residues of **155**.

The third anomeric proton at δ_H 5.16 showed a correlation to a proton resonance at δ_H 4.34 which showed a correlation to a proton signal at δ_H 2.55. The proton resonating at δ_H 4.34 showed a $^1J_{CH}$ correlation to a carbon at 62.8 indicating oxygenation at this centre and the signal at δ_H 2.55 integrated for two protons to give (Figure 6.31a). The final spin system was comprised of a methyl signal at δ_H 1.33 correlating to a proton resonating at δ_H 4.05 with this resonance showing a $^1J_{CH}$ correlation to a carbon at δ_C 67.6, which indicated the presence of an oxygen atom at this centre (Figure 6.31b).

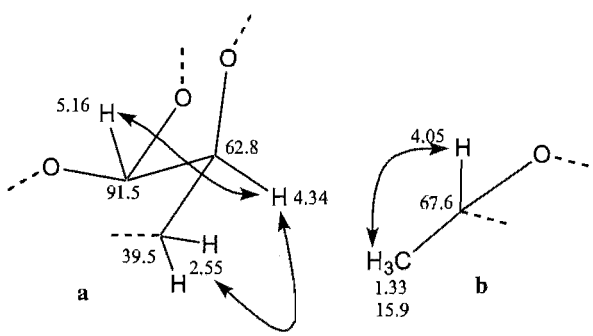

Figure 6.31a-b: COSY correlations for the third and fourth spin systems of **155**.

Due to the high molecular weight of **155** and the presence of the contaminating fatty acid material the number of correlations seen in the CIGAR spectrum was relatively low for the sugar residues. However, the correlations observed enabled the two fragments in Figure 6.31 to be connected. The ^{13}C NMR spectrum for **155** showed a carbonyl signal

at δ_C 208.0 indicative of a six-membered ring carbonyl and this was confirmed in the CIGAR spectrum. The methyl signal at δ_H 1.33 and the CH_2 signal at δ_H 2.55 both showed correlations to a carbonyl at δ_C 208.0. This sugar was a cinerulose residue (Figure 6.32).

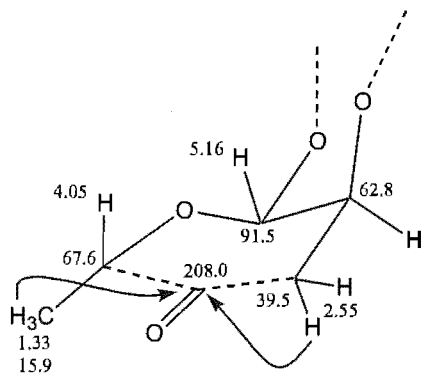

Figure 6.32: CIGAR correlations for the spin systems in Figure 6.29.

The presence of fragments in Figures 5.26, 5.28 and 5.30 confirmed that **155** was either 1-hydroxyaclacinomycin B (**167**) or spartanamycin A (**168**). The $^3J_{HH}$ coupling constant of 7 Hz between the methyl signal at δ_H 1.33 and the proton at δ_H 4.05 in the cinerulose residue was the same as that observed between the methyl at δ_H 1.33 and the proton at δ_H 4.81 in the rhodosamine residue (Figure 6.30a) suggesting that the stereochemistry was the same for both sugars which indicated that **167** was the correct structure thus **155** was 1-hydroxyaclacinomycin B.

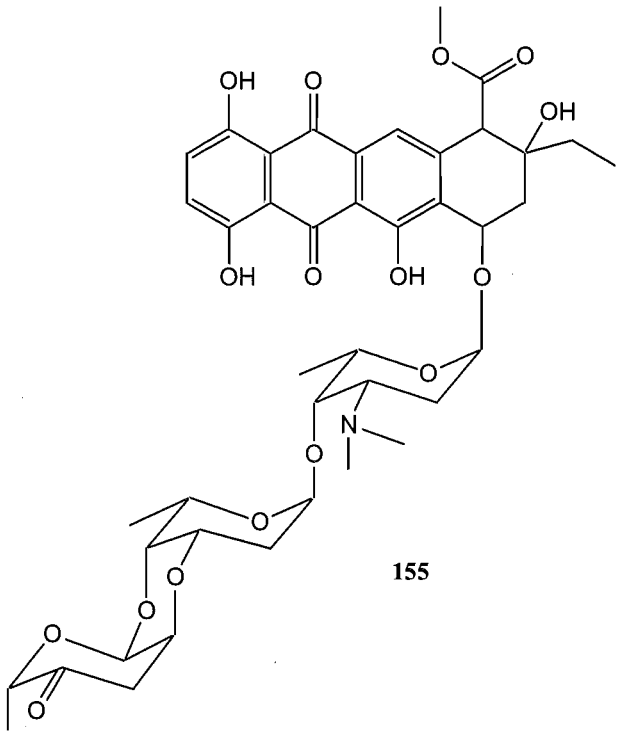

155

Summary

Five new pyrromycin derivatives were isolated and purified from culture extracts of Fox 21-2-6a with two of these derivatives (**154**, **157**) stereoisomers of pyrromycin (**169**), one an *N*-demethyl derivative (**156**) and the fourth (**158**) and fifth (**159**) derivatives displaying minor variations in the side chain of the anthraquinone D-ring. A sixth compound (**155**) was also isolated, and shown to be the known compound 1-hydroxyaclacinomycin B.

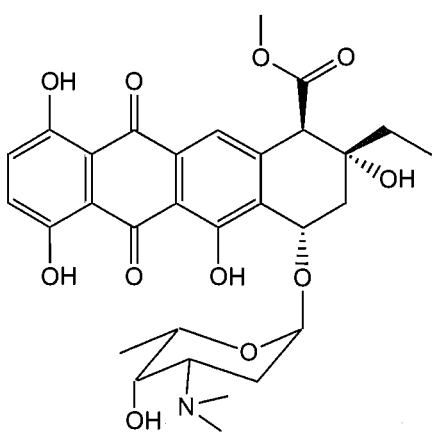

169

6.6 Discussion

The anthraquinone core of all these compounds is derived from units of acetyl CoA. In the case of the pyrromycin derivatives (**154** - **157**) the anthraquinone core is comprised of a starter unit of propionyl CoA plus nine acetyl CoA units connected in a head to tail fashion as shown in Figure 6.33.

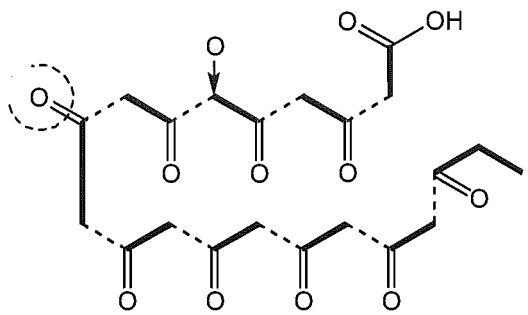

Figure 6.33: Biosynthetic origin of the polyketide anthraquinone core of pyrromycin (**169**)

In the case of **158** however, the propionyl CoA starter unit is replaced with one acetate unit and in **159** it is replaced with two. The only compounds similar to **158** and **159** previously isolated were either the aglycones or the di- or trisaccharides[102] which poses the question - are these compounds of natural origin, produced by the organism being investigated or are they artefacts of the extraction and isolation process produced by hydrolysis of the trisaccharide parent compounds present in the extract?

The pyrromycin derivatives were not thought to have arisen via a partial hydrolysis of the di- and trisaccharide forms as random hydrolysis should have resulted in tri-, di- and mono-saccharides as well as the appropriate aglycones. However, only the monosaccharide or the trisaccharide were observed. An inspection of the original analytical HPLC trace of the second extract also supported the theory that these compounds were present in the original extract as there were many small peaks eluting at the appropriate time in the HPLC trace and with the appropriate UV-visible spectrum (Figure 6.3). However, these compounds were only present in very minor amounts when compared to the amount of the total extract.

During chromatography it was also noted that both extracts of Fox 21-2-6a contained a large volume of fatty acid material in a number of the red fractions which was almost impossible to remove and indeed, all of the fractions from the first extract except for RKP 2.245.2 and RKP 2.245.3 showed a high level of fatty acids. All attempts to

separate the red compounds from the fatty acids present in the first extract were unsuccessful which suggested that the fatty acids were bound to the cytotoxic components possibly rendering them harmless towards the producing organism but creating a metabolic pool which could release the toxic compounds when the producing organism was damaged. This was also observed in the second extract but not to the same extent. The only difference between the first and second extracts was in the length of time that they were cultured, the first for 30 days and the second for only 18 days. This difference in growth time suggested that the longer the culture was left to grow the higher the levels of toxic metabolites became, possibly increasing to the tolerance threshold of the producing organism. The producing organism could then reduce the levels of toxin without degrading the toxin but rather sequestering the toxic metabolites by converting them to a less toxic form, typically by esterification of any available sites on the toxin.

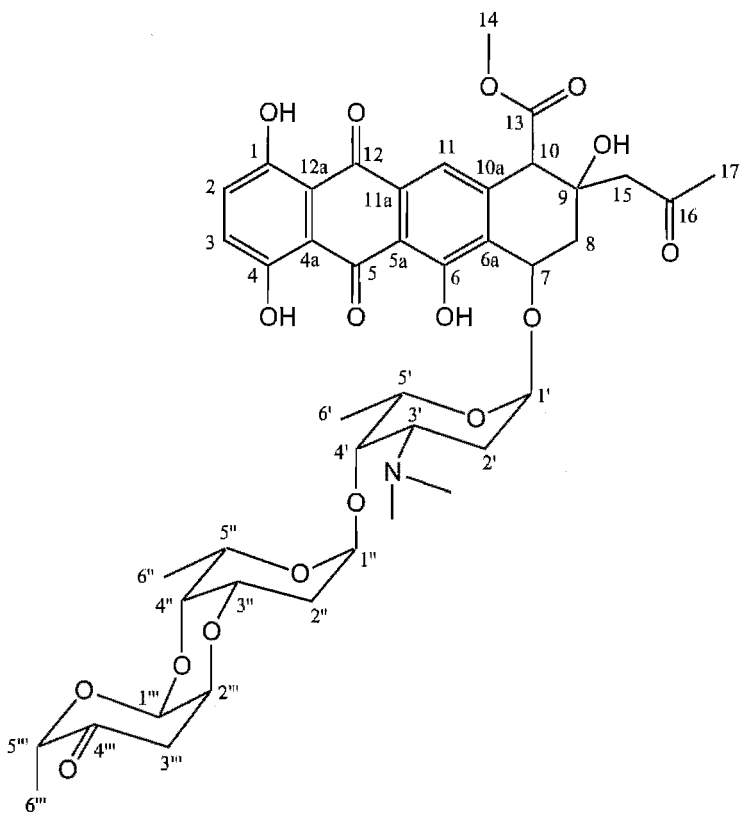

Figure 6.34: Numbering system for **154 - 159** in Tables 6.1 - 6.6

Table 6.1: ^{1}H and ^{13}C NMR data for **154** in CD_3OD

Number	^{1}H, multiplicity, (J_{HH} Hz)	COSY / TOCSY	HSQC / APT	CIGAR	NOESY
1 OH			159.4		
2 H	7.08 s		131.1	159.4 , 159.0 , 113.5	
3 H	7.08 s		131.5	159.4 , 159.0 , 113.4	
4 OH			159.0		
4a			113.4		
5			191.6		
5a			116.0		
6 OH			163.6		
6a			133.1		
7 H	5.10 d (5)	2.56 , 2.28	72.9	163.6 , 144.1 , 133.1 , 101.9 , 72.2	5.55 , 2.56 , 2.28
8 ax H	2.56 dd (5, 15)	5.10 , 2.10	36.2		5.10 , 2.28
8 eq H	2.28 d (15)	5.10 , 4.07 , 2.56 , 1.56	36.2	133.1 , 72.9 , 72.2 , 58.5	5.55 , 5.10 , 2.56
9 OH			72.2		
10 H	4.07 s	7.51 , 2.28	58.5	172.8 , 144.1 , 133.1 , 121.2 , 72.2 , 36.2	1.76
10a			144.1		
11 H	7.51 s	4.07	121.2	186.7 , 133.1 , 116.0 , 58.5	4.07
11a			133.8		
12			186.7		
12a			113.4		
13			172.8		
14 OMe	3.75 s		53.5		
15 α H	1.76 m	1.56 , 1.11	33.6	72.2 , 36.2 , 7.5	4.07 , 1.56 , 1.11
15 β H	1.56 m	2.28 , 1.76 , 1.11	33.6	72.2 , 58.5 , 7.5	1.76
16 CH_3	1.11 t (7)	1.76 , 1.56	7.5	72.2 , 33.6	1.76
1' H	5.56 d (2.5)	3.96 , 3.52 , 2.28 , 2.08	101.9	72.9 , 68.2 , 63.9	5.10 , 2.28 , 2.08
2' ax H	2.28 d (15)	5.55 , 3.96 , 3.52 , 2.08	28.1		
2' eq H	2.08 dt (4, 12.5)	5.55 , 3.96 , 3.52 , 2.28	28.1		5.55 , 4.26 , 3.52
3' H	3.52 br m	5.55 , 3.96 , 2.28 , 2.08	63.9		4.26 , 3.96 , 2.08
4' H	3.96 br s	5.55 , 4.26 , 3.52 , 2.28 , 2.08	66.1	63.9 , 28.1	4.26 , 3.52
5'H	4.26 q (6.5, 13)	3.96 , 1.33	68.2	66.1 , 17.2	3.96 , 3.52 , 2.28 , 1.33
6' CH_3	1.33 d (6.5)	4.26	17.2	68.2 , 66.1	4.26
7' $N(Me)_2$	2.87		40.7	63.9 , 40.7	

Number	^{1}H, multiplicity, (J_{HH} Hz)	HSQC	COSY / TOCSY	NOESY
2 H	7.38 s	131.2		
3 H	7.38 s	131.2		
7 H	4.96 t (2.5)	73.8	2.62 , 2.32	5.58
8 ax H	2.62 dd (7.5 , 14)	37.3	4.96 , 2.32	
8 eq h	2.32 dd (8 , 14)	37.3	4.96 , 2.62	
10 H	3.99 s	57.9		
11 H	7.60 s	121.1		
14 OMe	3.78 s	53.1		
15 H	1.49 m	33.1	0.98	
16 CH_3	0.98 t (7)	7.7	1.49	
1' H	5.58 br s	100.9	2.06	4.96
2' ax H	2.29 dd (8 , 14)	27.9	2.06	
2' eq H	2.06 br s	27.9	5.58 , 3.95 , 3.52 , 2.29	
3' H	3.52 br d (11)	64.0	3.95 , 2.06	4.17 , 3.95
4' H	3.95 br s	66.0	4.16 , 3.52 , 2.06 , 1.33	4.17 , 3.52 , 2.91
5' H	4.17 q (7, 12.5)	68.2	3.95 , 1.33	3.95 , 3.52 , 1.33
6' H	1.33 d (6)	17.2	4.17 , 3.95	4.17
7 $N(Me)_2$	2.91 , 2.85	41.8 , 40.9	2.91 , 2.85	3.95

Table 6.2: ^{1}H and ^{13}C NMR data for **157** in CD_3OD

Number	^{1}H, multiplicity, (J_{HH} Hz)	HSQC	COSY / TOCSY	CIGAR
2 H	7.37 s	131.2		
3 H	7.37 s	131.2		
7 H	5.13 d (5)	72.4	2.58 , 2.20	
8 ax H	2.58 dd (6 , 15)	39.4	5.13 , 2.20	
8 eq h	2.20 d (15)	39.4	5.13 , 2.58	
10 H	4.09 s	59.5		172.8 , 144.0 , 70.2
11 H	7.67 s	121.0		
14 OMe	3.71 s	53.2		172.8
16 CH_3	1.38 s	27.8		70.2 , 59.5 , 39.4
1' H	5.56 br s	101.5	2.15 , 2.02	
2' ax H	2.15 m	28.0	5.56 , 3.46 , 2.02	
2' eq H	2.02 dt (3.5 , 12.5)	28.0	5.56 , 3.91 , 2.15	
3' H	3.46 br d (11.5)	63.8	3.91 , 2.15	
4' H	3.91 br s	66.0	4.24 , 3.46 , 2.02	
5' H	4.24 q (7.5, 14)	68.1	3.91 , 1.31	
6' H	1.31 d (6.5)	17.1	4.24	68.1 , 66.0
7 $N(Me)_2$	2.88 , 2.78	41.9 , 41.0		63.8 , 41.9 , 41.0

Table 6.3: ^{1}H and ^{13}C NMR data for **158** in CD_3OD

Number	^{1}H, multiplicity, (J_{HH} Hz)	HSQC	COSY / TOCSY	CIGAR
2 H	7.36 s	131.1		
3 H	7.36 s	131.1		
7 H	5.10 br s	72.5	2.53	
8 H	2.53 br s	36.7	5.10	
10 H	4.24 s	58.1		72.2
11 H	7.71 s			
14 OMe	3.71 s	53.4		172.3
15 α H	3.04 d (16.5)	51.7	2.66	
15 β H	2.66 d (16.5)	51.7	3.04	
17 CH_3	2.25 s	32.5		210.6 , 51.7
1' H	5.49 br s	101.7	2.15 , 2.03	
2' ax H	2.15 m	28.0	5.49 , 3.93 , 3.46 , 2.03	
2' eq H	2.03 m	28.0	5.49 , 3.93 , 3.46 , 2.15	
3' H	3.46 br d (11.5)	63.9	3.93 , 2.15 , 2.03	
4' H	3.93 br s	66.1	4.26 , 3.46 , 2.15 , 2.03	
5' H	4.26 q (7, 13)	68.2	3.93 , 1.32	17.2
6' H	1.32 d (6.5)	17.2	4.26	68.2 , 66.1
7 $N(Me)_2$	2.88 br s , 2.77 br s	41.7 , 40.9	2.77 , 2.88	41.7 , 40.9

Table 6.4: ^{1}H and ^{13}C NMR data for **159** in CD_3OD

Table 6.5: ^{1}H and ^{13}C NMR data for the anthraquinone moiety of **155** in $CDCl_3$

Number	^{1}H, multiplicity, (J_{HH} Hz)	COSY / TOCSY	HSQC / APT	CIGAR	NOESY
1 OH			157.9		
2 H	7.29 s		129.9	157.9 , 158.5 , 112.4 , 112.2	
3 H	7.29 s		130.2	157.9 , 158.5 , 112.4 , 112.2	
4 OH			158.5		
4a			112.2		
5			190.4		
5a			114.9		
6 OH			162.1		
6a			130.7		
7 H	5.24 br s	2.59 , 2.28	71.1	130.7 , 71.7	5.55 , 2.59
8 ax H	2.59 br t	5.24 , 2.28	33.9		2.28
8 eq H	2.28 br t	5.24 , 2.59	33.9	71.1 , 56.8	2.59
9 OH			71.7		
10 H	4.09 s		56.8	171.0 , 142.2 , 130.7, 120.2 , 71.7 , 33.9	7.70
10a			142.2		
11 H	7.70 s		120.2	185.7 , 130.7 , 114.9 , 56.8	4.09
11a			133.0		
12			185.7		
12a			112.4		
13			171.0		
14 OMe	3.70 s		52.5	171.0	
15 α H	1.76 m	1.52 , 1.09	31.8	71.7 , 33.9 , 6.7	1.52 , 1.09
15 β H	1.52 m	1.76 , 1.09	31.8	71.7 , 56.8 , 6.7	1.76 , 1.09
16 CH_3	1.09 t (7.5)	1.76 , 1.52	6.7	71.7 , 31.8	1.76 , 1.52

Number	^{1}H, multiplicity, (J_{HH} Hz)	COSY / TOCSY	HSQC / APT	CIGAR	NOESY
1' H	5.55 br s	2.30	101.2		5.24
2' ax H	1.58 br	2.30	33.8		2.30
2' eq H	2.30 br t	5.55 , 3.48 , 1.58	33.8		1.58
3' H	3.48 br	3.97 , 2.30	50.7		
4' H	3.97 br s	4.81 , 3.48	72.5		5.26
5' H	4.81q (7)	3.97 , 1.33	77.9	18.0	1.33
6' H	1.33 d (7)	4.81	18.0	77.9	5.26 , 4.81
7' N(Me)$_2$	2.35 br s		41.1		
1'' H	5.26 br s	2.50	99.1		2.50 , 1.33
2'' ax H	2.00 dd (4.5, 12.5)	4.43 , 2.50	26.3	99.1 , 66.2	4.34 , 2.50
2'' eq H	2.50 dd (4.5, 12.5)	5.26 , 2.00	26.3		5.26 , 4.34 , 2.00
3'' H	4.43 br d	4.06 , 2.00	66.2		4.06
4'' H	4.06 br s	4.53 , 4.43	66.2		4.53 , 4.43
5'' H	4.53 br s	4.06 , 1.21	65.8		4.06
6'' H	1.21 d (7)	4.53	15.8	65.8	
1''' H	5.16 d (3)	4.34	91.5	66.2 , 62.8	4.34
2''' H	4.34 d (3.5)	5.16 , 2.55	62.8		5.16 , 2.55 , 2.50 , 1.95
3''' H	2.55 d (4.5)	4.34	39.5	208.0 , 91.5 , 67.6	4.34
4''' H			208.0		
5''' H	4.05 br s	1.33	67.6		1.33
6''' H	1.33 d (7)	4.05	15.9	208.0 , 67.6	4.05

Table 6.6: ^{1}H and ^{13}C NMR data for the sugar residues of **155** in $CDCl_3$

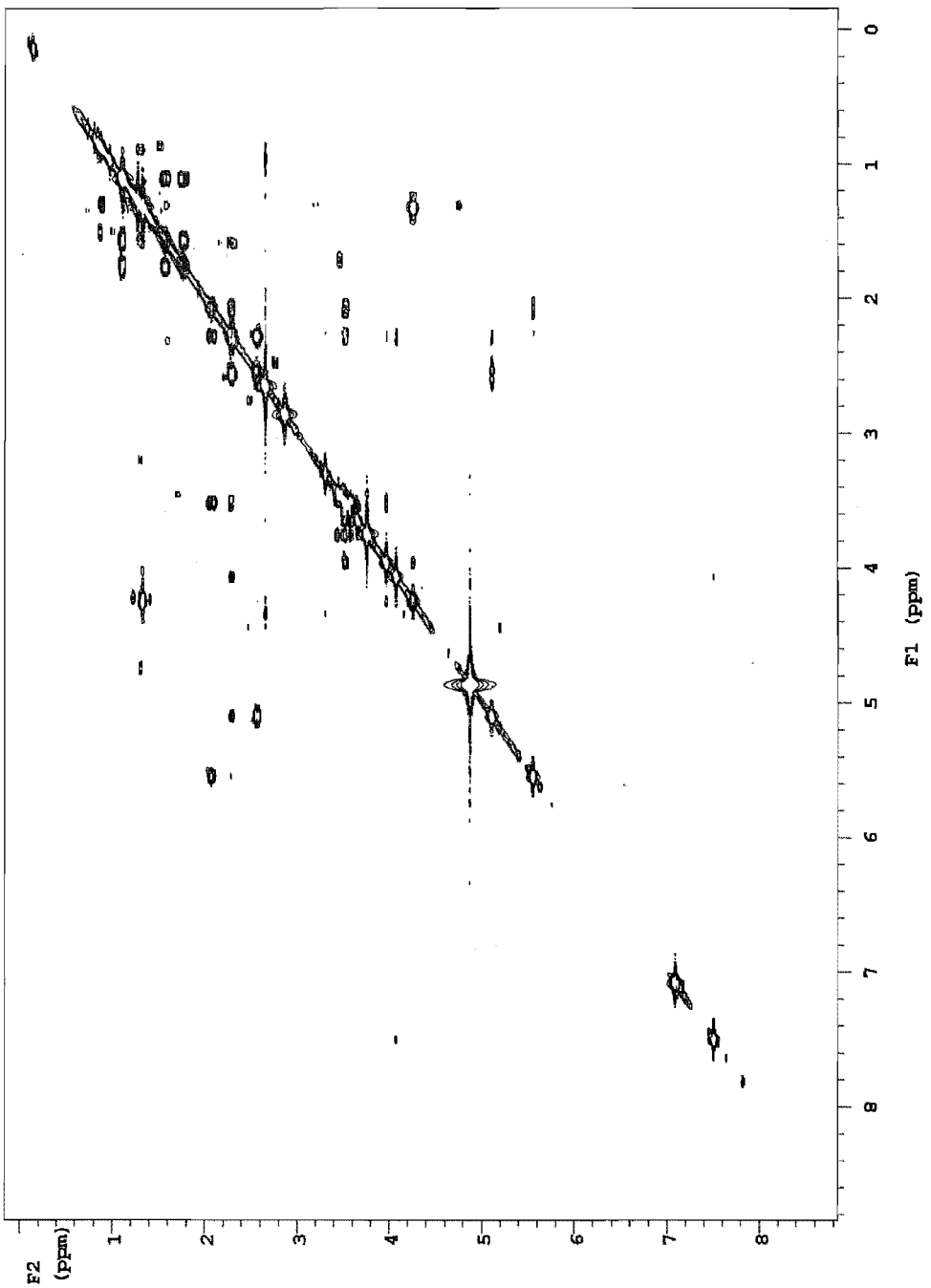

Figure 6.35: COSY spectrum of **154** in CD_3OD

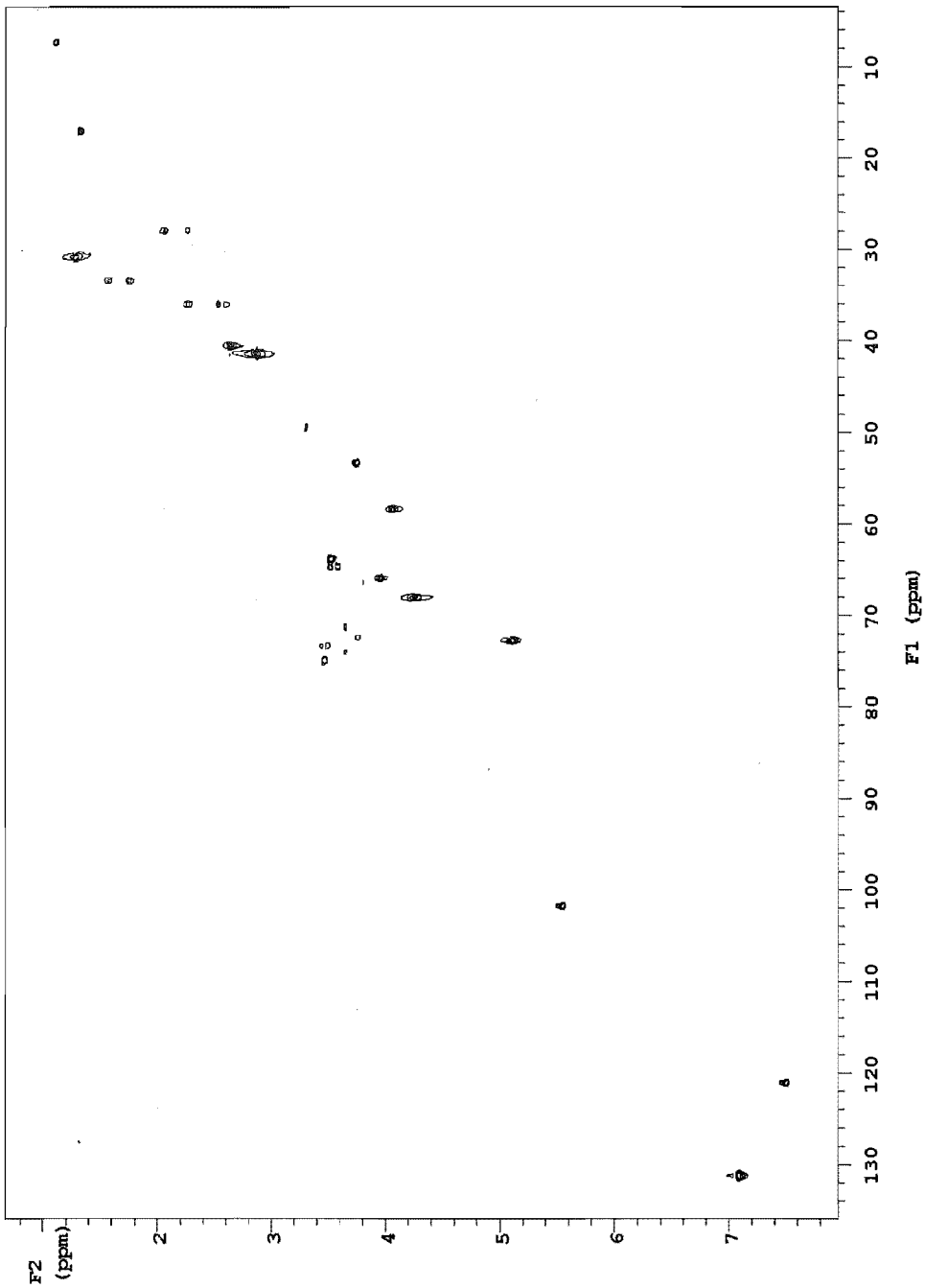

Figure 6.36: HSQC spectrum of **154** in CD_3OD

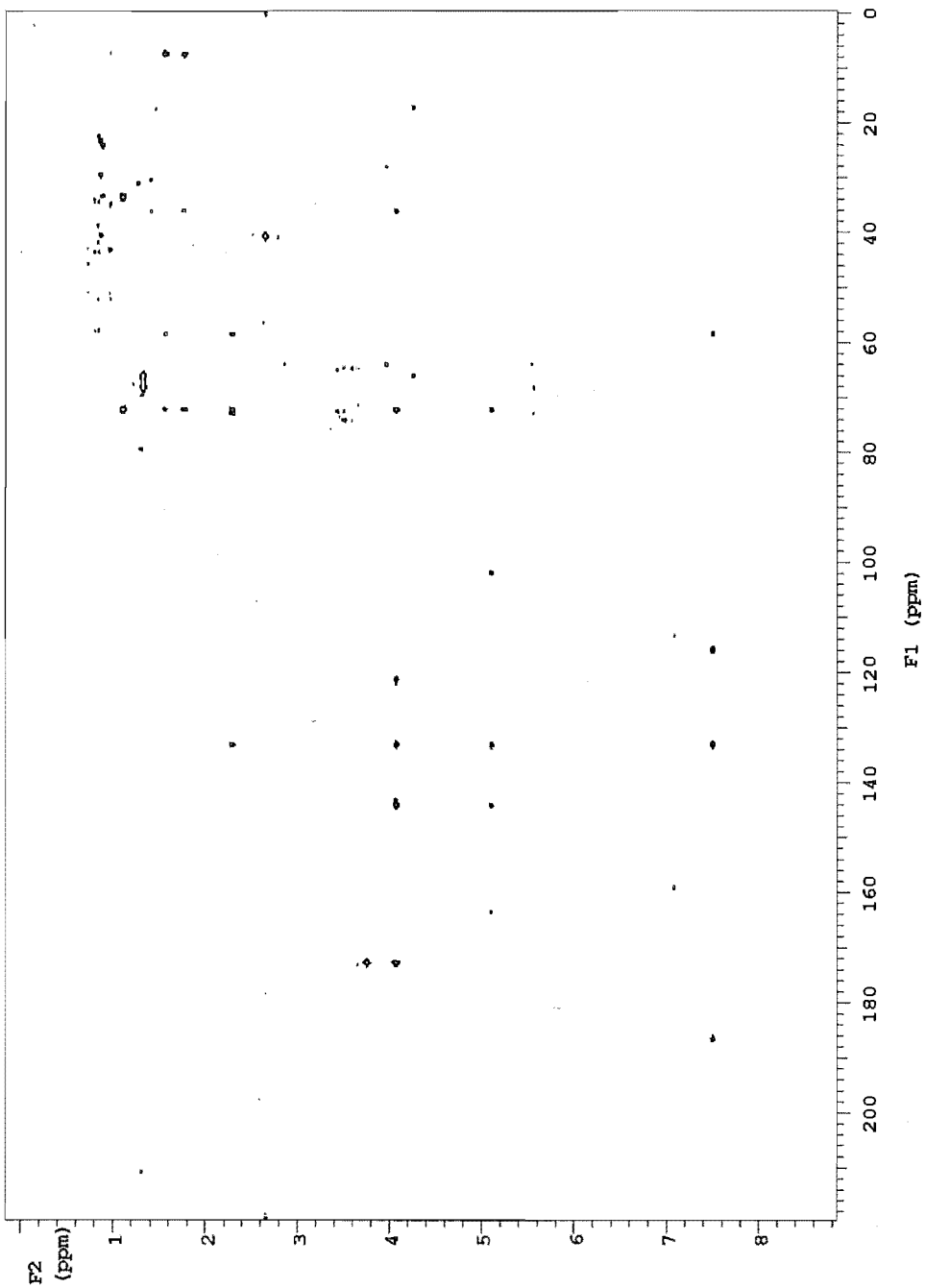

Figure 6.37: CIGAR spectrum of **154** in CD_3OD

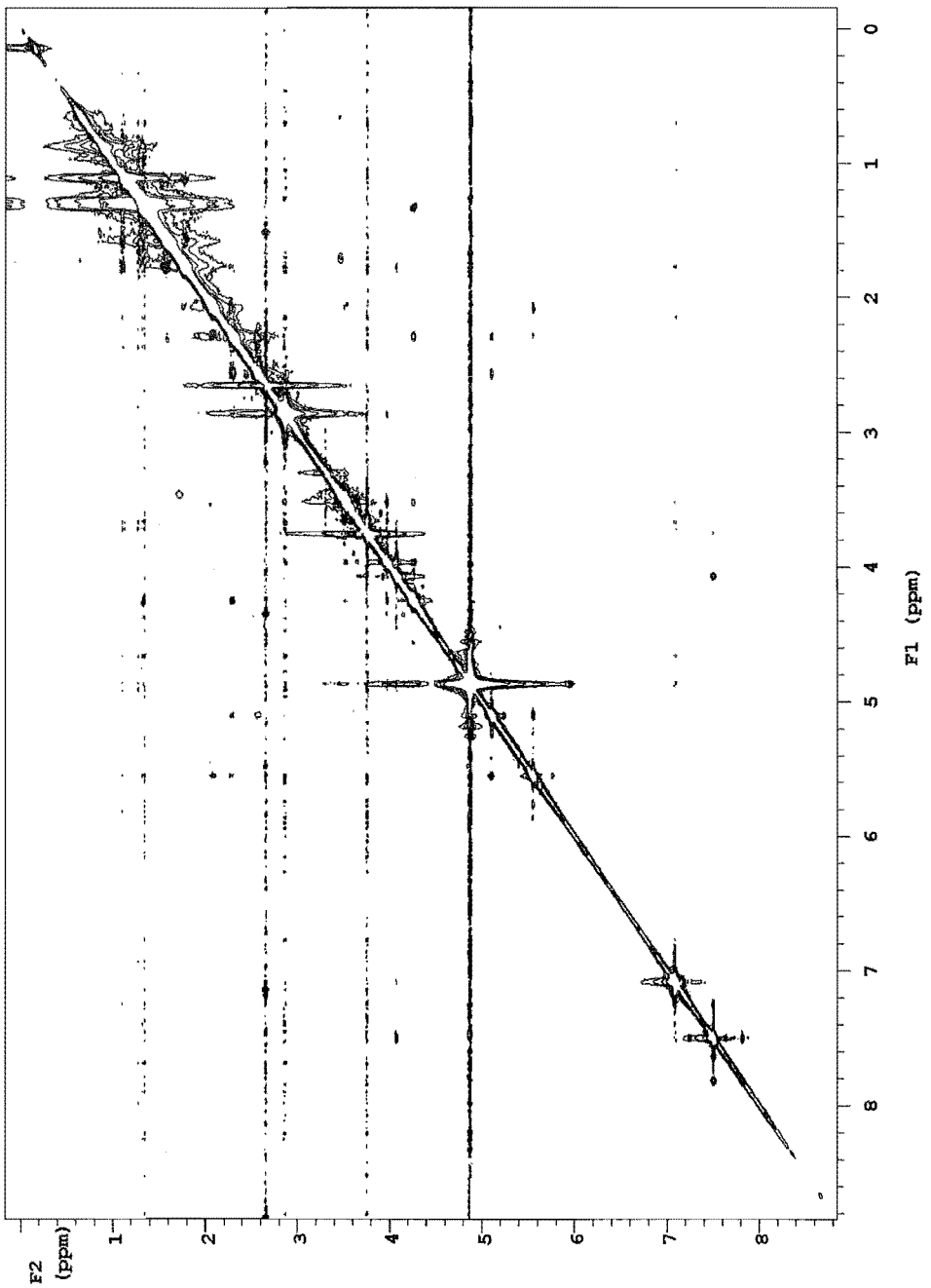

Figure 6.38: NOESY spectrum of **154** in CD_3OD

CHAPTER SEVEN

KAI 11-2-1 ~ *STREPTOMYCES* SP

7.1 Introduction.

Extracts from three *Streptomyces* spp cultured from various macro-algae collected from Kaikoura (Kai 40-1-1, 84 and Kai 11-2-1) all showed excellent cytotoxicity towards the P388 cell line (with IC_{50} values ranging from 286 ng/mL - < 97.5 ng/mL). Initial investigations (Section 7.2.1) of the crude extracts showed that the antitumour activity was centered on a range of peaks in a moderately complex HPLC chromatogram (Figure 7.3). Three actinomycins with exceptional cytotoxicity against the P388 cell line (**177**, < 1.0 ng/mL, **178**, 12.5 ng/mL, **179**, 13.6 ng/mL) were identified from culture extracts. The chromatography of these compounds is discussed in Sections 7.3 and 7.5 and the structural elucidations described in Section 7.4 of this chapter.

7.1.1 The actinomycins

The actinomycins are a commonly occurring group of antibiotics that have been isolated from numerous different *Streptomyces* spp. One of the more common actinomycins, actinomycin D, has been utilised as an anticancer drug against a small number of tumours, the most notable of which is Wilms Tumor.[170] This is a cancerous tumour of the kidneys common in children under 14 years of age, accounting for 6 - 7 % of all childhood cancers. Unfortunately, the clinical uses for actinomycins have been limited due to both their high toxicity and because the number of cancers that respond well to actinomycin treatments are relatively few.[171]

Actinomycins are a family of chromopeptolides comprised of a phenoxazinone moiety called actinocin (**170**) and two five membered amino acid depsipeptide rings, such as those seen in **171**.

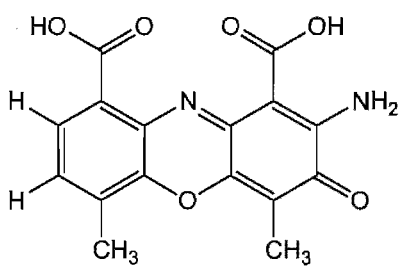

170

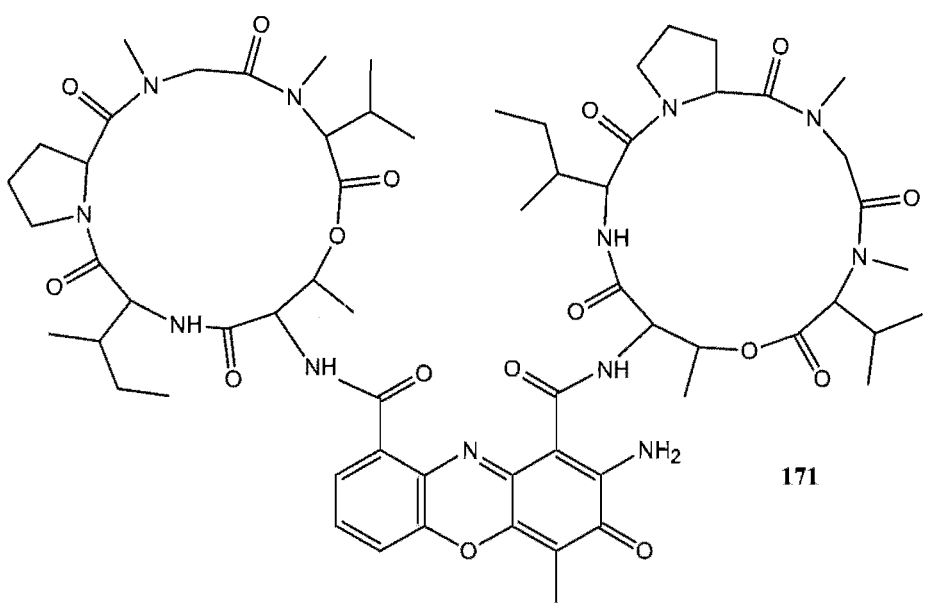

171

After the initial discovery of the actinomycins in 1940 by Waksman and Woodruff from *Streptomyces antibioticus*[153] numerous attempts to elucidate the structure were made culminating in the determination of the structure of actinomycin C_3 in 1956[172] and actinomycin D in 1957.[173] Elucidation of these structures confirmed the presence of two five membered depsipeptide rings rather than a single ten membered dilactone ring as proposed by Perutz.[174] The actinomycins show some features in common with other antibiotics such as etamycin A (**172**)[175] which contains a depsipeptide ring and cryptomycin A (**173**) which contains the phenoxazinone moiety. Other than the non-peptide phenoxazinones such as cinnabarin (**174**) and xanthommatin (**175**), cryptomycin A and the aurantins (**171**) are the only compounds, other than the actinomycins, known to contain the phenoxazinone moiety.[102]

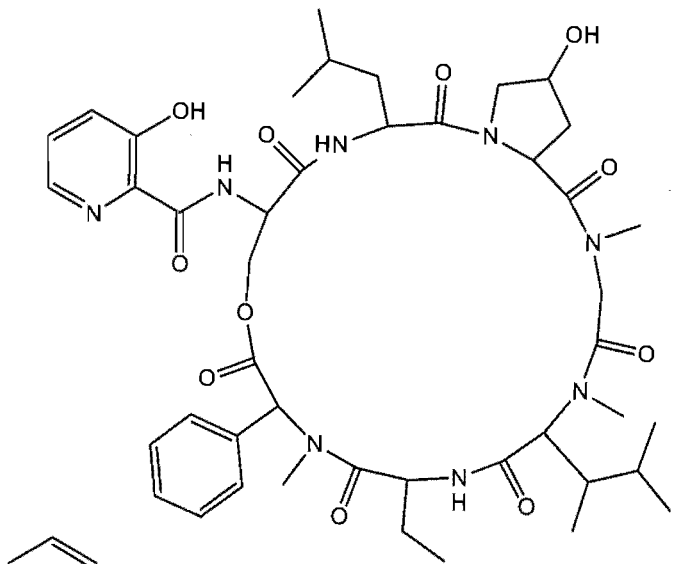

172

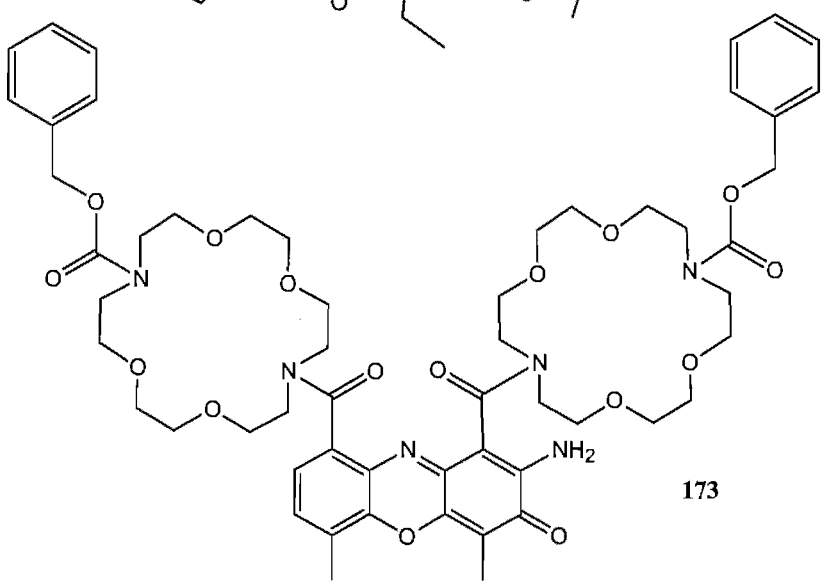

173

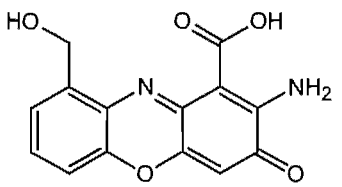

174

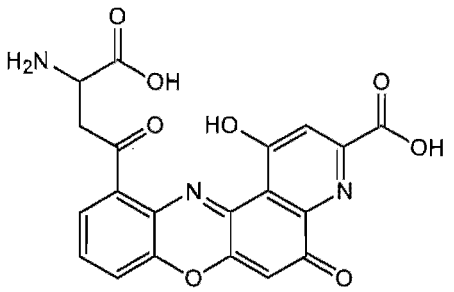

175

7.1.1.1 Nomenclature

The original actinomycin A complex was thought to be uniform, but after a similar complex (actinomycin C) was subjected to countercurrent distribution it appeared to separate into three main components (C_1, C_2 and C_3).[176] This assumption was proved incorrect with five actinomycins subsequently isolated from this complex. After discovering that all the actinomycins previously isolated, except for actinomycin D were mixtures, a naming system was developed. The new actinomycin was given a letter from the complex it was isolated from and then given a subscript number to further identify the compound. However, because of the ever increasing number of the actinomycins being found and because the complexes contained identical actinomycins this led to some degree of confusion. A second naming system was proposed based on the R_f values on paper chromatography. However, this method of naming was not widely adopted. The variability between these naming systems created further confusion and as such a third naming system for the actinomycins based on amino acid abbreviations was proposed.[153] This system split the two depsipeptide rings into α- and β- rings and then numbered the five amino acid residues 1 through 5 starting at the threonine residue (Figure 7.1) and listing only those changes from a parent actinomycin. Thus, actinomycin D is abbreviated as Val_2-AM.

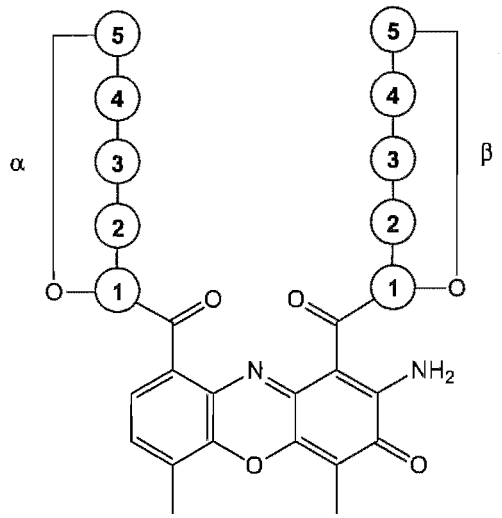

Figure 7.1: Amino acid numbering system for the actinomycins

7.1.1.2 Structure activity relationships

Numerous studies have shown that the phenoxazinone moiety of the actinomycins is able to intercalate with DNA between $d(G\text{-}C)_n$ (deoxyguanosine/deoxycytosine) base pairs[177] thereby inhibiting cellular proliferation. The naturally occurring weak antibiotic questiomycin A (**176**),[178, 179] which also contains a similar structure to the phenoxazinone moiety of the actinomycins, also functions by intercalating with DNA. However, the biological activity of the actinomycins is greatly increased primarily because of the presence of the two depsipeptide rings.

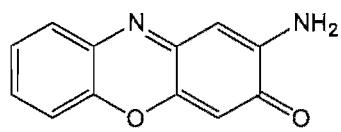

176

Semi-synthetic studies on the actinomycins have shown that alterations in the phenoxazinone moiety generally decrease the biological activity of the actinomycins by interfering with DNA intercalation.

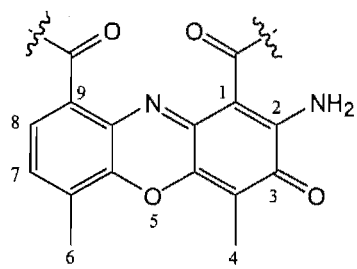

Figure 7.2: Numbering system for the phenoxazinone of the actinomycins

Any modification of the 2- amino group of the phenoxazinone system (Figure 7.2) has been shown to drastically reduce or even completely remove the biological activity of the actinomycins, with a similar effect observed when the methyl groups at C^4 and C^6 were replaced by either H or OCH_3.[180, 181]

After the phenoxazinone moiety of the actinomycin molecule has intercalated with DNA it would normally be able to easily dissociate away from the DNA strand. However, the two depsipeptide rings are able to wrap around the DNA helix thereby forming a relatively stable DNA - actinomycin complex thereby preventing dissociation of the actinomycin molecule.

Changes in the depsipeptide rings of the actinomycins alter the 3-dimensional conformation of the peptides which can either enhance or reduce the DNA binding efficacy of the various actinomycins. If one or both of the depsipeptide rings are opened at either the lactone or the sarcosine - *N*-methylvaline peptide bonds the biological activity is abolished because the now linear peptides do not bind well to DNA thereby preventing formation of the stable actinomycin - DNA complex. Variations in the amino acid residues of the depsipeptides have been noted in all five positions and generally reduce the DNA binding efficacy with very few exceptions. One of these exceptions, actinomycin V (X_2) which contains a 4-ketoproline residue in the 3-position of the β-ring has been shown to increase the antimicrobial activity but decrease the anti-tumour activity.[176]

7.2 Culturing and extraction of Kai 11-2-1

7.2.1 Preliminary investigations

Kai 11-2-1, a *Streptomyces* sp, was isolated from a conglomeration of the red algae *Jania micrarthrodia* and *Haliptilon roseum* collected below the low tide zone 20 km north of Kaikoura on the east coast of the South Island of New Zealand in September 1999.

When grown under microscale conditions (1 mL broth) an EtOAc extract displayed significant cytotoxicity towards the P388 cell line and as such was selected for chemical investigation. Extraction with EtOAc of a one month old culture grown in 100 mL

starch casein broth (SCB) followed by concentration under vacuum yielded a dark yellow powdery solid with significant cytotoxicity (504 ng/mL).

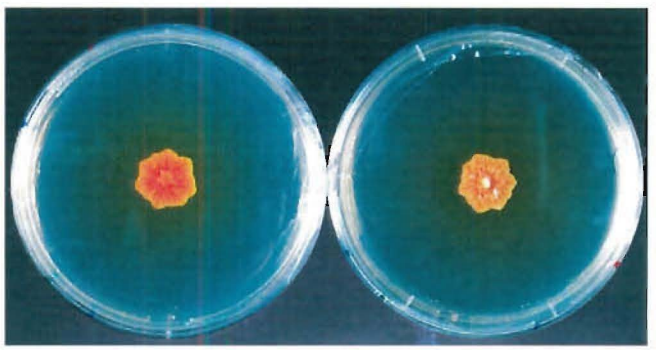

Figure 7.3: Isolate Kai 11-2-1 (*Streptomyces* sp) grown on a seawater PDA plate.

7.2.1.1 Chemical screening

As before (Section 3.2.1.1) the small scale EtOAc extract was chromatographed on CBA, C_{18} and LH20 cartridges. The initial fractionation of this extract with these column cartridges suggested that even minor amounts of the biologically active material were extremely cytotoxic as almost all fractions showed total cell death. Therefore the fractions were dried and re-assayed at a known concentration until the biological activity was observed in only one fraction.

Chromatography on CBA concentrated the cytotoxicity into the first fraction with slight carry over to the next two fractions. Chromatography on C_{18} concentrated the activity into the second fraction with some activity seen in the third fraction. Significant biological activity was observed in the first two LH20 fractions which, when combined with the CBA and C_{18} results indicated that the compound(s) of interest were large (> 1000 Da), of medium to low polarity and uncharged.

7.2.1.2 HPLC bioassay

The biological profile of this extract showed that the major region of activity was centred on a single large peak in the HPLC chromatogram, eluting at approximately 19 minutes (Figure 7.4) and which possessed a very distinctive UV-visible spectrum with characteristic absorption maxima (Figure 7.5).

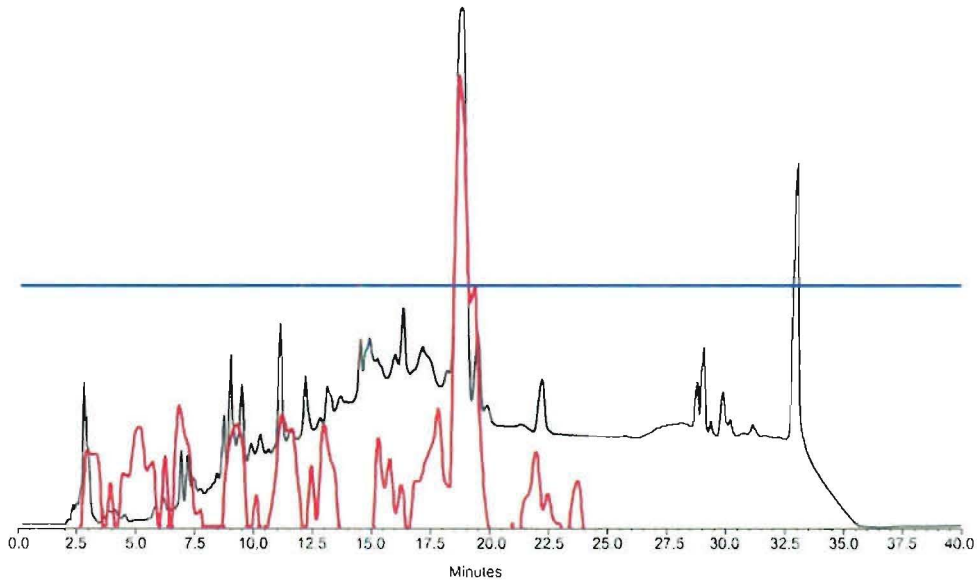

Figure 7.4: Spectrum max plot HPLC trace (black) and bioactivity data (red) of Kai 11-2-1 extract showing region of biological activity (the blue line represents 50% cell death).

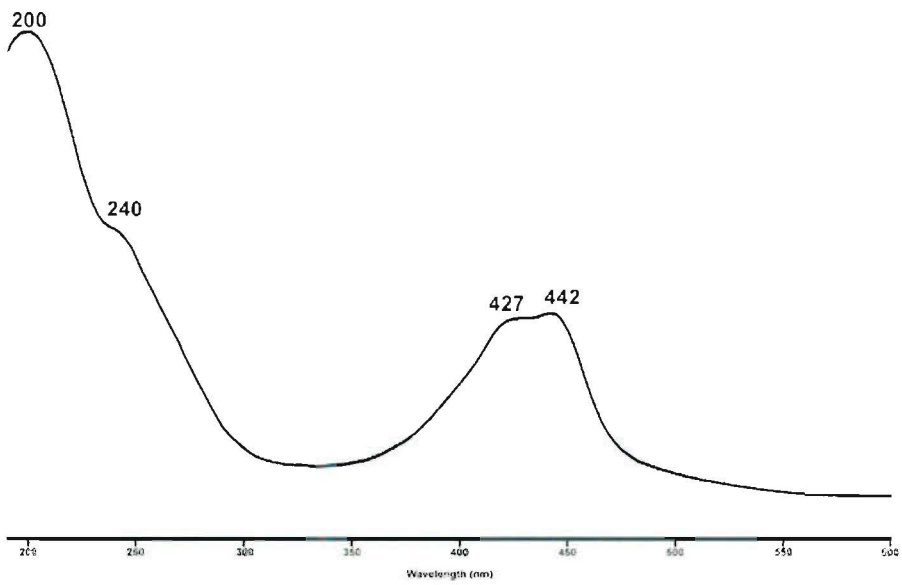

Figure 7.5: UV profile of bioactive peak from HPLC trace (19 minutes) as determined from the microtitre plate assay

ESI-MS of the bioactive wells from the microtitre plate showed a complex series of peaks between 620 - 640 Da and 1250 - 1280 Da. Upon closer inspection it was seen that the ions between 620 - 640 Da were doubly charged which indicated that the corresponding molecular ions were twice the size, between 1240 - 1280 Da. There were six major peaks observed at 1255, 1269, 1277, 1291, 1293 and 1307, which

corresponded to a pair of molecular ions differing by 14 Da at 1255 and 1269, and the sodium and potassium adducts, 1277 and 1291 MNa^+, 1293 and 1307 K^+ respectively. While the extracts of Kai 11-2-1 were being purified only two databases were available for dereplication, The Berdy Natural Products Database (BNPD) and Scifinder® Scholar. The BNPD is a text based database and allows searches to be carried out on a wide variety of different fields, including mass, producing organism and UV maxima. Scifinder® Scholar is an online database provided by the American Chemical Society. Although a much larger number of compounds can be search for in this database, an initial search based on molecular weight is not possible, limiting the usefulness of this database for dereplication. A search in the BNPD on the UV maxima and molecular weight of 1255 Da found a single match, actinomycin D. A second search on the molecular mass of 1269 found a further ten possible matches, nine of which were actinomycins and one an aurantin. A ^1H NMR spectrum was not able to be obtained from either the HPLC microtitre plate wells or from the chemical screening fractions (Section 7.2.1.1). This was because both the mass isolated in the microtitre plate wells was very low (< 250 μg) and the chemical screening fractions were not sufficiently pure. To determine if the molecular ion at 1269 Da was due to either a new actinomycin derivative or one of the ten possible matches seen in the BNPD a new extract was required.

7.2.2 Large scale culturing and extraction

To obtain adequate extract for identification of the compound responsible for the molecular ion at 1269 Da the microbial isolate Kai 11-2-1 was cultured in a further 2 L of starch casein broth under the same conditions as described in Section 7.2.1. Repeated extraction of this culture with distilled EtOAc, followed by solvent removal under vacuum yielded a deep red solid (129.6 mg) with significantly more biological activity than that of the small scale extract (< 97.5 ng/mL).

7.3 Chromatography of 177

The chromatographic steps for the large scale extract of Kai 11-2-1 are shown in Scheme 7.1. A more detailed description of the chromatographic steps carried out on this extract can be found in the Experimental Section.

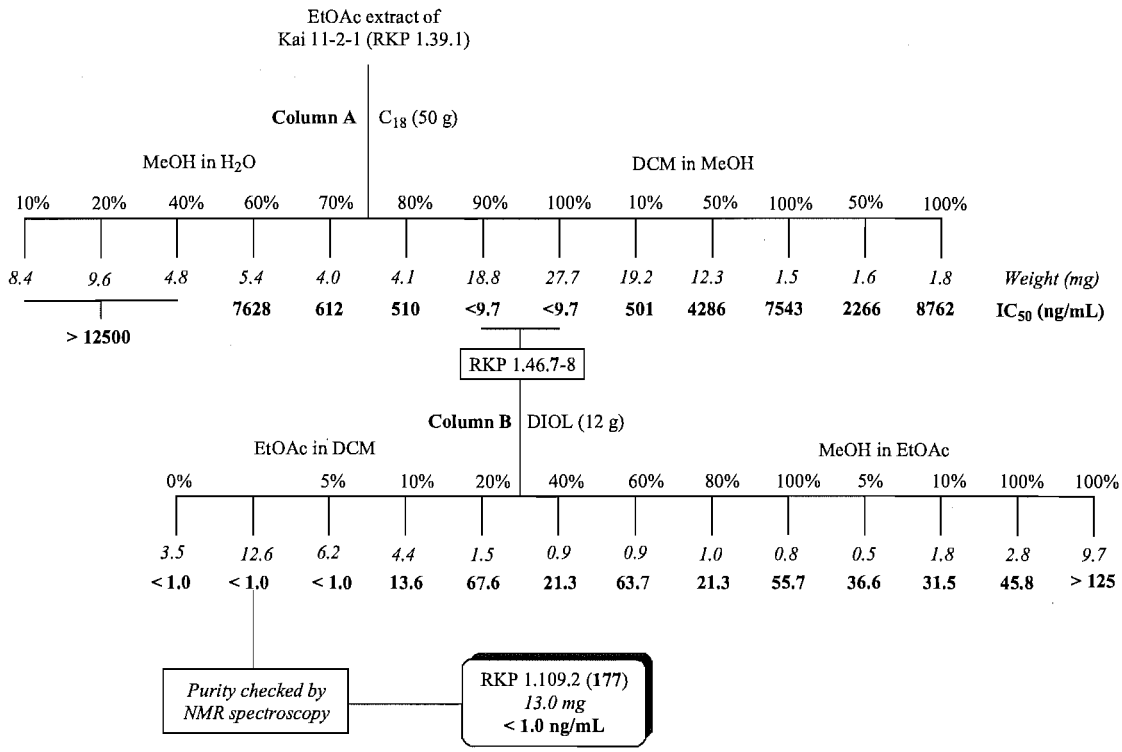

Scheme 7.1: Purification flow chart of an extract prepared from the microbial isolate Kai 11-2-1.

The large scale culture extract (129.6 mg) was initially fractionated on reverse-phase C_{18} (column A), using the same stepped gradient solvent system that was used for the elution of compound **141** from C_{18} (Scheme 5.1). Almost all the fractions that eluted from the C_{18} column displayed some measure of cytotoxicity however, it had previously been noted during the chemical screen that even minor traces of **177** resulted in significant levels of cytotoxicity and because of this only the two most cytotoxic fractions were purified further. Analysis of two most active fractions (RKP 1.46.7-8) and the two side fractions (RKP 1.46.6 and 9) by reverse-phase HPLC (Figure 7.6) showed that significant quantities of **177** were only present in fractions 7 and 8. ESI-

MS spectra showed a similar series of ions to those seen in samples from the microtitre plate assay.

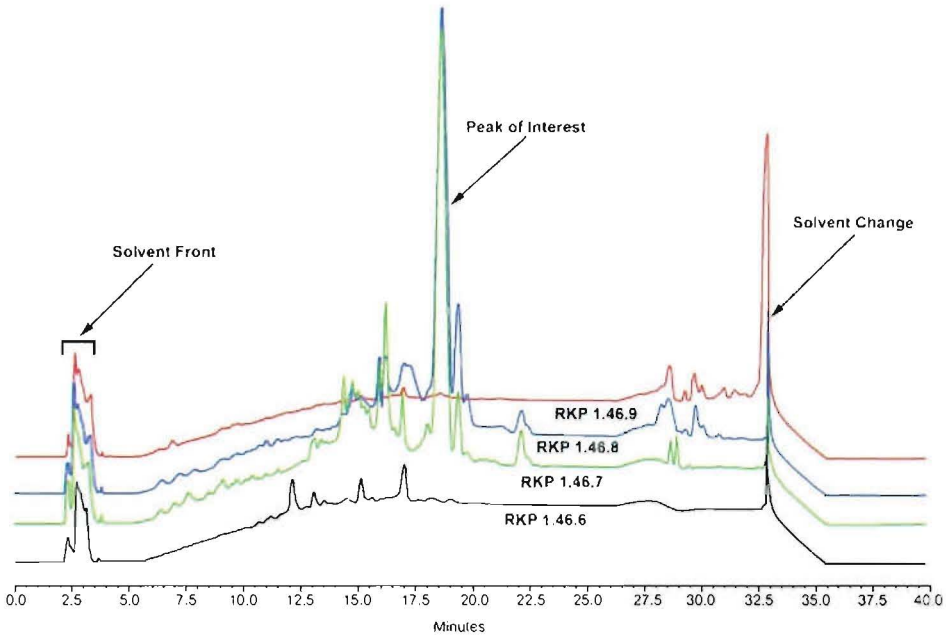

Figure 7.6: HPLC chromatogram of RKP 1.46.6-9

Based upon the analytical HPLC and ESI-MS data RKP 1.46.7 and 8 were combined then further purified with normal phase chromatography on DIOL (column B). The combined bioactive fractions were eluted off column B with the same stepped gradient system used for column B in Section 3.3. During elution the first and last fractions from this column showed distinct bands of colour within the fraction and as such these bands were collected individually.

An exceptionally high level of cytotoxicity was observed in the first three fractions from column B with a slow tailing off of the cytotoxicity in the remaining fractions. Analytical HPLC of the first four fractions (Figure 7.7) showed that fraction two was the most pure with slightly lower purity in RKP 1.109.1 and 3. The ESI MS spectra of these three fractions showed that the molecular ion corresponding to **177** (MH^+ 1269) was enriched in RKP 1.109.2 with lower levels in RKP 1.109.1 and 3. RKP 1.109.2 was subsequently examined with 1D and 2D NMR spectroscopy, with the structural elucidation of **177** discussed in Section 7.4.

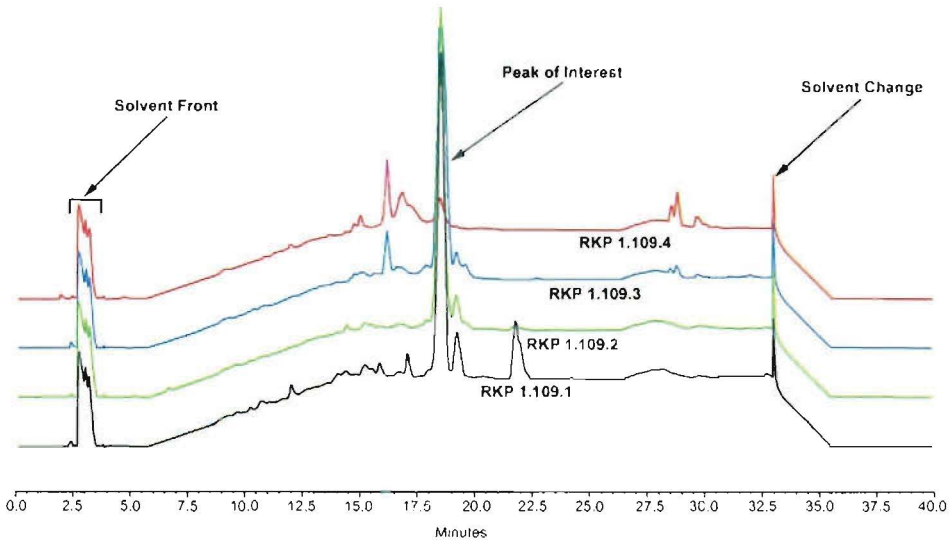

Figure 7.7: HPLC chromatogram of RKP 1.109.1-4

7.4 Structural elucidation

7.4.1 Structural elucidation of 177

The ^{1}H NMR spectrum of **177** in $CDCl_3$ showed a great deal of complexity (Figure 7.8) hindering a direct comparison with the literature data. The ^{1}H NMR spectrum showed numerous methyl signals between δ_H 1.4 and δ_H 0.8, four *N*-methyl signals (δ_H 2.93 - 2.88) and two aromatic methyls (δ_H 2.54 and δ_H 2.21). The presence of these two aromatic methyl signals indicated that **177** was an actinomycin rather than an aurantin, reducing the number of possible matches to **177** from ten to nine. The remaining nine possibilities for **177** arose from variations at the second and third amino acid residues in both the α and β rings (Figure 7.1). The variations resulted from the insertion of a CH_2 group in the amino acid residues at position 2 or 3 or replacement of a CH_2 group with a ketone at position 3.

The ^{1}H NMR spectrum highlighted a further four amide protons and two aromatic protons between δ_H 8.2 and δ_H 7.0. A pair of doublets at δ_H 6.55 and δ_H 5.95, two multiplets at δ_H 5.22 and δ_H 5.14 and a series of complex multiplets between δ_H 5.0 and δ_H 2.0 were also seen.

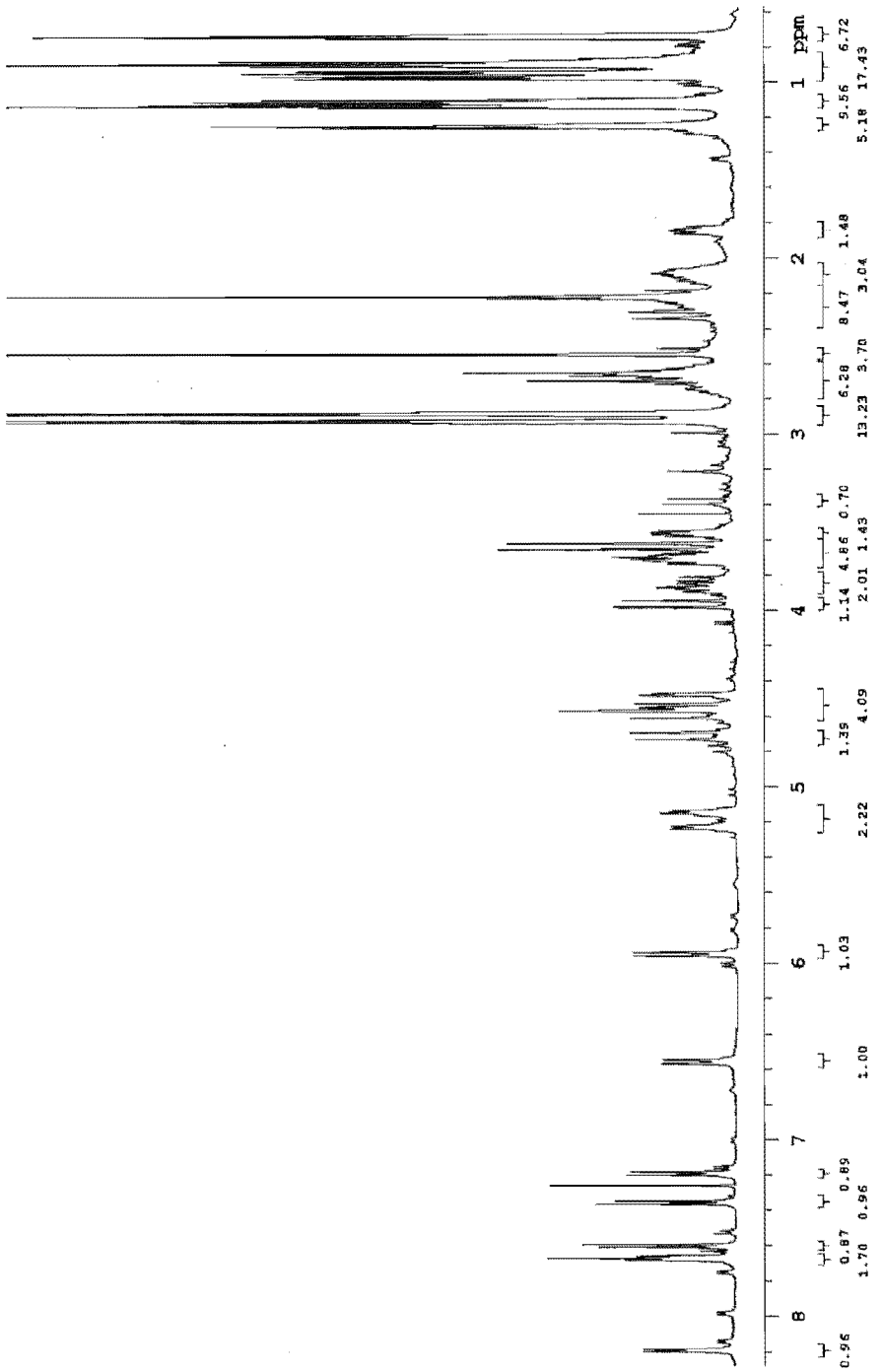

Figure 7.8: ^{1}H NMR spectrum of **177** in $CDCl_3$

The ^{13}C APT spectrum obtained for this sample showed over 60 signals (Figure 7.9). Of the low field carbons (δ_H 180 - 80), thirteen were assigned as carbonyl carbons between δ_C 180 - 150, ten were aromatic quaternary carbons between δ_C 150 - 100 and two were aromatic CH carbons at δ_C 130.3 and δ_C 126.2. There were thirty five high

field carbons from δ_C 75.0 - δ_C 17.0 which all arose from the various amino acid residues present. There were also two very high field aromatic methyl signals at δ_C 15.0 and δ_C 7.7. Again the complexity of the NMR spectrum hindered a direct comparison to the literature data of the possible matches obtained from a search of the BNPD.

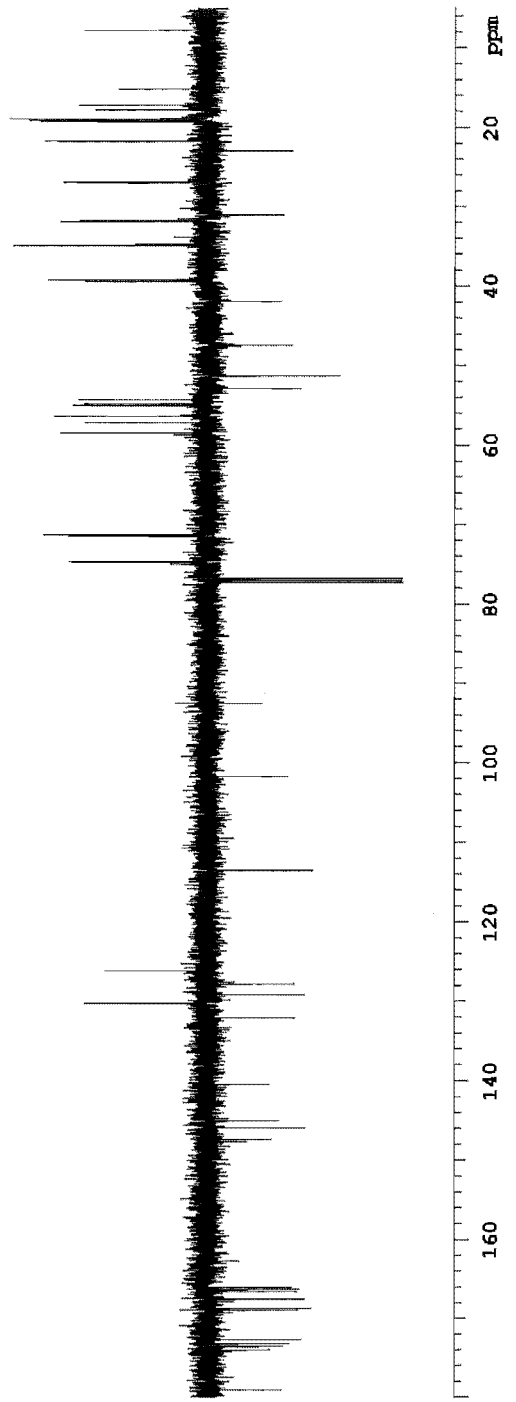

Figure 7.9: ^{13}C APT spectrum of **177** in $CDCl_3$

As the complexity of the ^{1}H NMR and ^{13}C NMR spectra precluded a direct comparison to the literature data, **177** was examined by further 2D NMR experiments. From COSY (Figure 7.25), TOCSY (Figure 7.26) and HSQC (Figure 7.27) spectra twelve spin systems were determined. These included two threonine, two valine, one proline, two *N*-methylvaline and two sarcosine residues, an aromatic system, a CH-CH_2 system and a lone CH_2 group.

The proton at δ_H 4.47 showed correlations to an amide proton at δ_H 7.67 and a proton multiplet at δ_H 5.22, which was in turn coupled to a methyl at δ_H 1.24. The proton at δ_H 5.22 was attached to a carbon at δ_C 74.6 indicating that this carbon was oxygenated (Figure 7.10a) to give rise to the first threonine residue. A second threonine residue showed the same correlations with slightly different chemical shifts, δ_H 7.19, 4.55, 5.14 and δ_H 1.13 respectively (Figure 7.10b).

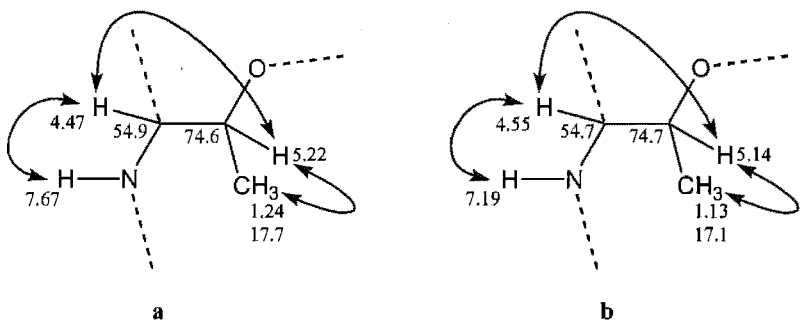

Figure 7.10a-b: Correlations observed for the two threonine residues of **177**.

Another proton at δ_H 3.56 showed correlations to an amide proton at δ_H 7.65 and a multiplet at δ_H 2.11. The proton at δ_H 2.11 also showed correlations to a pair of methyl signals at δ_H 1.11 and δ_H 0.90 (Figure 7.11a) to give rise to one of the valine residues. A second valine residue was also identified with chemical shifts of δ_H 8.19, 3.69, 2.21, 1.14 and δ_H 0.89 respectively (Figure 7.11b).

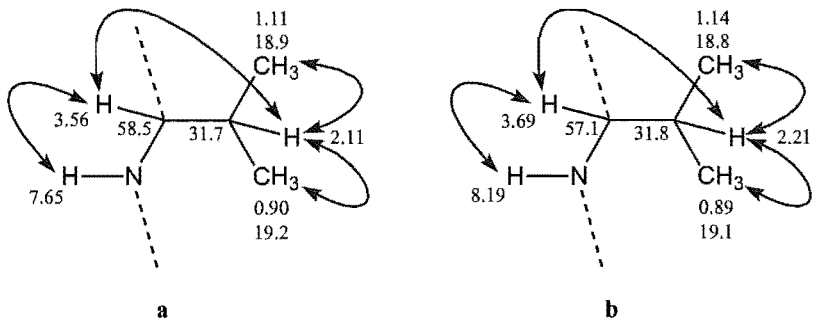

Figure 7.11a-b: Correlations observed for the two valine residues of **177**.

A proton resonance at δ_H 4.70 showed long range coupling to an *N*-methyl signal at δ_H 2.87. The proton signal at δ_H 4.70 also showed a correlation to a proton signal at δ_H 3.63. The HSQC spectrum indicated that both of these protons were attached to the same carbon atom indicating that this was a sarcosine residue (Figure 7.12a). A second sarcosine residue was also identified with chemical shifts of δ_H 2.88, 4.58 and δ_H 3.63 respectively (Figure 7.12b).

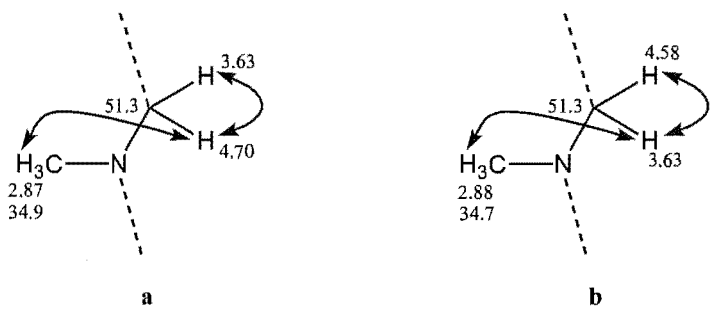

Figure 7.12a-b: Correlations observed for the two sarcosine residues of **177**.

A methyl group at δ_H 0.73 showed a correlation to a proton at δ_H 2.64, which in turn showed a correlation to another methyl group at δ_H 0.93. The multiplet signal at δ_H 2.64 showed two $^1J_{CH}$ correlations in the HSQC spectrum to carbon atoms at δ_C 71.2 and δ_C 26.8 respectively. This indicated that there were two protons at δ_H 2.64 which was further corroborated in the ^{1}H NMR spectrum as this multiplet integrated for two protons. The CIGAR spectrum displayed correlations from the methyl groups at δ_H 0.73 and δ_H 0.93 and the multiplet at δ_H 2.64 to both the carbons at δ_C 71.2 and δ_C 26.9 indicating that these two carbons were connected to each other. An *N*-methyl signal at

δ_H 2.92 also showed a CIGAR correlation to the carbon at δ_C 71.2 indicating that this fragment was an *N*-methylvaline residue (Figure 7.13a). A second *N*-methylvaline residue was also identified with almost identical chemical shifts of δ_H 0.74, 0.97, 2.69 and δ_H 2.93 respectively (Figure 7.13b).

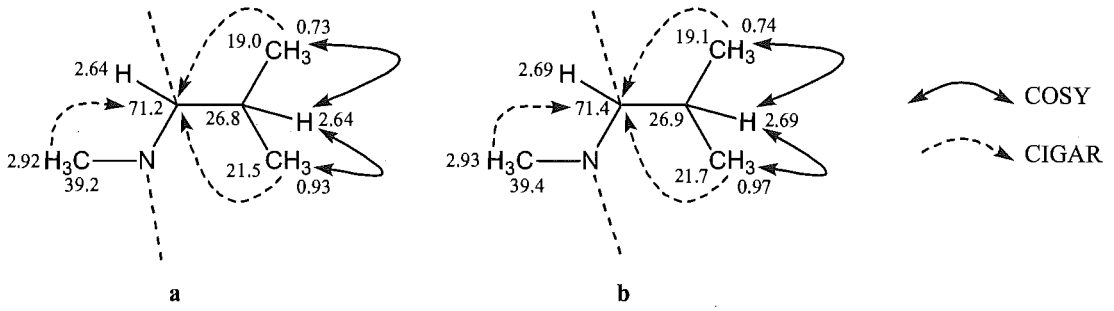

Figure 7.13a-b: Correlations observed for the two *N*-methylvaline residues of **177**.

The distinct doublet at δ_H 5.95 showed correlations to a pair of protons at δ_H 2.74 and δ_H 1.83 which were attached to the same carbon at δ_C 31.0. This pair of protons showed correlations to another pair of protons at δ_H 2.27 and δ_H 2.07 attached to a carbon at δ_C 22.9. The protons at δ_H 2.27 and δ_H 2.07 showed correlations to protons resonating at δ_H 3.88 and δ_H 3.71 attached to a carbon at δ_C 47.4. The chemical shift of this last carbon (δ_C 47.4) suggested that a nitrogen atom was attached to this carbon. A CIGAR correlation from the proton at δ_H 5.95 to the carbon at δ_C 47.4 enabled cyclisation of this fragment to give rise to a proline residue (Figure 7.14).

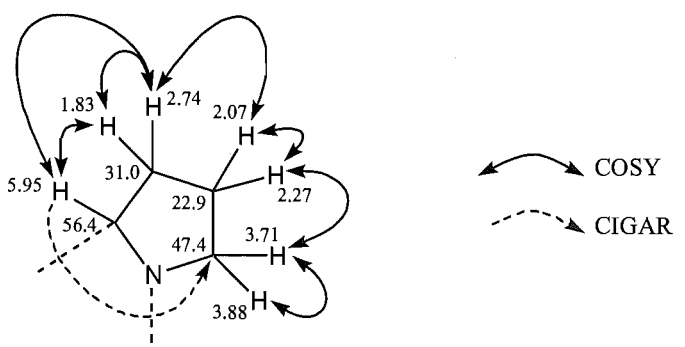

Figure 7.14: Correlations observed for a proline residue in **177**.

An aromatic proton signal at δ_H 7.60 showed a single correlation to another aromatic proton signal at δ_H 7.35. The proton resonance at δ_H 7.35 also showed long range coupling to a methyl signal at δ_H 2.54 (Figure 7.15).

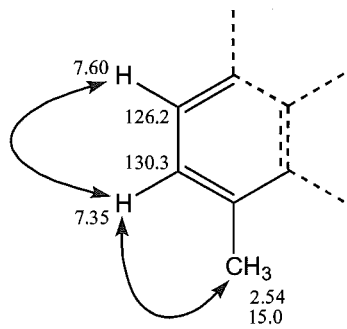

Figure 7.15: Correlations observed for the aromatic portion of **177**.

Correlations were seen from the proton signal at δ_H 6.55 to proton signals at δ_H 3.84 and δ_H 2.30. The signals at δ_H 3.84 and δ_H 2.30 both showed $^1J_{CH}$ correlations to the same carbon resonance at δ_C 41.9. The final spin system contained a pair of doublet protons at δ_H 4.55 and δ_H 3.96 which showed a $^1J_{CH}$ correlation to a carbon at δ_C 52.8. The chemical shifts of the carbons at δ_C 54.2 and δ_C 52.8 indicated the presence of nitrogen atoms attached to these two carbons (Figure 7.16a-b).

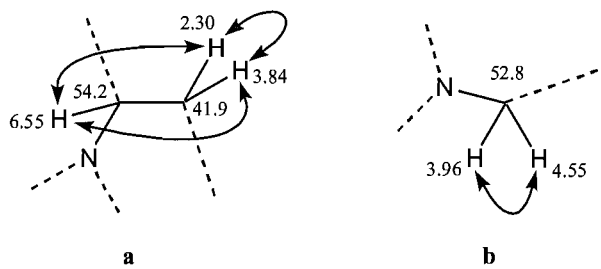

Figure 7.16a-b: Correlations observed for the protons at δ_H 6.55, 4.55, 3.96, 3.84 and δ_H 2.30.

Actinomycin D (**179**) contains a pair of identical depsipeptide rings containing five amino acid residues each. However, the COSY and TOCSY spectra of **177** identified only nine residues with the tenth residue replaced by the two fragments in Figure 7.16a and b. The five protons seen in Figure 7.16a and b (δ_H 6.55, 4.55, 3.96, 3.84, 2.30) all showed strong correlations in the CIGAR spectrum to a signal at δ_C 33.8. However, this

signal was not observed in the ^{13}C APT spectrum and because of this it was thou[illegible] be a foldback in the CIGAR spectrum (Figure 7.28). Thus the actual shift for these correlations was calculated to be δ_C 208.8 indicating the presence of a carbonyl group within a ring system. A ROESY correlation from the proton at δ_H 6.55 to the proton at δ_H 4.55 closed the ring system to give 4-ketoproline (Figure 7.17).

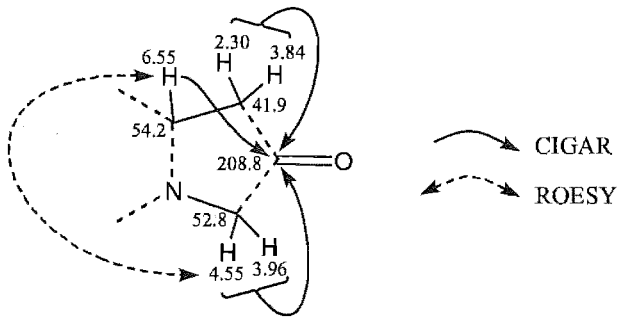

Figure 7.17: CIGAR correlations to the carbonyl group at δ_C 208.8.

After the presence of 4-ketoproline had been confirmed the number of possible matches to **177** from the BNPD was reduced to just one, actinomycin V. A comparison between the literature data[182-184] for actinomycin V and the experimental data for **177** showed almost identical ^{1}H and ^{13}C NMR data suggesting that **177** was actinomycin V. However, during the interpretation of the CIGAR spectrum questions arose regarding the position of the 4-ketoproline residue in the depsipeptide rings of **177**. If the 4-ketoproline residue was present in the α-depsipeptide ring then **177** was novel, whereas if it was in the β-depsipeptide ring then it was actinomycin V. Both of these compounds would be expected to show identical chemical shifts in the ^{1}H and ^{13}C NMR spectra due to the symmetry of the molecule.

The valine α-proton at δ_H 3.56, the amide proton resonance at δ_H 7.65 and the threonine β-proton signal at δ_H 5.14 all showed correlations to a carbonyl at δ_C 168.7. The proton signal at δ_H 5.14, the *N*-methylvaline α-proton peak at δ_H 2.64 and the *N*-methyl resonance at δ_H 2.92 all showed correlations to a carbonyl signal at δ_C 167.50. The *N*-methyl resonance at δ_H 2.92 also showed correlations to a carbonyl at 166.3, as did the sarcosine proton resonance at δ_H 4.70. The *N*-methyl group of this sarcosine residue showed a correlation to a carbonyl group at 173.1, as was also the case for the proline α-proton at δ_H 5.95. The proline α-proton showed a correlation to a second carbonyl at δ_C 173.5. No further correlations were seen to the carbonyl at δ_C 173.5. However, all previously identified actinomycins contain a pair of five membered depsipeptide rings

thus the carbonyl at δ_C 173.5 is most likely connected to the free end of the valine residue (Figure 7.18a).

The second depsipeptide ring also contained threonine, valine, *N*-methylvaline and sarcosine residues connected in the same way as that in Figure 7.18a. However, the proline residue was replaced with a 4-ketoproline. The proton at δ_H 5.22 and the *N*-methylvaline α-proton at δ_H 2.69 both showed correlations to a carbonyl at δ_C 167.51. The *N*-methyl group at δ_H 2.93 and the sarcosine proton at δ_H 4.58 showed correlations to a carbonyl at 165.9. The *N*-methyl group of the sarcosine residue at δ_H 2.88 and the β-protons of the 4-ketoproline residue at δ_H 2.30 and 3.84 all showed correlations to a carbonyl group at 172.7. The proton at δ_H 4.55 in the 4-ketoproline residue and the α-proton at δ_H 3.69 of the valine residue both showed correlations to a carbonyl at δ_C 174.0. The valine amide proton resonance at δ_H 8.19 and the threonine α-proton at δ_H 4.47 showed correlations to a carbonyl at δ_C 168.9 thereby closing the second depsipeptide ring (Figure 7.18b). Finally the amide protons of the threonine residues at δ_H 7.19 and δ_H 7.67 both showed correlations to carbonyl groups at δ_C 166.0 and δ_C 166.5 respectively.

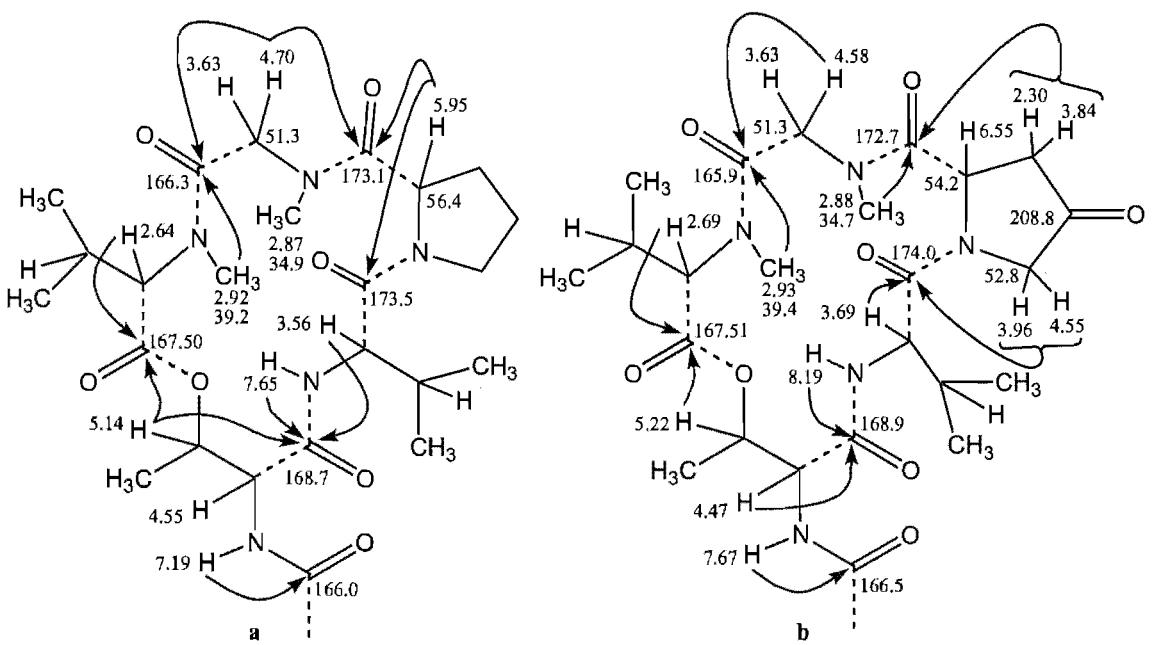

Figure 7.18a-b: CIGAR correlations for the depsipeptide rings.

If the 4-ketoproline residue was in the α-ring the aromatic proton at δ_H 7.60 would be expected to show a $^3J_{CH}$ correlation to the carbonyl at δ_C 166.5. Whereas if it was in the

β-ring the $^3J_{CH}$ correlation would be to δ_C 166.0. A correlation from the aromatic proton at δ_H 7.60 to the carbonyl at δ_C 166.0 was observed, thus the 4-ketoproline residue was located in the β-ring. Therefore **177** was indeed actinomycin V.

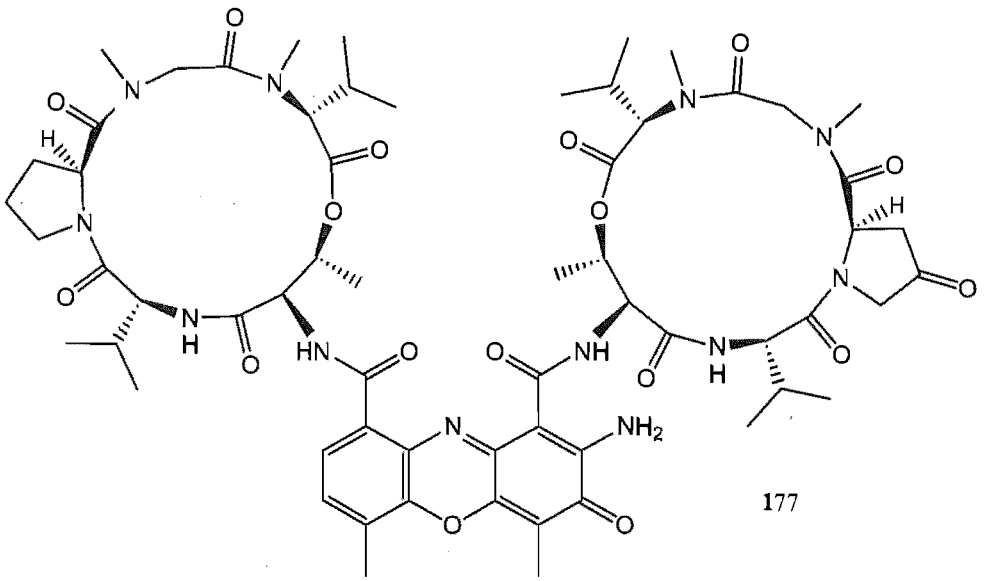

177

Unfortunately at the time of work on this compound a high resolution mass spectrum was unable to be obtained. However, after **177** had been identified as actinomycin V a high resolution ESI-MS showed a molecular formula the same as that for actinomycin V of $C_{62}H_{84}N_{12}O_{17}$ (27 double bond equivalents).

7.4.1.1 Confirmation of multiplet signal assignments

After identification of **177** as actinomycin V, spectral simulation using the experimental coupling constants and chemical shifts of the multiplets between δ_H 5.0 - 3.0 in the ^1H NMR spectrum was performed with ACDLabs ^1H NMR viewer to confirm that the correct signal assignments had been made.

7.4.1.2 Multiplets between δ_H 5 - 4

There were two well defined signals between δ_H 4.75 and δ_H 4.65 and a relatively complex multiplet between δ_H 4.62 - δ_H 4.50 which arose from a sarcosine proton, a threonine α-proton and a δ-proton in the 4-ketoproline residue. The coupling constants for the threonine α-proton were unable to be determined directly from this multiplet

(Figure 7.19a). However, the other threonine α-proton signal was well separated and as such the coupling constants were estimated from this signal instead. Spectral simulation of this multiplet with coupling constants of $^2J_{HH}$ = 17 Hz for δ_H 4.58, $^2J_{HH}$ = 19 Hz for δ_H 4.55 and $^3J_{HH}$ = 2 Hz and 5.5 Hz for δ_H 4.55 plus a line width of 2 Hz showed a very similar multiplet indicating that this was the correct signal assignment for these protons (Figure 7.19b).

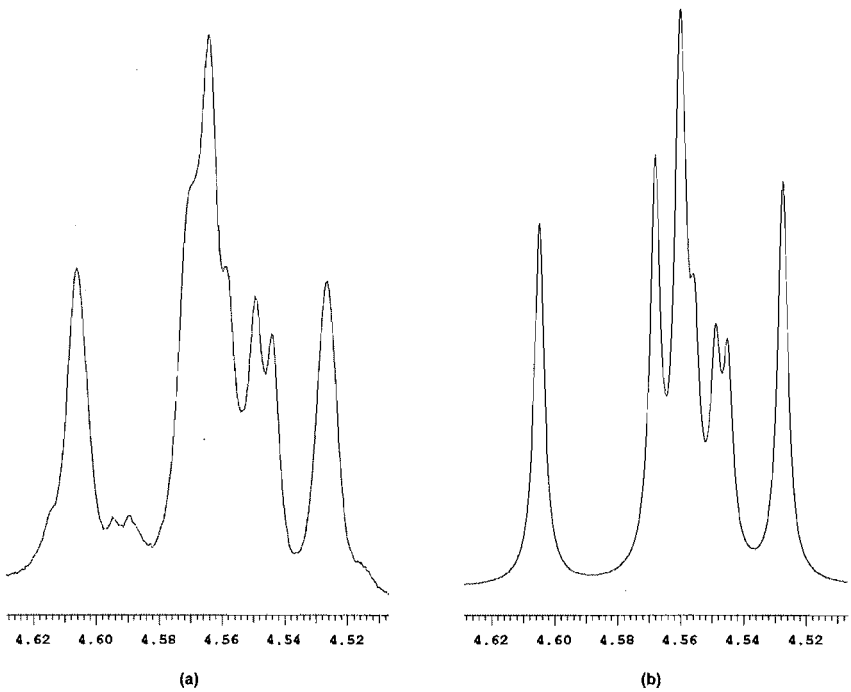

Figure 7.19: Experimental (a) and simulated (b) peaks for the multiplet between δ_H 4.50 - 4.62

7.4.1.3 Multiplets between δ_H 4 - 3

There were two complex multiplets between δ_H 4.0 - 3.0 both of which integrated for two protons. The first of these multiplets, between δ_H 3.92 and δ_H 3.80 arose from a δ-proton in the proline residue and a β-proton in the 4-ketoproline residue (Figure 7.20a-b).

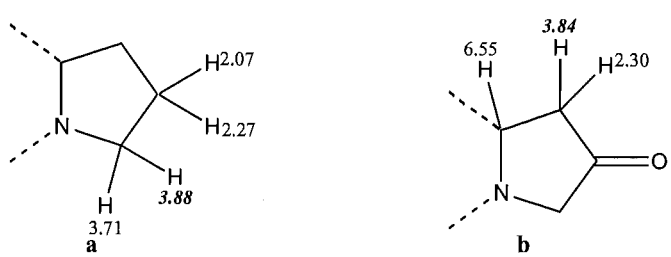

Figure 7.20a-b: Position of the signals at δ_H 3.88 and δ_H 3.84 in **176**

Spectral simulation of this multiplet with $^3J_{HH}$ coupling constants of 6.5, 10.5 and 11 Hz for δ_H 3.88, and a $^3J_{HH}$ of 11 Hz plus a $^2J_{HH}$ of 15.5 Hz for δ_H 3.84 with a line width of 3 Hz showed a multiplet almost identical to the experimental one (Figure 7.21).

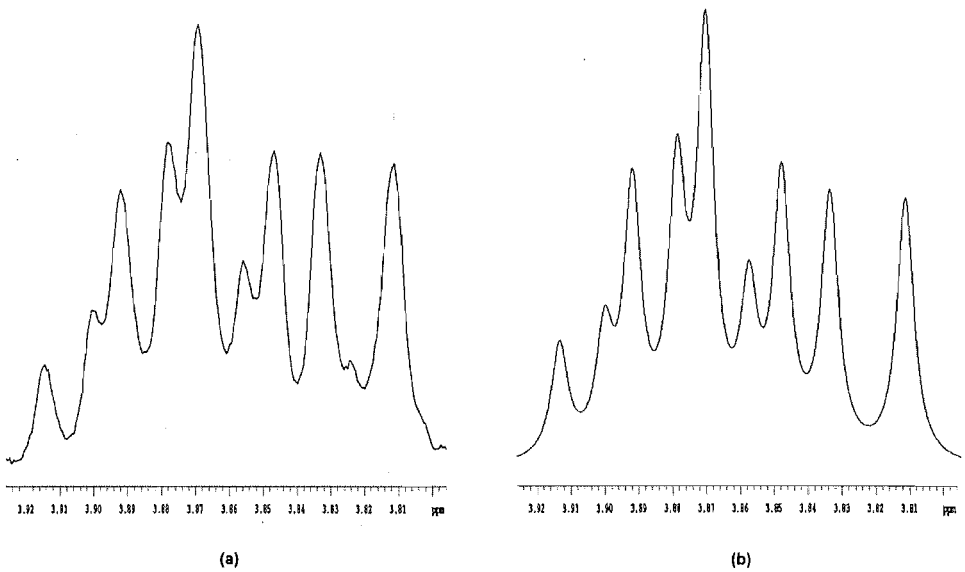

Figure 7.21: experimental (a) and simulated (b) peaks for the multiplet between δ_H 3.92 - 3.80

The second of these multiplets, between δ_H 3.75 and δ_H 3.67, arose from the second δ-proton on the proline residue (Figure 7.22a) and an α-proton from the valine residue in the β-ring (Figure 7.22b).

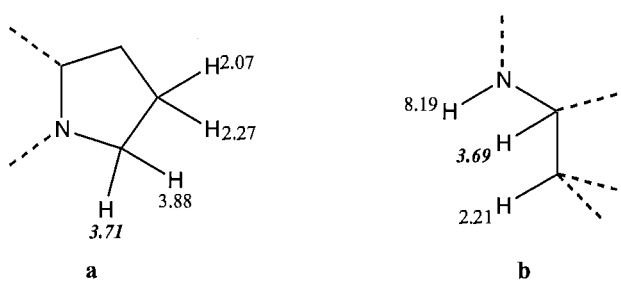

Figure 7.22a-b: Position of the signals at δ_H 3.71 and δ_H 3.69 in **176**

Spectral simulation of this multiplet with coupling constants of $^3J_{HH}$ = 1, 9 and 11 Hz for δ_H 3.71 and $^3J_{HH}$ = 6 and 9.5 Hz for δ_H 3.69 and a line width of 3 Hz showed a multiplet displaying many similarities to the experimental one (Figure 7.23).

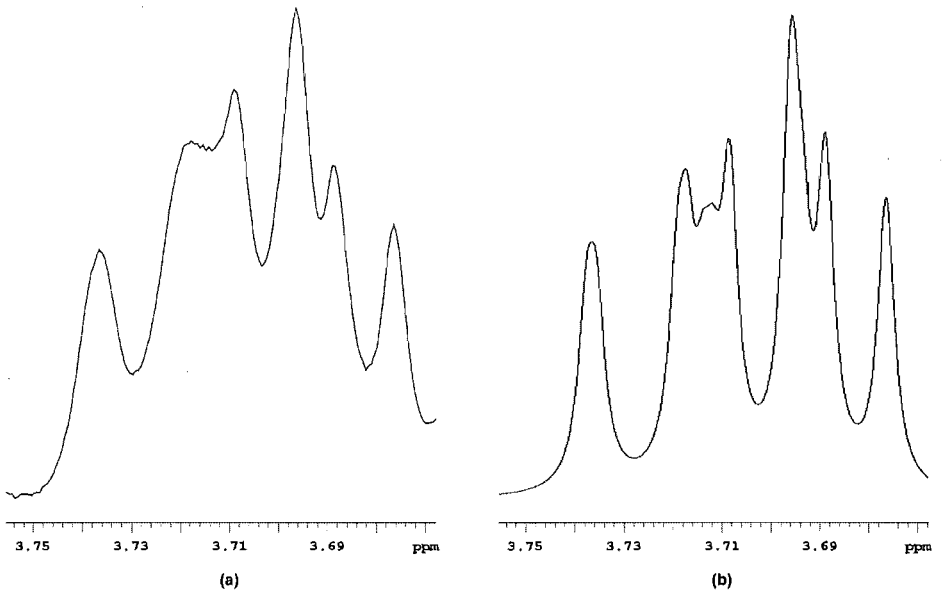

Figure 7.23: experimental (a) and simulated (b) peaks for the multiplet between δ_H 3.92 - 3.80

7.4.1.4 Relative stereochemistry of 177

Further work on the stereochemistry of **177** was deemed unnecessary because the experimental ^{1}H and ^{13}C chemical shifts and the $^{n}J_{HH}$ coupling constants were almost identical to those already reported for actinomycin V.[183-185] As the NMR data for **177** were identical to those for actinomycin V the only way that **177** could be novel is if all the stereogenic centres were inverted. It is more likely however, that only one or possibly two stereogenic centres could have been inverted. This would result in alterations in the ^{1}H and ^{13}C NMR data as well as the $^{n}J_{HH}$ coupling constants, but as this was clearly not the case the stereochemistry was assumed to be the same as that in actinomycin V (**177**).

7.4.2 Structural elucidation of 178

A slightly later eluting fraction, RKP 1.109.4, from the diol column showed an enrichment of a molecular ion 2 Da higher than **177** (MH^+ 1271). However, due to the low mass (4.4 mg) and the relatively low purity of the recovered sample no further work

was performed. Even though this was the case the increase of 2 Da in the mass spectrum, combined with the slight increase in polarity suggested that either one of the available carbonyl groups had been replaced with a hydroxyl group or that one of the two depsipeptide rings had been hydrolysed at the ester bond. Hydrolysis of the ester bonds was discounted as it has previously been shown that opening of one or both of the lactone rings results in a considerable decrease in biological activity and RKP 1.109.4 showed significant activity towards the P388 cell line (13.6 ng/mL).[176, 186]

There are fourteen carbonyl groups in actinomycin V, twelve of which form the peptide backbone, one is present in the 4-ketoproline residue and one in the aromatic ring system. Replacement of the amide carbonyls was discounted as this would significantly alter the conformation of the depsipeptide rings which has been shown to greatly alter the biological properties of the actinomycins.[170] This left two accessible carbonyl groups present in actinomycin V, one in the aromatic system and one in the 4-ketoproline residue. The carbonyl in the aromatic ring system could not have been replaced by a hydroxyl group as this would have altered the conjugation of the aromatic system and caused a hypsochromic shift of the UV maxima. The alteration must therefore be at the 4-ketoproline residue to give rise to an actinomycin X_0 derivative (**178**), naturally occurring as two different diastereoisomers, $X_{0\beta}$ or $X_{0\delta}$.[185] The 4-hydroxyproline residue in the actinomycin X_0 diastereoisomers is not a reduced form of 4-ketoproline, but is instead incorporated as 4-hydroxyproline.[176]

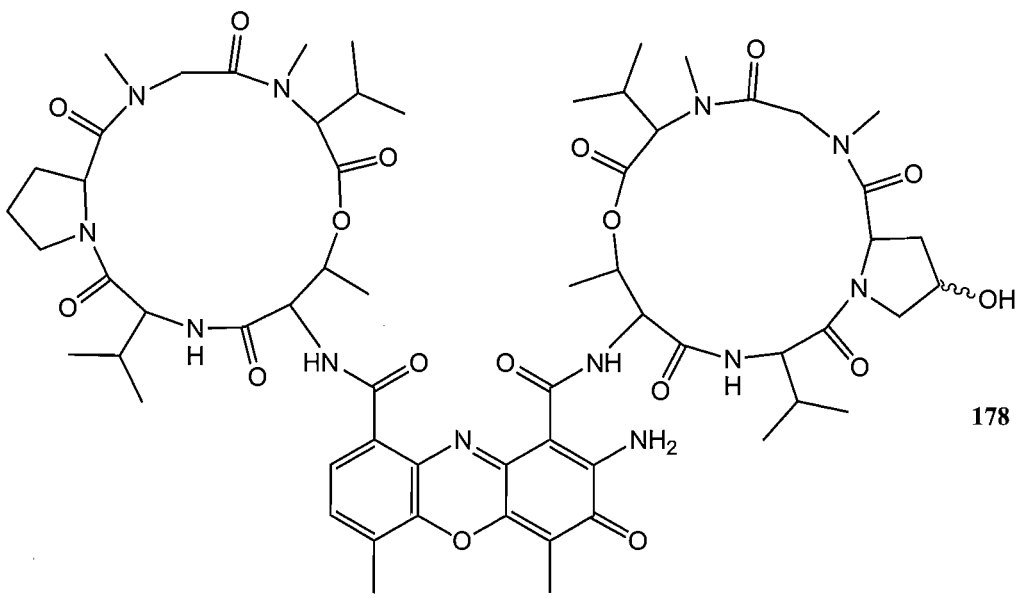

178

7.5 Chromatography of 179 in Spanish extracts

A further two powdered extracts were received from BioMar SA with preliminary investigations of these extracts suggesting that the biologically active components were also actinomycins. The chromatographic steps for these two extracts were identical to each other and displayed almost identical bioactivity profiles, varying only in recovered mass. The results for one of these two extracts, Kai 40-1-1, are shown in Scheme 7.2, with a more detailed description of the chromatographic steps carried out on both these extracts found in the experimental section.

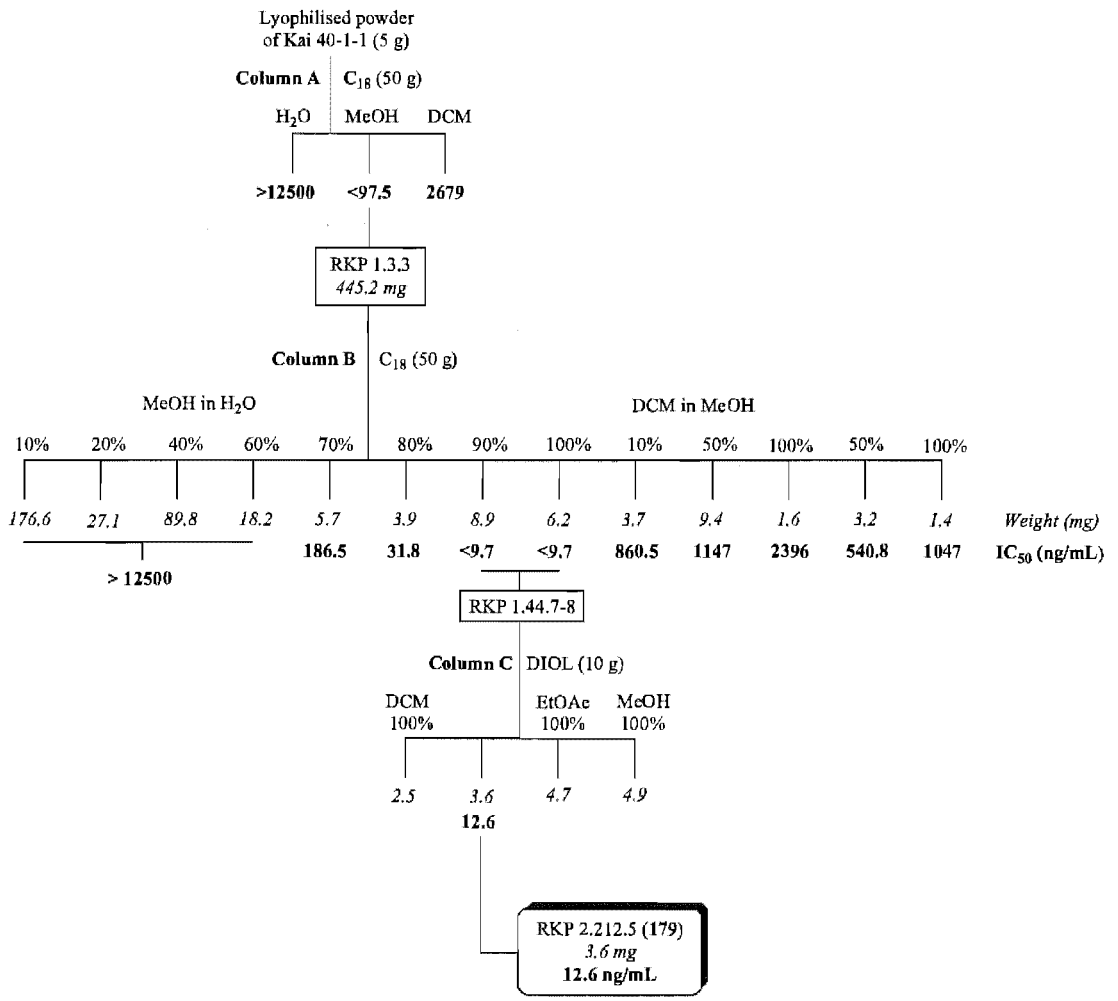

Scheme 7.2: Purification flow chart of an extract from the microbial isolate Kai 40-1-1.

The powdered extracts (5 g) were initially re-suspended in distilled water (100 mL) then crudely fractionated by vacuum liquid chromatography (VLC) on reverse phase C_{18} (50

g) washing first with 200 mL each of H_2O, then MeOH and finally DCM. The highest level of cytotoxicity was seen in the second fraction with the most mass eluting in the first thus the second fraction of both extracts were purified further on reverse phase C_{18} column chromatography using the same stepped gradient solvent system used for the extract prepared from Kai 11-2-1. As with Kai 11-2-1 the major zone of biological activity was between 90 and 100 % MeOH and the ESI-MS spectra of these fractions indicated a mass of 1254 Da. A search on the available databases with this mass and the UV maxima from Figure 7.3 indicated that **179** was actinomycin D. A further chromatographic step on normal phase DIOL (column C) of these two extracts was undertaken to confirm this identification. The two fractions from each extract, RKP 1.44.7-8 and RKP 1.60.7-8 respectively, were both eluted off separate normal phase DIOL columns with 30 mL each of DCM, EtOAc and MeOH. The ^{1}H NMR spectrum of the two DCM fractions were identical to a ^{1}H NMR spectrum of authentic actinomycin D and literature reports[183] confirming that **179** was actinomycin D.

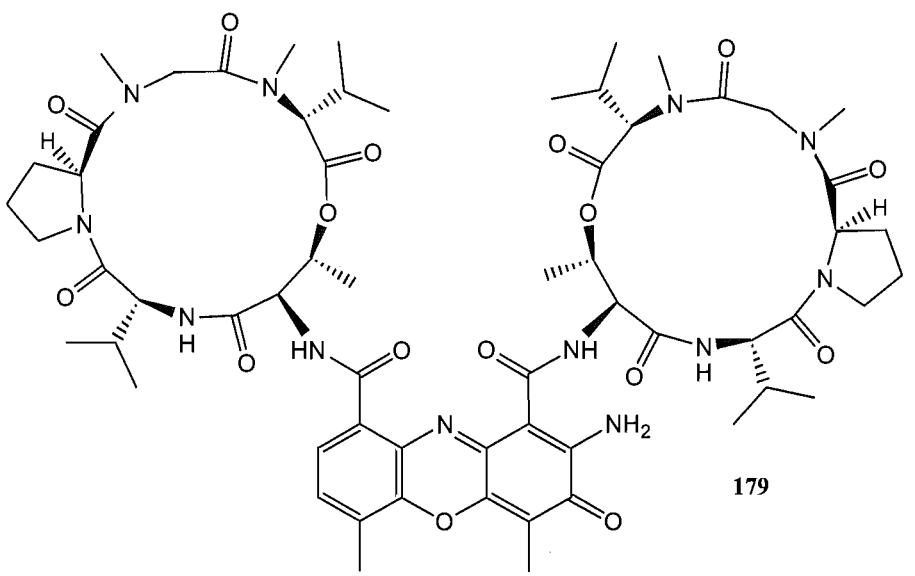

179

7.6 Discussion

The stereochemistry of **177** was not determined (Section 7.4.1.1) however, the absolute stereochemistry of the amino acid residues could easily be resolved using LC-MS and a modified Marfey's method.[187] This would involve hydrolysis of the actinomycin to the constituent amino acid residues then derivatisation of the free amino acids with FDLA

(1-fluoro-2,4-dinitrophenyl-5-L-leucine amide) for detection by a photodiode array detector. For comparison authentic amino acids are also subjected to the same procedures.

The therapeutic potential of actinomycin V is relatively low in comparison to that of actinomycin D however, the free amine group on the phenoxazinone could be utilised in the production of various prodrugs. It has previously been shown that modification or removal of the 2-amino group in the actinomycin chromophore significantly reduces or completely destroys the biological activity of the actinomycins.[176] However, in some semi-synthetic analogues of actinomycin D (**180** - **186**)[188] the observed antitumour activities were only slightly reduced compared to that of actinomycin D.

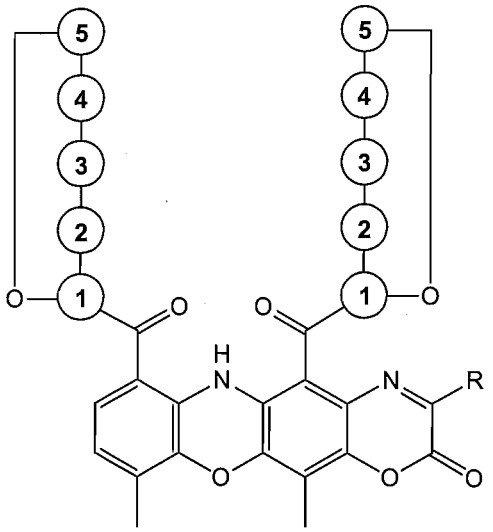

180 R = H
181 R = CH_3
182 R = C_2H_5
183 R = CH_2CO_2H
184 R = $CH_2CH_2CO_2H$
185 R = CH_2F
186 R = C_6H_5

Three of these analogues (**182**, **185** and **186**) also promoted a marked increase in the life span of the test organism and it was suggested that compounds **180** - **186** were being hydrolysed through the imine bond and the lactone *in vivo* to regenerate actinomycin D.

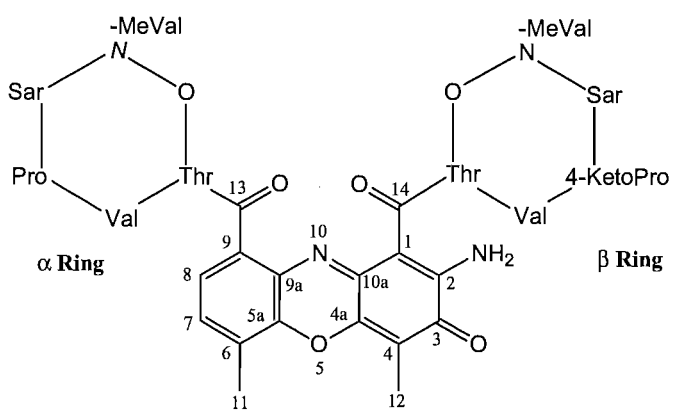

Figure 7.24: Numbering system of 177 used for Tables 7.1 - 7.3

Number	^{1}H, Multiplicity, (J_{HH}, Hz)	APT/HSQC	COSY	TOCSY	CIGAR	ROESY
1		101.7				
2		147.6				
3		179.0				
4		113.5				
4a		145.0				
5a		140.5				
6		127.8				
7	7.35, d, (8)	130.3	7.60 , 2.54	2.54 , 7.60	140.5 , 132.1 , 126.2 , 15.0	7.6
8	7.60, d, (7.5)	126.2	7.35	7.35	166.0 , 130.3 , 129.1 , 127.8	7.35 , 1.13
9		132.1				
9a		129.1				
10a		145.9				
11	2.21, s	7.7			179.0 , 145.0 , 113.5	2.54
12	2.54, s	15.0	7.35	7.60 , 7.35	140.5 , 130.3 , 127.8	7.35 , 2.21
13		166.0				
14		166.5				

Table 7.1: ^{1}H and ^{13}C NMR data for the aromatic portion of **177** in $CDCl_3$

Table 7.2: ^{1}H and ^{13}C NMR data for the α - ring portion of **177** in $CDCl_3$

Number	^{1}H, Multiplicity, (J_{HH}, Hz)	APT/HSQC	COSY	TOCSY	CIGAR	ROESY
Thr 1		168.7				
2	4.55, dd, (2.5, 5.5)	54.7	7.19 , 5.14	7.19 , 5.14 , 1.13	168.7 , 74.7	7.65 , 7.19 , 5.14 , 1.13
3	5.14, dd, (2.5, 6)	74.7	4.55 , 1.13	7.19 , 4.55 , 1.13	167.50	7.65 , 4.55 , 1.13
4	1.13, d, (6)	17.1	5.14	7.19 , 5.14 , 4.55 , 0.88	74.7 , 54.7	7.65 , 5.14 , 4.55 , 2.21
NH	7.19, d, (7.5)		4.55	5.14 , 4.54 , 1.13	166.0 , 168.7 , 54.7	4.55 , 1.13
Val 1		173.5				
2	3.56, q, (6, 9.5)	58.5	7.65 , 2.11	7.65 , 2.11 , 1.11 , 0.90	168.7 , 31.7 , 18.9	7.65 , 5.95 , 2.11 , 1.11 , 0.90
3	2.11, m, (7, 7, 9.5)	31.7	3.56 , 1.11 , 0.90	7.65 , 3.56 , 1.11 , 0.90	58.5 , 19.2 , 18.9	7.65 , 3.56 , 1.11 , 0.90
4	0.9, d, (7.5)	19.2	2.11	7.65 , 3.56 , 2.11 , 1.11	58.5 , 31.7 , 18.9	3.56 , 2.11
5	1.11, d, (7)	18.9	2.11	7.65 , 3.56 , 2.11 , 0.90	58.5 , 31.7 , 19.2	5.14 , 3.56 , 2.11
NH	7.65, d, (5.5)		3.56	3.56 , 2.11 , 1.11 , 0.90	168.7 , 58.5 , 31.7	5.14 , 4.55 , 3.56 , 2.11 , 1.11
Pro 1		173.1				
2	5.95, d, (1, 9)	56.4	2.74	3.88 , 3.71 , 2.74 , 2.27 , 2.07 , 1.83	173.5 , 173.1 , 47.4 , 31.0 , 22.9	4.70 , 3.56 , 2.74 , 1.83
3 α	2.74, m	31.0	5.95 , 2.07 , 1.83	5.95 , 3.88 , 3.71 , 2.27 , 2.07 , 1.83	173.1	5.95 , 2.07 , 1.84
3 β	1.83, m, (1, 7, 12)	31.0	5.95 , 2.74 , 2.27	5.95 , 3.88 , 3.71 , 2.74 , 2.27 , 2.07	173.1 , 47.4 , 22.9	5.95 , 2.93 , 2.74 , 2.27 , 2.07
4 α	2.27, m	22.9	3.71 , 1.83	5.95 , 3.88 , 3.71 , 2.74 , 2.07 , 1.83		3.71 , 2.74 , 2.07 , 1.84
4 β	2.07, m	22.9	3.88 , 3.71 , 2.74 , 2.27	5.95 , 3.88 , 3.71 , 2.74 , 2.27 , 1.83	56.4 , 31.0	3.88 , 2.74 , 2.27
5 α	3.71, m, (1, 9, 11)	47.4	3.88 , 2.07	5.95 , 3.88 , 2.74 , 2.27 , 1.83	31.0	3.88 , 2.27
5 β	3.88, m, (6.5, 10.5, 11)	47.4	2.07	5.95 , 3.71 , 2.74 , 2.27 , 1.83		4.47 , 3.71 , 2.07 , 1.24
Sar 1		166.3				
2 α	4.70, d, (17.5)	51.3	3.63 , 2.87	3.63	173.1 , 166.3 , 34.9	5.95 , 3.63 , 2.87
2 β	3.63, d, (17)	51.3	4.70	4.7	165.9 , 172.7 , 34.7	5.95 , 4.70 , 2.87 , 0.73
NCH_3	2.87, s	34.9			173.1 , 51.3	
MeVal 1		167.5				
2	2.64, m, (5.5, 6)	71.2	0.93 , 0.73	0.93 , 0.73	167.50 , 166.3 , 71.2 , 39.2 , 26.8 , 21.5 , 19.0	2.92 , 0.94 , 0.73
3	2.64	26.8	0.93 , 0.73	0.93 , 0.73	167.50 , 166.3 , 71.2 , 39.2 , 26.8 , 21.5 , 19.0	2.92 , 0.94 , 0.73
4	0.93, d, (6)	21.5	2.64	2.64 , 0.73	167.50 , 71.2 , 26.8 , 19.0	2.64
5	0.73, d, (5.5)	19.0	2.64	2.64 , 0.93	167.50 , 71.2 , 26.8 , 21.5	3.63 , 2.92 , 2.64 , 0.93
NCH_3	2.92, s	39.2			166.3 , 71.2	

Number	^{1}H, Multiplicity, (J_{HH}, Hz)	APT/HSQC	COSY	TOCSY	CIGAR	ROESY
Thr 1		168.9				
2	4.47, dd, (2, 5.5)	54.9	7.67 , 5.22	7.67 , 5.22 , 1.24	168.9 , 167.51	8.19 , 7.67 , 5.22 , 3.88 , 1.24
3	5.22, dd, (2.5, 6)	74.6	4.47 , 1.24	7.67 , 4.47 , 1.24	167.51	8.19 , 4.47 , 1.24 , 1.14
4	1.24, d, (6.5)	17.7	1.24	7.67 , 5.22 , 4.47	74.6 , 54.9	5.22 , 4.47 , 3.88
NH	7.67, d, (6)		4.47	5.22 , 4.47 , 1.24	168.9 , 166.5 , 54.9	4.47
Val 1		174.0				
2	3.69, q, (6.5, 10)	57.1	8.19 , 2.21	8.19 , 2.21 , 1.14 , 0.89	174.0 , 168.9 , 31.8	8.19 , 6.55 , 2.21 , 1.14 , 0.89
3	2.21, m, (7, 7.5, 10)	31.8	3.69 , 1.14 , 0.89	8.19 , 3.69 , 1.14 , 0.89	57.1 , 19.1	8.19 , 3.69 , 1.14 , 0.89
4	0.89, d, (7)	19.1	2.21	8.19 , 3.69 , 2.21 , 1.14	57.1 , 31.8 , 18.8	3.69 , 2.21
5	1.14, d, (7)	18.8	2.21	8.19 , 3.69 , 2.21 , 0.89	57.1 , 31.8 , 19.1	8.19 , 5.22 , 3.69 , 2.21 , 0.90
NH	8.19, d, (6)		3.69	3.69 , 2.21 , 1.14 , 0.89	168.9 , 57.1 , 31.8	5.22 , 4.47 , 3.69 , 2.21 , 1.14
4-KetoPro 1		172.7				
2	6.55, d, (1, 10)	54.2	3.84 , 2.30	3.84 , 2.30	174.0 , 41.9 , 208.8	4.55 , 3.69 , 3.84
3 α	3.84, dd, (11, 18)	41.9	6.55 , 2.30	6.55 , 2.30	208.8 , 172.7 , 54.2	6.55 , 2.30
3 β	2.30, d, (1, 18)		6.55 , 3.84	6.55 , 3.84	208.8 , 172.7	3.84
4		208.8				
5 α	4.55, d, (19)	52.8	3.96	3.96	208.8 , 174.0 , 54.2	3.96
5 β	3.96, d, (19)		4.55	4.55	208.8	4.55 , 3.69
Sar 1		165.9				
2 α	4.58, d, (17.5)	51.3	3.63 , 2.88	3.63	172.7 , 165.9 , 34.7	6.55 , 3.63 , 2.88
2 β	3.63, d, (17)		4.58	4.58	173.1 , 166.3 , 34.9	6.55 , 4.58 , 2.88 , 0.74
NCH_3	2.88, s	34.7			172.7 , 51.3	
MeVal 1		167.5				
2	2.69, m, (6, 6)	71.4	0.97 , 0.74	0.96 , 0.74	167.51 , 165.9 , 71.4 , 39.4 , 26.9 , 21.7	2.93 , 0.97 , 0.74
3	2.69	26.9	0.97 , 0.74	0.96 , 0.74	167.51 , 165.9 , 71.4 , 39.4 , 26.9 , 21.7	2.93 , 0.97 , 0.74
4	0.97, d, (6)	21.7	2.69	2.69 , 0.74	167.51 , 71.4 , 26.9 , 19.1	2.69
5	0.74, d, (6)	19.1	2.69	2.69 , 0.97	167.51 , 71.4 , 26.9 , 21.7	3.63 , 2.93 , 2.69 , 0.97
NCH_3	2.93, s	39.4			167.51 , 165.9 , 71.4	

Table 7.3: ^{1}H and ^{13}C NMR data for the β - ring portion of **177** in $CDCl_3$

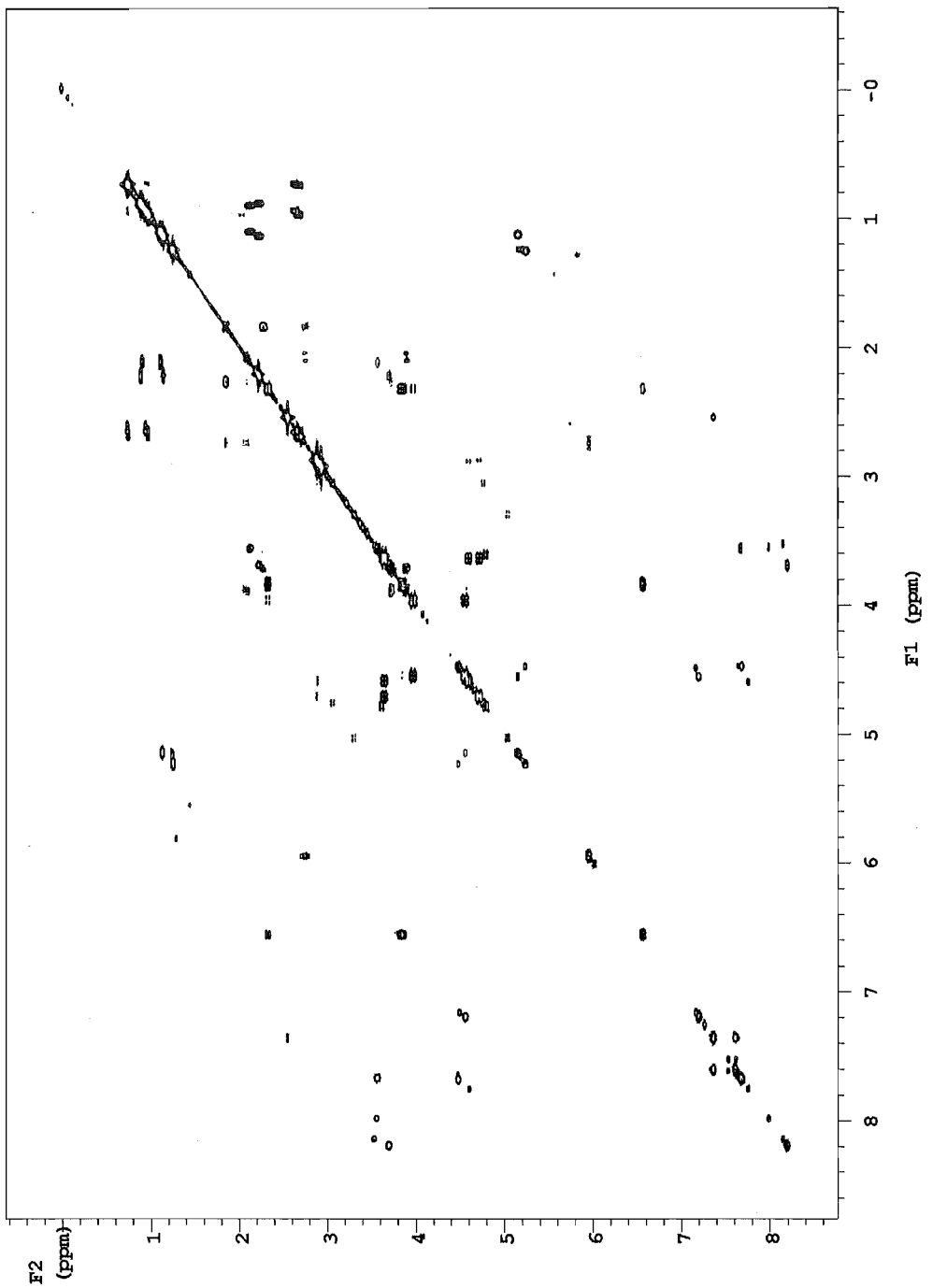

Figure 7.25: COSY spectrum of **177** in CDCl3

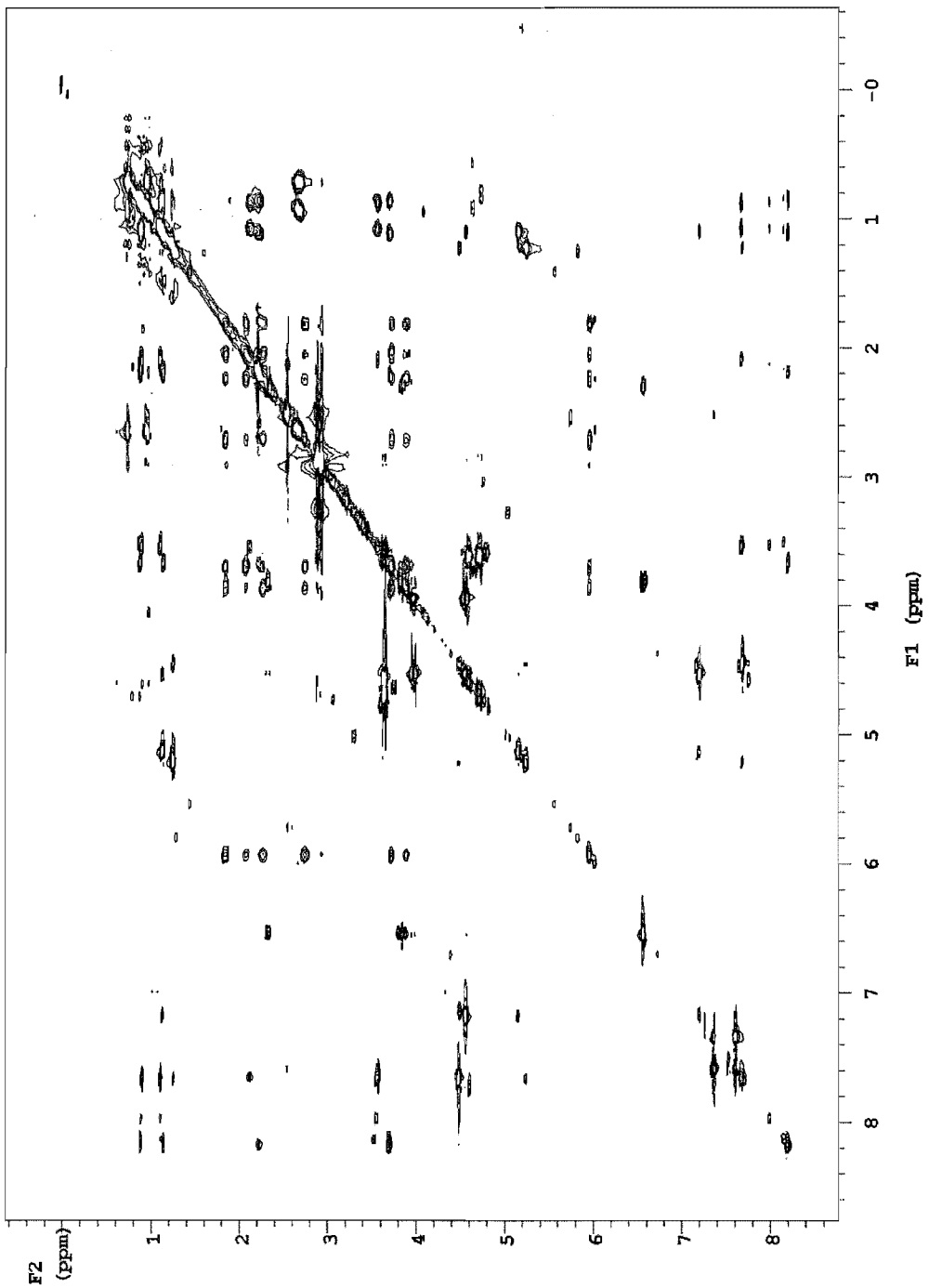

Figure 7.26: TOCSY spectrum of **177** in CDCl3

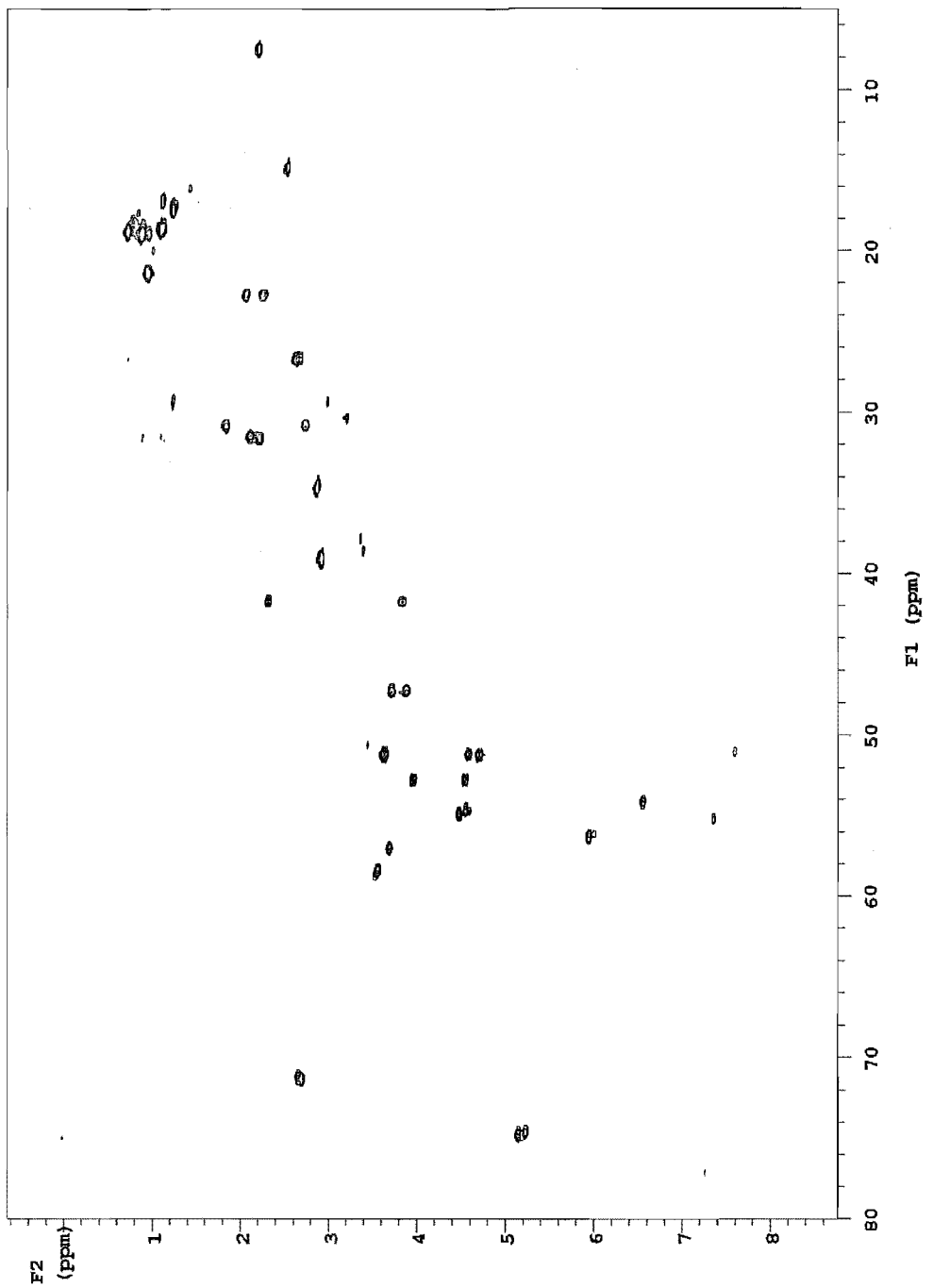

Figure 7.27: HSQC spectrum of **177** in CDCl3

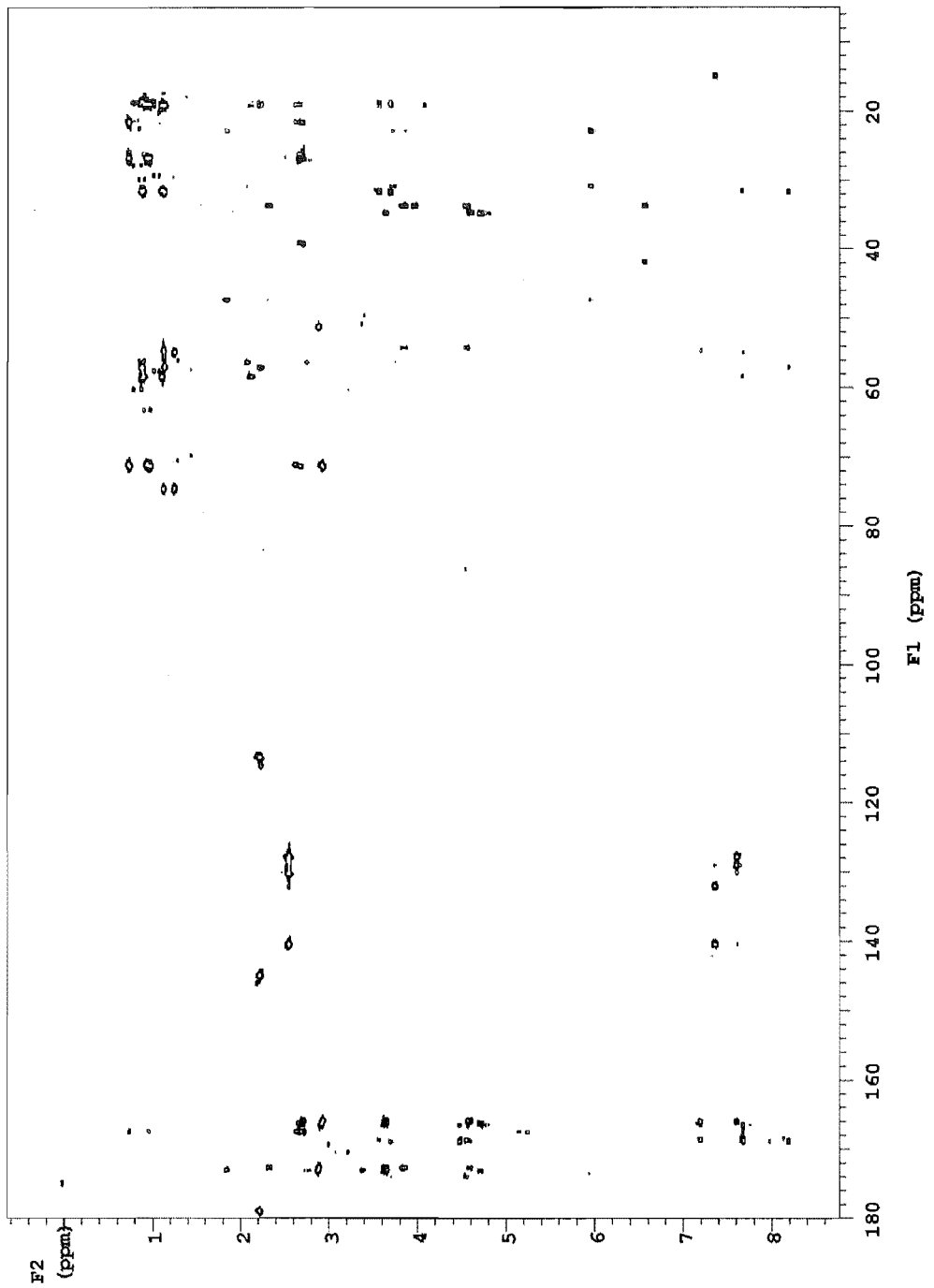

Figure 7.28: CIGAR spectrum of **177** in CDCl3

CONCLUSIONS

This body of work serves to demonstrate that marine derived micro-organisms, especially fungi and actinomycetes, are capable of producing a wide variety of secondary metabolites. Even though no compound isolated and characterised in this study possessed a new carbon skeleton a high proportion did display modifications to known carbon skeletons and are in that sense novel.

Only a small number of the total micro-organisms isolated in this study were able to be investigated. The results obtained from the microassay however, indicated that a high proportion of these micro-organisms (~ 30 %) produce bioactive metabolites. Those microbes that were not investigated in this study remain a lucrative source of potentially novel metabolites. Indeed this high percentage of active microbial isolates almost certainly will lead, in the future, to the discovery of compounds with novel carbon skeletons as well as known compounds and new derivatives of known carbon skeletons.

In brief, marine derived micro-organisms are capable of producing a plethora of potentially useful bioactive compounds.

CHAPTER EIGHT

EXPERIMENTAL

8.1 General Methods.

8.1.1 Preparation of macro-algae and driftwood samples

Small sections of surface sterilized macro-algae and driftwood were plated out on minimal and complex media (Section 8.1.2) containing antibiotics such as streptomycin and chloramphenicol to inhibit bacterial growth.[32]

Macro-algae

Sections of macro-algae were rinsed with sterile distilled water, blotted dry on sterile filter paper, cut into small pieces (approximately 0.5 cm^2) and placed onto a minimal isolation medium (medium I) and a complex medium (medium II).

Driftwood samples

The outer layer of driftwood samples were aseptically scraped to remove any superficial organisms. Thin slices of the driftwood were then plated onto medium I and medium II.

8.1.2 Media and incubation conditions

Medium I

Filtered seawater agar (SA). 15 g/L agar, fresh seawater (filtered though coarse miracloth) 1000 mL, 100 µg/L chloramphenicol, 100 µg/L ampicillin, 50 µg/L streptomycin sulphate.

Medium II

Seawater potato dextrose agar (sPDA). Gibco PDA 39 g/L, fresh filtered seawater 1000 mL, 100 µg/L chloramphenicol, 100 µg/L ampicillin, 50 µg/L streptomycin sulphate.

Medium III

Seawater potato dextrose agar (sPDA). Gibco PDA 39 g/L, fresh filtered seawater 1000 mL.

Medium IV

Potato dextrose agar (PDA). Gibco PDA 39 g/L, distilled water 1000 mL

Medium V

Starch-casein agar. Glycerol 10 g/L, peptone 140 0.3 g/L, KNO_3 2 g/L, NaCl 2 g/L, K_2HPO_4 2 g/L, $MgSO_4.7H_2O$ 50 mg/L, $CaCO_3$ 20 mg/L, $FeSO_4.7H_2O$ 10 mg/L, distilled water 1000 ml, pH adjusted to 7.0 prior to sterilization.

Incubation and isolation conditions

After plating out, the macro-algae and driftwood samples were incubated at 15°C and 20°C for seven days, after which the plates were examined daily for developing fungal hyphae under a stereomicroscope. Once hyphae had been detected on the macro-algal

or driftwood sections (typically after 10 days incubation) the hyphae were transferred to a nutrient rich medium (medium II). Any hyphae or sporulating structures were observed with a stereomicroscope and transferred to medium II with a sterile glass capillary.

8.1.3 Maintenance of fungal stock cultures

Terrestrial and facultative micro-organisms were stored in 10 % glycerol in distilled water and obligate marine micro-organisms were stored in 10 % glycerol in seawater. All were stored at - 80°C.

8.1.4 Sample Extraction

Fungal cultures were homogenised with an Ultra-turrax® (Janke & Kunkle) for five minutes or until the mycelial mat was sufficiently macerated, then filtered through celite under vacuum. The filtered broth was subsequently extracted three times with EtOAc at a ratio of 5:1. The solid mycelial residue was re-suspended in EtOAc at a ratio of 1:5 (100 mL EtOAc for every 20 g wet weight) and extracted three times. The initial EtOAc extraction was for one hour, the second overnight and the third for a final hour. All organic phases were combined, dried over anhydrous $MgSO_4$, and taken to dryness on a rotary evaporator. A small volume (50 mL) of the aqueous phase was also taken to dryness on a rotary evaporator. Both the aqueous and organic phases were then transferred to a pre-weighed vial, the weight determined and assayed for antitumour activity.

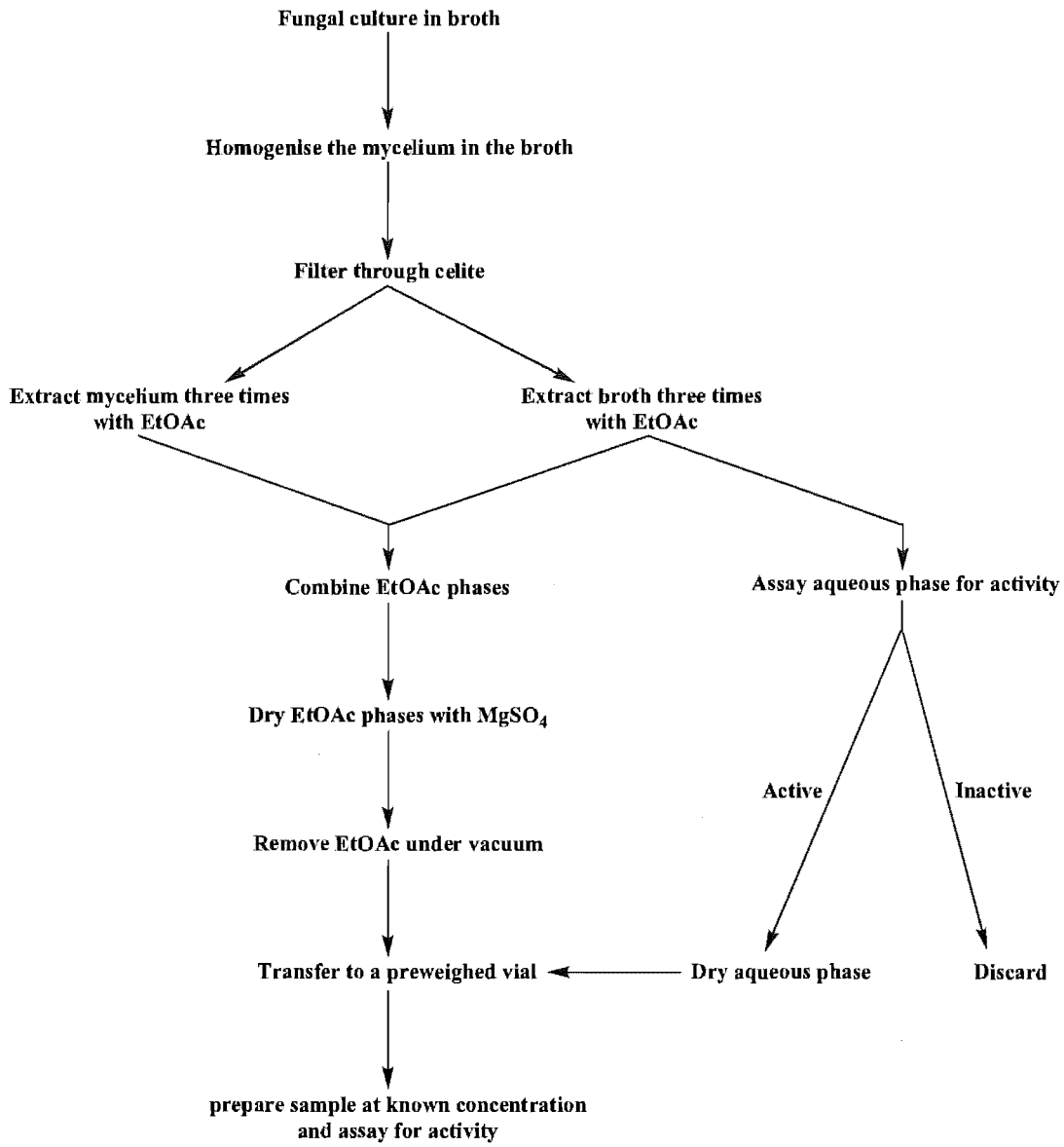

Scheme 8.1: Flow chart showing procedure used for metabolite extraction from fungal cultures.

8.1.5 P388 Assay

Prior to further investigation, crude extracts were assayed for biological activity against the murine leukaemia cell line P388. This assay consists of a serial dilution of the sample of interest followed by incubation for 72 hours with P388 cells. Cell viability is determined colorimetrically by the addition of the yellow dye MTT tetrazolium. Unhealthy or dead cells cannot metabolise this dye leaving a yellow colour, whereas healthy cells reduce this dye to MTT formazan resulting in an intense purple colour.

The concentration of sample required to reduce cell growth by 50 %, when compared to controls, is expressed as an IC_{50} in ng/mL. All samples were dissolved in double distilled MeOH prior to submission to the assay.

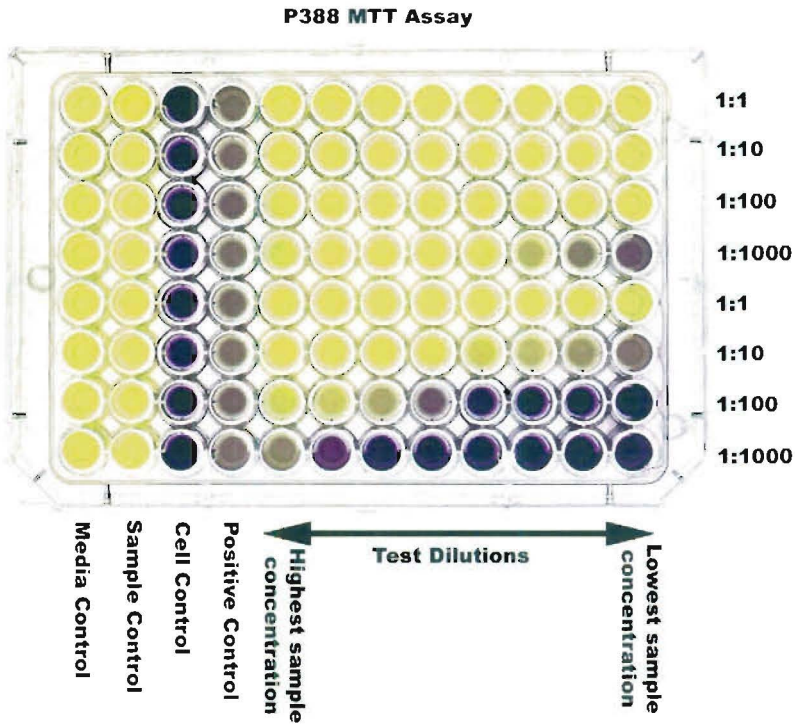

Figure 8.1: P388 assay dilution plate, purple indicates viable cells and yellow dead or inactive cells.

8.1.6 HPLC microtitre plate screening

As part of the dereplication process (Section 2.4) all small scale extracts were initially examined in the HPLC microtitre plate screen. An aliquot of the crude extract (250 µg) was analysed by reverse phase C_{18} HPLC using the following gradient solvent system: 2 minutes of 10 % ACN/H_2O; a linear gradient to 75 % ACN/H_2O for 12 minutes; isocratic at 75 % for another 10 minutes; a linear gradient for 2 minutes to 100 % ACN followed by isocratic at 100 % ACN for 4 minutes then returned to 10 % ACN/H_2O in 2 minutes and re-equilibrated for 8 minutes; with a flow rate 1 mL/min. The eluant was collected into 96 well microtitre plates and assayed for cytotoxicity against the P388 cell line.

8.1.7 Column Chromatography

Column chromatography was performed with glass columns of stated dimensions. All solvents used for chromatography were of commercial grade and distilled once, except for MeOH which was doubly distilled. Reverse phase C_{18} and some normal phase diol columns were run under pressure (0.5 kPa) with oxygen-free N_2 gas.

Normal phase flash and preparative chromatography was performed with Merck DIOL (40 μm APD). Samples fractionated by normal phase (DIOL) flash chromatography were dissolved in a minimal volume of 50:50 MeOH/DCM and adsorbed to fresh DIOL (0.2 g). Residual solvent was removed under vacuum on a rotary evaporator.
A standard elution profile was created for normal phase (DIOL) column chromatography (12g, 1.2 x 60 cm). Columns were equilibrated to 100 % DCM prior to sample loading then eluted with the following gradient solvent system: 100 % DCM (30 mL), 5 %, 10 %, 20 %, 40 %, 60 %, 80 %, 100 % EtOAc/DCM (20 mL); 5 %, 10 % MeOH/EtOAc (15 mL) and 100 % MeOH (35 mL).

Reverse phase chromatography used Bakerbond C_{18} (40 μm prep LC packing). Samples fractionated on reverse phase C_{18} were also dissolved in a minimal volume of appropriate solvent and adsorbed to fresh C_{18} at a ratio of 1:50. All remaining solvent was removed under vacuum with a rotary evaporator.
A standard elution profile was created for reverse phase C_{18} column chromatography (50g, 3 x 60 cm). Columns were equilibrated to 10 % MeOH/H_2O prior to sample loading then eluted with the following gradient solvent system: 10 %, 20 %, 40 %, 60 %, 70 %, 80 %, 90 %, 100 % MeOH/H_2O (100 mL); 10 % DCM/MeOH (100 mL); 50 % DCM/MeOH, 100 % DCM, 50 % DCM/MeOH, 100 % MeOH (200 mL).

Size exclusion chromatography was carried out with Sephadex LH20 (Pharmacia Biotech AB). Samples fractionated with Sephadex LH20 were dissolved in a minimal volume of initial eluting solvent.

8.1.8 High Pressure Liquid Chromatography (HPLC)

Analytical HPLC was carried out on a Shimadzu LC-10ADvp liquid chromatograph, with an SPD-M10Avp photodiode array detector. Columns were kept at a constant temperature of 40°C with a CTO-M10ADvp oven. Reverse phase HPLC was carried out on a Phenomenex Prodigy C_{18} 5-ODS column (3 µm, 250 x4.6 mm). A standard flow rate of 1 mL/min was used with variable concentrations of ACN (HPLC grade) in H_2O (Milli-Q). In some projects the milli-Q H_2O was acidified with 0.05% TFA. All samples were filtered through a 0.45 µm syringe filter immediately prior to injection.

8.1.9 Structural Elucidation

Structures were elucidated based on 1D and 2D NMR experiments and high resolution mass spectrometry. This was further backed up with additional experiments such as UV-visible and CD spectroscopy. Where appropriate compounds were identified by comparison of experimental data and those found in the literature. Literature searches were performed using multiple databases including, MarinLit, Berdy Natural Products Database, Antibase, Chapman & Hall Natural Products Dictionary, version 9.1, August 2000, and Scifinder Scholar. If the metabolite of interest was not found in any of the above databases, but especially Scifinder Scholar, it was designated as new.

8.1.9.1 Mass Spectrometry

EI mass spectra were obtained on a Kratos MS80RFA spectrometer, operating with a 4kV accelerating potential, 70eV and a source temperature of 250°C.

Electrospray Ionisation (ESI) mass spectra were recorded on a Micromass LCT spectrometer using a probe voltage of 3200V, an operating temperature of 150°C and a source temperature of 80°C. A 10 µL injection of sample was made from a 10 µg/mL sample. When obtaining positive ESI mass spectra some samples were protonated with 10 µL/mL formic acid prior to injection. When recording negative ESI mass spectra samples were deprotonated as required with 10 µL/mL DEA prior to injection.

LC-APcI Mass Spectra were obtained with a Waters 2790 HPLC coupled to a Micromass LCT spectrometer. Reverse phase HPLC was carried with a Phenomenex Prodigy C_{18} 5-ODS column (3 μm, 250 x4.6 mm) at a flow rate of 1 mL/min with varying concentrations of ACN (HPLC grade) and H_2O (Milli-Q). APcI spectra were recorded with a drying gas flow rate of 300 L/hr, a probe voltage of 3200V and a cone voltage of 45V. A probe operating temperature of 300°C and a source temperature of 150°C were used.

8.1.9.2 Nuclear Magnetic Resonance (NMR)

^{1}H NMR and ^{13}C NMR spectra were recorded on a Varian INOVA 500 spectrometer at 23°C, operating at 500 MHz and 125 MHz respectively. Other experiments described herein, including, 1D-TOCSY, 2D-TOCSY, COSY, 1D-NOESY, 2D-NOESY, APT, HSQC and CIGAR were all recorded on the INOVA 500 spectrometer at 500 MHz. The spectrometer was fitted with a pulsed field gradient MLD driver with a 5 mm Indirect Detection Probe.

Chemical shifts in this thesis are described in parts per million (ppm), on the δ scale, and referenced to the appropriate solvent peaks:

$CDCl_3$ referenced to $\mathbf{C}HCl_3$ at δ_H 7.26 ppm (^{1}H) and $\mathbf{C}DCl_3$ at δ_C 77.0 ppm (^{13}C);

CD_3OD referenced to CHD_2OD at δ_H 3.30 ppm (^{1}H) and $\mathbf{C}D_3OD$ at δ_C 49.3 ppm (^{13}C);

DMSO-d_6 referenced to $CD_3(CHD_2)SO$ at δ_H 2.50 ppm (^{1}H) and $(\mathbf{C}D_3)_2SO$ at δ_C 39.6 ppm (^{13}C).

^{1}H NMR spectra were recorded with an acquisition time (AT) of 1.892 s and ^{13}C NMR were recorded with an AT of 1.3 s and a delay (D1) of 1 s. COSY, 2D TOCSY, 2D NOESY and 2D ROESY experiments were all recorded with an AT of 0.228 s and a D1 of 1.0 s. Both the mixing times and spectral windows for each experiment varied according to the sample being examined.

HSQC experiments with the pulsed field gradient system were run with an AT of 0.140 s, a D1 of 1.0 s and $^1J_{CH}$ = 140 Hz. CIGAR experiments were recorded with the same D1 as in the HSQC experiments, but with an AT of 0.250 s and $^nJ_{CH}$ = 8.0 Hz.

8.1.9.3 UV-Vis Spectroscopy

Purified samples were dissolved in MeOH at a concentration of 1 mg/mL. The UV-vis spectra of these samples were recorded with a Hewlett Packard 8452 diode array detector using a 10 mm quartz curvette.

8.1.9.4 Circular Dichroism Spectroscopy

CD spectra were measured in 0.1-0.01 mg/mL MeOH using a 10 mm quartz cell on a Jasco J 20-C spectropolarimeter.

8.1.9.5 Optical Rotation

Rotation values were obtained on a Perkin Elmer 341 polarimeter at 20°C with a wavelength of 589 nm. The optical rotation was then calculated using the following equation:

$$[\alpha]_D^{20°C} = \frac{\alpha}{LC}$$

Where L is the cell pathlength (dm) and C is the concentration (g/L).

8.1.10 Solvents

Commercial grade solvents were all distilled once prior to use with the exception of MeOH and H_2O. MeOH was distilled twice and H_2O was treated by reverse osmosis and subsequently filtered through a 0.45 μm Millipore filter before use.

8.2 Experimental for Chapter 3

8.2.1 Chromatography of Oka 2-1-1

The large scale culture extract was adsorbed to C_{18} (2 g) and fractionated on a reverse phase (C_{18}) column (50 g, 3 x 60 cm), using the standard stepped gradient system (Section 8.1.7) for elution. Thirteen fractions were collected and analysed by reverse phase HPLC and assayed for cytotoxicity against the P388 cell line. The three fractions (RKP 1.127.5-7) which eluted between 70-90% MeOH/H_2O showed the highest cytotoxicity towards the P388 cell line and showed common components in the HPLC traces eluting between 11 and 14 minutes. Based on these results these fractions were combined and further purified by normal phase chromatography on DIOL (12 g, 1.2 x 60 cm). The combined bioactive fractions (RKP 1.127.5-7) were eluted using the standard DIOL elution profile (Section 8.1.7). Eleven fractions were collected, assayed for cytotoxicity and analysed with analytical reverse phase (C_{18}) HPLC and NMR spectroscopy. Cytotoxicity was seen in the first two fractions from 0-10 % EtOAc/DCM (RKP 2.209.1-2), and the fifth and sixth fractions from 40-60 % EtOAc/DCM (RKP 2.209.5-6). Based on cytotoxicity, HPLC and NMR spectroscopy the first two fractions (RKP 2.209.1-2) were combined.

Analytical HPLC and NMR spectroscopy of the two later eluting fractions (RKP 2.209.5-6) showed that RKP 2.209.5 was relatively pure, whereas RKP 2.209.6 was not. The major component of RKP 2.209.5 (**109**) was identified by 2D NMR spectroscopy and mass spectrometry as the 4-hydroxy derivative of **104**.

Analytical HPLC and NMR spectroscopy of RKP 2.209.1-2 highlighted many impurities in the combined fraction thus it was further purified on a small scale normal phase (DIOL) column (1 g, 0.5 x 7.5 cm). The combined fraction was eluted with 100 % DCM (2 x 1 mL) and 100 % EtOAc (2 x 1 mL) collecting four fractions (RKP 2.226.1-4). The ^{1}H NMR spectra of these four fractions indicated that the middle two fractions (RKP 2.226.2-3) were very pure and thus were combined. On the basis of 1D and 2D NMR spectroscopy and mass spectrometry the major component of the combined fraction (RKP 2.227.1) was identified as a novel trichothecene (**104**).

Compound (104)

HR ESIMS MCs^+ 527.1049 ($C_{21}H_{30}O_7Cs$ requires 527.1046). ^1H NMR ($CDCl_3$) δ 5.79 (d, J_{HH} = 5.5 Hz, 1H, H10), 5.28 (d, J_{HH} = 5.5 Hz, 1H, H8), 4.47 (dt, J_{HH} = 5, 12 Hz, 1H, H3), 4.43 (d, J_{HH} = 6 Hz, 1H, H11), 4.25 (d, J_{HH} = 12.5 Hz, 1H, H15α), 3.95 (d, J_{HH} = 12.5 Hz, 1H, H15β), 3.50 (d, J_{HH} = 4.5 Hz, 1H, H2), 3.07 (d, J_{HH} = 4 Hz, 1H, H13α), 2.86 (d, J_{HH} = 4 Hz, 1H, H13β), 2.45 (m, J_{HH} = 6 Hz, 1H, H18), 2.34 (dd, J_{HH} = 5.5, 15 Hz, 1H, H7β), 2.27 (dd, J_{HH} = 3.5, 14.5 Hz, 1H, H4α), 2.14 (dd, J_{HH} = 3.5, 14.5 Hz, 1H, H4β), 2.05 (s, 3H, 22Me), 1.95 (d, J_{HH} = 15 Hz, 1H, H7α), 1.74, (s, 3H, 16Me), 1.17, (d, J_{HH} = 7 Hz, 3H, 19Me), 1.16, (d, J_{HH} = 7 Hz, 3H, 20Me), 0.80 (s, 3H, 14Me). ^{13}C NMR ($CDCl_3$) δ 176.7 (C=O), 170.4 (C=O), 136.2 (C), 124.1 (CH), 79.6 (CH), 69.0 (CH), 68.5 (CH), 67.7 (CH), 65.4 (C), 64.9 (CH_2), 48.6 (CH_2), 45.5 (C), 42.1 (CH_2), 41.7 (C), 34.1 (CH), 27.5 (CH_2), 21.1 (CH_3) 20.3 (CH_3), 19.2 (CH_3), 18.5 (CH_3), 12.1 (CH_3). UV (MeOH, nm) 195.

Compound (109)

HR ESIMS MNa^+ 433.1849 ($C_{21}H_{30}O_8Na$ requires 433.1838). ^1H NMR ($CDCl_3$) δ 5.77 (d, J_{HH} = 5.5 Hz, 1H, H10), 5.28 (d, J_{HH} = 5.5 Hz, 1H, H8), 4.49 (d, J_{HH} = 2.5 Hz, 1H, H4), 4.34 (d, J_{HH} = 13 Hz, 1H, H15α), 4.24 (d, J_{HH} = 5.5 Hz, 2H, H3 H11), 4.01 (d, J_{HH} = 12.5 Hz, 1H, H15β), 3.63 (d, J_{HH} = 5 Hz, 1H, H2), 3.03 (d, J_{HH} = 4 Hz, 1H, H13α), 2.77 (d, J_{HH} = 4 Hz, 1H, H13β), 2.49 (m, J_{HH} = 7 Hz, 1H, H18), 2.40 (dd, J_{HH} = 5.5, 14.5 Hz, 1H, H7β), 2.05 (s, 3H, 22Me), 1.90, (d, J_{HH} = 15.5 Hz, 1H, H7α), 1.74, (s, 3H, 16Me), 1.18, (d, J_{HH} = 7 Hz, 3H, 19Me), 1.17, (d, J_{HH} = 7 Hz, 3H, 20Me), 0.80 (s, 3H, 14Me). UV (MeOH, nm) 195.

8.3 Experimental for Chapter 4

8.3.1 Chromatography of Wai 7-1-1

The crude extract was adsorbed to C_{18} (2 g) and initially fractionated with reverse phase (C_{18}) column chromatography. The extract was eluted using a modified version of the C_{18} elution profile (Section 8.1.7) with nineteen fractions collected. The first thirteen

fractions were eluted with the same profile as that described in Section 8.1.7, but this did not recover a large majority of the crude extract from the column. The remainder of the extract was recovered by washing the column with 100 % MeOH, 50 % DCM/MeOH and 100 % DCM containing 0.05 % TFA (200 mL) followed by 100 % DCM, 50 % DCM/MeOH, 100 % MeOH containing 0.1 % NH_3 (200 mL). All fractions were assayed against the P388 cell line and examined by analytical reverse phase (C_{18}) HPLC. Cytotoxicity was only observed in the fractions eluting at 80 and 90 % MeOH/H_2O (RKP 1.95.6-7) and the HPLC trace of these two fractions indicated the presence of the bioactive peak eluting at 17.5 minutes as determined in preliminary investigations (Section 4.2.1.2). These two fractions were subsequently combined, adsorbed to DIOL (1 g) and further purified on a normal phase (DIOL) column (12 g, 1.2 x 60 cm). The combined fractions were eluted using a modified version of the DIOL elution profile (Section 8.1.7) with sixteen fractions collected. The first 10 fractions were eluted with the same profile as that described in Section 8.1.7 with the remaining six fractions eluted as follows: 20 %, 40 %, 60 %, 80 %, 100 % MeOH/EtOAc (15 mL) and 100 % MeOH with 0.05 % TFA (35 mL). The first twelve fractions all possessed some cytotoxicity with the major region of activity occurring from fraction two to eight (RKP 1.115.2-8). Analysis of these seven fractions by ^1H NMR spectroscopy indicated that they all contained the same major compound, but still contained contaminants. These seven fractions were subsequently combined, loaded onto a small Sephadex LH20 column (1 g, 0.5 x7.5 cm) and eluted with 100 % MeOH. Six fractions (1 mL) were collected and NMR analysis showed that fractions four and five (RKP 1.169.4-5) were pure compounds identical to cephalochromin (**116**).

8.3.2 Chromatography of Fox 35-2-5

The EtOAc extract was taken to dryness under vacuum and redissolved in MeOH (50 mg/mL). An aliquot (200 µL) was loaded onto a Sephadex LH20 column (1 g, 0.5 x 7.5 cm) equilibrated to 100 % MeOH and eluted with 100 % MeOH collecting six fractions (1 mL). To obtain enough sample mass this was repeated five times. Examination by ^1H NMR spectroscopy located cephalochromin (**116**) in the fourth and fifth fractions (RKP 1.186.4-5).

Compound (116)

HR ESIMS MH^+ 519.1297 ($C_{28}H_{23}O_{10}$ requires 519.1291). ^1H NMR (DMSO-d_6) δ 15.1(s, 2H, 5 OH), 10.1 (s, 2H, 6OH), 9.9 (s, 2H, 8OH), 6.52 (s, 2H, H7), 5.72 (s, 2H, H10), 4.55 (ddq, J_{HH} = 3, 6, 12.5 Hz, 2H, H2), 2.93 (dd, J_{HH} = 12.5, 17.5 Hz, 2H, H3β), 2.74 (dd, J_{HH} = 3, 17.5 Hz, 2H, H3β), 1.37 (d, J_{HH} = 6 Hz, 6H, 11Me). ^{13}C NMR (DMSO-d_6) δ 198.2 (C4), 164.9 (C5), 160.1 (C8), 158.7 (C6), 155.0 (C10a), 141.6 (C9a), 107.2 (C9), 104.3 (C5a), 101.7 (C4a), 100.1 (C7), 98.6 (C10), 73.0 (C2), 42.8 (C3), 20.6 (C11). UV (MeOH, nm) 234, 272, 294, 328, 422. CD (MeOH 0.01 mg/mL) 294 nm (θ 45 x 10^4), 266 nm (θ -35 x 10^4).

8.4 Experimental for Chapter 5

8.4.1 Chromatography of Gil 12-1-3

The large scale EtOAc extract of Gil 12-1-3 was adsorbed to C_{18} (2 g), loaded on a reverse phase (C_{18}) column (50 g, 3 x 60 cm) equilibrated to 10 % MeOH/H_2O and eluted using the standard C_{18} elution profile (Section 8.1.7). Thirteen fractions were collected, assayed for cytotoxicity and examined by analytical reverse phase C_{18} HPLC. The cytotoxic fractions (RKP 1.93.4-5) eluted between 40 and 60 % MeOH/H_2O and showed the bioactive peak eluting at 8.5 minutes in the HPLC trace. Thus they were combined. The combined fractions were adsorbed to DIOL (1 g) and further purified with normal phase (DIOL) column chromatography (12 g, 1.2 x 60 cm) using the standard DIOL elution profile (Section 8.1.7). Eleven fractions were collected, assayed for cytotoxicity and examined by reverse phase HPLC. Based on cytotoxicity and HPLC the fractions that eluted between 80 % EtOAc/DCM and 5 % MeOH/EtOAc (RKP 1.125.7-9) were combined. A ^1H NMR spectrum of the combined fractions showed the presence of phthalate plasticizers which were removed with another chromatographic step on a small scale normal phase (DIOL) column (1 g, 0.5 x7.5 cm) equilibrated to 100 % DCM (column C). The sample was eluted from this column with 100 % DCM (3 x 1 mL), 100% EtOAc (3 x 1 mL) and 100% MeOH (3 x 1 mL) collecting any coloured bands as they eluted. An intense yellow band (RKP 1.171.3)

eluted in EtOAc and was subsequently identified with 2D NMR experiments and mass spectrometry as a novel altersolanol (**141**).

Chromatography of the side fractions

Before an identification had been made it was believed that more of **141** would be required for an identification thus all cytotoxic side fractions from the first round of chromatography were combined, adsorbed to DIOL (1 g) and purified on a normal phase (DIOL) column (12 g, 1.2 x 60 cm) equilibrated to 100 % DCM. The side fractions were eluted with the standard DIOL elution profile collecting eleven fractions which were examined by HPLC only. Three yellow fractions which showed the bioactive peak eluting at 8.5 minutes in the HPLC trace were combined with the bioactive chemical screening fractions of the small scale extract and purified on normal phase DIOL (12 g, 1.2 x 60 cm) equilibrated to 100 % DCM (column E). The combined fractions were eluted with 100 % DCM (100 mL), 100 % EtOAc (100 mL) and 100 % MeOH (100 mL). Bands of colour were collected as they eluted, then examined by HPLC and the fractions containing the bioactive peak (RKP 2.229.2-3) were further purified on another small scale normal phase (DIOL) column (1 g, 0.5 x7.5 cm) with the same elution profile used for column C. Nine fractions were collected and examined by NMR spectroscopy which showed that RKP 2.234.6 was the only fraction containing **141** and as such this fraction was combined with the earlier fraction RKP 1.171.3 to give RKP 2.257.1.

After combining the fractions a number of new signals were observed in the ^{1}H NMR spectrum, thus the combined sample (RKP 2.257.1) was subjected to a final purification step on analytical reverse phase (C_{18}) HPLC. RKP 2.257.1 was purified using the same gradient solvent system that was used for the microtitre plate screen (Section 8.1.6) and collecting the bioactive peak (8.5 minutes) as it eluted.

Compound (141)

HR ESIMS MNa^+ 359.0743 ($C_{16}H_{16}O_8Na$ requires 359.0743). ^{1}H NMR (CD_3OD) δ 7.15 (d, J_{HH} = 2.5 Hz, 1H, H8), 6.74 (d, J_{HH} = 2.5 Hz, 1H, H6), 4.73 (d, J_{HH} = 7 Hz, 1H, H4), 4.51 (s, 1H, H1), 3.91 (s, 3H, *O*Me7), 3.84 (d, J_{HH} = 7 Hz, 1H, H3), 1.42 (s, 1H, 2Me). ^{1}H NMR (DMSO-d_6) δ 12.12 (s, 1H, 5OH), 7.12 (d, J_{HH} = 2 Hz, 1H, H8), 6.94 (d, J_{HH} = 2 Hz, 1H, H6), 5.79 (d, J_{HH} = 6 Hz, 1H, 1OH), 5.14 (d, J_{HH} = 6 Hz, 1H, 4OH),

5.00 (d, J_{HH} = 7 Hz, 1H, 3OH), 4.58 (t, J_{HH} = 6.5, 7 Hz, 1H, H4), 4.56 (s, 1H, 2OH), 4.42 (d, J_{HH} = 6 Hz, 1H, H1), 4.01 (s, 3H, 7*O*Me), 3.73 (t, J_{HH} = 6.5, 7 Hz, 1H, H3), 1.34 (s, 3H, 2Me). UV (MeOH, nm) 220, 268, 434.

8.5 Experimental for Chapter 6

8.5.1 Chromatography of the first Fox 21-2-6a extract

The first extract of Fox 21-2-6a was adsorbed to C_{18} (2 g) and fractionated on a reverse phase (C_{18}) column (50 g, 3 x 60 cm) equilibrated to 10 % MeOH/H_2O. The extract was eluted from the C_{18} column using the standard elution profile (Section 8.1.7) with a total of fourteen fractions collected. The fourteenth fraction eluted with 100 % MeOH containing 0.05 % TFA. Fractions eight to eleven (RKP 1.57.8-11) showed peaks that eluted between 10 and 12 minutes and had previously been shown to be bioactive. These fractions were also the only ones to possess cytotoxicity. Based on the cytotoxicity and HPLC traces fractions eight and nine (RKP 1.57.8-9) were combined as were fractions ten and eleven (RKP 1.57.10-11).

The first combined fraction (RKP 1.57.8-9) was fractionated on a normal phase (DIOL) column (12 g, 1.2 x60 cm) and eluted with the standard DIOL elution profile (Section 8.1.7). Eleven fractions were collected from this column, but none showed cytotoxicity and thus these fractions were not examined further.

The second combined fraction (RKP 1.57.10-11) was also purified on a normal phase (DIOL) column with the standard elution profile and again, eleven fractions were collected. Cytotoxicity was observed in all but the first fraction and analytical reverse phase (C_{18}) HPLC showed that the fractions contained the appropriate peaks responsible for the cytotoxicity. Based on HPLC traces and cytotoxicity data fractions two to nine (RKP 1.124.2-9) were combined. The combined fractions (RKP 1.124.2-9), fraction one (RKP 1.124.1) and fraction eleven (RKP 1.124.11) were chromatographed on three separate Sephadex LH20 (20 g, 1.2 x 60 cm) columns. The three LH20 columns were all eluted with 100 % MeOH collecting bands of colour as they eluted. Five fractions were collected from each LH20 column with colour observed in the second and fourth fractions of each column. However, only one fraction (RKP 2.245.2) possessed any

significant cytotoxicity, but the mass was too low for this fraction to be examined further.

8.5.2 Chromatography of the second Fox 21-2-6a extract

The second crude extract of Fox 21-2-6a was adsorbed to C_{18} (5 g) and fractionated on a reverse phase (C_{18}) column (50 g, 3 x 60 cm) conditioned to 10 % MeOH/H_2O. The extract was eluted from the column using the standard elution profile developed for C_{18}, but the final two fractions also contained 0.05 % TFA. Based on the chromatographic steps used for the first extract of Fox 21-2-6a the fractions were combined as follows: Fractions one to seven (RKP 2.267.1-7), fractions eight to eleven (RKP 2.267.8-11) and fractions twelve and thirteen (RKP 2.267.12-13). A very high level of cytotoxicity was seen in the second (RKP 2.267.8-11) and third (RKP 2.267.12-13) set of combined fractions from the C_{18} column, but no cytotoxicity was observed in the first set of fractions (RKP 2.267.1-7).

RKP 2.267.12-13

This combined fraction was adsorbed to DIOL (5 g), loaded onto a normal phase (DIOL) column (40 g, 1.2 x 60 cm) equilibrated to 100 % Pet. Ether and eluted with the following gradient solvent system: 100 % PE, 20 %, 40 %, 60 %, 80 %, 90 %, 100 % DCM/PE, 20 %, 40 %, 60 %, 80 %, 90 %, 100 % EtOAc/DCM, 20 %, 50 %, 100 %, MeOH/EtOAc (70 mL). Of the sixteen fractions collected fractions six to sixteen (RKP 2.270.6-16) all contained cytotoxic components.

Analysis of the first five cytotoxic fractions (RKP 2.270.6-10) with ^1H NMR spectroscopy showed a very high level of fatty acids which were unable to be removed from the fractions thereby preventing further purification of these fractions.

Analytical reverse phase (C_{18}) HPLC analysis of fractions eleven to fourteen (RKP 2.270.11-14) showed a single common component eluting at 11.5 minutes and as such these four fractions were combined. NMR spectroscopy of this combined fraction highlighted the presence of fatty acids which were removed by taking the fraction to dryness under vacuum and washing twice with 100 % Pet. Ether (2 mL). The remaining

MeOH soluble residue was combined with a fraction (RKP 2.307.8-15) from another column.

Analytical HPLC and NMR spectroscopy indicated that the last two fractions (RKP 2.270.15-16) from this column contained common components which were also shown to be identical to those seen in fractions from a later DIOL column (RKP 2.307.18-28) and as such all these fractions were combined.

RKP 2.267.8-11

This combined fraction was adsorbed to DIOL (5 g), loaded onto a normal phase (DIOL) column (40 g, 1.2 x 60 cm) equilibrated to 100 % Pet. Ether and eluted with the following gradient solvent system: 100 % Pet. Ether (100 mL), 10 %, 20 %, 40 %, 60 %, 80 %, 100 % DCM/Pet. Ether, 10 %, 20 %, 40 %, 60 %, 80 %, 100 % EtOAc/DCM, 10 %, 20 %, 40 %, 60 %, 80 % MeOH/EtOAc (70 mL). Of the twenty fractions collected cytotoxicity was observed in fraction nine (RKP 2.274.9) onwards.

Reverse phase HPLC analysis of fractions ten to thirteen (RKP 2.274.10-13) showed a single common component eluting at 13.5 minutes thus these four fractions were combined. Fractions fourteen and fifteen (RKP 2.274.14-15) also showed a common component eluting at 13.5 minutes in the HPLC trace, but were combined with a fraction from a later column (RKP 2.309.2-3). The last four cytotoxic fractions from this column (RKP 2.274.16-20) all showed a similar series of peaks eluting between 9 and 15 minutes in the HPLC and as such were combined.

RKP 2.274.10-13

This combined fraction was adsorbed to DIOL (100 mg), loaded onto a small normal phase (DIOL) column (1 g, 0.5 x 7.5 cm) equilibrated to 100 % Pet. Ether and eluted with the following gradient solvent system: 100 % DCM (2 x 1.6 mL), 100 % MeOH (3 x 1.6 mL). Five fractions were collected and examined by analytical reverse phase (C_{18}) HPLC and ^{1}H NMR spectroscopy. Fractions two (RKP 2.303.2) and four (RKP 2.303.4) were both intensely coloured, but HPLC and NMR spectroscopy of fraction two indicated a large mass of fatty acids present. HPLC and NMR analysis of the fourth fraction (RKP 2.303.4) indicated the presence of two compounds and thus this fraction was further purified on another small normal phase (DIOL) column.

RKP 2.303.4

This fraction was adsorbed to DIOL (100 mg), loaded onto a small normal phase (DIOL) column (1 g, 0.5 x 7.5 cm) equilibrated to 100 % DCM and eluted with the following gradient solvent system: 100 % DCM (7.2 mL), 100 % EtOAc (2.4 mL) 20 % MeOH/EtOAc (1.6 mL), 50 % MeOH/EtOAc (3.2 mL). Five fractions were collected and analysed by analytical reverse phase (C_{18}) HPLC and ^{1}H NMR spectroscopy. Fractions two (RKP 2.309.2) and four (RKP 2.309.4) were both intensely coloured and HPLC and NMR analysis of both fractions showed a high level of purity. The second fraction (RKP 2.309.2) was combined with fractions (RKP 2.274.14-15) from an earlier column, taken to dryness under vacuum and washed with 10 mL Pet. Ether to remove any residual fatty acids. The MeOH soluble residue (RKP 2.348.2) was identified by NMR spectroscopy and mass spectrometry as 1-hydroxyaclacinomycin T (**155**).

The fourth fraction (RKP 2.309.4) was combined with fractions from two other chromatographic sequences (RKP 2.270.11-14 and RKP 2.307.8-15).

RKP 2.274.16-20

The last of the fractions from the DIOL column of RKP 2.267.8-11 (RKP 2.274.16-20) were taken to dryness under vacuum and washed with 100 % Pet. Ether. The MeOH soluble residue was adsorbed to DIOL (0.5 g) and loaded onto a normal phase (DIOL) column (20 g, 0.5 x 100 cm) equilibrated to 10 % MeOH/EtOAc and eluted with the following gradient solvent system: 10 - 25 % MeOH/EtOAc (18 mL) in 1 % increments, 25 - 50 % MeOH/EtOAc (18 mL) in 5 % increments, 100 % MeOH (5 x 18 mL). Twenty eight fractions were collected, analysed by analytical reverse phase HPLC and examined with ^{1}H NMR spectroscopy. The gradient elution profile used for analytical HPLC of these twenty eight fractions is as follows: 2 minutes of 40 % ACN/H_2O; a linear gradient to 70 % ACN/H_2O for 8 minutes; isocratic at 75 % for 3 minutes; a linear gradient for 2 minutes to 100 % ACN followed by isocratic at 100 % ACN for 3 minutes then returned to 40 % ACN/H_2O in 1 minute and re-equilibrated for 4 minutes; with a flow rate 1 mL/min.

RKP 2.307.1-7

The first seven fractions (RKP 2.307.1-7) from this column contained a high level of fatty acids thus these fractions were not examined further.

RKP 2.307.8-15

The next eight fractions (RKP 2.307.8-15) showed a single common component eluting at 6.5 minutes and showed identical ^{1}H NMR spectra to RKP 2.309.4 and RKP 2.270.11-14 and as such these fractions were all combined. The combined fractions were taken to dryness under vacuum and washed with 100 % Pet. Ether to remove any residual fatty acids. The major component of this fraction was identified by 1D and 2D NMR spectroscopy and mass spectrometry as the novel pyrromycin derivative, 9-*epi*-pyrromycin (**154**).

RKP 2.307.18-28

Analytical HPLC analysis of the last eleven fractions showed a number of common components eluting between 4 and 7 minutes which were also seen in fractions from an earlier DIOL column (RKP 2.270.15-16) and as such these fractions were combined. The combined fractions were dissolved in a minimum volume of MeOH, loaded onto a Sephadex LH20 column (20 g, 1.2 x 60 cm) equilibrated to 100 % MeOH and eluted with 100 % MeOH. Fractions were collected based on colour, but only one band of colour was observed (RKP 2.320.2) eluting from this column

RKP 2.320.2

Analytical reverse phase C_{18} HPLC of RKP 2.320.2 indicated that there were at least five major components in this fraction all with the same UV spectra and all eluting within two minutes of each other. The final purification of this fraction was carried out on analytical reverse phase (C_{18}) HPLC. The fraction was eluted with an isocratic solvent system of 32 % ACN/H_2O and the individual components (compounds **154** and **156 - 159**) were collected as they eluted.

Compound (154)

HR ESIMS MH^+ 586.2297 ($C_{30}H_{36}NO_{11}$ requires 586.2288). ^{1}H NMR (CD_3OD) δ 7.51 (s, 1H, H11), 7.08 (s, 2H, H2 H3), 5.56 (d, J_{HH} = 2.5 Hz, 1H, H1'), 5.10 (d, J_{HH} = 5 Hz, 1H, H7), 4.26 (q, J_{HH} = 6.5, 13 Hz, 1H, H5'), 4.07 (s, 1H, H10), 3.96 (s, 1H, H4'), 3.75 (s, 3H, 14*O*Me), 3.52 (m, 1H, H3'), 2.87 (s, 6H, 7'*N*(Me)$_2$), 2.56 (dd, J_{HH} = 5, 15 Hz, 1H, H8ax), 2.28 (d, J_{HH} = 15 Hz, 2H, H8eq H2'ax), 2.08 (dt, J_{HH} = 4, 12.5 Hz, 1H, H2'eq), 1.76 (m, 1H, H15α), 1.56 (m, 1H, H15β), 1.33 (d, J_{HH} = 6 Hz, 3H, 6'Me), 1.11

(t, J_{HH} = 7 Hz, 3H, 16Me). ^{13}C NMR (CD_3OD) δ 191.6 (C5), 186.7 (C12), 172.8 (C13), 163.6 (C6), 159.4 (C1), 159.0 (C4), 144.1 (C10a), 133.8 (C11a), 133.1 (C6a), 131.5 (C3), 131.1 (C2), 121.2 (C11), 116.0 (C5a), 113.4 (C12a, C4a), 101.9 (C1'), 72.9 (C7), 72.2 (C9), 68.2 (C5'), 66.1 (C4'), 63.9 (C3'), 58.5 (C10), 53.5 (C14 *O*Me), 40.7 (*N*Me), 36.2 (C8), 33.6 (C15), 28.1 (C2'), 17.2 (C6'), 7.5 (C16). UV (MeOH, nm) 202, 234, 258, 290, 492. $[\alpha]_D$ = +128.0° (0.25 mg/mL, MeOH).

Compound (155)

HR ESIMS MH^+ 826.3280 ($C_{42}H_{52}NO_{16}$ requires 826.3286). ^{1}H NMR ($CDCl_3$) δ 7.70 (s, 1H, H11), 7.29 (s, 2H, H2 H3), 5.55 (br s, 1H, H1'), 5.26 (br s, 1H, H1''), 5.24 (br s, 1H, H7), 5.16 (d, J_{HH} = 3 Hz, 1H, H1'''), 4.81 (q, J_{HH} = 7 Hz, 1H, H5'), 4.53 (br s, 1H, H5''), 4.43 (br d, 1H, H3''), 4.34 (d, J_{HH} = 3.5 Hz, 1H, H2'''), 4.09 (s, 1H, H10), 4.06 (br s, 1H, H4''), 4.05 (br s, 1H, H5'''), 3.97 (br s, 1H, H4), 3.70 (s, 3H, 14*O*Me), 3.48 (br, 1H, H3'), 2.59 (br t, 1H, H8ax), 2.55 (d, J_{HH} = 4.5 Hz, 2H, H3'''), 2.50 (dd, J_{HH} = 4.5, 12.5, 1H, H2''eq), 2.35 (br s, 6H, 7'*N*(Me)$_2$), 2.30 (br t, 1H, H2'eq), 2.28 (br t, 2H, H8eq), 2.00 (dd, J_{HH} = 4.5, 12.5, 1H, H2''ax), 1.76 (m, 1H, H15α), 1.58 (br s, 1H, H2'ax), 1.52 (m, 1H, H15β), 1.33 (d, J_{HH} = 7 Hz, 6H, H6', H6'''), 1.21 (d, J_{HH} = 7 Hz, 3H, H6''), 1.09 (t, J_{HH} = 7.5 Hz, 3H, 16Me). ^{13}C NMR ($CDCl_3$) δ 208.0 (C4'''), 190.4 (C5), 185.7 (C12), 171.0 (C13), 162.1 (C6), 158.5 (C4), 157.9 (C1), 142.2 (C10a), 133.0 (C11a), 130.7 (C6a), 130.2 (C3), 129.9 (C2), 120.2 (C11), 114.9 (C5a), 112.4 (C12a), 112.2 (C4a), 101.2 (C1'), 99.1 (C1''), 91.5 (C1'''), 77.9 (C5'), 72.5 (C4'), 71.7 (C9), 71.1 (C7), 67.6 (C5'''), 66.2 (C3'', C4''), 65.8 (C5''), 62.8 (C2'''), 56.8 (C10), 52.5 (C14 *O*Me), 50.7 (C3'), 41.1 (C7' *N*(Me)$_2$), 39.5 (C3'''), 33.9 (C8), 33.8 (C2'), 31.8 (C15), 26.3 (C2''), 18.0 (C6'), 15.9 (C6'''), 15.8 (C6''), 6.7 (C16). UV (MeOH, nm) 202, 234, 258, 290, 492.

Compound (156)

HR ESIMS MH^+ 572.2126 ($C_{29}H_{34}NO_{11}$ requires 572.2132). ^{1}H NMR (CD_3OD) δ 7.71 (s, 1H, H11), 7.38 (s, 2H, H2 H3), 5.51 (d, J_{HH} = 3 Hz, 1H, H1'), 5.14 (d, J_{HH} = 4.5 Hz, 1H, H7), 4.24 (q, J_{HH} = 7, 13.5 Hz, 1H, H5'), 4.10 (s, 1H, H10), 3.92 (s, 1H, H4'), 3.68 (s, 3H, 14*O*Me), 3.52 (m, 1H, H3'), 2.60 (s, 3H, 7'*N*Me), 2.49 (dd, J_{HH} = 5.5, 15 Hz, 1H, H8ax), 2.31 (m, 2H, H8eq, H2'ax), 1.90 (m 1H, H2'eq), 1.76 (m, 1H, H15α), 1.54 (m,

1H, H15β), 1.29 (d, J_{HH} = 6.5 Hz, 3H, 6'Me), 1.08 (t, J_{HH} = 7 Hz, 3H, 16Me). UV (MeOH, nm) 202, 234, 258, 290, 492.

Compound (157)

HR ESIMS MH^+ 586.2290 ($C_{30}H_{36}NO_{11}$ requires 586.2288). ^1H NMR (CD_3OD) δ 7.60 (s, 1H, H11), 7.38 (s, 2H, H2 H3), 5.58 (br s, 1H, H1'), 4.96 (t, J_{HH} = 2.5 Hz, 1H, H7), 4.17 (q, J_{HH} = 7, 12.5 Hz, 1H, H5'), 3.99 (s, 1H, H10), 3.95 (br s, 1H, H4'), 3.78 (s, 3H, 14*O*Me), 3.52 (br d, J_{HH} = 11 Hz, 1H, H3'), 2.91 (s, 3H, 7'*N*Me), 2.85 (s, 3H, 7'*N*Me), 2.62 (dd, J_{HH} = 7.5, 14 Hz, 1H, H8ax), 2.32 (dd, J_{HH} = 8, 14 Hz, 1H, H8eq), 2.29 (dd, J_{HH} = 8, 14 Hz, 1H, H2'ax), 2.06 (br s, 1H, H2'eq), 1.49 (m, 2H, H15), 1.33 (d, J_{HH} = 6 Hz, 3H, 6'Me), 0.98 (t, J_{HH} = 7 Hz, 3H, 16Me). UV (MeOH, nm) 202, 234, 258, 290, 492. $[\alpha]_D$ = +224.0° (0.125 mg/mL, MeOH).

Compound (158)

HR ESIMS MH^+ 572.2138 ($C_{29}H_{34}NO_{11}$ requires 572.2132). ^1H NMR (CD_3OD) δ 7.67 (s, 1H, H11), 7.37 (s, 2H, H2 H3), 5.56 (br s, 1H, H1'), 5.13 (d, J_{HH} = 5 Hz, 1H, H7), 4.24 (q, J_{HH} = 7.5, 14 Hz, 1H, H5'), 4.09 (s, 1H, H10), 3.91 (br s, 1H, H4'), 3.71 (s, 3H, 14*O*Me), 3.46 (br d, J_{HH} = 11.5 Hz, 1H, H3'), 2.88 (br s, 3H, 7'*N*Me), 2.78 (br s, 3H, 7'*N*Me), 2.58 (dd, J_{HH} = 6, 15 Hz, 1H, H8ax), 2.20 (d, J_{HH} = 15 Hz, 1H, H8eq), 2.15 (m, 1H, H2'ax), 2.02 (dt, J_{HH} = 3.5, 12.5 Hz, 1H, H2'eq), 1.38 (s, 3H, 16Me), 1.31 (d, J_{HH} = 6.5 Hz, 3H, 6'Me). UV (MeOH, nm) 202, 234, 258, 290, 492.

Compound (159)

HR ESIMS MH^+ 614.2237 ($C_{31}H_{36}NO_{12}$ requires 614.2238). ^1H NMR (CD_3OD) δ 7.71 (s, 1H, H11), 7.36 (s, 2H, H2 H3), 5.49 (br s, 1H, H1'), 5.10 (br s, 1H, H7), 4.26 (q, J_{HH} = 7, 13 Hz, 1H, H5'), 4.24 (s, 1H, H10), 3.93 (br s, 1H, H4'), 3.71 (s, 3H, 14*O*Me), 3.46 (br d, J_{HH} = 11.5, 1H, H3'), 3.04 (d, J_{HH} = 16.5 Hz, 1H, H15α), 2.88 (br s, 3H, 7'*N*Me), 2.77 (br s, 3H, 7'*N*Me), 2.66 (d, J_{HH} = 16.5 Hz, 1H, H15β), 2.53 (br s, 2H, H8), 2.25 (s, 3H, 17Me), 2.15 (m, 1H, H2'ax), 2.03 (m, 1H, H2'eq), 1.32 (d, J_{HH} = 6.5 Hz, 3H, 6'Me). UV (MeOH, nm) 202, 234, 258, 290, 492.

8.6 Experimental for Chapter 7

8.6.1 Chromatography of Kai 11-2-1

The crude large scale extract was adsorbed to C_{18} (2 g) and purified with reverse phase (C_{18}) column chromatography and eluted with the standard C_{18} elution profile (Section 8.1.7) collecting thirteen fractions. Cytotoxicity was observed in almost all fractions from the third fraction to the last fraction, but was concentrated in fractions seven and eight (RKP 1.46.7-8). Based on cytotoxicity and analytical reverse phase C_{18} HPLC fractions seven and eight were combined then further purified with normal phase (DIOL) chromatography (12g, 1.2 x 60 cm). The combined fraction (RKP 1.46.7-8) was eluted using the standard column elution profile described in Section 8.1.7, but the first fraction was split into two as an intensely coloured band eluted within this fraction. The second fraction (RKP 1.109.2) was identified by ^{1}H NMR spectroscopy and MS as actinomycin V (X_2) (**177**) and the fourth fraction was identified as actinomycin X_0 (**178**) from mass spectrometry.

Compound (177)

HR ESIMS MH^+ 1269.6134 ($C_{62}H_{85}N_{12}O_{17}$ requires 1269.6156). ^{1}H NMR ($CDCl_3$) 8.19 (d, J_{HH} = 6 Hz, 1H, β Val NH), 7.67 (d, J_{HH} = 6 Hz, 1H, β Thr NH), 7.65 (d, J_{HH} = 5.5 Hz, 1H, α Val NH), 7.60 (d, J_{HH} = 7.5 Hz, 1H, H8), 7.35 (d, J_{HH} = 8 Hz, 1H, H7), 7.19 (d, J_{HH} = 7.5 Hz, 1H, α Thr NH), 6.55 (d, J_{HH} = 1, 10 Hz, 1H, β Pro H2), 5.95 (d, J_{HH} = 1, 9 Hz, 1H, α Pro H2), 5.22 (dd, J_{HH} = 2.5, 6 Hz, 1H, β Thr H3), 5.14 (dd, J_{HH} = 2.5, 6 Hz, 1H, α Thr H3), 4.70 (d, J_{HH} = 17.5 Hz, 1H, α Sar H2α), 4.58 (d, J_{HH} = 17.5 Hz, 1H, β Sar H2α), 4.55 (d, J_{HH} = 19 Hz, 1H, β Pro H5α), 4.55 (dd, J_{HH} = 2.5, 5.5 Hz, 1H, α Thr H2), 4.47 (dd, J_{HH} = 2, 5.5 Hz, 1H, β Thr H2), 3.96 (m, J_{HH} = 19 Hz, 1H, β Pro H5β), 3.88 (m, J_{HH} = 6.5, 10.5, 11 Hz, 1H, α Pro H5β), 3.84 (dd, J_{HH} = 11, 18 Hz, 1H, β Pro H3α), 3.71 (m, J_{HH} = 1, 9, 11 Hz, 1H, α Pro H5α), 3.69 (q, J_{HH} = 6.5, 10 Hz, 1H, β Val H2), 3.63 (d, J_{HH} = 17 Hz, 1H, α Sar H2β, β Sar H2β), 3.56 (q, J_{HH} = 6, 9.5 Hz, 1H, α Val H2), 2.93 (s, 3H, β Val *N*Me), 2.92 (s, 3H, α Val *N*Me), 2.88 (s, 3H, β Sar *N*Me), 2.87 (s, 3H, α Sar *N*Me), 2.74 (m, 1H, α Pro H3α), 2.69 (m, J_{HH} = 6, 6 Hz, 2H, β *N*Me Val H2, β *N*Me Val H3), 2.64 (m, J_{HH} = 5.5, 6 Hz, 2H, α *N*Me Val H2, α

*N*Me Val H3), 2.54 (s, 3H, H12), 2.30 (d, J_{HH} = 1, 18 Hz, 1H, β Pro H3β), 2.27 (m, 1H, α Pro H4α), 2.21 (s, 3H, H11), 2.21 (m, J_{HH} = 7, 7.5, 10 Hz, 1H, β Val H3), 2.11 (m, J_{HH} = 7, 7, 9.5 Hz, 1H, α Val H3), 2.07 (m, 1H, α Pro H4β), 1.83 (m, J_{HH} = 1, 7, 12 Hz, 1H, α Pro H3β), 1.24 (d, J_{HH} = 6.5 Hz, 3H, β Thr H3), 1.14 (d, J_{HH} = 7 Hz, 3H, β Val H4), 1.13 (d, J_{HH} = 6 Hz, 3H, α Thr H3), 1.11 (d, J_{HH} = 7 Hz, 3H, α Val H4), 0.97 (d, J_{HH} = 6 Hz, 3H, β Val H4), 0.93 (d, J_{HH} = 6 Hz, 3H, α Val H4), 0.90 (d, J_{HH} = 7.5 Hz, 3H, α Val H3), 0.89 (d, J_{HH} = 7 Hz, 3H, β Val H3), 0.74 (d, J_{HH} = 5.5 Hz, 3H, β Val H5), 0.73 (d, J_{HH} = 5.5 Hz, 3H, α Val H5). ^{13}C NMR ($CDCl_3$) 208.8 (β Pro C4), 179.0 (C3), 174.0 (β Val C1), 173.5 (α Val C1), 173.1 (α Pro C1), 172.7 (β Pro C1), 168.9 (β Thr C1), 168.7 (α Thr C1), 167.5 (α *N*Me Val C1, β *N*Me Val C1), 166.5 (C14), 166.3 (α Sar C1), 166.0 (C13), 165.9 (β Sar C1), 147.6 (C2), 145.9 (C10a), 145.0 (C4a), 140.5 (C5a), 132.1 (C9), 130.3 (C7), 129.1 (C9a), 127.8 (C6), 126.2 (C8), 113.5 (C4), 101.7 (C1), 74.7 (α Thr C3), 74.6 (β Thr C3), 71.4 (β *N*Me Val C2), 71.2 (α *N*Me Val C2), 58.5 (α Val C2), 57.1 (β Val C2), 56.4 (α Pro C2), 54.9 (β Thr C2), 54.7 (α Thr C2), 54.2 (β Pro C2), 52.8 (β Pro C5), 51.3 (α Sar C2, β Sar C2), 47.4 (α Pro C5), 41.9 (β Pro C3), 39.4 (β *N*Me Val *N*CH_3), 39.2 (α *N*Me Val *N*CH_3), 34.9 (α Sar *N*CH_3), 34.7 (β Sar *N*CH_3), 31.8 (β Val C3), 31.7 (α Val C3), 31.0 (α Pro C3), 26.9 (β *N*Me Val C3), 26.8 (α *N*Me Val C3), 22.9 (α Pro C4), 21.7 (β *N*Me Val C4), 21.5 (α *N*Me Val C4), 19.2 (α Val C4), 19.1 (β Val C4, β *N*Me Val C5), 19.0 (α *N*Me Val C5), 18.9 (α Val C5), 18.8 (β Val C5), 17.7 (β Thr C4), 17.1 (α Thr C4), 15.0 (C12), 7.7 (C11). UV (MeOH, nm) 200, 240, 427, 442.

8.6.2 Chromatography of Kai 40-1-1 and 84

These two extracts underwent identical purification steps. Powdered extracts (5 g) of these two micro-organisms were re-suspended in distilled water (100 mL) then adsorbed to reverse phase C_{18} (50 g) and fractionated by vacuum liquid chromatography (VLC). The extracts were eluted with 100 % H_2O (200 mL), 100 % MeOH (100 mL) and 100 % DCM (100 mL) collecting three fractions. Significant cytotoxicity was only seen in the second fractions (RKP 1.3.3 and RKP 1.3.4) of both extracts. These fractions were adsorbed to C_{18} (2 g) and loaded onto reverse phase C_{18} columns (50 g, 3 x 60 cm)

equilibrated to 10 % MeOH/H_2O (column B). Column B was eluted with the standard C_{18} elution profile (Section 8.1.7) with thirteen fractions collected, assayed for cytotoxicity and examined by HPLC. Both extracts showed cytotoxicity from the fifth fraction onwards, but this cytotoxicity was concentrated in fractions seven and eight (RKP 1.44.7-8 and RKP 1.51.7-8 respectively). These fractions were subsequently combined and further purified on normal phase (DIOL) columns (10 g, 1.2 x 60 cm) equilibrated to 100 % DCM. Both combined fractions were eluted with 100 % DCM (30 mL), 100 % EtOAc (30 mL) and 100 % MeOH (30 mL) collecting bands of colour as they eluted. The major principle in both of the second fractions (RKP 2.212.5 and RKP 2.212.2) was identified by ^{1}H NMR spectroscopy and MS as actinomycin D (**179**).

REFERENCES

1. Gibson, D.M. and S.B. Krasnoff, *Exploring the Potential of Biologically Active Compounds from Plants and Fungi*, in *Biologically Active Natural Products: Agrochemicals*, H.G. Cutler and S.J. Cutler, Editors. 1999, CRC Press: Boca Raton, Florida.
2. Potier, P., *Search and Discovery of New Antitumour Compounds.* Chemical Society Reviews, 1992: p. 113-119.
3. Hawksworth, D.L., *The Fungal Dimension of Biodiversity: Magnitude, Significance and Conservation.* Mycological Research, 1991. **95**: p. 641-655.
4. Coll, J.C., S.L. Barre, P.W. Sammarco, W.T. Williams, and G.J. Bakus, *Chemical Defences in Soft Corals (Coelenterata: Octocorallia) of the Great Barrier Reef: A Study of Comparative Toxicities.* Marine Ecology - Progress Series, 1982. **8**: p. 271-278.
5. Assmann, M., R.W.M. van Soest, and M. Kock, *New Antifeedant Bromopyrrole Alkaloid from the Caribbean Sponge Stylissa caribica.* Journal of Natural Products, 2001. **64**(10): p. 1345-1347.
6. Dreyfus, M., E. Harri, H. Hofmann, H. Kobel, W. Pache, and H. Tscherter, *Cyclosporin A and C, New Metabolites from Trichoderma polysporum (Link et Pers.) Rifai.* European Journal of Applied Microbiology, 1976. **3**: p. 125-133.
7. Pearce, C., *Biologically Active Fungal Metabolites.* Advances in Applied Microbiology, 1997. **44**: p. 1-80.
8. Endo, A., M. Kuroda, and Y. Tsujita, *ML-236A, ML-236B, and ML-236C, New Inhibitors of Cholesterogenesis Produced by Penicillium citrinum.* The Journal of Antibiotics, 1976. **29**: p. 1346-1348.
9. Newman, D.J. and S.A. Laird, *The Influence of Natural Products on 1997 Pharmaceutical Sales Figures*, in *The Commercial Use of Biodiversity*, K. ten Kate and S.A. Laird, Editors. 1999, Earthscan Publications: London. p. 333-335.
10. Pearce, C., *Discovering Novel Bioactive Compounds from Fungi*, in *Natural Products: Rapid Utilisation of Sources for Drug Discovery and Development*, N. Mulford and C. Sussman, Editors. 1995, IBC Biomedical Library:

Southborough, Massachusetts. p. 1.72-1.94.

11. Wu, J.C., *Mycophenolate Mofetil: Molecular Mechanisms of Action.* Perspectives in Drug Discovery and Design, 1994. **2**: p. 185-204.
12. Sayed, K.A.E., D.C. Dunbar, P. Bartyzel, J.K. Zjawiony, W. Day, and M.T. Hamann, *Marine Natural Products as Leads to Develop New Drugs and Insecticides*, in *Biologically Active Natural Products: Pharmaceuticals*, S.J. Cutler and H.G. Cutler, Editors. 2000, CRC Press: Boca Raton. p. 233-252.
13. Faulkner, D.J., *Marine Natural Products Chemistry: Introduction.* Chemical Reviews, 1993. **93**(5): p. 1671-1672.
14. Cafieri, F., E. Tattorusso, A. Mangoni, O. Taglialatela-Scafati, and R. Carnuccio, *A Novel Bromopyrrole Alkaloid from the Sponge Agelas longissima with Antiserotonergic Activity.* Bioorganic and Medicinal Chemistry Letters, 1995. **5**: p. 799-804.
15. Urban, S., S.J.H. Hickford, J.W. Blunt, and M.H.G. Munro, *Bioactive Marine Alkaloids.* Current Organic Chemistry, 2000. **4**(7): p. 765-807.
16. Blunt, J.W. and M.H.G. Munro, *Marinlit: A Database of the Literature on Marine Natural Products.* 2001, University of Canterbury.
17. Fusetani, N., S. Matsunaga, T. Yamashita, and S. Tsukamoto, *Bistellettadines A and B: Two Bioactive Dimeric Stellettadines from a Marine Sponge Stelletta sp.* The Journal of Organic Chemistry, 1999. **64**(11): p. 3794-3795.
18. Glombitza, K.W. and B. Sailler, *Phlorethols and Fucophlorethols from the Brown Alga Cystophora retroflexa.* Phytochemistry, 1999. **50**: p. 869-881.
19. Mayer, A.M.S. and V.K.B. Lehmann, *Marine Pharmacology in 1999: Antitumor and Cytotoxic Compounds.* Anticancer Research, 2001. **21**: p. 2489-2500.
20. Fusetani, N., *Drugs from the Sea.* 2000, Basel: Karger.
21. McKee, T.C., D.L. Galinis, L.K. Pannell, J.H. Cardellina II, J. Laakso, C.M. Ireland, L. Murray, R.J. Capon, and M.R. Boyd, *The Lobatamides, Novel Cytotoxic Macrolides from Southwestern Pacific Tunicates.* The Journal of Organic Chemistry, 1998. **63**(22): p. 7805-7810.
22. Rodriguez, A.D., E. Gonzalez, and S.D. Huang, *Unusual Terpenes with Novel Carbon Skeletons from the West Indian Sea Whip Pseudopterogorgia elisabethae (Octocorallia).* The Journal of Organic Chemistry, 1998. **63**(20): p. 7083-7091.
23. Bassett, S., S.P.B. Overden, R.W. Gable, and R.J. Capon, *Sigmosceptrins A-C:*

New Norditerpenes from a Southern Australian Marine Sponge, Sigmosceptrella sp. Australian Journal of Chemistry, 1997. **50**: p. 1137-1143.

24. Bennamara, A., A. Abourriche, M. Berrada, M. Charrouf, N. Chaib, M. Boudouma, and F.X. Garneau, *Methoxybifurcarenone: An Antifungal and Antibacterial Meroditerpenoid from the Brown Alga Cytoseira tamariscifolia.* Phytochemistry, 1999. **52**: p. 37-40.
25. Garrett, R.H. and C.M. Grisham, *Biochemistry.* Second ed. 1999, Fort Worth: Saunders College Publishing.
26. Munro, M.H.G., *Personal Communication.* 2002.
27. Shah, N.D., L.C. Vermeulen, J.P. Santell, R.J. Hunkler, and K. Hontz, *Projecting Future Drug Expenditures - 2002.* American Journal of Health-System Pharmacy, 2002. **59**(Jan 15): p. 131-142.
28. Bhakuni, D.S., *Some Aspects of Bioactive Marine Natural Products.* Journal of the Indian Chemical Society, 1998. **75**: p. 191-205.
29. Webster, N.S. and R.T. Hill. *Microbial Diversity and Bacterial Symbiosis in the Great Barrier Reef Sponge Rhopaloeides odorabile.* in *International Marine Biotechnology Conference 2000.* 2000. Townsville.
30. Hill, R.T., N.S. Webster, J. Ravel, and O. Peraud. *Molecular Approaches to the Isolation, Identification and Characterisation of Actinomycetes from the Marine Environment.* in *International Marine Biotechnology Conference 2000.* 2000. Townsville.
31. Kobayashi, J. and M. Ishbashi, *Bioactive Metabolites of Symbiotic Marine Micro-organisms.* Chemical Reviews, 1993. **93**: p. 1753-1769.
32. Johnson, T.W. and F.K. Sparrow, *Fungi in Oceans and Estuaries.* 1961, J Cramer: Weinheim. 668.
33. Tyndall, R.W. and P.W. Kirk, *Factors in Seawater Affecting Spore Germination in Marine Lignicolous Fungi.* Virginia Journal of Science, 1973. **24**: p. 136.
34. de Maisonneuve, C.D. and J.F.C. Montagne, *Pyrenomycetes Fr*, in *Exploration Scintifique De L'algerie, Botanique*, J.B. de Saint-Vincent and C.D de Maisonneuve, Editors. 1869: Paris. p. 443-608.
35. Fischer, B., *Die Bakterien Des Meers Nach Den Untersuchungen Der Plankton-Expedition Unter Gleichzeitger Berucksichtigung Einger Alterer Und Neuerer Untersuchungen.* Ergebnisse der Plankton-Expidition der Humbolt-Stiftung, 1894. **4**: p. 1-83.

36. Sparrow, F.K., *The Occurrence of Saprophytic Fungi in Marine Muds.* Biological Bulletins, 1937. **73**: p. 242-248.

37. Linder and Barghoorn, *Marine Fungi: Their Taxonomy and Biology.* Farlowia, 1944. **1**: p. 395-467.

38. ZoBell, C.E., *Marine Microbiology : A Monograph on Hydrobacteriology.* 1946, Waltham, Massachusetts.: The Chronica Botanica Company. 240.

39. Austin, B., *Marine Microbiology.* 1988, New York: Cambridge University Press. 222.

40. Schneider, J., *Fungi*, in *Microbial Ecology of a Brackish Water Environment*, G. Rheinheimer, Editor. 1977, Springer-Verlag: Berlin. p. 90-102.

41. Roth, F.J., P.A. Opurt, and D.G. Ahern, *Occurrence and Distribution of Fungi in a Subtropical Marine Environment.* Canadian Journal of Botany, 1964. **42**: p. 375-383.

42. Moore, R.T. and S.P. Meyers, *Thalassiomycetes I. Principles of Delimitation of the Marine Mycota with the Description of a New Aquatically Adapted Deuteromycete Genus.* Mycologia, 1959. **51**: p. 871-876.

43. Ritchie, D., *The Evolution of Salinity Tolerance in Fungi.* Transactions of the New York Academy of Sciences Series 2, 1960. **23**: p. 138-140.

44. Jones, E.B.G. and D.H. Jennings, *The Effect of Cations on the Growth of Fungi.* New Phytologist, 1965. **64**: p. 86-100.

45. Jones, E.B.G., P. Byrne, and D.J. Alderman, *The Response of Fungi to Salinity.* Vie Milieu supplement, 1971. **22**: p. 265-280.

46. Wood, E.J.F., *Microbiology of Oceans and Estuaries.* Elsevier Oceanography Series. Vol. 3. 1967, Amsterdam: Elsevier Publishing Company. 319.

47. Jones, E.B.G., *Aquatic Fungi: Freshwater and Marine*, in *Biology of Plant Litter Decomposition*, C.H. Dickenson and G.J.F. Pugh, Editors. 1974, Academic Press: New York. p. 337-383.

48. Pugh, G.J.F., *Fungi in Intertidal Regions*, in *Marine Mykologie II. Veroffentlichungen Des Instituts Fur Meeresforschung in Bremerhaven, Supplement 5*, A. Gaertner, Editor. 1974, Kommissionverlag Franz Leuwer: Bremer. p. 403-418.

49. Oppenheimer, C.H., *Symposium on Marine Microbiology.* 1963, Springfield, Illinois: Thomas. 769 pp.

50. Ravishankar, J.P. and T.S. Suryanarayanan, *Influence of Salinity on the Activity*

of Polyol Metabolism Enzymes and Peroxidase in the Marine Fungus Cirrenalia pygmea (Hyphomycetes). Indian Journal of Marine Sciences, 1998. **27**: p. 237-238.

51. Dietzman, G.R., *The Marine Environment as a Discovery Resource*, in *High Throughput Screening: The Discovery of Bioactive Substances*, J.P. Devlin, Editor. 1997, Marcel Dekker Inc.: New York. p. 99-115.
52. Mitchell, R. and C. Wirsen, *Lysis of Non-Marine Fungi by Marine Micro-Organisms.* Journal of General Microbiology, 1968. **52**: p. 335-345.
53. Kirk, P.W., *Isolation and Culture of Lignicolous Marine Fungi.* Mycologia, 1969. **61**: p. 174-177.
54. Kohlmeyer, J. and E. Kohlmeyer, *Synoptic Plates of Higher Marine Fungi.* 2nd ed. 1964, Weinheim: J Cramer. 64 pp.
55. Kohlmeyer, J. and E. Kohlmeyer, *Marine Mycology: The Higher Fungi.* 1979, London: Academic press.
56. Kirk, P.W., *Seasonal Distribution of Marine Lignicolous Fungi in Lower Chesapeake Bay.* American Journal of Botany, 1972. **59**: p. 667.
57. Hyde, K.D., V.V. Sarma, and E.B.G. Jones, *Morphology and Taxonomy of Higher Marine Fungi*, in *Marine Mycology : A Practical Approach*, K.D. Hyde and S.B. Pointing, Editors. 2000, Fungal Diversity Press: Hong Kong. p. 172-204.
58. Gerard, J., R. Lloyd, T. Barsby, P. Haden, M.T. Kelly, and R.J. Anderson, *Massetolides A-H, Antimycobacterial Cyclic Depsipeptides Produced by Two Psuedomonads Isolated from Marine Habitats.* Journal of Natural Products, 1997. **60**: p. 223-229.
59. Lindel, T., P.R. Jensen, and W. Fenical, *Lagunapyrones A-C: Cytotoxic Acetogenins of a New Skeletal Class from a Marine Sediment Bacterium.* Tetrahedron Letters, 1996(37): p. 1327-1330.
60. Yu, C.M., J.M. Curtis, J.L.C. Wright, S.W. Ayer, and Z.R. Fathi-Afshar, *An Unusual Fatty Acid and Its Glyceride from the Marine Fungus Microsphaeropis olivacea.* Canadian Journal of Chemistry, 1996. **74**: p. 730-735.
61. Farooq-Biabani, M.A. and H. Laatsch, *Advances in Chemical Studies on Low Molecular Weight Metabolites of Marine Fungi.* Journal Für Praktische Chemie Chemiker-Zeitung, 1998. **340**: p. 539-607.
62. Fenical, W., G.N. Belofsky, P.R. Jensen, and M.K. Renner, *New Cytotoxic*

Sesquiterpenoid Nitrobenzoyl Esters from a Marine Isolate of the Fungus Aspergillus versicolor. Tetrahedron, 1998. **54**: p. 171715-1724.

63. Höller, U., G.M. König, and A.D. Wright, *Three New Metabolites from Marine-Derived Fungi of the Genera Coniothyrium and Microsphaeropsis.* Journal of Natural Products, 1999. **62**(1): p. 114-118.
64. Liberra, K. and U. Lindequist, *Marine Fungi - a Prolific Source of Biologically Active Natural Products?* Pharmazie, 1995. **50**: p. 583-588.
65. Brotzu, G., *Ricerche Su Di Un Nuovo Antibiotico.* Lavori Dell'Istituto Di Igiene Di Cagliari, 1948: p. 3-11.
66. Schiehser, G.A., J.D. White, G. Matsumoto, J.O. Pezzanite, and J. Clardy, *The Structure of Leptosphaerin.* Tetrahedron Letters, 1986. **27**(46): p. 5587-5590.
67. Chen, C., N. Imamura, M. Nishijima, K. Adachi, M. Sakai, and H. Sano, *Halymecins, New Antimicroalgal Substances Produced by Fungi Isolated from Marine Algae.* The Journal of Antibiotics, 1996: p. 998-1006.
68. Rahbaek, L., C. Christophersen, J. Frisvad, H.S. Bengaard, S. Larsen, and B.R. Rassing, *Insulicolide A: A New Nitrobenzoyloxy-Substitiuted Sesquiterpene from the Marine Fungus Aspergillus insulicola.* Journal of Natural Products, 1997. **60**: p. 811-813.
69. Yu, C.-M., J.M. Curtis, J.A. Walter, J.L.C. Wright, S.W. Ayer, J. Kaleta, L. Querengesser, and Z.R. Fathi-Afshar, *Potent Inhibitors of Cysteine Proteases from the Marine Fungus Microascus longirostris.* The Journal of Antibiotics, 1995. **49**(4): p. 395-397.
70. Alam, M., E.B.G. Jones, M.B. Hossain, and D. van der Helm, *Isolation and Structure of Isoculmorin from the Marine Fungus Kallichroma tethys.* Journal of Natural Products, 1996. **59**(4): p. 454-456.
71. Onuki, H., H. Miyashige, H. Hasegawa, and S. Yamashita, *NI 15501A, a Novel Anthranilamide Derivative from a Marine Fungus Penicillium sp.* The Journal of Antibiotics, 1998: p. 442-444.
72. Jenkins, K.M., M.K. Renner, P.R. Jensen, and W. Fenical, *Exumolides A and B: Antimicroalgal Cyclic Depsipeptides Produced by a Marine Fungus of the Genus Scytalidium.* Tetrahedron Letters, 1998. **39**: p. 2463-2466.
73. Varoglu, M., T.H. Corbett, F.A. Valeriote, and P. Crews, *Asperazine, a Selective Cytotoxic Alkaloid from a Sponge-Derived Culture of Aspergillus niger.* The Journal of Organic Chemistry, 1997. **62**(21): p. 7078-7079.

74. Osterhage, C., R. Kaminsky, G.M. Konig, and A.D. Wright, *Ascosalipyrrolidinone A, an Antimicrobial Alkaloid, from the Obligate Marine Fungus Ascochyta salicorniae.* The Journal of Organic Chemistry, 2000. **65**: p. 6412-6417.

75. Numata, A., T. Amagata, K. Minoura, and T. Ito, *Gymnastatins, Novel Cytotoxic Metabolites Produced by a Fungal Strain from a Sponge.* Tetrahedron Letters, 1997. **38**(32): p. 5675-5678.

76. Namikoshi, M., H. Kobayashi, T. Yoshimoto, and T. Hosoya, *Phomopsidin, a New Inhibitor of Microtubule Assembly Produced by Phomopsis sp. Isolated from Coral Reef in Pohnpei.* The Journal of Antibiotics, 1997: p. 563-565.

77. Smith, C.S., D. Abbanat, V.S. Bernan, W.M. Maiese, M. Greenstein, J. Jompa, A. Tahir, and C.M. Ireland, *Novel Polyketide Metabolites from a Species of Marine Fungi.* Journal of Natural Products, 2000. **63**(1): p. 142-145.

78. Renner, M.K., P.R. Jensen, and W. Fenical, *Neomangicols: Structures and Absolute Stereochemistries of Unprecedented Halogenated Sesterterpenes from a Marine Fungus of the Genus Fusarium.* The Journal of Organic Chemistry, 1998. **63**(23): p. 8346-8354.

79. Belofsky, G.N., P.R. Jensen, and W. Fenical, *Sansalvamide: A New Cytotoxic Cyclic Depsipeptide Produced by a Marine Fungus of the Genus Fusarium.* Tetrahedron Letters, 1999. **40**.

80. Sperry, S., G.J. Samuels, and P. Crews, *Vertinoid Polyketides from the Saltwater Culture of the Fungus Trichoderma longibrachiatum Separated from a Haliclona Marine Sponge.* The Journal of Organic Chemistry, 1998. **63**(26): p. 10011-10014.

81. Toske, S.G., P.R. Jensen, C.A. Kauffman, and W. Fenical, *Aspergillamides A and B: Modified Cytotoxic Tripeptides Produced by a Marine Fungus of the Genus Aspergillus.* Tetrahedron, 1998. **54**: p. 13459-13466.

82. Nielsen, J., P.H. Nielsen, and J.C. Frisvad, *Fungal Depside, Guisinol, from a Marine Derived Strain of Emericella unguis.* Phytochemistry, 1999. **50**: p. 263-265.

83. Verbist, J.-F., C. Sallenave, and Y.-F. Pouchus, *Marine Fungal Substances.* Studies in Natural Products Chemistry, 2000. **24**: p. 979-1092.

84. Adams, N.M., *Seaweeds of New Zealand.* 1994, Christchurch: Canterbury University Press.

85. Flannigan, B., *Mycotoxins*, in *Toxic Substances in Crop Plants*, J.P.F. D'Mello, C.M. Duffus, and J.H. Duffus, Editors. 1991, The Royal Society of Chemistry: Cambridge. p. 226-257.

86. ApSimon, J.W., B.A. Blackwell, L. Blais, D.A. Fielder, R. Greenhalgh, G. Kasitu, J.D. Miller, and M. Savard, *Mycotoxins from Fusarium Species: Detection, Determination and Variety.* Pure and Applied Chemistry, 1990. **62**(7): p. 1339-1346.

87. Moss, M.O. and J.E. Smith, *Mycotoxins*. 1985, Toronto: Wiley.

88. D'Mello, J.P.F., J.K. Porter, A.M.C. Macdonald, and C.M. Placinta, *Fusarium Mycotoxins*, in *Handbook of Plant and Fungal Toxicants*, J.P.F. D'Mello, Editor. 1997, CRC Press: Boca Raton, Florida.

89. Savard, M.E., J.D. Miller, B. Salleh, and R.N. Strange, *Chlamydosporol, a New Metabolite from Fusarium chlamydosporum.* Mycopathologica, 1990. **110**: p. 177-181.

90. Delmotte, P. and J. Delmotte-Plaquee, *A New Antifungal Substance of Fungal Origin.* Nature, 1953. **171**: p. 344.

91. Mirrington, R.N., E. Ritchie, C.W. Shoppee, W.C. Taylor, and S. Sternhell, *Constitution of Radicicol.* Tetrahedron Letters, 1964. 7: p. 365-370.

92. Nair, M.S.R. and S.T. Carey, *Metabolites of Pyrenomycetes XIII. Structure of (+)-Hypothemycin, an Antibiotic Macrolide from Hypomyces trichothecoides.* Tetrahedron Letters, 1980. **21**: p. 2011-2012.

93. Smith, J.E., I. Mitchell, and M.L.C. Chiu, *The Natural Occurrence of Fusarium Mycotoxins*, in *The Applied Mycology of Fusarium*, M.O. Moss and J.E. Smith, Editors. 1984, Cambridge University Press: Cambridge. p. 157-173.

94. Hidy, P.H., R.S. Baldwin, R.L. Greasham, C.L. Keith, and J.R. McMullen, *Zearalenone and Some Derivatives: Production and Biological Activities.* Advances in Applied Microbiology, 1977. **22**: p. 59-82.

95. Drysdale, R.B., *The Production and Significance in Phytopathology of Toxins Produced by Species of Fusarium*, in *The Applied Mycology of Fusarium*, M.O. Moss and J.E. Smith, Editors. 1984, Cambridge University Press: Cambridge. p. 95-105.

96. Cole, R.J., J.W. Kirksey, H.G. Cutler, B.L. Doupnik, and J.C. Peckham, *Toxin from Fusarium moniliforme: Effects on Plants and Animals.* Science, 1973. **179**: p. 1324-1326.

97. Vesonder, R.F. and P. Golinski, *Metabolites of Fusarium*, in *Fusarium. Mycotoxins, Taxonomy and Pathogenicity*, J. Chelkowski, Editor. 1989, Elsevier: Amsterdam. p. 1-40.

98. Breiphol, G. and B. Frank, *Biosynthesis of Moniliformin, a Fungal Toxin with Cyclobutanedione Structure.* Angewandte Chemie International Edition, 1984. **23**: p. 996-998.

99. Bezuidenhout, S.C., W.C.A. Gelderblom, C.P. Gorst-Allman, R.M. Horak, W.F.O. Marasas, G. Spiteller, and R. Vleggaar, *Structure Elucidation of the Fumonisins, a Mycotoxin from Fusarium moniliforme.* Journal of the Chemical Society, Chemical Communications, 1988: p. 743-745.

100. ApSimon, J.W., *The Biosynthetic Diversity of Secondary Metabolites*, in *Mycotoxins in Grain: Compounds Other Than Aflatoxin*, J.D. Miller and H.L. Trenholm, Editors. 1994, Eagan Press: St Paul, Minnesota. p. 3-18.

101. Seo, J.A., J.C. Kim, and Y.W. Lee, *Isolation and Characterisation of Two New Type C Fumonisins Produced by Fusarium oxysporum.* Journal of Natural Products, 1996. **59**(11): p. 1003-1005.

102. Laatsch, H., *Antibase 2001: A Database for Rapid Structure Identification of Microbial Metabolites.* 2001, Wiley-VCH Verlag Berlin GmbH: Weinheim.

103. Savard, M.E. and J.W. ApSimon, *Non-Trichothecene Secondary Metabolites of Fusarium: Recent Work.* Studies in Natural Products Chemistry, 1993. **13**: p. 519-551.

104. Gelderblom, W.C.A., W.F.O. Marasas, P.S. Steyn, P.G. Theil, K.J. van der Merwe, P.H. van Rooyen, R. Vleggaar, and P.L. Wessels, *Structure Elucidation of Fusarin C, a Mutagen Produced by Fusarium moniliforme.* Journal of the Chemical Society, Chemical Communications, 1984: p. 122-124.

105. Savard, M.E. and J.D. Miller, *Characterisation of Fusarin F, a New Fusarin from Fusarium moniliforme.* Journal of Natural Products, 1992. **55**(1): p. 64-70.

106. Bjeldanes, L.F. and S.V. Thomson, *Mutagenic Activity of Fusarium moniliforme Isolates in the Salmonella typhimurium Assay.* Applied and Environmental Microbiology, 1979. **37**(6): p. 1118-1121.

107. Burmeister, H.R. and R.D. Plattner, *Enniatin Production by Fusarium tricinctum and Its Effects on Germinating Wheat Seeds.* Phytopathology, 1987. **77**: p. 1483-1487.

108. Grove, J.F. and M. Pople, *The Insecticidal Activity of Beauvericin and Enniatin*

Complex. Mycopathologica, 1980. **70**(2): p. 103-105.

109. Bekker, A.R., G.P. Kononenko, N.A. Leonov, and N.A. Soboleva, *Gramilaurone, a Novel Natural Sesquiterpenoid from Fusarium graminearum Schw.* Tetrahedron Letters, 1991. **32**(16): p. 1893.
110. Hsieh, D.P.H., *Mode of Action of Mycotoxins*, in *Mycotoxins in Food*, P. Krogh, Editor. 1987, Academic Press: London. p. 149-176.
111. Pestka, J.J. and G.S. Bondy, *Immunotoxic Effects of Mycotoxins*, in *Mycotoxins in Grain: Compounds Other Than Aflatoxin*, J.D. Miller and H.L. Trenholm, Editors. 1994, Eagan Press: St Paul. p. 339-358.
112. Beardall, J.M. and J.D. Miller, *Diseases in Humans with Mycotoxins as Possible Causes*, in *Mycotoxin in Grain. Compounds Other Than Aflatoxin*, J.D. Miller and H.L. Trenholm, Editors. 1994, Eagan Press: St Paul, Minnesota. p. 487-539.
113. Scott, P.M., *The Natural Occurrence of Trichothecenes*, in *Trichothecene Mycotoxicosis: Pathophysiologic Effects*, V.R. Beasley, Editor. 1989, CRC Press: Boca Raton.
114. Renner, M.K., P.R. Jensen, and W. Fenical, *Mangicols: Structures and Biosynthesis of a New Class of Sesterterpene Polyols from a Marine Fungus of the Genus Fusarium.* The Journal of Organic Chemistry, 2000. **65**(16): p. 4843-4852.
115. Cueto, M., P.R. Jensen, and W. Fenical, *N-Methylsansalvamide, a Cytotoxic Cyclic Depsipeptide from a Marine Fungus of the Genus Fusarium.* Phytochemistry, 2000. **55**: p. 223-226.
116. Amagata, T., J.F. Rigot, N. Tarlov, F.A. Valeriote, and P. Crews. *Three New Cytotoxic Trichothecenes Produced by a Sponge-Derived Fusarium sp.* in *10th International Symposium on Marine Natural Products*. 2001. Hago, Okinawa, Japan.
117. Savard, M.E. and B.A. Blackwell, *Spectral Characteristics of Secondary Metabolites from Fusarium Fungi*, in *Mycotoxins in Grain: Compounds Other Than Aflatoxin*, J.D. Miller and H.L. Trenholm, Editors. 1994, Eagan Press: St Paul, Minnesota. p. 59-285.
118. Savard, M.E. and R. Greenhalgh, *Synthesis and NMR Analysis of New Natural Trichothecenes.* Journal of Natural Products, 1987. **50**(5): p. 953-957.
119. Sakuma, Y., J. Tanaka, and T. Higa, *New Naphthopyrone Pigments from the Crinoid Comanthus parvicirrus.* Australian Journal of Chemistry, 1987. **40**(9):

p. 1613-1616.

120. Rideout, J.A. and M.D. Sutherland, *Pigments of Marine Animals XV. Bianthrones and Related Polyketides from Lamprometra palmata gyges and Other Species of Crinoids.* Australian Journal of Chemistry, 1985. **38**(5): p. 793-808.

121. Messana, I., F. Ferrari, M.S.B. Cavalcanti, and E. Gacs-Baitz, *New Naphthopyrone Derivatives from Cassia pudibunda.* Heterocycles, 1990. **31**(10): p. 1847-1853.

122. Macias, M., M. Ulloa, A. Gamboa, and R. Mata, *Phytotoxic Compounds from the New Coprophilous Fungus Guanomyces polythrix.* Journal of Natural Products, 2000. **63**(6): p. 757-761.

123. Macias, M., A. Gamboa, M. Ulloa, R.A. Toscano, and R. Mata, *Phytotoxic Naphthopyranone Derivatives from the Coprophilous Fungus Guanomyces polythrix.* Phytochemistry, 2001. **58**(5): p. 751-758.

124. Brown, D.W., F.M. Hauser, R. Tommasi, S. Corlett, and J.J. Salvo, *Structural Elucidation of a Putative Conidial Pigment Intermediate in Aspergillus parasiticus.* Tetrahedron Letters, 1993. **34**(3): p. 419-422.

125. Koyama, K. and S. Natori, *Chaetochromins B, C, and D; Bis(Naphtho-γ-Pyrone) Derivatives from Chaetomium gracile.* Chemical and Pharmaceutical Bulletin, 1987. **35**(2): p. 578-84.

126. Tertzakian, G., R.H. Haskins, G.P. Slater, and L.R. Nesbitt, *The Structure of Cephalochromin.* Proceedings of the Chemical Society, 1964: p. 195-196.

127. Priestap, H.A., *New Naphthopyrones from Aspergillus fonsecaeus.* Tetrahedron, 1984. **40**(19): p. 3617-3624.

128. Koyama, K., K. Ominato, S. Natori, T. Tashiro, and T. Tsuruo, *Cytotoxicity and Antitumor Activities of Fungal Bis(Naphtho-γ-Pyrone) Derivatives.* Journal of Pharmacobio-Dynamics, 1988. **11**(9): p. 630-635.

129. Hedge, V.R., J.R. Miller, M.G. Patel, A.H. King, M.S. Puar, A. Horan, R. Hart, R. Yarborough, and V. Gullo, *SCH 45752 - an Inhibitor of Calmodulin-Sensitive Cyclic Nucleotide Phosphodiesterase Activity.* The Journal of Antibiotics, 1993. **46**(2): p. 207-213.

130. Carey, S.T. and M.S.R. Nair, *Metabolites of Pyrenomycetes V. Identification of an Antibiotic from Two Species of Nectria, as Cephalochromin.* Lloydia, 1975.

38(5): p. 448-449.

131. Koyama, K. and S. Natori, *Further Characterization of Seven Bis(Naphtho-γ-Pyrone) Congeners of Ustilaginoidins, Pigments of Claviceps virens (Ustilaginoidea virens).* Chemical and Pharmaceutical Bulletin, 1988. **36**(1): p. 145-152.

132. Koyama, K., S. Natori, and Y. Iitaka, *Absolute Configurations of Chaetochromin A and Related Bis(Naphtho-γ-Pyrone) Mold Metabolites.* Chemical and Pharmaceutical Bulletin, 1987. **35**(10): p. 4049-4055.

133. Koyama, K., K. Kinoshita, N. Hamada, S. Natori, and T. Iitaka, *Structures of Bis(Naphtho-γ-Pyrone) Mycotoxins.* Tennen Yuki Kagobutsu Toronkai Kon Yoshishu, 1987. **29**: p. 713-720.

134. Stoessl, A., C.H. Unwin, and J.B. Stothers, *On the Biosynthesis of Some Polyketide Metabolites in Alternaria solani: ^{13}C and ^{2}Hmr Studies.* Canadian Journal of Chemistry, 1983. **61**: p. 372-377.

135. Suemitsu, R., K. Horiuchi, M. Kubota, and T. Okamatsu, *Production of Alterporriols, Altersolanols and Macrosporin by Alternaria porri and A. solani.* Phytochemistry, 1990. **29**(5): p. 1509-1511.

136. Rotem, J., *The Genus Alternaria. Biology, Epidemiology and Pathogenicity.* 1994, St Paul, Minnesota: APS Press.

137. Stierle, A.C., J.H. Cardellina II, and G.A. Strobel, *Maculosin, a Host-Specific Phytotoxin for Spotted Knapweed from Alternaria alternata.* Proceedings of the National Academy of Science, 1988. **85**: p. 8008-8011.

138. Ayer, W.A. and L.M. Pena-Rodriguez, *Metabolites Produced by Alternaria brassicae, the Black Spot Pathogen of Canola, Part 1, the Phytotoxic Components.* Journal of Natural Products, 1987. **50**(3): p. 400-407.

139. Nishimura, S. and K. Kohmoto, *Host Specific Toxins and Chemical Structures from Alternaria Species.* Annual Review of Phytopathology, 1983. **21**: p. 87-116.

140. Yagi, A., N. Okamura, H. Haraguchi, T. Abo, and K. Hashimoto, *Antimicrobial Tetrahydroanthraquinones from a Strain of Alternaria solani.* Phytochemistry, 1993. **33**(1): p. 87-91.

141. Okamura, N., H. Haraguchi, K. Hasimoto, and A. Yagi, *Altersolanol-Related Antimicrobial Compounds from a Strain of Alternaria solani.* Phytochemistry,

1993. **34**(4): p. 1005-1009.

142. Gamboa-Angulo, M.M., F. Alejos-Gonzalez, F. Escalante-Erosa, K. Garcia-Sosa, G. Delgado-Lamas, and L.M. Pena-Rodriguez, *Novel Dimeric Metabolites from Alternaria tagetica.* Journal of Natural Products, 2000. **63**(8): p. 1117-1120.

143. Suemitsu, R., T. Yamamoto, T. Miyai, and T. Ueshima, *Alterporriol A: A Modified Bianthraquinone from Alternaria porri.* Phytochemistry, 1987. **26**(12): p. 3221-3224.

144. Stoessl, A. and J.B. Stothers, *Tetrahydroaltersolanol B, a Hexahydroanthronol from Alternaria solani.* Canadian Journal of Chemistry, 1983. **61**: p. 378-382.

145. Assante, G. and G. Nasini, *Identity of the Phytotoxin Stemphylin from Stemphylium botryosum with Altersolanol A.* Phytochemistry, 1987. **26**(3): p. 703-705.

146. Stack, M.E., E.P. Mazzola, S.W. Page, A.E. Pohland, R.J. Highet, and M.S. Tempesta, *Mutagenic Perylenequinone Metabolites of Alternaria alternata: Altertoxins I, II, and III.* Journal of Natural Products, 1986. **49**(5): p. 866-871.

147. Schade, J.E. and A.D. King, *Analysis of the Major Alternaria Toxins.* Journal of Food Protection, 1984. **47**(12): p. 978-995.

148. Lazarovits, G., R.W. Steele, and A. Stoessl, *Dimers of Altersolanol A from Alternaria solani.* Z. Naturforsch, 1988. **43c**: p. 813-817.

149. Sturdik, E. and L. Drobnica, *Interaction of Cytotoxic Antibiotic Dactylarin with Glycolytic Thiol Enzymes in Ehrlich Ascites Carcinoma Cells.* The Journal of Antibiotics, 1981. **34**: p. 708-712.

150. Blunt, J., *Personal Communication.* 2002: University of Canterbury.

151. Haasnoot, C.A.G., F.A.A.M. DeLeeuw, and C.A. Altona, *The Relationship between Proton-Proton NMR Coupling Constants and Substituent Electronegativities I. An Empirical Generalisation of the Karplus Equation.* Tetrahedron, 1980. **36**: p. 2783-2792.

152. Betina, V., *Bioactive Secondary Metabolites of Micro-organisms.* Progress in Industrial Microbiology. Vol. 30. 1994, Amsterdam: Elsevier.

153. Meienhofer, J. and E. Atherton, *Structure-Activity Relationships in the Actinomycins.* Advances in Applied Microbiology, 1973. **16**: p. 203-300.

154. Schatz, A., E. Bugie, and S.A. Waksman, *Streptomycin, a Substance Exhibiting Antibiotic Activity against Gram-Positive and Gram-Negative Bacteria.*

Proceedings of the Society for Experimental Biology and Medicine, 1944. **55**: p. 66-69.

155. Reading, C. and M. Cole, *Clavulanic Acid: A Beta-Lactamase-Inhibiting Beta-Lactam from Streptomyces clavuligerus.* Antimicrobial Agents and Chemotherapy, 1977. **11**(5): p. 852-857.

156. Behal, V., *Bioactive Products from Streptomyces.* Advances in Applied Microbiology, 2000. **47**: p. 113-156.

157. Harris, C.M. and T.M. Harris, *Structure of the Glycopeptide Antibiotic Vancomycin: Evidence for an Asparagine Residue in the Peptide.* Journal of the American Chemical Society, 1982. **104**(15): p. 4293-4295.

158. Harris, D.R., S.G. McGeachin, and H.H. Mills, *The Structure and Stereochemistry of Erythromycin A.* Tetrahedron Letters, 1965. **11**: p. 679-685.

159. Chong, C.N. and R.W. Rickards, *Macrolide Antibiotic Studies XVI. Structure of Nystatin.* Tetrahedron Letters, 1970. **59**: p. 5145-5148.

160. Burg, R.W., B.M. Miller, E.E. Baker, J. Birnbaum, S.A. Currie, R. Hartman, K. Yu-Lin, R.L. Monaglan, G. Olsen, I. Putter, J.B. Tunac, H. Wellick, E.O. Stampley, R. Oiwa, and S. Omura, *Avermectins, New Family of Potent Antihelminthic Agents: Production Organisms and Fermentation.* Antimicrobial Agents and Chemotherapy, 1979. **15**(3): p. 361-367.

161. Ehrlich, J., Q.R. Bartz, R.M. Smith, D.A. Joslyn, and P.R. Burkholder, *Chloromycetin, a New Antibiotic from a Soil Actinomycete.* Science, 1947. **106**: p. 417.

162. Long, L.M. and H.D. Troutman, *Chloramphenicol (Chloromycetin) VII. Synthesis through p-Nitroacetophenone.* Journal of the American Chemical Society, 1949. **71**: p. 2473-2475.

163. Berdy, J., *Recent Developments of Antibiotic Research and Classification of Antibiotics According to Chemical Structure.* Advances in Applied Microbiology, 1974. **18**: p. 309-406.

164. Bakina, E.V., I.V. Yartseva, L.S. Povarov, L.G. Alexandrova, K.A. Tulemysova, L.P. Mamonova, and M.N. Preobrazhenskaya, *Investigation of Anthracyclinones Produced by Streptomyces griseoruber.* Bioorganicheskaya Khimiya, 1989. **15**(10): p. 1423-1430.

165. Brockmann, H., H.J. Brockmann, J.J. Gordon, W. Keller-Schlierlein, W. Lewk, W.D. Ollis, V. Prelog, and I.O. Sutherland, *Identity of Rutilantinone with*

Pyrromycinone and the Position of the Carbomethoxy Group in Pyrromycinones. Tetrahedron Letters, 1960(8): p. 25-27.

166. Mitscher, L.A., W. McCrae, W.W. Andres, J.A. Lowery, and N. Bohonos, *Ruticulomycins, New Anthracycline Antibiotics.* Journal of Pharmaceutical Science, 1964. **53**(9): p. 1139-1140.
167. Arora, S.K., *Structure of Aklavinone, a DNA Binding Anthracycline Antibiotic.* The Journal of Antibiotics, 1985. **38**(12): p. 1788-1791.
168. Fujiwara, A., M. Tazoe, T. Hoshino, Y. Sekine, S. Masuda, and S. Nomura, *New Anthracycline Antibiotics, 1-Hydroxyauramycins and 1-Hydroxysulfurmycins.* The Journal of Antibiotics, 1981. **34**(7): p. 912-915.
169. Doyle, T.W., D.E. Nettleton, R.E. Grulich, D.M. Balitz, D.L. Johnson, and A.L. Vulcano, *Antitumour Agents from the Bohemic Acid Complex 4. Structures of Rudolphomycin, Mimimycin, Collinemycin and Alcindoromycin.* Journal of the American Chemical Society, 1979. **101**(23): p. 7041-7049.
170. Meienhofer, J. and E. Atherton, *Structure-Activity Relationships in the Actinomycins*, in *Structure-Activity Relationships among the Semisynthetic Antibiotics*, D. Perlman, Editor. 1977, Academic Press: New York. p. 427-529.
171. Farber, S., *Chemotherapy in the Treatment of Leukaemia and Wilms' Tumor.* Journal of the American Medical Association, 1966. **198**(8): p. 826-36.
172. Brockmann, H., G. Bohnsack, B. Franck, H. Gröne, H. Muxfeldt, and C. Süling, *Constitution of the Actinomycins.* Angewandte Chemie, 1956. **68**: p. 70-71.
173. Bullock, E. and A.W. Johnson, *Actinomycin Part V. The Structure of Actinomycin D.* Journal of the Chemical Society, 1957: p. 3280-3285.
174. Perutz, M.F., *X-Ray Diffraction of Actinomycin C_3.* Nature, 1964. **201**: p. 814.
175. Sheehan, J.C., H.G. Zachau, and W.B. Lawson, *The Structure of Etamycin.* Journal of the American Chemical Society, 1958. **80**: p. 3349-3355.
176. Mauger, A.B., *Part D - the Actinomycins*, in *Topics in Antibiotic Chemistry*, E.H. Chichester, Editor. 1980, Halsted Press: New York. p. 223-306.
177. Cerami, A., E. Reich, D.C. Ward, and I.H. Goldberg, *The Interaction of Actinomycin with DNA: Requirement for the 2-Amino Group of Purines.* Proceedings of the National Academy of Science, 1967. **57**(4): p. 1036-1042.
178. Anzai, K., K. Isono, K. Okuma, and S. Suzuki, *The New Antibiotics, Questiomycins A and B.* The Journal of Antibiotics, 1960. **13**(2): p. 125-132.
179. Gerber, N.N. and M.P. Lechevalier, *Phenazines and Phenoxazinones from*

Waksmania aerata and Pseudomonas iodinum. Biochemistry, 1964. **3**(4): p. 598-602.

180. Brockmann, H. and F. Seela, *Synthesis of 1,8-Didesmethyl-Actinomycin C_1.* Tetrahedron Letters, 1965. **52**: p. 4803-4305.

181. Brockmann, H. and F. Seela, *Synthesis of 4,6-Didemethyl- and 4,6-Dimethoxyactinomycin C_1.* Tetrahedron Letters, 1968(2): p. 161-163.

182. Lim, Y., J.H. Chang, J.H. Kim, J.W. Suh, J.K. Jung, and C.H. Lee, *Structure Elucidation of a Potent Anti-MRSA Antibiotic, AM3, Produced by Streptomyces sp.* Agricultural Chemistry and Biotechnology, 1995. **38**(6): p. 516-521.

183. Mauger, A.B. and W.A. Thomas, *NMR Studies of Actinomycins Varying at the Proline Sites.* Organic Magnetic Resonance, 1981. **17**(3): p. 186-190.

184. Ha, S.C. and S.D. Hong, *Characteristics of Antitumor Antibiotics HS-1 from a Streptomyces floridae SHS-1372.* Korean Journal of Applied Microbiology and Biotechnology, 1994. **22**(2): p. 169-174.

185. Lifferth, A., I. Bahner, H. Lackner, and M. Schafer, *Synthesis and Structure of Proline Ring Modified Actinomycins of the X-Type.* Z. Naturforsch, 1999. **54**(b): p. 618-691.

186. Yamaoka, K. and H. Ziffer, *The Optical Properties of Actinomycin D II. Optical Activity of the Deoxyribonucleic Acid Complex.* Biochemistry, 1968. **7**(3): p. 1001-1008.

187. Harada, K., K. Fujii, T. Mayumi, Y. Hibino, M. Suzuki, Y. Ikai, and H. Oka, *A Method Using LC/MS for Determination of Absolute Configuration of Constituent Amino Acids in Peptide --- Advanced Marfey's Method ---.* Tetrahedron Letters, 1995. **36**(9): p. 1515-1518.

188. Sengupta, S.K., D.H. Trites, M.S. Madhavarao, and W.R. Beltz, *Actinomycin D Oxazinones as Improved Antitumor Agents.* Journal of Medicinal Chemistry, 1979. **22**(7): p. 797-802.